Study of IgH locus recombination in human normal and in pathological condition, the Chronic lymphocytic leukemia

Israa Al Jamal

▶ **To cite this version:**

Israa Al Jamal. Study of IgH locus recombination in human normal and in pathological condition, the Chronic lymphocytic leukemia. Human health and pathology. Université de Limoges; Université Libanaise, 2022. English. NNT : 2022LIMO0067 . tel-03853099

HAL Id: tel-03853099
https://theses.hal.science/tel-03853099

Submitted on 15 Nov 2022

HAL is a multi-disciplinary open access archive for the deposit and dissemination of scientific research documents, whether they are published or not. The documents may come from teaching and research institutions in France or abroad, or from public or private research centers.

L'archive ouverte pluridisciplinaire **HAL**, est destinée au dépôt et à la diffusion de documents scientifiques de niveau recherche, publiés ou non, émanant des établissements d'enseignement et de recherche français ou étrangers, des laboratoires publics ou privés.

Thesis under joint supervision

Of

Lebanese University

And

University of Limoges

In partial fulfillment of the requirements of the degree of

Doctor of Philosophy

Discipline: Biology Science Health
Specialty: Immunology

Presented and defensed by
Israa Al Jamal

On September 23, 2022

Study of *IgH* locus recombination in human normal and in pathological condition, the Chronic Lymphocytic Leukemia

Thesis directors: Mme. Nathalie GACHARD, M. Nehman AL MAKDISSY
Thesis co-directors: Mme. Sophie PERON, Mme. Samar AL HAMAOUI

JURY:

M. Saïd AOUFOUCHI, Research Director, INSERM CNRS UMR8200, France	**Reporter**
Mme. Fanny BARAN-MARSZAK, PU-PH, Sorbonne University, France	**Reporter**
M. David RIZZO, MCU-PH, Limoges University, France	**Examiner**
Mme. Anne QUINQUENEL, MCU-PH, Reims University, France	**Examiner**
Mme. Sophie PERON, Researcher, CRIBL CNRS7276 INSERM1262, France	**Guest**
Mme. Samar AL HAMAOUI, University Professor, Lebanese University, Lebanon	**Guest**
M. Jean FEUILLARD, PU- PH, University of Limoges, France	**Guest**

License CC BY-NC-ND 4.0

During the first three years of my thesis, I was cofounded by the AZM and Saade association (AZM-UL) and the Lebanese association for Scientific research (LASeR). For the 4th year of my thesis I was funded by the “Fondation pour la Recherche Médicale, FRM”.

My work was warried out within the CRIBL Laboratory (UMR CNRS 7276, INSERM U1262) at the Faculty of Medicine and Pharmacy in the University of Limoges, FRANCE.

License CC BY-NC-ND 4.0

License CC BY-NC-ND 4.0

To Mother Mother 

To my Husband 

To my Family 

I dedicate this milestone of my life

To the memory of my dear uncle (**Mokhles**) who passed away too soon.

I hope that, from the new world where you are now, you appreciate this humble gesture as proof of gratitude from your niece who has always prayed for your soul.

You were always on my mind and in my heart during those years. I will not forget that you were the first person who encouraged me to continue my education and realize my dream, and you were the first person who called me ‘Doctor’, before I even started officially my PhD.

License CC BY-NC-ND 4.0

License CC BY-NC-ND 4.0

If you have a dream don't let anyone take it and always believe that the impossible is possible.

Selena

Strength does not come from winning. Your struggles develop your strength. When you go through hardship and decide not to surrender that is strength.

Mahatma Gandhi

License CC BY-NC-ND 4.0

License CC BY-NC-ND 4.0

Acknowledgements

That's life, for every beginning there are ends and here I am at the end of a chapter of my life, end of my PhD!!! A chapter full of great moments of learning and experiences. As they say: “one hand can never clap, the other hand should make some effort and show dedication to do the clapping”. Similarly, my thesis was not possible without the contribution of many of people. In this very emotional part of my manuscript, i will thank all the people who participated from near or far in this work.

First, I want to address my acknowledgments to the team director in the CBRS, CRIBL UMR7276, Pr. Jean FEUILLARD, for accepting me in his team to accomplish my thesis, for your encouragement and your professional advices during the meetings. My acknowledgments go also to the director of the AZM center, Pr. Mohamad KHALIL for welcoming and accepting me to do a thesis in collaboration with France.

I want to address my sincere acknowledgement to my thesis directors in the Lebanese and Limoges universities. I would like also to thank Dr. Nathalie GACHARD for accepting to be my director on the behalf of Limoges University and thank you for the scientific discussions we had during the CLL team meetings.

I want to address my special thanks to my co-director and my mentor throughout my thesis, Pr. Sophie PERON. Thank you for accepting me in thesis in France, thank you from all my heart, you were not only my thesis director but you were on a high level of humanity. I cannot forget when I went through difficult circumstances, how you tried the impossible to help me. Our project was not easy, but with the persistence of both of us, we reached where we are today. Thank you for the trust you placed in me from day one. Thank you for the kindness you showed me when we went to Paris and Vienna to participate in the SFH and EHA congress. Your words will remain engraved in my mind, “on va y arriver”.

I would like also to thank Pr. Nehman AL MAKDISSY and Dr. Samar Al HAMAOUI for accepting to be my director and co-director on behalf of the Lebanese University, which contributed to my funding during the first three years of my thesis. I truly appreciate your kindness.

I want to address my acknowledgements to the Jury members, reporters and examiners, Dr. Saïd AOUFOUCHI, Dr. Fanny BARAN-MARSZAK, Dr. Anne QUINQUENEL and Dr. David RIZZO for giving me the honor by accepting to judge my work and be a part of this committee.

During these years, I was able to work in a particularly pleasant environment, thanks to all the members of UMR CNRS7276, we are numerous and I cannot mention you one by one (to not forget anyone). Thank you for giving me the opportunity to live well the moments of research

License CC BY-NC-ND 4.0

within the unit. Thank you all for the discussions over my project that we had during the lab meeting.
Thanks to all the persons who helped me in any way I really appreciate your kindness.
To my old office colleague, Lilian, a big thank-you for your kindness and your help.
To my current not only colleagues but also friends and supporters, A thesis is not easy as we imagine, we pass through very difficult moments and we support each other even by small things, and I have the luck to have you, Jennifer, Lea, Stecy and Quentin. I will not forget the secret discussions we had, your support by leaving me 'post-it's on my desk to encourage me and to wish me luck. For sure, I will not forget the best moments we had at the lunchtime, when we ate the dessert prepared by anyone of us, and as Jennifer says: “C’est le bureau des grands parents”. You, my colleagues and friends, are amazing, soon I will leave you but I will not forget you and I wish you all the best for your theses, Stecy you are next!
Keeping in your minds my expression “OHHH MYYYY GODDD” to remember me.

To the LSR team, Kenza and Milène, I wish you luck and all the best in your PhD work, you will be in a safe and practical place in Sophie team’s. Kenza thank you for the (Orchide), you are a very beautiful and elegant person inside and out I wish you nothing but the best luck in your future.

To the Lebanese community, old CRIBL members and others, Zainab, Batoul, Racha, Nour, Iman, Hussein, Hussein A., Hassan, my colleagues who quickly became my friends, for the good times we spent together and for the friendship. I will never forget you and wishing you luck wherever you are now.
Now I arrived to the most emotional part, this acknowledgment cannot be ended without mentioning the most important person in my life close friends, family and parents. I will talk about quality and not the quantity.
To you **Lara**, I never forget the first time we met in Limoges and after that we became very close friends, I will not forget our trip together in Beirut, in Tripoli, and in France, for the shopping, we did it together and we have the more to come. Thank you for your support until this moment, thank you for taking my news even when you were in Lebanon.
To you **Jennifer “Jenny”** I am so lucky to have ~~a friend~~ a sister by choice like you, really my words could never describe your sincerity. An example of an educated, conscious person, and a sweet heart. My companion in traveling, in the office and at all times. When I was in a difficult period, I could not forget everything you did to make me happy, whether it’s chocolate, gift or even a kind word from a pure human, you. In this part really, it’s difficult to write all the things

License CC BY-NC-ND 4.0

but the thing I know very well is that I love you and I wish you the best of the best luck in all your life.

Yes, it is your turn right now, you **Leena**, I already have the tears in my eyes, it is very difficult to thank a very close person, you called me sister by choice, but you know, to me you are more than my sister you are the copy of me, seriously. We share almost the same personality in two different bodies, but you know well you mean too much to me, if you look in my chatting list, you will find yourself on the top of the list. We passed together a very amazing three years, every day in the same lab, same city, we ate together, we did everything together. I cannot mention everything in this small part but I know when the person shows you their real personality without lying or acting when angry or happy, they are a real human being and you are. In this difficult moment of my life really, I wish you were by my side, but this is life. Despite the distance, you are the closest person to me. I will stop writing but you know the rest, THANK YOU FOR YOUR PRESENCE IN MY LIFE. I wish you a life full of success and happiness with Hussein.

I would like to thank all my friends, not just outside of the lab here in France but also in Lebanon, for all their love and support. I would like to heavily thank all my family members, my grandparents, my cousins, my aunts and uncles for their moral support and endless love and affection.

To the most valuable people in my life; my mother, my father and my big brother Mohamad, my sisters Jana (Jano) and Chadia (Chado) thank you from all my heart. I love you all so much and I thank you for being there for me throughout these years, loving me and supporting me whenever I needed it. I wish you could be here to celebrate this day with me, but that is life!

Mama, the person who did the impossible, your sacrifices and your patience to reach what I am today. My words are unable to express my love for you. You are my idol in life, and I pray to God to protect you and keep safe and healthy. What I am today is a proof of your success. Without you, I am nothing. I am grateful to you all my life and proud to be your daughter.

Last but not least, I would like to express my love and pride to my best friend my partner in this life, to my husband MOHAMAD. Our journey started at the same time of the beginning of my PhD. We had to be far because of travel, but this thing was not an obstacle, you were by my side with your advices, with your love and with the purity of your heart. You were my psychological support, your trust in me and in my abilities helped me a lot to overcome many difficult stages. Today, as I am writing these words, the PhD will end, but our relationship will continue forever. I love you so much, you mean a lot to me and I thank you for everything. ♾️

License CC BY-NC-ND 4.0

Finally, I would like to thank GOD for giving me physical and mental health, for giving me patience and strength to defy all odds and achieve everything I am today.

I turn a page and I open another!!!!

License CC BY-NC-ND 4.0

Rights

This creation is available under a Creative Commons contract:
« Attribution-Non Commercial-No Derivatives 4.0 International »
online at https://creativecommons.org/licenses/by-nc-nd/4.0/

License CC BY-NC-ND 4.0

License CC BY-NC-ND 4.0

Table of contents

List of Figures 18
List of Tables 20
List of Abbreviations 22
Abstract 26
Résumé 28
Bibliographic Introduction 30
Chapter I: Immunity and normal B cell development 32
A. Immune response 32
1. Innate immunity 32
2. Adaptive immunity 34
3. B cells 34
B. Immunoglobulins 36
1. Organization and structure of Immunoglobulin Loci 36
1.1. *Ig Kappa light chain* (*Igκ*) locus 37
1.2. *Ig light chain lambda* (*Igλ*) locus 38
1.3. *Ig Heavy chain* (*IgH*) locus 39
1.4. Cis Regulatory elements of *IgH* locus 40
1.5. Functions of cis regulatory elements of *IgH* locus 41
2. Immunoglobulins Isotypes 44
3. Production of functional immunoglobulins 45
3.1. Ig diversification: Antigen Independent stage 46
3.1.1. V (D) J Recombination 46
3.1.2. Recombination Signal Sequences (RSS) 47
3.1.3. RAG1/2 proteins 48
3.1.4. Steps of V (D) J recombination 48
3.2. Ig diversification: antigen dependent phase 51
3.2.1. Activation induced cytidine deaminase (AID) 51
3.2.2. Somatic Hypermutation (SHM) 52
3.2.3. Class Switch Recombination (CSR) 54
3.2.4. Locus Suicide Recombination (LSR) 58
C. B cell development, from the early stages to their terminal differentiation 60
1. Early stages of B cell development, an antigen independent phase 60
1.1. Hematopoietic Stem Cell (HSC) 60
1.2. Multipotent progenitor (MPP) 60

License CC BY-NC-ND 4.0

1.3. Common lymphoid progenitor (CLP) 60
1.4. Early Pro-B: D_H-J_H recombination 61
1.5. Late Pro-B: V_H-DJ_H recombination 61
1.6. Large pre-B cells: pre-BCR expression 61
1.7. Small pre-B cells: V_LJ_L recombination 62
1.8. Immature B cells 62
2. Late and Ag dependent stage of B cell development 63
2.1. Transitional B cells 63
2.2. B1 Cells 64
2.4. Marginal zone B cells 64
2.4. Mature naïve B cells 65
2.3. Initiation of the germinal center (GC) 65
2.4. Memory B cells 68
2.5. Plasma cells 68
2.3. Regulatory B cells 69
2.6. BCR signaling 70
Chapter II: DSB DNA Repair pathways *72*
1. DNA and chromatin structure 72
2. DNA lesions agents 73
3. Pathological impact of DNA lesions 75
4. DNA Damage Response (DDR) 76
5. Double Strand Break DNA repair pathways 77
5.1. Non-Homologous End Joining DNA repair pathway (NHEJ) 77
5.1.1. Mechanism of NHEJ 78
5.1.2. Alteration of NHEJ 80
5.2. Alternative End Joining DNA repair pathway (Alt-EJ) 81
5.2.1. Mechanism of Alt-EJ 82
5.2.2. Alteration of Alt-EJ 84
5.3. Homologous Recombination DNA repair pathway (HR) 84
5.3.1. Mechanism of HR 85
5.3.2. Alteration of HR 87
5.4. Single Strand Annealing DNA repair pathway (SSA) 87
6. Junction structure after DNA ligation 89
7. Choice of the DSB DNA repair pathway in the cell 89
7.1. DNA end resection modulates the DSB repair pathway choice 90

License CC BY-NC-ND 4.0

7.2. Effect of the cell cycle phases on the DSB repair choice 93
7.3. Effect of chromatin state on DNA DSB repair pathway choice 94
Chapter III: B Lymphomas *98*
A. Chronic Lymphocytic Leukemia (CLL) *98*
1. Overview on CLL 98
2. Clinical and biological characteristics 98
2.1. Diagnostic 98
2.2. Prognostic 100
Mutational status of IgHV genes 100
ZAP-70 100
CD38 101
BCR signaling 102
Recurrent mutations 103
Cytogenetic alterations 104
2.3. Classification 105
2.4. Treatments of CLL 106
3. Cell of origin in CLL 108
4. Evolution of CLL 109
4.1. Clinical complications of CLL 109
4.2. Microenvironmental factors 110
4.3. AID in CLL 111
4.4. DSBs repair alteration 112
B. Hodgkin Lymphoma (HL) *112*
Thesis objectives *118*
Results *120*
Article I: Increased IgH locus suicide recombination in Chronic Lymphocytic Leukemia denotes MYC driven IgH rearrangements *122*
Article II: LSR as an indicator of cellular origin in CLL cases with superior outcomes? *142*
Preliminary data of Hodgkin Lymphoma *162*
Discussion and Future Perspectives *170*
Conclusions *176*
Bibliographic References *180*

License CC BY-NC-ND 4.0

License CC BY-NC-ND 4.0

List of Figures

Figure 1: Innate and adaptive immunity: Implication different types of cells. *33*
Figure 2: Origin of blood cells. *35*
Figure 3: Structure of immunoglobulin (IgG). *37*
Figure 4: Organization of human immunoglobulin light chains loci. *39*
Figure 5: Organization of human immunoglobulin heavy chain locus. *41*
Figure 6: Mechanisms of immunoglobulin loci rearrangement and mutation during B cell development. *46*
Figure 7: Schema of V (D) J recombination mechanism. *47*
Figure 8: Organization of Recombination Signal Sequence (RSS) on Ig loci. *48*
Figure 9: DNA repair during V (D) J recombination. *50*
Figure 10 : Schematic representation of DNA repair during SHM. *53*
Figure 11: Somatic Hypermutation of Ig loci induced by AID. *54*
Figure 12: Germinal transcripts on constant regions of IgH locus. *55*
Figure 13: R-loop and G-quadruplex structures. *56*
Figure 14: Schematic representation of CSR to IgG1. ..... *57*
Figure 15: Schematic representation of LSR mechanism. *59*
Figure 16: Schematic representation of early stages of B cell development. *62*
Figure 17. Checkpoints during early B cell development *63*
Figure 18: Organization of secondary lymphoid organs (SLO). *65*
Figure 19: Schematic representation of late B cell development and germinal center. *69*
Figure 20: Signaling pathway of B cell Receptor. *70*
Figure 21: Schematic representation of Chromosome structure. *73*
Figure 22 :Factors inducing DNA lesions and the pathways of DNA repair. *74*
Figure 23: Signaling pathway of DNA Damage Response. *77*
Figure 24: Schematic representation of the NHEJ repair pathway. *80*
Figure 25: Schematic representation of the Alt-EJ mechanism. *83*
Figure 26 : Schematic representation of presynaptic step of HR pathway. *86*
Figure 27: Schematic representation of the SSA pathway. *88*
Figure 28 : Schematic representation of the junction structure generated by DSB repair. *89*
Figure 29: representation of how end resection influences the choice of DSB repair pathway choice. *92*
Figure 30: Schematic representation of cell cycle effect on DNA repair choice. *94*
Figure 31: Schematic representation of the influence of the chromatin state and γH2AX and DDR. *95*
Figure 32: Histone modification impact the DSB repair choice. *96*
Figure 33: A cross talk exist between H3K36me3 and H4k16ac. *97*
Figure 34: Signs and symptoms of chronic Lymphocytic leukemia. *99*
Figure 35: BCR signaling in CLL. *102*
Figure 36 : Schematic representation of the inhibitors and their targets in CLL treatment. *108*
Figure 37: Tumor microenvironment in CLL. *110*
Figure 38: Crosstalk between CLL and MSC cells. *111*
Figure 39: Structure of LSR and CSR junctions in HL and healthy tonsils samples. *163*
Figure 40: CSR junction structure in HL sorted cells (CD20+ and H/RS cells). *165*
Figure 41: Gating strategy to isolate the different subpopulation of tonsils B cells. *174*

License CC BY-NC-ND 4.0

License CC BY-NC-ND 4.0

List of Tables

Table 1: Characteristics of immunoglobulin isotypes. *45*
Table 2: Markers of human transitional B cells. *64*
Table 3: Matutes score in in CLL diagnosis. *100*
Table 4: Characteristics of RAI and Binet classification. *106*
Table 5: International prognostic Index of CLL (CLL-IPI). *106*
Table 6: CSR junction counts in HL sorted cells. *164*

License CC BY-NC-ND 4.0

License CC BY-NC-ND 4.0

List of Abbreviations

3'RR 3' Regulatory Region

ɣ gamma

μ mu

α alpha

β Beta

δ delta

k Kappa

λ lambda

ε Epsilon

η Eta

Θ theta

A

A Adenosine

Ab Antibody

Ag Antigens

AID Activation Induced cytidine Deaminase

Alt-EJ Alternative End Joining

APOBEC Apolipoprotein B RNA Editing catalytic Component

ATM Ataxia-Telangiectasia Mutated

ATR Ataxia-Telangiectasia and Rad3 Related

APC Antigen Presenting Cell

ASTE1 Asteroid Homolog 1

B

BCR B Cell Receptor

BCL6 B-cell lymphoma 6

BER Base Excision Repair

BM Bone Marrow

Bp Base pair

53BP1 p53 Binding Protein 1

BRCA1/2 Breast Cancer 1/2

BRIGHT B Cell Regulator of IgH Transcription

BSAP B Cell Specific Activator Protein

BTK Bruton's Tyrosine Kinase

C

C Cytosine

CDC25 Cell Division Cycle 25

CDK2 Cyclin-dependent kinase 2

CDR Complementarity-Determining Regions

ChIP Chromatin ImmunoPrecipitation

CHK1/2 Check point 1/2

CLL Chronic Lymphocytic Leukemia

CLP Common Lymphoid Progenitor

CSR Class Switch Recombination

CtIP C-terminal-binding protein interacting protein

CXCR C-X-C type Chemokine Receptor

CXCL C-X-C-type Chemokine Ligand

D

D Diversity

DC Dendritic Cell

DNA Deoxyribonucleic Acid

DDR DNA Damage Repair pathway

DLBCL Diffuse Large B Cell Lymphoma

DNA-PKcs DNA Dependent Protein Kinase catalytic subunit

DSB Double Strand Break

DZ Dark Zone

License CC BY-NC-ND 4.0

E

E2A E box protein binding 2 A

EBF1 Early B cell Factor-1

EBI2 Epstein-Barr virus-induced molecule 2

ERK Extracellular-signal-Regulated

EXO1 Exonucléase1

F

FDC Follicular Dendritic Cell

FO Follicular

FOXO1 Fork head box protein O1

FR Frame Work

G

G Guanine

GC Germinal Center

H

H Histone

HDAC Histone deacetylases

HJ Holiday Junction

HMCES 5-hydroxymethlycytosine (5hmC)

HMGB High Mobility Group Box

HR Homologous Recombination

HS Hypersensitive region

HSC Hematopoietic Stem Cell

I

iE Intronic Enhancer element

Ig Immunoglobulin

IgH Ig Heavy chain

IgL Ig Light chain

IKZF1 Ikaros Zinc finger protein 1

IL Interleukin

J

J Junction

K

K Lysine

KAT5 Lysine Acetyltransferase 5

Kb Kilobase

KO Knock Out

L

LEDGF Lens epithelium–derived growth factor

LIG Ligase

LPS Lipopolysaccharides

LS Like Switch region

LSR Locus Suicide Recombination

LZ Light Zone

M

MARs Matrix Association Region

MDC1 Mediator of DNA damage checkpoint 1

MMEJ Microhomologies Mediated End Joining

MMR Mismatch Repair

MPP Multipotent Progenitor

MRE11 Meiotic Recombination 11 homolog

MSH MutS Homolog

MZ Marginal Zone

N

NBS1 Nijmegen Breakage Syndrome 1

NE Novel Enhancer

NES Nuclear Exporting Signal

NHEJ Non-Homologous End Joining

NF-κB Nuclear Factor Kappa B pathway

NK Natural Killer

NLS Nuclear Localization Signal

P

PARP 1 poly ADP-ribose polymerase I

Pax-5 Paired box gene 5

License CC BY-NC-ND 4.0

PAXX XRCC4-like small protein

PCR Polymerase Chain Reaction

PCs Plasma cells

PI3K phosphatidylinositol-3-kinase

PKA Protein Kinase A

PTIP Pax transactivation domain interacting protein

Pol Polymerase enzyme

PRDM1 PR domain zinc finger protein 1

R

Rif1 Rap1-interacting factor 1

RPA Replication Associated Protein A

RAG Recombination Activating-Genes

RSS Recombination Signal Sequence

S

S Switch region

S1P sphingosine 1-phosphate

SCID Severe Combined Immunodeficiency

SETD2 SET Domain Containing 2, Histone Lysine Methyltransferase

SHM Somatic HyperMutation

SLC Surrogate Light Chain

SSA Single Strand Annealing

SSB Single Strand Break

ssDNA Single Strand DNA

SHM Somatic Hypermutation

SLO Secondary Lymphoid Organs

SYK Spleen tyrosine kinase

T

T Thymine

TAD Topologically Associating Domain

TAM Tumor-Associated Macrophage

TCR T Cell Receptor

TdT Terminal deoxynucleotidyl Transferase

TFH T Follicular Helper

Th Helper T cells

TGF_{β} Transforming Growth Factor β

TLR Toll Like Receptor

Tp53 Tumor protein 53

U

U Uracil

UNG Uracil DNA Glycosylase

V

V Variability

VH Variable regions of heavy chains

VL Variable regions of light chains

W

WRN Werner Syndrome protein

X

XPF Xeroderma Pigmentosum complementation group F

XRCC1 X-ray Repair Cross Complementing protein 1

XRCC4 X-ray Repair Cross Complementing protein 4

XLF XRCC4-like Factor (cernunnos)

Y

Y Tyrosine

Z

ZAP-70 Zeta-chain-associated protein kinase 70

License CC BY-NC-ND 4.0

License CC BY-NC-ND 4.0

Abstract

In normal B cells, Activation Induced-cytidine deaminase (AID) is the key enzyme for class switch recombination (CSR) and somatic hypermutation of (SHM) on the heavy chain (H) and the light chain (for SHM) of Immunoglobulin (Ig). AID is also implicated in another *IgH* rearrangement, the locus suicide recombination (LSR). LSR occurs in activated B cells and recombines the *IgH* locus between the switch μ (Sμ) region and the 3'regulatory region (3'RR) of *IgH* locus. LSR results in the complete deletion of the cluster of *IgH* constant genes. When LSR hits the active *IgH* locus, it induces the loss of BCR expression and the death of the concerned B cells. CSR and d LSR proceed by introduction of double strand breaks (DSB) followed by DNA repair and junction production. Chronic lymphocytic leukemia (CLL) is an indolent non-Hodgkin B cell lymphoma. CLL is characterized by the clonal expansion of tumor cells (CD5+, CD23+ and CD19+). Tumor cells weakly express a B cell receptor (BCR) on the surface, it is composed in the vast majority of cases of Immunoglobulins (Ig) IgM and IgD. CLL tumor cells are rarely switched, raising the question of abnormalities in the Ig gene recombination machinery in this B cell lymphoma. In our study, and based on the count of LSR junction we identified two groups of CLL patients. A group with High LSR junction count (LSR^{High}) and a group with low LSR junction count (LSR^{Low}) based on the mean count of LSR junctions obtained in healthy peripheral mononuclear blood cells (PBMC). Deep analysis of these groups of CLL patients showed that in LSR^{High} CLLs cells, the accessibility of *IgH* locus could be increased in a MYC dependent manner resulting in shorter survival and implying an additional MYC driven AID independent mechanism of *IgH* recombination. Also, LSR^{High} and ^{Low} CLLs appear to be characterized by different features certainly due to different CLL tumoral transformation mechanisms. We showed also similarity of LSR junctions between CLL LSR^{Low} samples and healthy tonsils. We propose tumoral cells, in LSR^{Low} CLL, emerge from B cell population, which is normally restricted to the compartment of B cell activation achievement.

Key words High LSR count, low LSR count, CSR, MYC, CLL, prognosis, cell of origin.

License CC BY-NC-ND 4.0

License CC BY-NC-ND 4.0

Résumé

Dans les lymphocytes B (LB) normaux, l'Activation Induced-cytidine Deaminase (AID) est l'enzyme clé des mécanismes de commutation de classe (CSR) et l'hyper-mutation somatique (SHM) des chaînes lourde (H) et légère (L) d'immunoglobuline (Ig). AID est impliquée dans un autre mécanisme de réarrangement du locus *IgH*, la recombinaison suicide du locus *IgH* (LSR). La LSR se produit dans les cellules B activées et recombine le locus *IgH* entre la région de commutation μ (Sμ pour switch μ) et la région régulatrice (3'RR) en 3' du locus *IgH*. La LSR entraîne la suppression des gènes constants du locus *IgH*. Quand la LSR touche le locus *IgH* sur l'allèle productif, elle induit la perte d'expression du BCR et la mort des LB concernés. Les mécanismes de CSR et LSR nécessitent des cassures doubles brin (CDB) de l'ADN qui vont être réparées et générer la production de jonctions de recombinaison. La leucémie lymphoïde chronique (LLC) est un lymphome indolent non hodgkinien affectant les cellules B. la LLC est caractérisée par une prolifération clonale de cellules tumorales (CD5+, CD23+, CD19+). Les cellules tumorales expriment faiblement le BCR et l'Ig est majoritairement une IgM coexprimée avec l'IgD. Les cellules tumorales expriment rarement une Ig de classe commutée, ce qui pose la question sur une altération du processus permettant le réarrangement du locus *IgH* dans ces cellules cancéreuses. En utilisant le nombre de jonctions LSR détectées dans des prélèvements sanguins de patients atteints de LLC, nous avons identifié deux groupes distincts. Le premier groupe se présente avec un nombre augmenté de jonctions de LSR ($LSR^{augmentée}$), le second groupe, avec un nombre diminué de jonctions LSR, ($LSR^{diminuée}$) par rapport à la moyenne du compte de jonctions LSR d'échantillons de cellules mononuclées du sang périphérique (PBMC) de volontaires sains. L'analyse en détails de ces deux groupes a permis de montrer que dans les cellules du groupe $LSR^{augmentée}$ l'accessibilité du locus *IgH* est augmentée, une prolifération accrue, la surexpression de *MYC* et des indicateurs de mauvais pronostic. Ces cellules apparaissent subies un mécanisme de recombinaison du locus *IgH* aboutissant à la LSR indépendant de l'AID mais dépendant de MYC. Par ailleurs, nos résultats montrent que les LLC $LSR^{augmentée}$ et $LSR^{diminuée}$ présentent des caractéristiques différentes et suggèrent des mécanismes de transformation tumorale distincts. Nous avons également montré la similitude des jonctions LSR des cellules de LLC $LSR^{diminuée}$ et de cellules issues des amygdales de volontaires sains. Nous proposons que les cellules tumorales, dans la LLC $LSR^{diminuée}$, émergent de la population de cellules B qui est normalement limitée aux compartiments impliqués dans l'activation des cellules B.

Mots clés LSR augmentée, LSR diminuée, CSR, MYC, LLC, pronostic, Cellule d'origine.

License CC BY-NC-ND 4.0

License CC BY-NC-ND 4.0

Bibliographic Introduction

License CC BY-NC-ND 4.0

License CC BY-NC-ND 4.0

Chapter I: Immunity and normal B cell development

A. Immune response

The immune system is a complex network composed of cells, tissues and organs whose function is protection and defense the organism against the enormous number of pathogens that our organism encounters during life time and control of cellular deregulation potentially leading to tumoral transformation. Two different fundamental types of responses, linked between them, are known to compose our immunity: the innate and the adaptive immune responses which differ by their components, rapidity, specificity and potency (Marshall et al., 2018).

1. Innate immunity

Innate immune response constitutes the first line of defense, non-specific (react in the same way to all pathogens) and the most rapid response (from minutes to hours after infection). It eliminates the high number of pathogens that we encounter on a daily basis. Genetically inherited, not acquired during the life, immune innate response does not generate memory immunity in contrast to the adaptive immunity.

Innate immune response formed of four types of defensive lines: anatomic (skin and mucous membrane), physiologic (temperature, low pH, mucus and chemical mediators), endocytic and phagocytic cells (Macrophages, neutrophils and dendritic cells) and the inflammatory reaction (Marshall et al., 2018).

Pathogens that are not eliminated and succeed to cross the first lines of defense (physical and chemical barriers), are targeted by an inflammatory reaction by soluble factors (complement system and inflammatory proteins) and by cellular factors.

Complement system is defined as a biochemical cascade constituted of about 35 proteins present in the Blood. Complement contributes in pathogens detection, chemiotaxis of the phagocytic cells and pathogens lysis. Complement system activation can be accomplished via three principal pathways: the classical pathway by forming antigen-antibody complex, the alternative pathway, or the lectin pathway leading to opsonization of antigens (Ag) that facilitate the phagocytosis function, and induction of inflammatory reaction.

Cells implicated in the innate immune response are numerous and each of them fight the pathogen in non-specific way. These cells are represented in the (Figure 1) and their functions are mentioned in the text. The Dendritic cells (DC) are implicated as antigen presenting cells (APC) and play a role in phagocytosis. Mast cells implicated in allergic response by releasing

License CC BY-NC-ND 4.0

histamines, are important for wound healing producing cytokines that recruit Macrophages. In addition, the Granulocytes account for: the Neutrophils characterized by their phagocytosis function and are implicated in response to fungi and bacteria. Eosinophils defense against the parasites, bacteria and allergic reaction, and Basophils that react in the same way of Mast cells by producing histamines. Other phagocytes cells also constitute a part of innate immunity, and they are sub-divided into two main cell types: Neutrophils short-lived cells (12-15µm) with half-life from 6-8 hours and characterized by their high motility to migrate to the infection site by chemotaxis. Neutrophils are granulocytes abundant in the blood. The second type is the Macrophages that are long-lived cells (20µm) with half-life about 30 days able to eliminate bacteria and other pathogens.

The natural killer (NK) cells related to the responses Vis a Vis virus-infected cells and tumor cells. It eliminates pathogens dissemination by destroying the infected cells.

Finally, the γδ T cells able to recognize a restrict number of pathogenic motifs in their native structure through their invariant T cell receptor (TCR) for antigen. These T cell population shares with other T cells common molecular characteristics (Rearranged TCR genes) are at the interface between innate and adaptive immunity.

Failure in the innate response leads the initiation and the activation of the adaptive immunity.

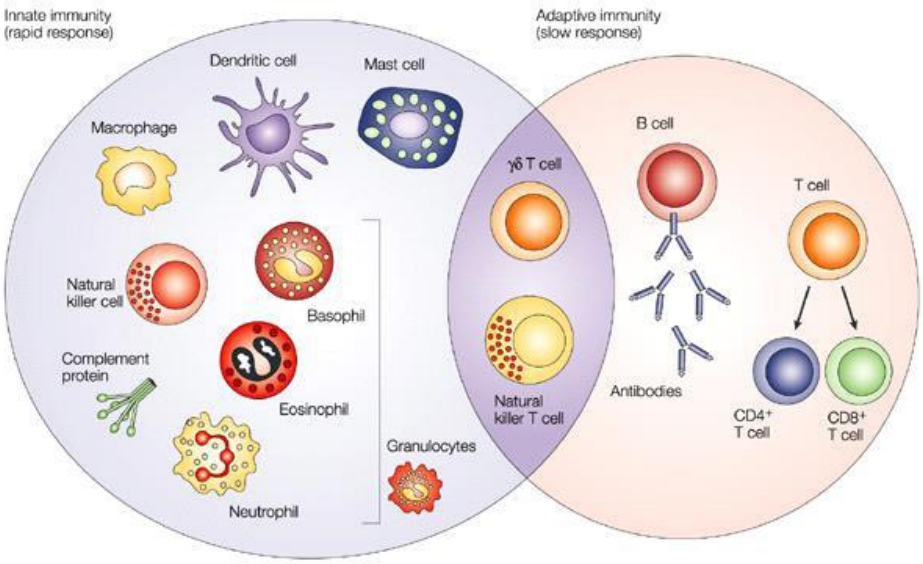

Figure 1: Innate and adaptive immunity: Implication different types of cells.
Innate immunity is constituted of phagocytic cells such as granulocytes, macrophages and dendritic cells, in addition to mast cells, and complement proteins. Adaptive immunity is composed of B cells and T cells (CD4+, CD8+) that respond in a specific way to the antigens. γδT cells and Natural Killer cells are implicated in both innate and adaptive immunity (Dranoff, 2004).

License CC BY-NC-ND 4.0

2. Adaptive immunity

Adaptive immunity constitutes the second line of defense after infection, it is not genetically determined and acquired during the life of each individual. Response generated Vis a Vis of pathogens is specific and is based on the differentiation between self-antigens and non-self-antigens.

Adaptive immune response is slower in generation of effectors able to kill or neutralize the antigen than innate response. Even this process takes more time it is more efficient, durable and generates an immune memory. Two adaptive immune responses are distinguished and well documented: the cellular immune response and the humoral immune response. Cellular immune response is characterized by the T cells (T from the thymus organ in which T cells continue their development) which, when they are activated, are able to kill and eliminate cells expressing at their surface non-self-antigen. Humoral immune response is ensured by B cells. The (B) name is attributed to these cells not referring to the bone marrow in which B cells develop in vertebrates but refers to the Bourse of Fabricius, organ in which these cells develop in birds.

In the continuing chapter, I will detail the mechanisms of development, activation and differentiation of B cells. I focus on human B cells because they constitute the center of interest in my thesis work. Moreover, it is important to mention that even the high similarities present with B cells from other species like mice, human B cells present inherent particularities.

3. B cells

B cells are key effectors of the humoral adaptive immune response. B cells are known as inflammatory regulators and effectors in the immune response by releasing antibodies and by presenting the antigen to activate T cells (Shang et al., 2020). Functional and efficient B cells are able to produce antibodies (Ab), secreted form of immunoglobulin (Ig), with high specificity and diversity that recognize wide number of foreign antigens. This function was demonstrated for the first time in 1960 (Cooper et al., 1960). Production of functional B cells is accomplished through a sequential process of differentiation, development and maturation. B cells are as all blood cells produced from hematopoietic stem cell (HSC) (Figure 2).

License CC BY-NC-ND 4.0

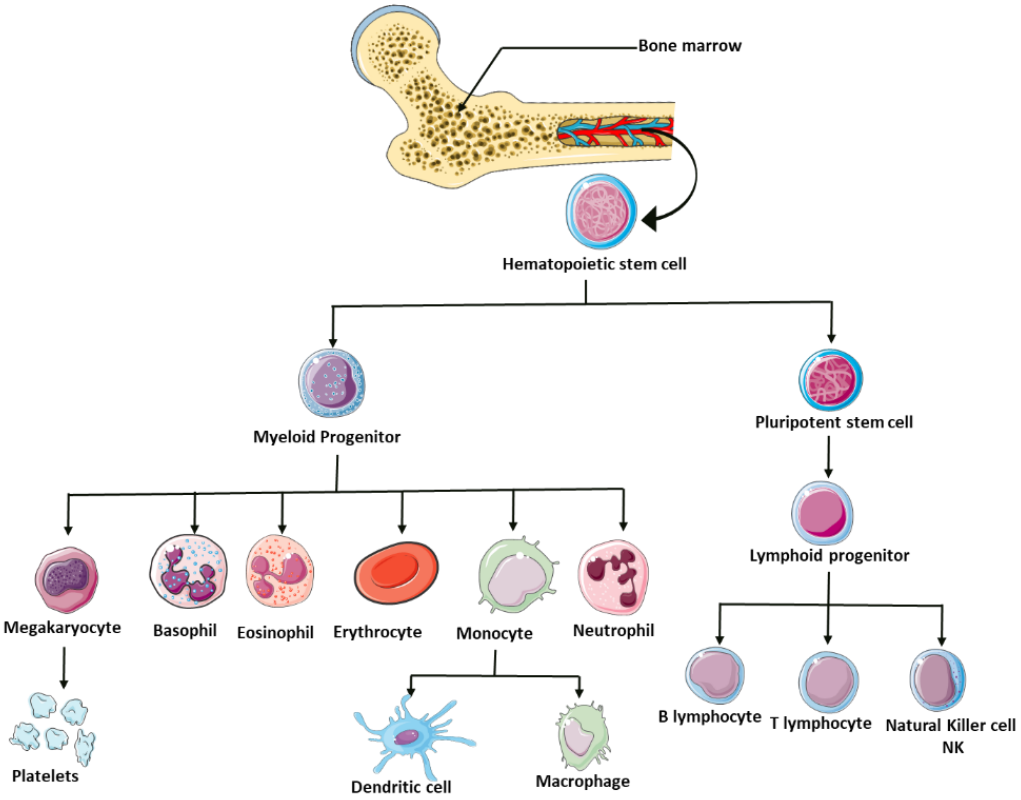

Figure 2: Origin of blood cells.
Hematopoietic stem cells give rise to all blood cells after differentiation into two progenitors. Lymphoid progenitors differentiate to the lymphatic cells like B lymphocytes, T lymphocytes and Naturel Killer cells. The myeloid progenitors can differentiate into the other subpopulations of blood cells like erythrocytes, granulocytes, etc…

Early stages of B cell development, which give rise to naïve B cells, take place in the bone marrow and the fetal liver. This process starts in the bone marrow of embryo from 12 weeks of pregnancy and continues after during all the life of persons. Early B cell development is antigen independent, as during all the steps, B cells are not exposed to foreign antigens. It is a very organized mechanism, constituted of several steps and checkpoints allowing the production non-self-reactive B cells. Briefly, in the bone marrow, Common Lymphoid progenitor (CLP) give rise to Pro-B cells, then Pre-B cells and after the immature naïve B cells. These latter exiting the bone marrow, enter into transitional (T) state characterized by the presence of three subgroups T1, T2 and T3. T1 give rise to T2 then T3 B cells, which continue their development into naïve mature B cells. These cells join the secondary lymphoid organs (SLO) such as spleen and lymph nodes through peripheral blood circulation where they undergo late B cell development.

In SLO, the majority of B cells are grouped into microstructure called follicles forming the follicular B cells (FO), these follicles are in contact with T cell rich zone, and surrounded Marginal Zone (MZ) enriched in macrophages and MZ B cells.

License CC BY-NC-ND 4.0

Late stages of B cell development, is an Ag-dependent phase, induced after interaction of naïve B cells with foreign antigens. Terminal maturation produces functional B cells: the plasma cells producing antibodies and the memory B cells.

As expression of functional Ig is a prerequisite for the normal development of B cells and their functions in immune responses, the continuing chapter describes Igs, their coding genes, their structure and their functions. After, the stages of B cell development will be detailed.

B. Immunoglobulins

1. Organization and structure of Immunoglobulin Loci

Antibodies, Ig in the secreted form, constitute the central effector of humoral immune response. Igs are glycoproteins are composed by the association of two identical Ig Light chains (IgL) encoding by the *Kappa* (□) locus or the *Lambda* (□) locus, and two identical Heavy chains (IgH) encoded by the *IgH* locus (Matsumoto, 2022). Disulfide bonds link IgH and IgL. Each light chain is composed of two domains, the variable (V_L) and one constant domain (C_L). In contrast, the heavy chain is composed of variable domain (V_H) and three or four constant domains (C_H1, C_H2, C_H3 and C_H4) according to the immunoglobulin isotype. V_H and V_L form the variable fragment (Fv) a part of the fragment antigen-binding region (Fab) (formed from V_L, V_H, C_L and C_H1). V_H and V_L both present three hypervariable complementarity-determining regions (CDR1, CDR2, and CDR3) permitting the recognizing and binding of wide number of Ag. Framework Regions with lower rate of variability called (FR1, FR2, FR3, and FR4) flank CDRs. C_H1 of the IgH is linked by a hinge to the rest of the constant region C_H2 C_H3 or C_H2 C_H3 C_H4, which constitutes the crystallized fragment of Ig (Fc). The link between C_H1 and C_H2 contribute to the Y form of immunoglobulins with the sulfhydryl linkages between the light and heavy chains (Figure 3) (Schroeder and Cavacini, 2010).

License CC BY-NC-ND 4.0

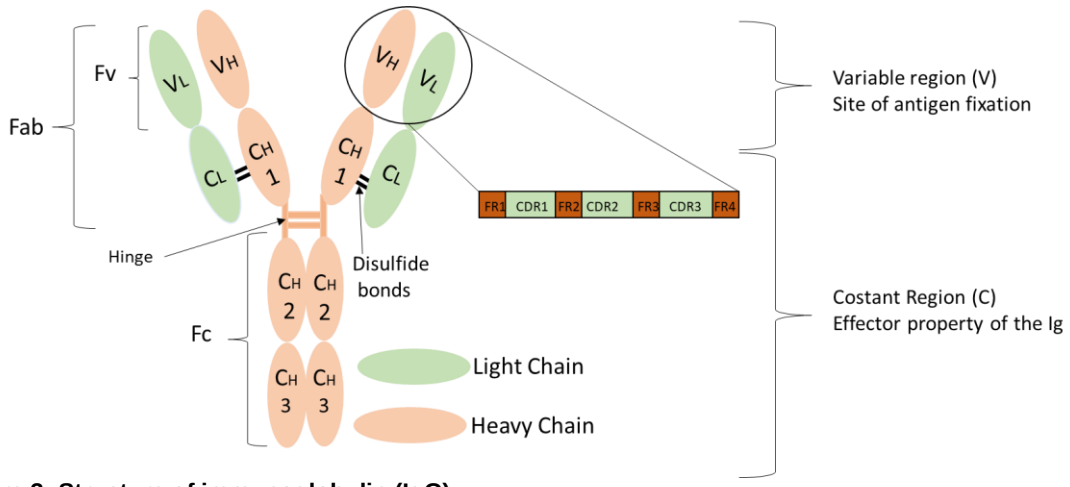

Figure 3: Structure of immunoglobulin (IgG).
Immunoglobulin is constituted of two light chains (IgL) (in green) and two heavy chains (IgH) (in orange). Variable (VL, VH) domain of Ig constitutes the site of antigen binding, it is formed by three complementarity-determining regions (CDRs) flanked by the Framework regions (FR). This part of Ig constitutes the variable fragment Fv of Fab. The constant (CL, CH) domains are implicated in the effector function of Ig. The hinge interspaces the CH1 exon 1 to the constant region (Fc). The two parts Fab and Fc are determined by the digestion analysis of immunoglobulins by capsaicin.

Immunoglobulins loci are located on three different chromosomes.

1.1. *Ig Kappa light chain* (*Igκ*) locus

The chromosome 2q11.2 encodes human immunoglobulin Kappa light chain locus (*Igκ*) (chromosome 6 in mouse) which is about 1820kb of length ("Immunoglobulin Kappa Chain - an overview | ScienceDirect Topics,"). *Igκ* consists of 76 genes Vκ with only 52 functional genes, 5 genes constitute the Jκ and one constant gene Cκ. Diversity segment (D) is not present in light chains (Figure 4A) (Townsend et al., 2016). Igκ chain is more frequent and predominant in normal serum, in human ratio of κ/λ is 1.5 to 2 (60/40), this predominance also increased in mouse while κ chain is expressed 19-fold more than λ chain (95/5).

Regulatory elements of *Igκ* locus

In human, in 5' of each functional V segment a promoter was detected containing the transcriptional initiating site implicated in the recruitment of the transcriptional machinery (Lenhard, Sandelin, & Carninci, 2012). Regulation of Ig gene expression in B cells is not achieved only due to the promoter activity but also due to the presence of enhancers and insulators.

Igκ locus is characterized by the presence of three enhancers located differently on the locus and highly conserved in mammals.

License CC BY-NC-ND 4.0

Between the Jk-Ck we identify the intronic enhancer element (iEκ), an important factor for B cell development regulation, presenting a similarity with the Eμ presents on the *IgH* locus concerning the placement and the stage specific function. These conclusions were obtained from studies replacing the iEk by an Eμ in mice and resulting in early rearrangement of the *κ* locus during the Pro-B cells. Eμ, as described below, promotes the rearrangement on the *IgH* at this B cell stage. iEκ was demonstrated to be important in the mechanism of demethylation of the DNA on one IgK allele and conducting the allelic exclusion (Inlay et al., 2002).

Another enhancer was also identified in mouse *Igκ* locus located on the 3' of Ck called 3'Ek. 3'Eκ activity is specific to B cells in which it regulates the somatic hypermutation (SHM) and then the maturation of Ig affinity (Odegard & Schatz, 2006). The 3'Eκ element is implicated in the allelic exclusion (Zhou, Xiang, Ding, & Garrard, 2012) and directs the nuclear positions of *Igκ* and *IgH* loci (Hewitt et al., 2008). Deletion of both iEk and 3'Ek abolishes the rearrangement of the *Igκ* locus (Inlay et al., 2002) suggesting an essential function of theses both elements in promoting the Igκ rearrangement.

A third enhancer was discovered on the mouse *Igκ* locus and was characterized, called distal enhancer dEκ (Liu et al., 2002; Xiang and Garrad., 2008). dEk was shown to be implicated in the regulation of rearranged Igκ transcription (Zhou et al., 2010). Additional enhancer was identified called Hypersensitive Sequence (HS10) located 40 kb before the iEκ and seems indispensable for the high level of *Igκ* expression in plasma cells (Zhou et al., 2012).

1.2. *Ig light chain lambda* (*Igλ*) locus

The chromosome 22q11.2 encodes the human immunoglobulin Lambda light chain (Igλ) locus (Mikocziova et al., 2021) of 1050kb in length. *Igλ* consist of 30 Variable genes (V_λ), 7 joining genes (J_λ) and 7 constant genes (C_λ). The J segments precede each constant genes and form $J_\lambda C_\lambda 1$ to $J_\lambda C_\lambda 7$. It is important to mention here that only four constant genes of seven are functional (1-3 and 7) leading to four subtypes of Lambda light chain λ1, λ2, λ3 and λ7. The $C_\lambda 4$, $C_\lambda 5$ $C_\lambda 6$ are considered as pseudogenes (Figure 4B) (Townsend et al., 2016).

Cis regulatory elements of *Igλ* locus

Two important transcriptional enhancers are identified on the *Igλ* locus, the Eλ3-1 and Eλ2-4 characterized by their 90% of homology. Eλ3-1 is located approximately 35Kb in the 3' of Cλ3 gene and the Eλ2-4 is distant approximately from 15.5 Kb to the 3' of Cλ4 gene (Hagman et al., 1990). It was demonstrated that Eλ3-1 enhancer is implicated in the restriction of rearrangement mechanism in specific stage of B cell development in addition to his function in regulation of the recombination between V_λ and Jλ genes (Haque et al., 2013). Additionally, four hypersensitive regions from (HS1 to HS4) were shown to be located downstream of JCλ1.

License CC BY-NC-ND 4.0

HS1 was demonstrated to be important in Vλ-Jλ recombination and the regulation of rearrangement during specific stage rearrangement (Haque et al., 2013).

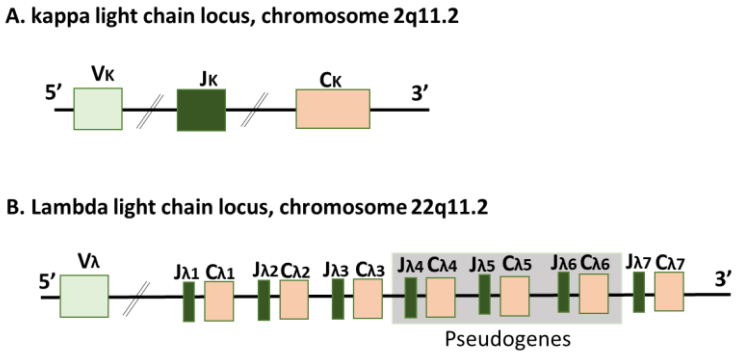

Figure 4: Organization of human immunoglobulin light chains loci.
A. *Igκ* is encoded by the chromosome 2q11.2 in human. From 5' to 3', it is composed of variable segment (Vk) Joining segments (Jk) and one constant gene (Ck). **B.** *Igλ* is encoded by the chromosome 22q11.2 in human, from 5' to 3' it is composed of Variable segments (Vλ), 7 constant genes (Cλ1, Cλ7) preceded by 7 joining segments (Jλ1, Jλ7). Cλ4, Cλ5, Cλ6 are pseudogenes.

1.3. *Ig Heavy chain* (*IgH*) locus

Immunoglobulin heavy chain (IgH) is encoded by chromosome 14q32.33 in human (chromosome 6 in mouse) and is about 1250kb in length. The 5' of the *IgH* locus is localized near to the telomere region of chromosome 14, this localization was demonstrated by studying translocations in leukemia and lymphomas (Lefranc et al., 2005). The constant segment is localized near the centromere region. *IgH* locus is composed from the 5' (telomere region) to 3' (centromere region) of different principal segments: Variable (V), Diversity (D), Joining (J), and Constant (C). Organization of VDJ segments is similar between species (human, mouse) in contrast to the species dependency of the constant region (Birshtein, 2014). Variable (IgHV) segments containing >100 IgHV genes (38-46 functional genes), Diversity segments consist of approximately 27 IgHD genes, Joining segments IgHJ consist of 6 genes(For review (Khatri et al., 2021)). These segments are rearranged during the mechanism of V (D) J recombination in order to produce a functional immunoglobulin. The 5' part of variable regionis called distal and the 3' part is called proximal. V (D) J recombination is detailed after in the continuity of this chapter.

The constant segments (IgHC) formed of 11 IgHC genes, 9 of them are functional and encode for the different isotypes and subtypes of Immunoglobulins Cμ (IgM), Cδ (IgD), Cγ3 (IgG3), Cγ1 (IgG1), Cα1 (IgA1), Cγ2 (IgG2), Cγ4 (IgG4), Cε (IgE), Cα2 (IgA2) and two pseudogenes Cψγ and Cψε ("IMGT Repertoire (IG and TR) 1. Locus and genes,").

License CC BY-NC-ND 4.0

In human, the *IgH* locus upon the evolution is submitted to different types of translocation and duplication resulting in the presence of two clusters of constant segments. Cluster 1 consists of Cμ, Cδ, Cγ3, Cγ1, Cψε and Cα1. The second cluster consists of Cψγ, Cγ2, Cγ4, Cε, and Cα2. Each constant gene is encoded by three exons (C_H1, C_H2, and C_H3) for IgG, IgA and IgD isotypes and four exons (C_H1, C_H2, C_H3, C_H4) for IgE and IgM. C_H3 of (IgG, IgA and IgD) and C_H4 of (IgE, IgM) contain a specific region (secretory exon) that can be conserved or eliminated by alternative splicing to determine the secreted form of each antibody. In addition to the secretory exon, there are two specific exons M1, M2 that encode the intracytoplasmic and transmembrane hinge and determine the membrane form of immunoglobulins (Lefranc et al., 2009). Each C_H gene is preceded by a highly repetitive region called switch region S (Sμ, Sγ, Sε and Sα) excepting the Cδ (IgD) which preceded in mice *IgH* locus by pseudo switch region ψδ. S regions are composed of repeated motifs of pentamers: GGGGT, GGGCT and GAGCT, with a variable length from 1 to 12 kb, targeted by the Activation Induced-cytidine Deaminase (AID) during CSR (Shinkura et al., 2003) (Figure 5). These S regions are preceded by promoters initiating the transcription (Iμ, Iγ, Iε and Iα) leading to the accessibility of the locus required for the locus recombination.

1.4. Cis Regulatory elements of *IgH* locus

The Regulation of *IgH* locus transcription and accessibility is regulated by different elements including cis regulatory elements. Two major cis-regulatory elements are identified on *IgH* Locus, the Eμ (5' intronic enhancer), important to the V (D) J recombination mechanism and during early stages of B cell development, and the 3'Regulatory Region (3'RR). In addition, other elements present on the variable region: the promoter PDQ52 (in mice), and in the 5' of the locus, 30kb from JH segments, DNaseI hypersensitive sites (5'HS1, 5'HS2, 5'HS3a and 5'HS3b) shown to be implicated in the regulation of B cell development (Pawlitzky et al., 2006).

The first discovered enhancer on *IgH* locus is the Eμ element. Eμ is an intronic enhancer of 1Kb and located between the junction segments (J_H) and Switch μ region (Sμ). Eμ is composed of two Matrix Association Region (MAR) which flank the central core of Eμ (cEμ) (Figure 5) (Perlot and Alt, 2008).

Human *IgH* locus due to the duplication of the constant part contains two 3' regulatory regions, 3'RR1 and 3'RR2, located downstream of Cα1 and Cα2 respectively. 3'RR1 and 3'RR2 are composed of super core enhancers segments hypersensitive (HS) to DNase I. Each 3'RR we can identify three HS regions so-called HS3, HS1.2 and HS4 respectively from 5' to 3' (L madisen et al., 1994). An inverted repeat sequence (IRIS) as well flanks HS1.2 (Sepulveda et al., 2005). Sequences with high homology with S regions containing a repeated sequence are detected in both 3'RR regions called like switch regions (LS). In the 3'RR2 we can identify from

License CC BY-NC-ND 4.0

(LS1-LS6) (Péron et al., 2012b) in contrast in 3'RR1(LS1-LS5) with small difference in the repartition (Figure 5). In mice, *IgH* locus is also characterized by the presence of three insulators in the 3', HS5, HS6 and HS7 (Garrett et al., 2005).

Recently, novel enhancers were also identified on *IgH* locus called (NEs). NE1 was shown to have a crucial function in controlling the chromatin conformation to promote the transcription of VH region, which is required during the mechanism of V (D) J recombination (Bhat et al., 2022). The other NEs need to be characterized and studied.

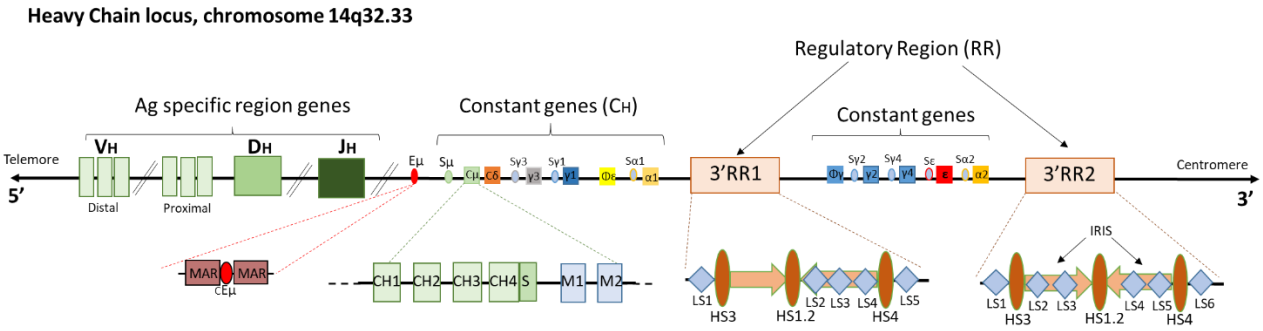

Figure 5: Organization of human immunoglobulin heavy chain locus.
IgH locus is encoded by the chromosome 14q32.33 in human, 5' is telomeric, 3' is centromeric. Variable (V) segments are divided in distal (5') and proximal (3') regions represented in light green. Diversity (D) genes are in green and the Joining segments (JH) are in dark green. The enhancer Eμ, in red, is composed of core Eμ flanked by matrix association regions (MAR). Switch regions (Sμ, Sγ, Sα, Sε) precede each constant gene (Cμ, Cγ, Cα, Cε) respectively, except Cδ. Each constant gene is composed of 3 or 4 exons (CH1, CH2, CH3 or CH4) determining the Ig isotype. IgM has 4 exons. The secretory exon (S) after CH3 or CH4 allow the expression of the secreted form of immunoglobulin. Two membrane exons are present (M1, M2) in blue, in the constant gene and are responsible for the transmembrane from of Immunoglobulins. Human heavy chain locus presents a duplication of the constant region and of the 3'regulatory region (3'RR). 3'RR1 and 3'RR2 present some differences; in general, they are composed in human of 3 DNAse1 hypersensitive regions (HS3, HS1.2, and HS4) represented in dark orange. These HS are flanked by inverted repeat sequence (IRIS) represented in light orange arrows. In 3'RR1 we can detect 5 like switch regions (LS1, LS5) with small differences in the repartition of those present in the 3'RR2 (LS1,6).

1.5. Functions of cis regulatory elements of *IgH* locus

Due to the high similarity of *IgH* locus between human and mice, in the literature mice are used as model to decipher the function of the different elements of *IgH* locus.

Functions of the 3'RR

The activity of 3'RR is lineage and stage specific and is initiated in the pre-B cell stage contributing in the regulation of the pre-BCR expression (Guglielmi et al., 2003). During the V D J recombination it was shown that 3'RR is dispensable and the deletion of the whole 3'rr in mouse has no impact on the efficiency of th e rearrangement (Rouaud et al., 2012). In activated B cells, 3'RR contributes to the *IgH* locus transcription during Class Switch Recombination

License CC BY-NC-ND 4.0

(CSR) and SHM (For review (Saintamand et al., 2017)). The regulatory region in 3' of the *IgH* locus is known to be the most important element regulating the CSR (Saintamand et al., 2015). It was demonstrated in mouse that the lack of the totality of 3'RR on *IgH* locus conduct to severe deficiency in CSR in all immunoglobulin isotypes and abrogation in the SHM (Pinaud et al., 2011; Vincent-Fabert et al., 2010). Redundancy in the function of the different HS elements of 3'RR in mouse was shown. Deletion of the HS3b present normal CSR, proliferation and transcription (Bébin et al., 2010).

The 3'RR is characterized by the presence of different binding sites of activator or repressor transcription factors acting in trans (For review (Pinaud et al., 2011)). As an example, in murine *IgH* locus, HS1.2 is activated by the binding of the OCT-2, OCA-B (transcription factors specific to B cell) to their oct domain located on HS1.2 which promotes cell activation and their inhibition highly affect the differentiation of B cells (Tang and Sharp, 1999).

Another binding site also present on HS1.2 is specific to NF-κB protein, which is characterized by two activities regarding the stage of development. Binding of NF-κB is repressor during the early stages of B cells development. In contrast, NF-κB has an activator activity during late stages of B cell development (Michaelson et al., 1996). HS1.2 is characterized by the presence of the lineage factor binding site for Pax-5. In resting B cells, Pax-5 binds on its site and interacts with NF-κB to repress HS1.2. In contrast, this activity is inverted in plasma cells which do not express Pax-5. NF-κB play an activator function of HS1.2 and leads to the synthesis of IgH (Neurath et al., 1994).

In activated mature B cells, the 3'RR is enriched by epigenetic marks such as H3K27ac related to the activation of transcription, H3K4me2 and H3K4me1 implicated in the chromatin remodeling to the euchromatin form and the activation of transcription (Whyte et al., 2013). In contrast to the limited impact of 3'RR during the early stages of B cell development, in plasma cells the 3'RR has an important function in the physiologic activity of plasma cells in Ab secretion. It was shown that complete deletion of 3'RR in mouse affect importantly the secreted Abs (Vincent-Fabert et al., 2010).

Functions of cEμ

Eμ activity is specific of B cell lineage and is implicated during the early stages of B cell development especially in the pro-B cells (Inlay et al., 2006). The cEμ is characterized by the presence of different binding sites of activator and inhibitor transcription factors. In non-B cells Eμ is inactivated by the binding of the EZB protein. In contrast, in B cells, activation of Eμ is correlated to the fixation of activator protein E2A protein on its specific binding site on Eμ during the V (D) J mechanism (Romanow et al., 2000). Eμ maintains the stability of sequential

License CC BY-NC-ND 4.0

V (D) J recombination of heavy chain locus regulating the DNA accessibility to recombinase enzymes by the chromatin remodeling. Also, Eμ controls the V (D) J recombination of *IgH* prior those of IgL as shown by insertion of Eμ in the Kappa locus resulting in premature VκJκ recombination at the pre-B cell stage rather than in pro-B cell stage.

Eμ is required for the *IgH* locus transcription activation and its deletion block the DH-JH recombination. Studies demonstrated that the transcription of Eμ and the promoter PDQ52 earlier than the D-JH recombination, suggesting a function of Eμ in the activation of the germline transcription of DH and JH. This was demonstrated by the Eμ deletion of which has no effect on VH germline transcription (Afshar et al 2006., Bolland et al., 2007).

V (D) J recombination requires contraction of the locus and loop formation in cis of loci of both heavy and light chains allow to bring the recombination acceptor and donor segments close each other. The distance between V_H and D_H is about 2.5MB. In mice, the cEμ is able to interact first with the promoter PDQ52 and then with the Intergenic Control Region 1 (IGCR1) located between the V and D segments, to regulate the sequential mechanism of V (D) J recombination. The first loop limits the accessibility of VH in the early Pro-B cell stage to allow only the D_H-J_H. Then a second loop formed between cEμ and IGCR1 allows the initiation of the V-DJ_H recombination and the recruitment of the RAG enzyme already recruited to the first loop (Guo et al., 2011). During the late stage of B cell development, it seems that Eμ is dispensable for CSR, it was shown that deletion of Eμ in mouse model does not affect the switch upon stimulation (Saintamand et al., 2017). In addition, the Eμ deletion did not affect the transcriptional enhancer epigenetic marks enrichment such as H3K4me3 on the *IgH* locus (Saintamand et al., 2017).

In conclusion, all of these studies suggest that Eμ regulates the development of B cells, by its action on V (D) J rearrangements as well as by the expression of heavy chain of Ig, from the pro-B stage to the immature B stage (Marquet et al., 2014; Peng and Eckhardt, 2013).

Functions of MARs element:

The precise function of MARs is still not well defined. MARs are formed of small DNA sequences enriched by A/T or G/C. It is about 200pb to 1Kb in length. Two types of MARs are defined, the constitutive and the facultative. The later one flanks the Eμ core. The constitutive MARs are permanently attached to the matrix, and the facultative MARs are attached in a reversible way in response to tissue specific nuclear factors and they are repressed in non-B cells. These MARs activate the transcription and increased the accessibility of the linked regions in B cells (Kim et al., 2017). MARs activation is due to the fixation of B cell regulator

License CC BY-NC-ND 4.0

factor (Bright) that regulates the transcription of *IgH* locus in differentiated B cells (Lin et al., 2007). MARs are also implicated in SHM of *IgH* locus and are not necessary to the V (D) J recombination (Marquet et al., 2014).

2. Immunoglobulins Isotypes

Antigen encounter conducts to the expression of different classes or isotypes of immunoglobulin (IgM, IgD, IgG, IgA and IgE). They are encoded from different constant genes of the *IgH* locus and present different biological functions, localization, molecular weight, half-life time, structure. These isotypes can be present in transmembrane or secreted form except IgD, present only in the transmembrane form. IgD is expressed on immature and mature B cell surface with the co-expression with IgM.

IgM constitute the first expressed Ig on B cells. During the B cell development in bone marrow μ chains are synthetized (IgM) to constitute the BCR. IgM are also the first antibodies produced during the primary immune response. IgM secretion in pentameric form allows to strongly activate the classical pathway of the complement.

IgG are the major Ig present in the serum, divided into four subclasses IgG1, IgG2, IgG3 and IgG4 (IgG1, IgG2a, IgG2b, IgG3 in mice). IgG subclasses present some differences concerning the type of recognized Ag. For example, IgG1 interact with parasite and virus whereas IgG3 are mainly involved in reactions directed against bacteria through complement recruitment. IgG can reach the placenta and join the embryo blood.

IgA are secreted in monomeric or dimeric, preponderantly, forms especially in the secretion mucosa, saliva or glands. IgA constitute the protective barrier against pathogens entry in surface with direct contact with the outside of the organisms (for review (Johansen et al., 2000).

Pentameric structure of IgM or the dimeric of IgA is due to the presence of polypeptide chain (J) of 15kDa.

Finally, IgE is produced after allergic reaction and parasites infection (Brezski and Georgiou, 2016). During the hypersensitivity reaction, IgE ligate the allergic molecules and bind to FcεRI present on the surface of mast cells. This leads to the production of histamine by these cells (Galli and Tsai, 2012).

Some of the characteristics of each isotype of immunoglobulins are summarized in the (Table 1).

License CC BY-NC-ND 4.0

Table 1: Characteristics of immunoglobulin isotypes.

	IgM Pentamer	IgD Monomer	IgG Monomer	IgA Monomer Dimer	IgE Monomer
Structure	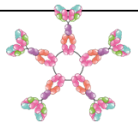			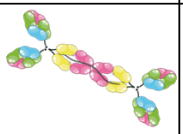	
Heavy chain	μ	δ	γ	α	ε
Antigen binding site	10	2	2	4	2
Isotypes	1	1	4 (IgG1, IgG2, IgG3, IgG4)	2 (IgA1, IgA2)	1
Molecular weight (KDa)	900	185	150	160	200
Biological function	*Antigen receptor in naives B cells *Complement activation	Antigen receptor in naives B cells	Secondary Immune response	Mucosal immunity	Hyper sensibility and parasital immunity
Localisation	Intravascular compartment		Plasma	Serum and mucosal secretion	Serum

3. Production of functional immunoglobulins

Immunoglobulin is a constituent of the BCR expressed on the surface of B cells and implicated in the signaling of survival, proliferation and differentiation of these cells. The *Ig* loci when in their germline conformation are nonfunctional and do not allow the expression of Ig and BCR. To produce a specific, functional and diversified BCR on the B cell surface, these loci occur several mechanisms during the different stages of B cell development. During the early stages, the mechanism of V (D) J recombination takes place in order to generate functional variable regions in the light and heavy chains. During the late stages of development, in SLO, two mechanisms occur, the SHM contributing to the affinity maturation and the CSR that diversifies the Ig isotypes (Figure 6). The molecular mechanism of V (D) J recombination, SHM and CSR is detailed after in this chapter.

License CC BY-NC-ND 4.0

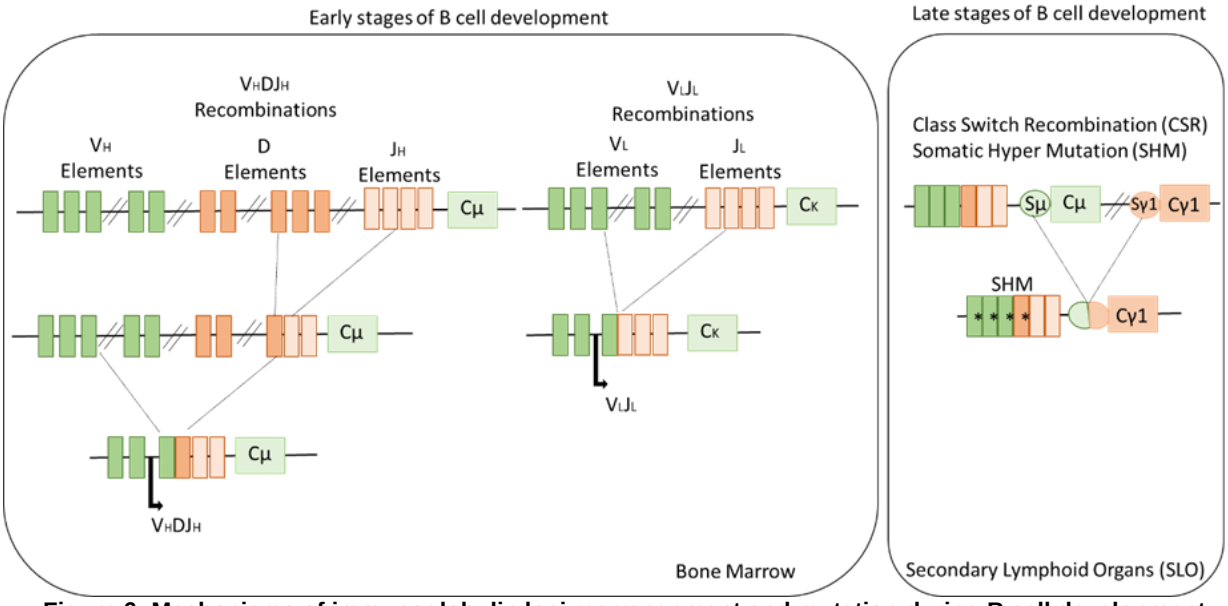

Figure 6: Mechanisms of immunoglobulin loci rearrangement and mutation during B cell development. During early stages of B cell development in the bone marrow independently of antigen encounter, the V(D)J rearrangements (VHDJH and VLJL) take place to produce a functional Ig. After activation induced after Ag binding. During the late stages of B cell development in the SLO, the Ig loci undergo the SHM in the variable region (IgH and IgL) and CSR (IgH) in order to produce specific isotypes with high affinity against the antigen.

3.1. Ig diversification: Antigen Independent stage

3.1.1. V (D) J Recombination

V (D) J mechanism occurs in B cells during the early stage of development in bone marrow. V (D) J mechanism generate functional coding *Ig* loci allowing production of functional Ig with diversified repertoire allowing the recognition of wide number of Ag. More than three million specific functional antibodies are produced and constitute the arm of the immune system (Khatri et al., 2021).

V (D) J recombination is a random mechanism assembling V, D (for IgH) and J segments. It is an ordered mechanism: it occurs on the *IgH* locus before the *IgL* locus. It occurs in sequential way with D-J recombination and then V to the recombined DJ genes (Schatz and Ji, 2011). During the D_H-J_H rearrangement, a random segment of D is assembled with one J exon. D_H-J_H occurs on both alleles to optimize the choice of functional DJ production. The second step is the recombination between functional D_H-J_H and the V_H segments on one allele, the second allele is submitted to allelic exclusion (Jung et al., 2006).

To ensure this mechanism, studies demonstrate the presence of specific DNA segments highly conserved called Recombination Signal Sequences (RSS). RSS define the specific site

License CC BY-NC-ND 4.0

of recombination (Khatri et al., 2021) (Figure 7). On the light chain the V J recombination occur in one step due to the absence of the D segments on these loci (*Igκ, Igλ*).

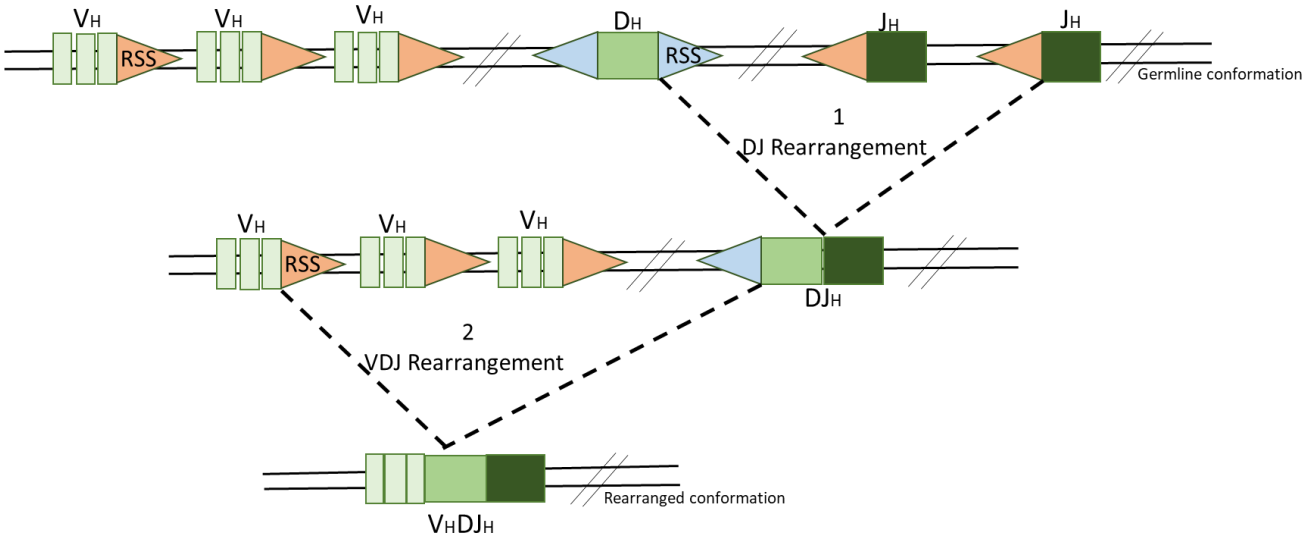

Figure 7: Schema of V (D) J recombination mechanism.
V (D) J recombinations are sequential processes occurring first in the heavy chain locus between the diversity and the joining segments D_H-J_H and then between the variable and the already rearranged segments DJ_H. The recombination signal sequence (RSS) present in the 3'of the variable genes and 5' of joining genes are represented in orange, RSS flanking the diversity segments are represented in blue. RSS are crucial in the mechanism of V (D) J recombination.

3.1.2. Recombination Signal Sequences (RSS)

RSS segments are present on the variable regions of the *IgH* and *IgL* loci. RSS are located immediately downstream (3') to the V segments, upstream (5') and downstream (3') of D segments on the *IgH* locus, and upstream (5') of J genes. RSS are composed from two highly conserved fragments, an heptamer (5'-CACAGTG-3') and a nonamer (5'-ACAAAAACC-3'), spaced by a linker of 12 or 23 nucleotides (nt) (Figure 7). The heptamer is known to be essential for the recombination mechanism especially at the initiation steps. The first three nucleotides are the most highly conserved part compared to the rest of the sequence. The RSS organization with the nonamer, the linker and the heptamer, contributes to the sequential and ordered V (D) J recombination mechanism. Recombination cannot occur between two RSS had the same nucleotide number in the spacer. The rule 12/23 is a crucial key for the initiation of the V (D) J mechanism. More precisely, in the *IgH* locus, the spacer in RSS of V and J regions is 23 nt in length, in contrast spacer of RSS in D segments is formed of 12nt. In kappa light chain, spacer of RSS at variable genes is constituted by 12 nt and 23nt in the J segments. This is inverted in the lambda light chain (Figure 8). Additionally, the Nonamer and heptamer orientation is not conserved in all the RSS of the locus, this orientation can be inverted according to the flanked region.

License CC BY-NC-ND 4.0

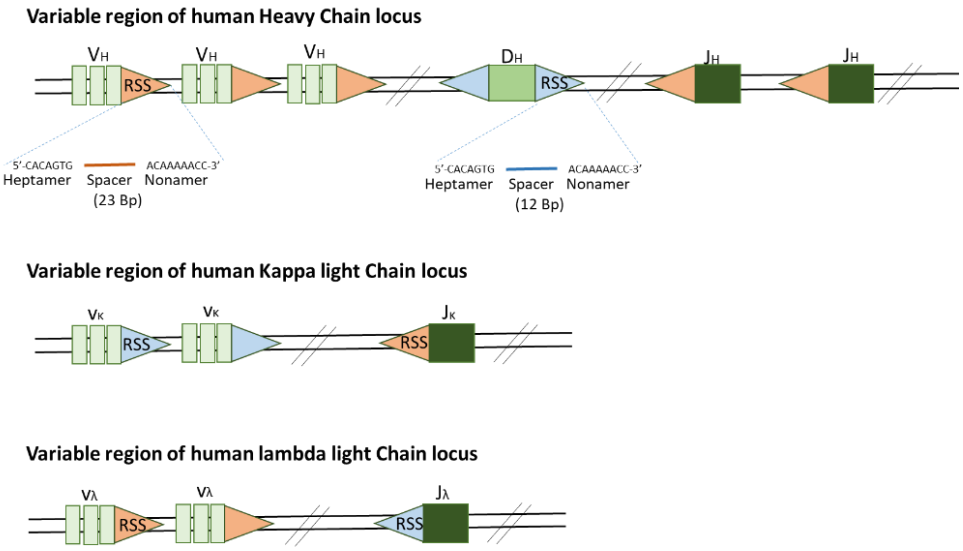

Figure 8: Organization of Recombination Signal Sequence (RSS) on *Ig* loci.
RSS are important structures for the initiation of the VDJ recombination. RSS consist of a conserved sequence of 7 nucleotide (heptamer), and a sequence of 9 nucleotides (nonamer) interspaced by 12 or 23 nt.The V(D)J recombination respect the rule 12/23. RSS with a spacer of 23 nucleotide are represented in orange color and RSS with 12 nucleotides are in blue color.

3.1.3. RAG1/2 proteins

Recombination Activating-genes 1 and 2 (RAG1/2), are proteins specific of lymphoid tissue. RAG1 protein presents a core domain crucial for the recognition of the nonamer of RSS regions, the non-core domain is more implicated in the regulation function. In the literature, RAG1 is more established than RAG2. RAG2 is implicated in the activation of the RAG1 facilitating its binding on the specific DNA site (Chi et al., 2020). RAG enzymes are specifically expressed during some stages of B cell development. Expression of these enzymes can be regulated by several factors implicated in the B cell lineage commitment i.e. E2A, IKaros, Pax-5 and FOXO1 proteins. Factors regulating RAG expression in B cells are different from those regulating RAG expression in T cells (Chen et al., 2011). These proteins positively regulate RAG1/2 expression during the light chain rearrangement in early B cell development. In contrast, these same factors negatively regulate RAG1 expression after functional Pre-BCR production (Timblin and Schlissel, 2013, p. 1).

3.1.4. Steps of V (D) J recombination

Generation of double strand breaks

Heterotetrameric RAG1/2 recombinase enzyme, with the High Mobility Group Box proteins (HMGB1 or HMGB2), creates DNA single strand cleavage between the 5' of the RSS heptamer and the flanked region. Both HMG1A and HMG1B are crucial to generate *in vivo* the DNA

License CC BY-NC-ND 4.0

break and they act as RAG2 cofactors (Vant gent et al., 1994). The production of a free 3'-hydroxyl end, in the presence of Mg^{2+}, induces a transesterification reaction leading to the formation of a DNA double strand break (DSB) harboring hairpin structure at the coding segments. The RSS end and the DNA segment located in between the targeted RSS are released. Accessory molecules are recruited and contribute to the formation of post cleavage complex and then process and repair double strand breaks (Figure 9) (For review (Chi et al., 2020)). At this point, single-stranded DNA-dependent 3'to 5'ATP dependent helicase complex (Ku70-ku80) and the phosphorylated DNA-PKcs recruit the Artemis to the DNA DSB site. Artemis processes the coding DNA end by through endonuclease activity to open the hairpin and generates incompatible overhangs (Goodarzi et al., 2006; Weterings et al., 2009). In addition, polymerases (Polμ, λ) and Terminal deoxynucleotidyl transferase (TdT) are recruited to the DNA ends. This recruitment requires the presence of Ku80. TdT adds nucleotides in a non-templated way, to the coding end region. TdT is expressed only in early stages of B cell development during V (D) J recombination of heavy and light chains of Ig.

Repair of the DNA breaks

Coding segment (hairpin) is repaired by the classical non-homologous end joining (NHEJ) DNA repair pathway. The first step of DNA repair by NHEJ is the recruitment of the Ku70/Ku80 of DNA-PKCs to the DNA ends. Ku complex provides DNA extremity protection from degradation and recruits the downstream molecules of the NHEJ pathway. Ligation of processed ends is ensured by the ligase IV (LIGIV) and his cofactor XRCC4/XLF. During the V (D) J recombination, the coding joints are conserved on the chromosome, in contrast, segment between two recombined segments is excised as a signal region. Repair of the signal ends is directly ensured by the activity of LIGIV and XRCC4, which bind the blunt end (Figure 9) (Ma et al., 2002).

License CC BY-NC-ND 4.0

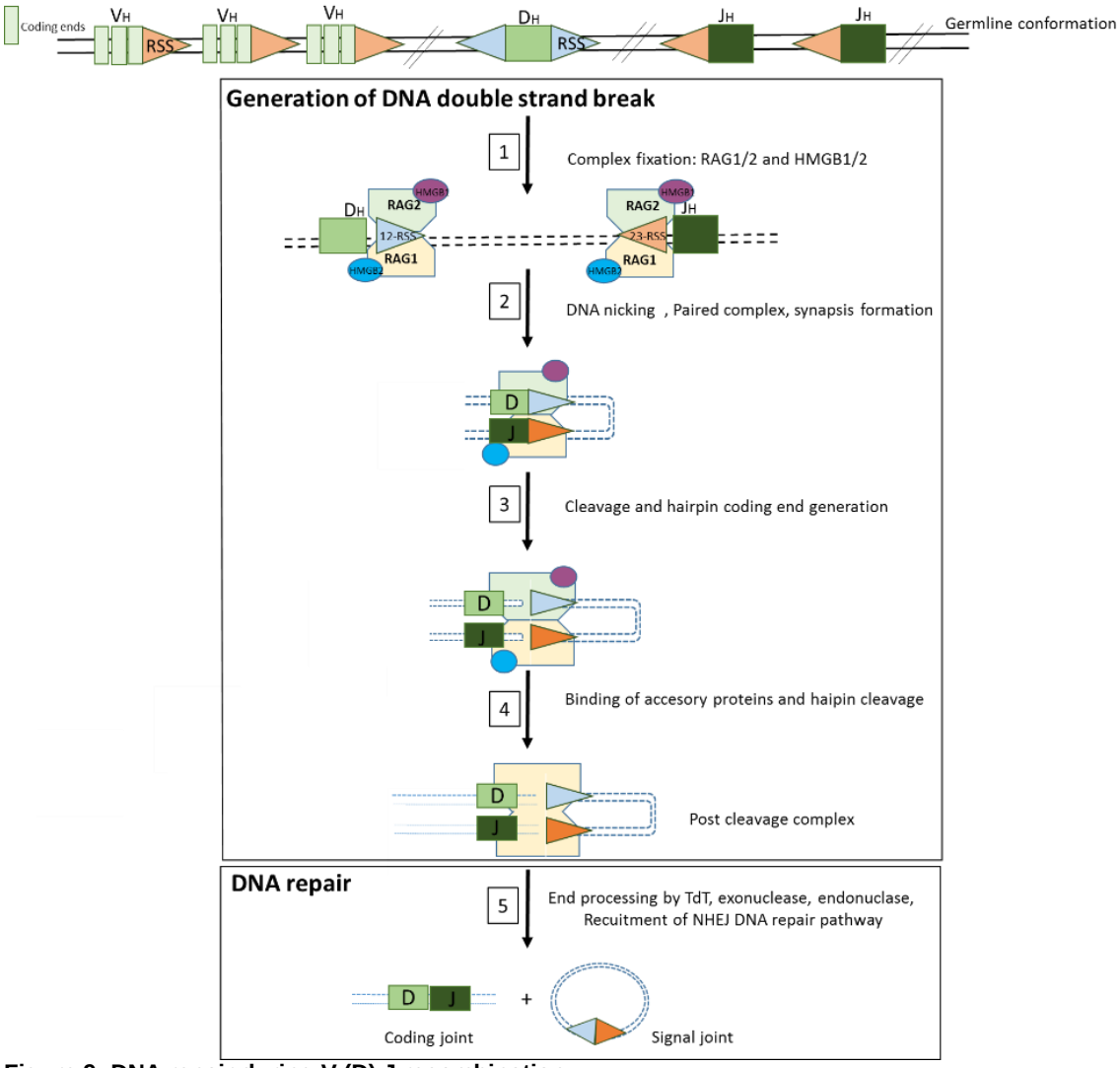

Figure 9: DNA repair during V (D) J recombination.
The mechanism of VDJ recombination is divided into two steps: generation of DNA double strand breaks and DNA repair phase. The first step is initiated by the recruitment of RAG1/2 proteins and their cofactors to the RSS regions to generate the synapse, and results in the generation of double strand breaks. During the second step, the end of breaks is processed by TdT enzyme, exonuclease and endonuclease polymerase leading to the recruitment of NHEJ DNA repair pathway. At the end, a coding joint is generated in the variable segments and the signal joint is excised as an episomal DNA.

Different points are known to regulate this mechanism, concerning the activity of RAG1/2, and the chromatin state (conformation, epigenetic marks). Pro-B cells are characterized by the accessibility of the *IgH* locus, by the abundance of H3K4me3 and H3K9ac, known as active forms of histone, on RSS region facilitating the binding of RAG enzyme making chromatin accessible to of V (D) J rearrangement. In contrast, binding of RAG to RSS can be negatively regulated by other epigenetic marks such as H4K20me3 and H3K9me3. These marks contribute to the heterochromatin structure, the inactive form of the chromatin (Kudithipudi et al., 2017). Additionally, cell cycle phases can regulate the V (D) J mechanism by regulating the level of RAG expression, more precisely the RAG1/2 are expressed only during G0-G1 cell

License CC BY-NC-ND 4.0

phases (Galloway et al., 2016). Furthermore, the regulatory elements present on the *Ig* loci contribute also to the regulation of the V D J mechanism (See section 1.5 Functions of cis regulatory element of the *IgH* locus). Briefly, these elements contribute to the loop formation on the locus during the V (D) J recombination.

3.2. Ig diversification: antigen dependent phase

Antigen encounter with naïve B cells induces their terminal maturation in the germinal center of SLO. Two different mechanism occur, SHM and CSR, leading to the differentiation of B cells into memory B cells and plasma cells (antibody secreting cells).

SHM proceed to the introduction of point mutations on the variable region of the *IgH* as well of the *IgL*. These mutations can result in affinity maturation of Ig. CSR leads to the diversification of Ig isotypes from IgM to IgG, IgA and IgE in specific response to the antigen. This mechanism occurs between the Sμ and one Sx (Switch region preceding the different CH). SHM and CSR depend on the activity of Activation induced cytidine deaminase (AID) the key mutator enzyme during the late B cell differentiation in adaptive immunity (Leeman-Neill et al., 2018).

3.2.1. Activation induced cytidine deaminase (AID)

AID is a small protein about 198 amino acid (26kDa) encoded by *AICDA* gene located on the chromosome 12 in human (chromosome 6 in mouse). AID is a part of the APOBEC family (Apolipoprotein B RNA editing catalytic component), accounting for 12 proteins, known by their functions as RNA-editing enzymes, a subgroup of a zinc-dependent deaminase superfamily. Different domains characterize the AID protein: the nuclear localization signal (NLS) in the N-terminal region, a catalytic domain (APOBEC-like) and the nuclear export signal (NES) in the C-terminal region. Due to the similarities with the APOBEC family, AID was first considered to target the RNA and to participate in RNA editing (For review (Hongo et al. 2002)). The absence of clear demonstration on this activity, in addition to several studies showing that AID targets specifically single strand DNA. Thus, AID is considered to target the DNA and not the RNA but till now this subject is still not definitely assumed. AID is implicated during SHM and CSR by his deaminase activity that deaminates and converts cytosine ‘C’ to uracil ‘U’ creating a mismatch U:G. This mismatch is recognized by the mechanism of base excision repair (BER) and mismatch repair (MMR) (Zan and Casali, 2013). AID enzyme was detected in germinal centers in SLO, in *in vitro* stimulated cells (Muramatsu et al., 1999) and, at a lower level, during the central tolerance in bone marrow (Kuraoka et al ., 2011). Also, AID is aberrantly expressed in malignant cells such as breast cancer cells, leukemic cells in Chronic lymphocytic leukemia (CLL), in Diffuse Large B cell lymphoma (DLBCL). Additionally, AID is normally expressed in germline cells during spermatogenesis (Sschreck et al., 2006). In malignant cells, including CLL, in addition to the full length of the protein, AID mRNA can be alternatively spliced into

License CC BY-NC-ND 4.0

four mRNA variants contributing in the cell transformation (Albesiano et al., 2003, Oppezzo et al., 2003).

Localization of AID in the cell compartment regulates its activity. AID protein is localized in the cytoplasm, upon cell activation, the importin-α-nuclear import, present in the cytoplasm interacts with the NLS domain of AID and contribute to its translocation into the nucleus. In the nucleus, AID targets the *IgH* locus during the SHM and CSR. At the end of its activity and to inhibit excess of activity, AID is then exported form the nucleus due to the interaction of the exportin CRM1 with the NES domain of AID (for review (Patenaude et al., 2010).

Germline transcription is not sufficient for the induction of the mutagenic activity of AID on the Ig. Data demonstrated the capability of AID to interact with the replication protein A (RPA), able to bind and stabilize single strand of DNA (ssDNA) (Chaudhuri et al., 2004). In addition, phosphorylation of AID on (ser38) by the cyclic-AMP-dependent protein kinase A (PKA) is important for interaction with RPA (Vuong zt al., 2009). AID and RPA are recruited to the target sites after their transcription activation. Phosphorylated AID recruits the RPA to ssDNA to stabilized facilitating the deaminase activity of AID on the concerned motifs (RGYW).

3.2.2. Somatic Hypermutation (SHM)

SHM occurs during the mechanism of B cell maturation upon the activity of AID on the variable region of *IgH* and *IgL* loci of Ig in specific motifs WWRCT characterized by their high mutability and low frequency of G. SHM mechanism is recently reviewed in (Tang et al., 2022).

Incorporation of U in the DNA strand resulting from AID activity is abnormal and need to be eliminated. First, the cell replication machinery can ignore the U and read it as T resulting in transition dC>dT on the affected strand and dG>dA on the second strand or this abnormal uracil leads to the recruitment of two different mechanism: Base excision Repair (BER) and Mismatch repair (MMR).

The principal mechanism known to eliminate uracil residue from DNA is Base Excision Repair (BER). BER is initiated by the Uracil-DNA glycosylases (UNG1) which excise the U resulting in an abasic site production (AP site). Apurinic site recruits the AP endonuclease 1 (APE1) that leads to 3'-OH formation in the terminus of DNA damage site and initiates the final step of BER by recruitment of polymerase B (polβ) that synthetizes a corrected base in the place of the damaged one and the ligase activity for nick sealing resulting in mutation insertion in the concerned strand.

Additionally, generated mismatch activates the MMR mechanism. The U:G is recognized by the MutS homolog (MSH) heterodimer MSH2/MSH6 complex. MSH2/MSH6 recruits other

License CC BY-NC-ND 4.0

factors such as MLH1 and the post meiotic segregation 2 (PMS2). All together able to introduce a nick in the 5' of the mismatch. So, Exonuclease 1 (EXO1) is recruited and eliminates bases of the segment containing the mismatch from the nick. Finally, the low fidelity polymerase eta(η) enzyme is recruited and synthetizes nucleotides and results in introduction of mutation especially in the residue A:T (Figure 10) (Chi et al., 2020). At the end of this mechanism, cells that express non self-reactive BCR with high affinity to exogenous antigens are selected to continue their differentiation into plasma cells producing specific and functional antibodies and memory B cells (LeBien and Tedder, 2008). Recently, it has been demonstrated that the DNA repair factor 5-hydroxymethylcytosine binding, ES cell specific (HMCES) is implicated in the protection of the DNA on the abasic site from deleterious deletion that can occur. This HMCES interacts and protects the break produced on the uracil site without any impact on the SHM implicated molecules and promotes production of functional antibodies (Wu et al., 2022).

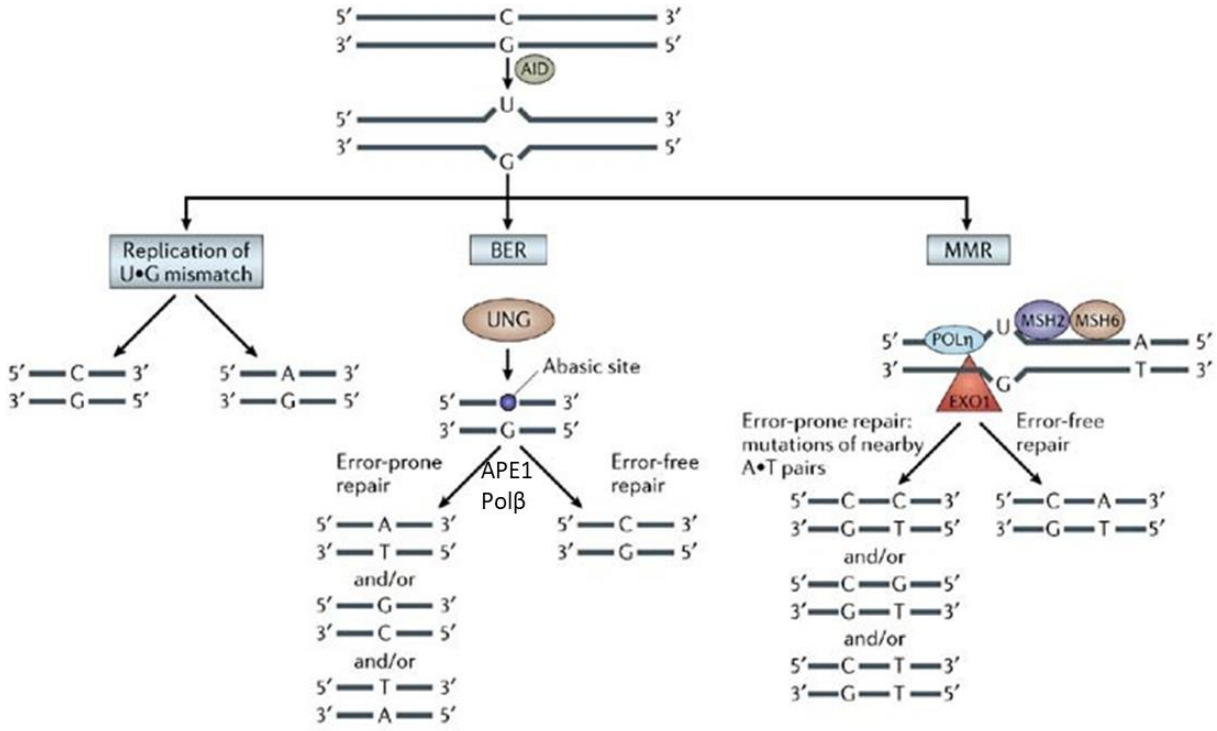

Figure 10 : Schematic representation of DNA repair during SHM.
AID activity result in uracil introduction in the DNA strand creating a mismatch U:G which will be repaired by three mechanisms. First, the machinery of cell replication ignores the U and read it as T resulting in transition from C to T on the affected strand and G to A in the complementary strand. Second, this abnormal uracil is removed by the UNG creating abasic site, which recruits the APE1. The endonuclease activity of APE1 lead to 3'OH generation of the damage site, Polβ is recruited to synthetize the corrected base (error free) or by error prone resulting in mutation insertion. Third the U:G is recognized by the MutS complex (MSH2/MSH6) creating a nick on the damage site, EXO1 is recruited to eliminate the base on the mismatch site then Polη synthetize the base in corrected way error free or by insertion of mutation (error prone) (Odegard and Schatz, 2006).

License CC BY-NC-ND 4.0

Frequency of introduced mutations resulting from AID activity in the variable region is represented in the (Figure 11).

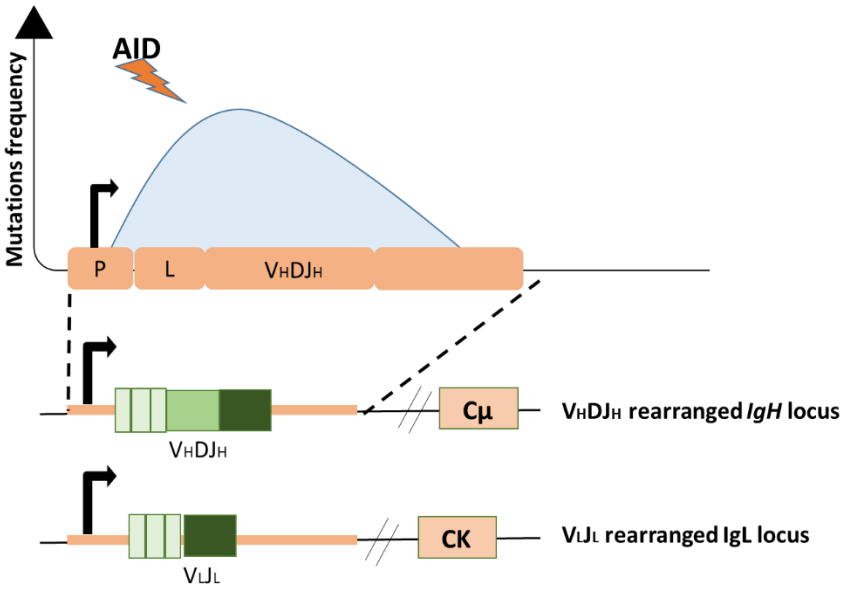

Figure 11: Somatic Hypermutation of *Ig* loci induced by AID.
Mutation frequency on the variable regions of *IgH* and *IgL* Loci induced by AID enzyme is represented by the light blue. Mutation begin upstream of the transcription site and extend up to 2Kb from this site. P: promoter, L: leader. Figure adapted from (Peled et al., 2008).

3.2.3. Class Switch Recombination (CSR)

CSR is a mechanism of genetic DNA rearrangement occurring on the *IgH* locus, it not affects the V region (For review (Chi et al., 2020)). CSR occurs during the terminal maturation of B cells and allows effective humoral immune response. This mechanism leads to the diversification of the Ig isotypes by the substitution of the IgM expressed on naïve B cells by another class of Ig (IgG, IgA and IgE) in a specific response to the antigen (Xu et al., 2012). It occurs between two S regions, the Sμ region, known as donor region, and an acceptor region, Sγ, Sα, Sε. S regions are located upstream of a constant gene (Cμ, Cγ, Cα, Cε). CSR leads to the deletion of the DNA between the two implicated S regions. Cδ is not preceded by a S region but studies reveal that CSR to IgD may be possible due to the presence of pseudo-S region (Rouaud et al., 2014). CSR is AID dependent, recently it has been demonstrated that in the absence of AID, CSR mechanism can be detected even at low level (Dalloul et al., 2021a). Initiation of CSR in the germinal centers of SLO requires several signals given by Ag encounter, cytokine production and interaction with the microenvironment cells. Activated B

License CC BY-NC-ND 4.0

cells produce signals inducing the germline transcription of the concerned S regions of the *IgH* locus. Germline transcription of S regions is absolutely required for CSR (Abarrategui and Krangel, 2009) since these transcripts permit the accessibility of the S DNA segments (Sμ and Sx).

Each transcription unit is constituted of a promotor (P) initiating the transcription via the RNA polymerase II enzyme, an intervening exon (Ix), the Switch (Sx) region and finally the (Cx) segment (Figure 12).

Germline transcription of the Sμ-Cμ region is constitutive in B cells (SC li et al., 1994). In contrast, the transcription of the acceptor S region is controlled by signals produced in response to the cytokine participating in the B cell stimulation. In murine cells, the interaction between the Toll-like 4 (TLR4) expressed on B cells with the lipopolysaccharide (LPS) induce the CSR to IgG2 and IgG3. In human B cells, production of IL-4 by CD4+ T cells in addition to the CD40-L stimulates the transcription of Iγ1 and Iε lead to IgG1 and IgE production respectively. The transforming growth factor TGFβ induce the transcription of Iα unit and then IgA production (Stavnezer et al., 2008).

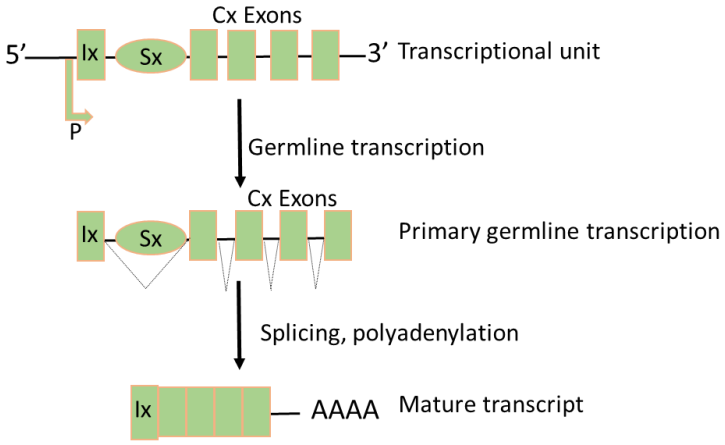

Figure 12: Germinal transcripts on constant regions of *IgH* locus.
Transcriptional unit of each constant gene is composed of one promoter (P), an intervening sequence (I), the switch region (S) and the constant exons (C). Cell stimulation leads to the germline transcription resulting in the production of primary germline transcript, which is submitted to splicing and polyadenylation to generate the mature non-coding transcript. Figure adapted from Chaudhuri and Alt., 2004.

AID is induced by the interaction between the CD40L on the activated CD4+ T cell surface with CD40 receptor present on B cells, or after LPS interaction with the TLR4. AID is localized in the cytoplasmic compartment and, upon activation, AID is imported to the nuclear compartment as described before. S regions are crucial for the CSR, their deletion results in CSR deficiency (Luby et al., 2001, Kamlichi et al., 2004). In addition, the orientation of these

License CC BY-NC-ND 4.0

S regions also important for the CSR. Inversion in S region results in important decrease in the CSR mechanism (Kinoshita et al., 1998).

Germline transcription of the S regions on the *IgH* locus generates neo-transcript RNA. This RNA strand hybridizes with the transcribed strand of the DNA matrix and generates hybrid RNA/DNA. In contrast, the opposite DNA strand, single stranded RPA coated, generates an R-loop. R-loop permits the single strand to be accessible to active PKA phosphorylated AID recruited by the RPA which stabilizes the single strand as described above (Pavri, 2017). S regions are rich in G motifs on the single strand and AID activity is facilitated by a G-quadruplex (G4) structure. G4 stabilize the formed R-loop. In addition to their presence on the single strand, G-quadruplex can be detected on the DNA strand present in the complex (RNA/DNA) (Figure 13).

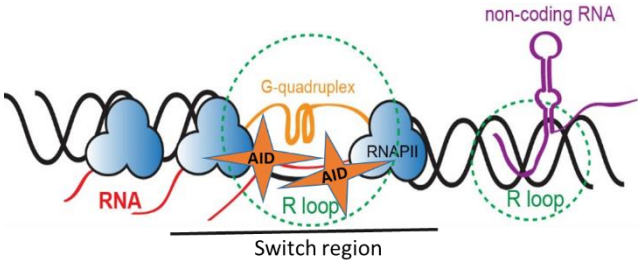

Figure 13: R-loop and G-quadruplex structures.
RNA polymerase II represented in blue synthetizes RNA in the switch region during germline transcription. Neo-synthetized RNA hybridizes with the DNA strand, the opposite strand still in single from and is coated by RPA. R-loop in green stabilized by the G-quadruplex in light orange generated in G rich region facilitates the activity of AID represented in orange in this region.

Briefly, AID recruited from the cytoplasmic to the nuclear compartment, interacts with S region and deaminates cytosines (C) to a uracil (U) creating DNA mismatches U:G. U:G mismatches are operated by the BER and MMR leading to single strand DNA breaks SSB (Cheng et al., 2009). Accumulation of SSB results in DSB generation on the two S regions (donor and acceptor). DSB generation on donor and acceptor segment leads to the excision of the DNA region located between them as an episome. It was shown that 3'RR constitute a major regulator of CSR mechanism thanks to its interaction with Eμ forming a loop on the *IgH* locus. In activated B, the 3'RR-Eμ loop is reinforced by a supplemental chromosome contraction allowing the rapprochement of the acceptor S region to 3'RR-Eμ-Sμ leading to the formation of Sμ-Sx synapsis (Wuerffel et al., 2007).

License CC BY-NC-ND 4.0

DNA ends are then ligated by NHEJ DNA repair pathway (Figure 14). Studies demonstrated that in case of the deficiency of this pathway, CSR still unexpectedly detected and repaired by the Alt-EJ pathway (Yan et al., 2007).

Finally, CSR and SHM mechanisms generate a functional BCR, implicated in the principal function in B cells, the transduction of signals controlling the B cell fate, survival, proliferation and differentiation. Each B cell express a unique type of BCR.

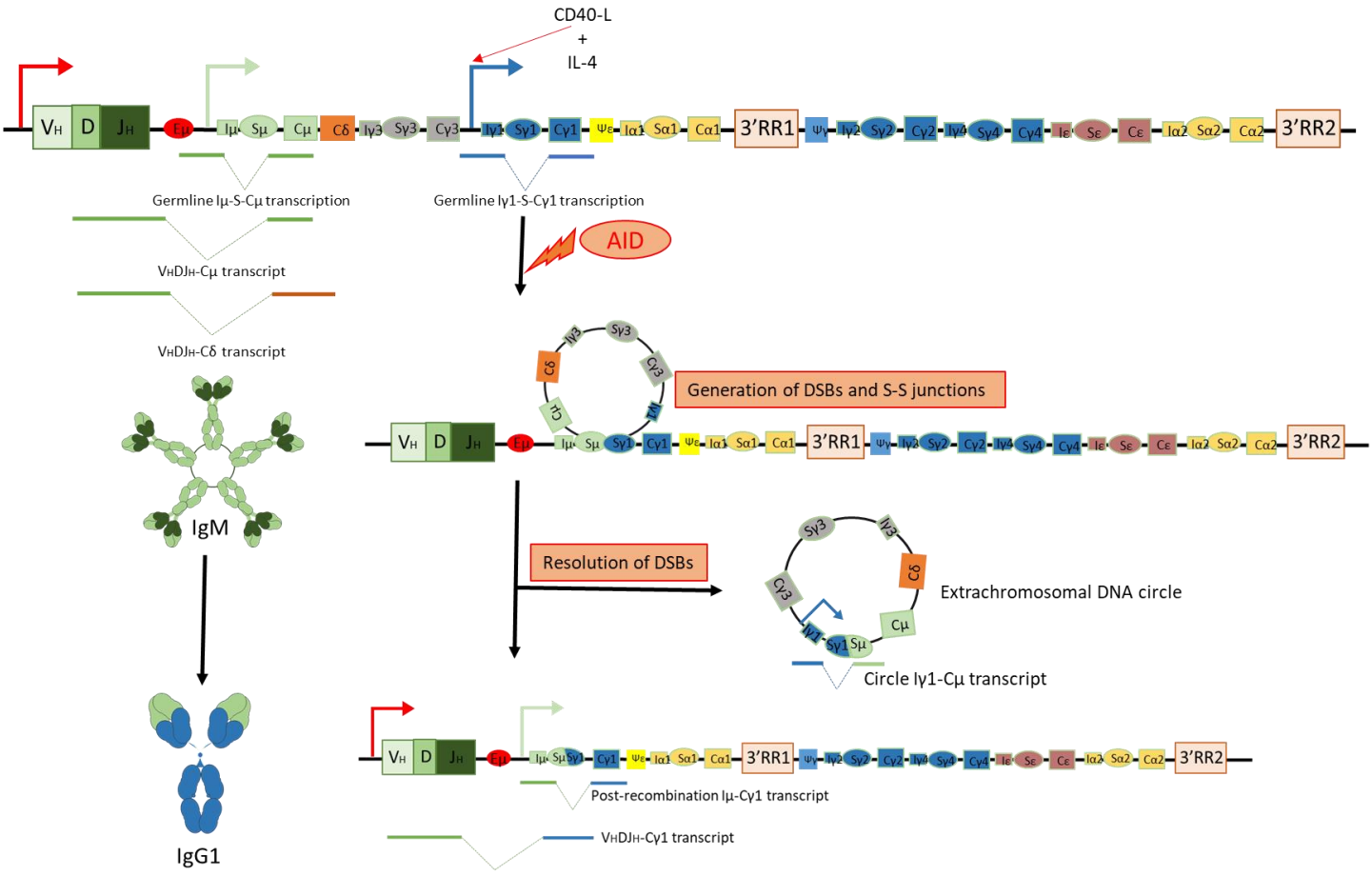

Figure 14: Schematic representation of CSR to IgG1.
Cell stimulation with CD40L and IL-4 induces the germline transcription of Igγ1 transcriptional unit in addition to the Igμ transcript. AID is expressed after B cell stimulation and is recruited to the transcribed S regions. AID DNA lesions lead to the production of DNA double strand breaks in the concerned switch regions. Repair of DSBs by NHEJ generates a Sμ/Sγ1 junction and the constant part between the two S regions is excised as a circle eliminated after cell proliferation. Ligated segment is transcribed from promoter upstream of the variable region leading to the expression of IgG1 isotype.

License CC BY-NC-ND 4.0

3.2.4. Locus Suicide Recombination (LSR)

Locus Suicide Recombination (LSR) is another genetic rearrangement detected on the *IgH* locus. It was detected for the first time in mouse. LSR occurs between the Sμ (donor segment) and one of the LS regions (acceptor segment) of the 3'Regulatory Region (3'RR1 and 3'RR2 in human) (Péron et al., 2012b). As detailed above, in the *IgH* locus organization, 3'RR is constituted of HS segments (HS1.2, HS3 and HS4) flanked by LS regions. LS are characterized by the presence of repeated sequences in tandem (Peron et al., 2012) and present high similarities with the Switch gamma 1 region (Sγ1). Presence of LS regions within the 3'RR is conserved among species, which potentially suggests an important physiologic function. Concerning the LSR mechanism and his detection, first, Peron et al. demonstrated in mouse the presence of germline transcription of the 3'RR (HS1.2, HS4). These transcripts were detected after stimulation of murine cells with LPS inducing CSR to Sγ1. Other studies showed that the 3'RR transcription is detected even in resting cells without any stimulation and can be sens and antisense transcription (Kaspryk et al., 2021). In addition, a mutation rate close to those of Sμ region was detected in these regions (0.42%) (Peron et al., 2012). Altogether, these observations suggest this region could be a new target of AID. This suggestion was confirmed when a mechanism of recombination was detected between the Sμ and 3'RR region, this mechanism called Locus Suicide Recombination (LSR) (Peron et al., 2012).

LSR leads to the excision of all genes encoding the immunoglobulin constant part as an episome (Figure 15). When this mechanism hits the functional allele, B cell loses the expression of IgH, Ig and BCR on their surface which lead to cell death by apoptosis since BCR was showed to be important in transduction of cell survival signals via his alpha beta domains (Maruyama et al., 2001) LSR can also occur on the non-functional allele, without compromising BCR expression on the cells. This idea is supported by the detection of LSR in human normal peripheral blood (Dalloul et al., 2019). LSR is suspected to occur in the germinal centers on the SLO, AID is expressed after cell activation in this organ. Detection of LSR in B cells of peripheral blood is due the exited cells from the SLO where the mechanism is occurred.

The physiologic function of the LSR is still pending. The rates of LSR is lower than CSR rate in normal cells. Among the suggested functions, LSR can be the counterpart of the CSR mechanism controlling the homeostasis of B cells, targeting the tumoral cells, auto-reactive cells and/or cells with low affinity to the Ag. In another way, it can result as an accidental rearrangement during cell stimulation and activation of CSR.

Concerning the molecular mechanism of the LSR, similarly to the CSR, it is initiated by the germline transcription of the LS segments in the 3'RR. Activation of AID and generation of

License CC BY-NC-ND 4.0

DNA double strand breaks in the LS are followed by DNA repair. Studies concerning the DNA repair during LSR mechanism in mouse suggested a greater involvement of the Alternative End Joining (Alt-EJ) DNA repair pathway than the NHEJ compared to CSR (Boutouil et al., 2019a).

As mentioned before CSR can be detected in cells deficient to AID, raising the question of LSR detection in AID KO condition? This question is tackled in the first part of my thesis work. on the other hand, the second part of my thesis work focusses on this part of LSR DNA repair in human in normal and pathological conditions. In order to improve the knowledge concerning this mechanism and to evaluate its function in human.

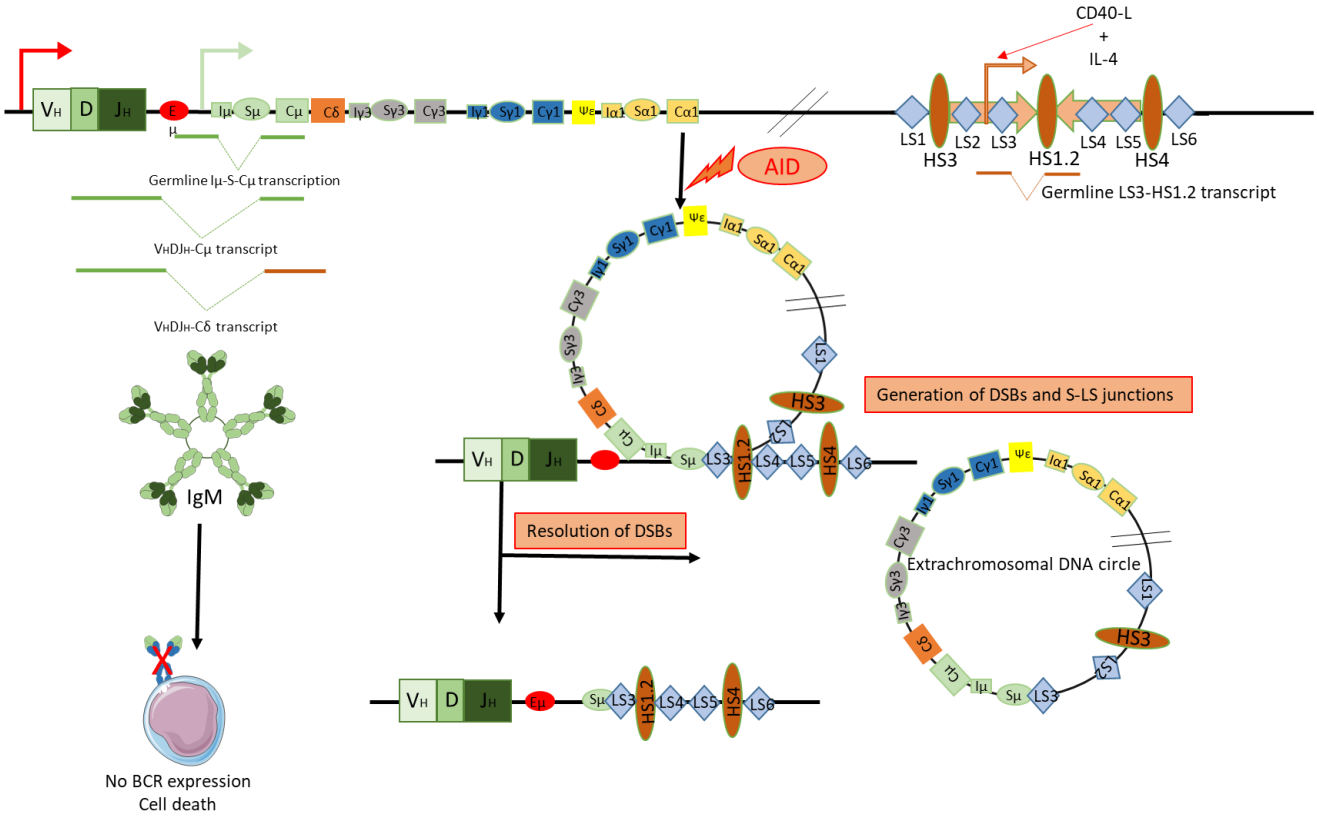

Figure 15: Schematic representation of LSR mechanism.
B Cells stimulated with CD40L and IL-4 undergo germline transcription of the like switch regions of the 3'regulatory region in addition to the Sμ. AID induced after B cell stimulation, is recruited to the transcribed regions and induces DNA lesions leading to the generation of DNA double strand breaks. DNA repair ligate Sμ to the concerned LS region in contrast the region located between Sμ and LS is excised as an extrachromosomal DNA circle.

License CC BY-NC-ND 4.0

C. B cell development, from the early stages to their terminal differentiation

Development of B cells is characterized by the mechanisms allowing B cells to produce functional Ig and to become mature B cells. These latter which finally have to undergo terminal differentiation to turn into antibody producing cells (plasma cells) and memory B cells.

1. Early stages of B cell development, an antigen independent phase

Given the wealth of literature on the model and hierarchy of B cell development, available publications identify markers to classify the different populations during differentiation from the hematopoietic stem cell in the bone marrow (Chao et al., 2008).

1.1. Hematopoietic Stem Cell (HSC)

HSC are pluripotent cells with a capacity of self-renewal which can differentiate into all blood cell types (HAWLEY et al., 2006). Flow cytometry studies of surface markers characterize the HSC as: $CD45RA^-$, $CD38^-$, CD90+, lin^- and $CD34^+$. This phenotype is used to isolate HSC population in bone marrow. Also these cells express the CXCR4, a receptor to CXCL12 ligand secreted by the stromal cells present in the microenvironment and contribute to the HSC retention in bone marrow (Baum et al., 1992; Mahony and Bertrand, 2019). HSC by differentiation give rise to multipotent progenitor cells MPP (Figure 16).

1.2. Multipotent progenitor (MPP)

MPP derives from the HSC and is characterized by the phenotype Lin^- $CD34^+$ $CD38^-$ $CD90^-$ IL7-$R\alpha^+$ $CD10^-$ $CD45RA^-$. MPP can differentiate into all mature cells of the blood. MPP is able to bind IL-7, secreted by the bone marrow stromal cells, due to the expression of IL-7 receptor. This binding induces signaling pathway initiating the differentiation into common lymphoid progenitor (CLP)(Melchers, 2015) (Figure 16).

1.3. Common lymphoid progenitor (CLP)

CLP give rise to T lymphocytes, NK and B lymphocytes. The different steps of B cells lymphopoiesis from the CLP are detailed thereafter. Immunophenotyping of the CLP population as $CD127^+$ $CD38^+$ Lin^- $CD34^+$. Until this stage of development, the *IgH* and *IgL* loci are still in the germline conformation (Figure 16).

License CC BY-NC-ND 4.0

1.4. Early Pro-B: D_H-J_H recombination

Early pro-B cells express the key transcription factor implicated in lineage commitment, the paired box gene 5 known as Pax-5 that encodes the B cell lineage specific activator protein (BSAP). Pax-5 activates the transcription of factors implicated in B cell specific lineage and represses the non-B lineage factors (for review (Cobaleda et al., 2007)). Pax-5 expression is regulated by the E12 and E47 proteins that regulate also RAG1/2 and EBF (kee et al., 2000).

Expression of the RAG1/2 and TdT enzymes characterizes this stage. Recombination between D and J segments takes place on both allele of *IgH* locus in this population. In contrast, IgL loci are in the germline conformations. At this stage, cells do not express a BCR on the surface neither pre-BCR nevertheless pro-B cells express the alpha (α) and beta (β) BCR Subunits. Pro-B cells are characterized by the surface expression of CD34, CD38, CD10 and CD127 and they are negative for the B cell lineage marker CD19 (Figure 16).

1.5. Late Pro-B: V_H-DJ_H recombination

At this stage RAG1/2 and the TdT are still expressed and the recombination of V segment occurs with the rearranged segment DJ on the *IgH* locus (V_HDJ_H recombination). Pax-5 able to interact with the coding region of the VH and also interact with RAG1/2 to mediates VH to DJH recombination (Kishi et al., 2002). *IgL* loci remain in the germline conformations. At this stage, Pro-B cells are characterized by the expression of CD45R (similar isoform to B220 murine), class II of CMH, CD19, CD40, CD34 and CD10 (Figure 16).

1.6. Large pre-B cells: pre-BCR expression

Pro-B cells give rise to large pre-B cells $CD38^+$ IgM^+. The recombined μ chain is associated with the surrogate light chain constituted by VpreB and λ5. IgM with the two subunits Igα/β (CD79A, B) at this stage form the pre-BCR. Expression of pre-BCR represents a checkpoint in the development of B cell progenitors which results in the downregulation of RAG1/2 and TdT expression (For review (Fritz et al., 2015)).

The functionality of the pre-BCR expressed on the cell surface is assessed in the interaction with galectin1 expressed by stromal cells of bone marrow (Elantak et al., 2012). Galectin1 able to bind to the VpreB and to induce cell signaling. Success in this signaling pathway indicates a functional pre-BCR and invites the rearrangement of the *IgL* loci. In contrast, failure in the signal transduction conducts to the arrest of the B cell development (Figure 17).

At this stage, B cells are positive for CD45R, CMH class II, CD19 and CD40. In addition, loss of CD34 characterize this stage of development (Figure 16).

License CC BY-NC-ND 4.0

1.7. Small pre-B cells: V_LJ_L recombination

V_LJ_L recombination takes place during this development stage, cells re-express the RAG1/2 and TdT. Phenotype of these cells can be defined as CD45R$^+$, CMH-II$^+$, CD19$^+$ and CD40$^+$ in addition to the pre-BCR already expressed from the large pre-B cell stage.

1.8. Immature B cells

Immature B cells expressing a complete BCR (IgM) on the surface formed of rearranged *IgH* and *IgL* loci. Immature B cells still express the RAG1/2 and TdT leading to the second checkpoint (central tolerance). Central tolerance consists on negative selection for B cells expressing non-autoreactive BCR. BCR able to recognize the self-antigens presented in the bone marrow are eliminated by apoptosis; or reinter in a new phase of light chain rearrangement to produce a new BCR (Figure 17).

Immature B cells express at the membrane CD45R, IgM, CD19, CD40 and class II of CMH. In these cells, IgD is expressed at the cell surface due the mechanism of alternative splicing of IgH RNA. IgD is detected at low levels on the membrane of these cells.

Cells expressing non-autoreactive BCR are allowed to exit the bone marrow and join the peripheral blood and secondary lymphoid organs and tissues as transitional B cells. In the peripheral blood, we can detect several subpopulations of B cells that differ by the stage of differentiation and activation (Leandro, 2013).

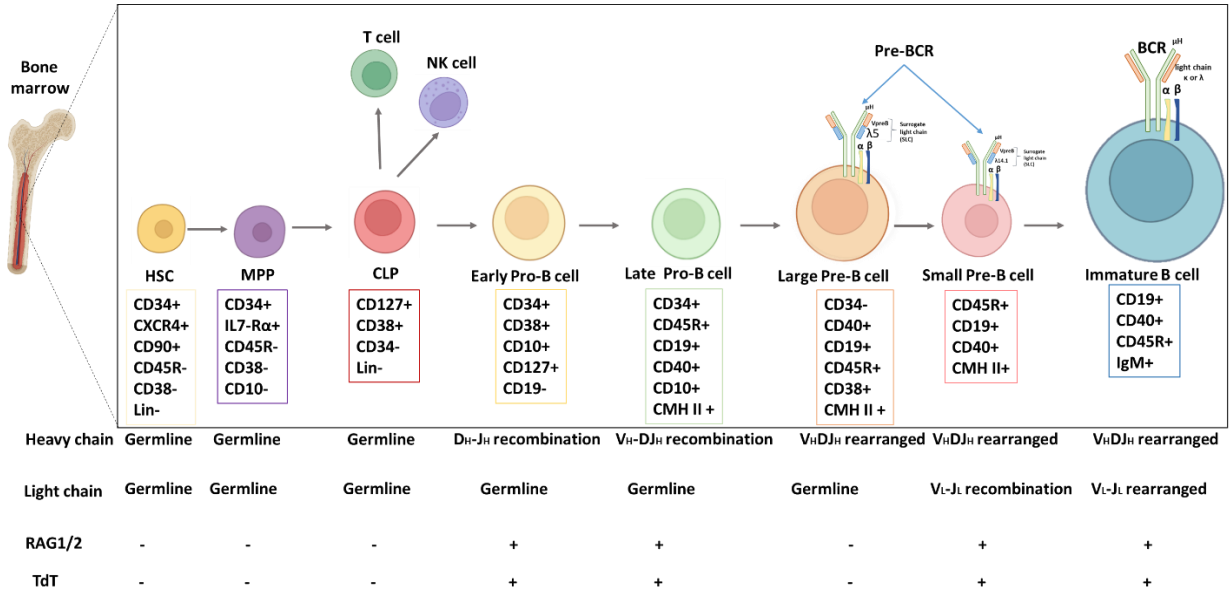

Figure 16: Schematic representation of early stages of B cell development.
This figure represents specific markers of B cells during the early stages of development. Immunoglobulin loci status and RAG1/2 and TdT expression are indicated.

License CC BY-NC-ND 4.0

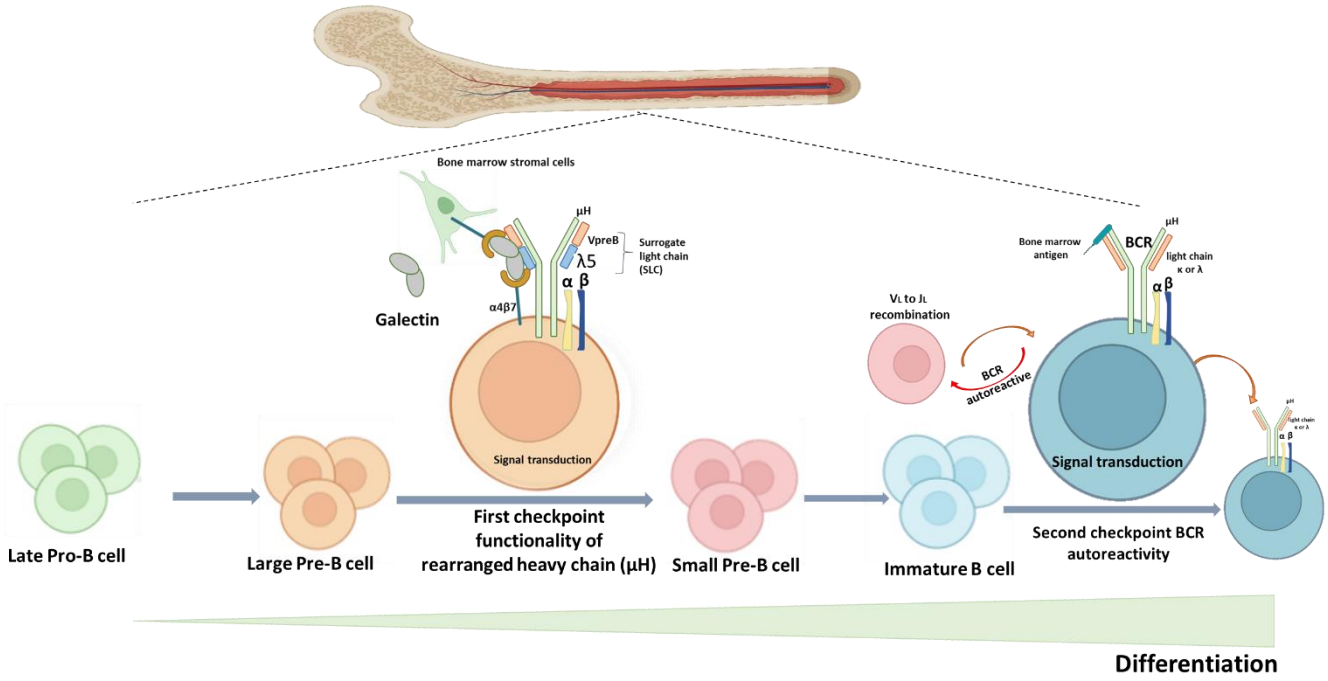

Figure 17. Checkpoints during early B cell development.
In bone marrow (BM), expression of the pre-BCR in large B cell leads to the first checkpoint that tests the functionality of the heavy chain of Ig. Stromal cells of the BM produce the galectin1 which binds to the pre-BCR via α4β7 receptor and to the SLC formed of (λ5 VpreB). Signal is transduced when pre-BCR is functional allowing cells to continue their development. Absence of signal induces the arrest of B cell development. The second checkpoint takes place in immature B cells and auto-reactivity of BCR is assessed. B cells are exposed to BM antigens, presence of signal indicates that the BCR is autoreactive and invites the cells to reenter in a novel round of light chain rearrangement, cells with negative signals are able to exit from the bone marrow to continue their development.

2. Late and Ag dependent stage of B cell development

2.1. Transitional B cells

After exiting from bone marrow, transitional B cells, constitute the transitional state from immature to mature B cells. Transitional B cells can be detected first circulating in the peripheral blood and characterized by the co-expression of IgM, IgD, and the expression of CD10. Cells migrate to the lymph nodes, the spleen or to the mucosa associated lymphoid tissue (MALT) to continue their development in response to chemo-attraction signals produce by the sphingosine 1-phosphate (S1P). Transitional B cells are classified into different subpopulations and they represent 5-10% of all B cell subpopulations. In human, three transitional B cell phases are detected before their commitment in follicular (FO) or marginal zone (MZ) B cells. The transitional T1, T2 and T3 B cell populations are reviewed in (Darwiche et al, 2018). T1 is detected in blood and spleen. High levels of T1 is observed in the systemic lupus erythematosus (SLE) disease after treatment by prolactin (Ledesma-Soto et al., 2012).

License CC BY-NC-ND 4.0

T2 state is present only in the spleen and will give rise to the mature naïve B cells (sims et al., 2005). The third group of Transitional B cells T3 is not able to continue their development and represent the group of anergic or autoreactive B cells (Melchers et al., 2006). Passage from immature to the different transitional stages and then mature naïve B cells is characterized by the gradual loose of some markers such as CD5 and CD10 and upregulation of other such as CD21. Markers used to characterize and isolate these three subpopulations are represented in (Table 2) (Martin et al., 2016).

Table 2: Markers of human transitional B cells.

Markers of human transitional cells	T1	T2	T3
	IgM^+, IgD^+ , $CD27^-$		
	$CD10^{Hi}$, $CD24^{Hi}$, $CD38^{Hi}$		$CD10^-$,$CD24^{int}$,$CD38^{int}$
	$CD21^-$	$CD21^+$	

2.2. B1 Cells

Two populations of mature B cells are described in human as well as in mouse, the B1 cells and the conventional B2 cells. B1 cells are implicated in the microbial defense and elimination of cell debris (housekeeping cells). They are found in the peripheral blood as well as in the umbilical cord blood. In human, B1 represent (5 to 10% of B cells), phenotypically characterized by the expression of $CD20^+$, $CD27^+$, $CD38^{low/int}$, $CD43^+$ and $CD5^{+/-}$. They are able to produce antibodies in a spontaneous way, IgM in the most of cases. This later characteristic is similar to mouse B1 cells (Griffin et al., 2011, Quach et al., 2016). Non-secreting B1 cells highly express the Pax-5 and they did not express the XBP1 and BLIMP1 which are characteristics for plasma cells (Tanaka et al., 2016).

2.4. Marginal zone B cells

In SLO, MZ B cells emerged from B2 B cell population are located in the spleen in the interface region between white and red pulp. MZ B cells share similar characteristics with B1 B cells. Low diversity of BCR is observed in MZ B cells and they are able to recognize microorganisms sharing common patterns (Pillai et al., 2005). MZ B cells are known to be involved in T-independent immune responses, and they are able to give rise rapidly to short-lived plasma cells (Balázs et al., 2002; Martin et al., 2001). Also, they are able to differentiate into long lived plasma cells in response to T-dependent stimulation. These antibody producing cells produce IgG or IgA isotypes with high affinity (MacLennan et al., 2003; Song and Cerny, 2003). Finally,

License CC BY-NC-ND 4.0

a suggested role for the MZ B cells is transporting antigens to the follicles rich in follicular B cells (FO) (Cinamon et al., 2008; Ferguson et al., 2004).

2.4. Mature naïve B cells

The co-expression of IgD in intermediated levels with IgM characterizes the naïve non-switched B cells in addition to the expression of CD20, CD19, CD21 (CR2, known as a receptor of C3d molecules of the complement), CD29 (integrin beta-1), CD35, CD40 receptor of the (CD154 Known as CD40 ligand) and BAFFR.

Antigen encounter with naïve B cells induces their activation resulting in proliferation, interaction with different types of immune cells and germinal center (GC) formation permitting to B cells to continue their development and maturation. Based on that, the first step after antigen encounter is GC generation in the SLO.

2.3. Initiation of the germinal center (GC)

SLO are characterized by a specific organization formed of follicles containing the follicular B cells and separated by inter-follicular region enriched by T lymphocytes, the limit between the T zone and B zone is named T/B border (Figure 18). Germinal centers are defined as transitory structures formed in the SLO after antigen B cell encounter. In GC, B cells continue their development, maturation and differentiation and to give rise an effective immune response (Huang, 2020).

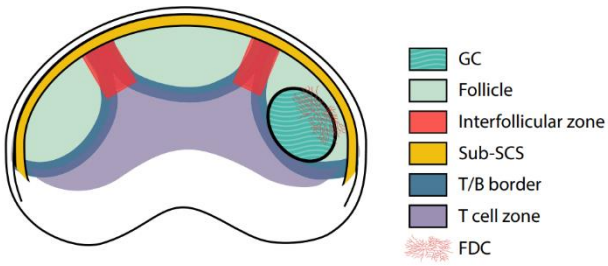

Figure 18: Organization of secondary lymphoid organs (SLO).
SLO are composed of follicles in which proliferation of T cell dependent Ag-activated B cells in presence of the follicular dendritic cells (FDC) allows the formation of germinal center structure (GC). Follicles are separated by the interfollicular zone. The limit between the T cell zone and B cell zone is called T/B border.

Naïve follicular B cells present in the follicular region of SLO, are activated by the encounter of a soluble antigen drained by the lymphatic vessels or cortical sinuses or by antigen presenting cell (APC) like follicular dendritic cells (FDC) present in the follicle (Figure 19) or by macrophages.

License CC BY-NC-ND 4.0

Activation of B cells leads to the expression of CD86, CMH II, EBI2 (Epstein Barr virus induced G protein coupled receptor 2) at their surface, in addition the chemotactic receptor, CCR7. This latter attracts activated B cells to the inter-follicular bordering the T-cell zone where CCL19 and CCL21, the ligands of CCR7, are expressed by the stromal cells (Link A et al 2007). CD4+ T lymphocytes are activated with the peptide presented via class II of CMH on dendritic cells which interacts with their TCR (Haberman et al., 2019). Migration of B cells to the border permits the interaction with CD4+ T cells (T-dependent response).

B-T cell interaction at the border zone is crucial because signal resulted from antigen encounter in naïve B cells is not sufficient for fully B cell differentiation. Additional co-stimulatory signal is given by the interaction with CD4+ T cells. Co-localization of B cells and CD4+ T cells in the border zone and their interaction is facilitated by the interaction of highly expressed level of EBI2 on the membrane of B and T cells and its ligand oxysterol produced by the stromal cells (Gatto and Brink, 2013).

At this stage, B cells can differentiate into short-lived plasma cells producing non-switched (IgM) antibodies with low affinity. These cells are produced short time after infection. B cells can also return in the center of the follicle to generate the germinal center. Cells returning to the center of follicle cannot be accomplished without regulation of the transcriptional level of some factors. B and T cells downregulate CCR7 and EBI2 and upregulate the B cell lymphoma (BCL6) (Pereira et al., 2009). BCL6 is an important regulating factor during B cell development in the SLO, it downregulates the expression of IRF4 and BLIMP1 implicated in the differentiation to plasma cells. In contrast, high expression of these two factors by plasma cells in turn downregulate BCL6 expression (Ochiai et al., 2013).

Downregulation of EBI2 and CCR7 in CD4+ T cells allows them to return to the follicles where their differentiation goes on into T follicular helper cells (Tfh). Localization of B and T cells into the center of follicles is maintained through the expression of CXCR5R on B and Tfh cells (Stebegg et al., 2018).

When B cells return to the follicle center they play the role of APC, presenting Ag peptides on class II of CMH to CD4+ T cells. This interaction permits to B cells to receive survival and differentiation signals. Activated B cells proliferate, while resting B cells migrate to the periphery of GC constituting the mantle zone where CD4+ T cells are detected at low levels (Nygren et al., 2014). The germinal center pass from the immature structure (pre-GC) to the mature structure constituted by two different compartments (light zone (LZ) and Dark zone (DZ)) with specific characteristics and cells. Architecture of germinal center is due to the chemokines produced by stromal cells in the GC. The dark zone (DZ) of GC is enriched by centroblasts which are $CXCR4^{high}$ $CD83^{low}$, $CD86^{low}$, $CD40^{low}$ and $BCL6^{high}$. Centroblasts are characterized by the loss of their membrane immunoglobulin expression and their high rate of

License CC BY-NC-ND 4.0

proliferation, and they are submitted to the SHM mechanism (Victora et al., 2010). Maintaining of centroblasts in the DZ is due to the presence of CXCL12 expressed by germinal center stromal cell of dark zone. CXCL12 is the ligand of CXCR4 highly expressed by centroblast cells (Stebegg et al., 2018). Centroblasts migrate from the DZ to the LZ under the effect of CXCL13 produced by the FDC. CXCL13 interacts with his receptor CXCR5 expressed on centrocytes, the characteristic B cells in LZ. Centrocytes are smaller than centroblasts, these cells downregulate the expression of CXCR4. Their phenotype is $CXCR4^{low}$, $CD83^{high}$, $CD86^{high}$ and they re-express an Ig at the cell surface.

In LZ, in addition to the centrocytes, Tfh cells, FDC and regulatory T cells are found. Tfh has a crucial function in the mature GC generation by maintaining the production of IL-21 and IL-4 cytokines and expressing CD40L leading to synapse formation with B cells (Victora et al., 2012). FDC are implicated in the process consisting on the positive selection of B cells harboring BCR with high affinity due SHM occurred on *Ig* loci in DZ. This selection occurs via their interaction with FDC through the binding of the BCR to the Ag exposed at the FDC surface. BCR with high affinity are able to bind the antigen and cells are allowed to continue their differentiation. In addition, it has been demonstrated that B cells expressing a high Ag-affinity BCR can also return to the DZ and be submitted to additional proliferation rounds and SHM process resulting in improvement of BCR affinity (Victora et al., 2012).

In contrast, B cells exiting from the DZ with low affinity BCR are disable to present the Ag and are eliminated by apoptosis or enter in anergic state (Rajewsky, 1996). It was demonstrated that centrocytes cells are able to proliferate (Wang and Carter, 2005). Centrocytes re-express the CXCR4 at high levels and the decrease in their costimulatory signals permit to these cells to return to the DZ to proliferate (Schwickert et al., 2007).

Positively selected cells in the LZ proceed to the CSR in order to diversify the immunoglobulin isotype from IgM to IgG, IgA, or IgE. Switched B cells differentiate into plasma cells or memory B cells. It was shown that positively selected cells with the higher affinity for Ag are conducted to differentiated into plasma cells. In contrast selected cells with lower affinity BCR are induced to give rise to the memory B cells as reviewed in (Palm and Henry, 2019) .

Recently published study demonstrate that CSR mechanism occurs before the SHM (Roco et al., 2019), but we cannot precisely determine SHM and CSR are time ordered and this question is still in debate.

License CC BY-NC-ND 4.0

2.4. Memory B cells

We can distinguish different memory B cell populations. Memory B cells can be produced after the encounter with the Ag in a T dependent way, via the interaction CD40L/CD40, outside of the GC, in the marginal zone of the spleen. The second population of memory B cells are produced during the GC reaction, in a T cell dependent activation with low level of CD40L/CD40 interaction producing high rate of memory B cell clonality compared to MZ memory B cells (Taylor et al., 2012). These cells carry the immune memory and the determinant function during the secondary immune response which is rapid and highly specific. The secondary infection induces these memory B cells to differentiate into plasma cells producing specific antibodies. Survival of memory B cells is controlled by the balance between pro and anti-apoptotic factors like PUMA and MCL-1 respectively. PUMA as important factor regulating the cell survival of activated B cells, in this context, Clybouw and colleagues showed that loss of PUMA results in the accumulation of memory B cells and not plasma cells (Clybouw et al., 2011). In addition, MCL1 was showed to play an important function in plasma cells which contributes to the maintenance of their survival (Peperzak et al., 2013).

2.5. Plasma cells

Plasma cells are differentiated cells after Ag encounter capable to produce neutralizing antibodies raised against the Ag. Plasma cells can be detected in the bone marrow, and in peripheral tissues (lymph nodes and spleen) but not in blood. These cells are characterized by the loss of BCL6, Pax-5, CD19 and CD20. In contrast, this cell population emerged from B cells is expressing specific factors: PRDM1, XBP1, CD38, and CD138. BLIMP1 constitutes the key factor of plasma cell differentiation that encoded by the *PRDM1* gene. BLIMP1 positively regulates XBP1 which not specific for plasma cells but expressed in secretory cells, required for plasma cell differentiation. In contrast, it negatively regulates Pax-5 implicated in the lineage B commitment (Kassambara et al., 2015).

License CC BY-NC-ND 4.0

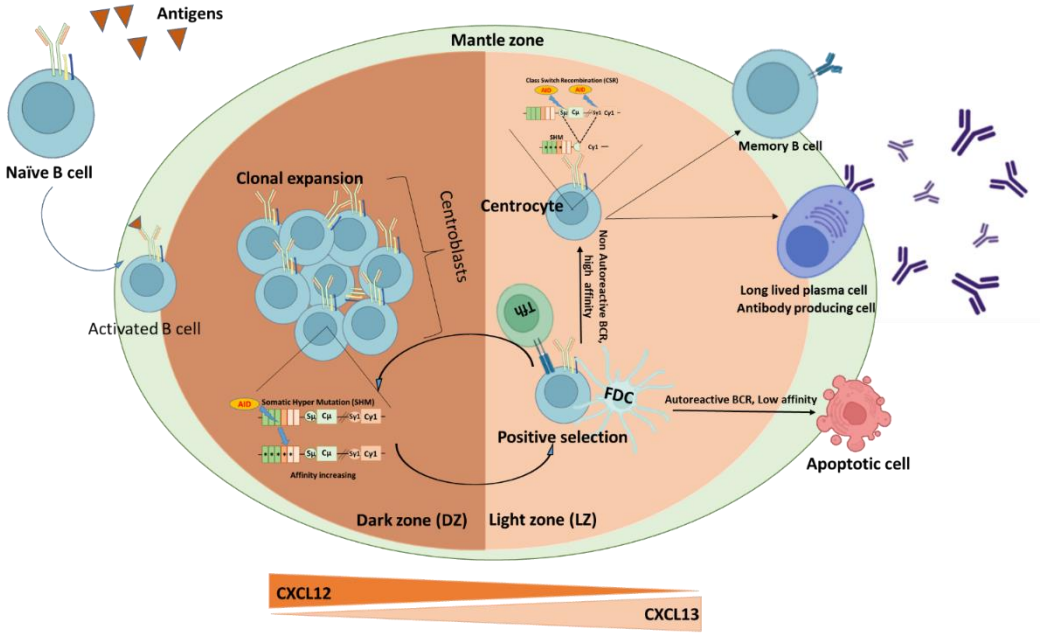

Figure 19: Schematic representation of late B cell development and germinal center.
The antigen binding leads to the germinal center (GC) generation and activation of naïve B cells. GC is formed in the SLO, it is composed of two distinct regions: the dark zone (DZ) enriched with proliferating B cells where SHM mechanism takes place, and the light zone (LZ), in which B cells are selected on the basis of the affinity of the BCR. B Cells in the DZ called centroblasts are retained due the high expression of CXCL12 receptor on their surface. Negatively selected B cells are eliminated by apoptosis or invited to return to the dark zone to undergo another round of SHM to improve BCR affinity. Positively selected B cells undergo CSR to diversify the Ig isotype and then differentiate into long-lived plasma cells (antibody producing cell) and memory B cells.

2.3. Regulatory B cells

The concept of the presence of cells able to inhibit the immune response was described in 1970 (Gerson and Kondo., 1970). B regs constitute a subpopulation of B cells known for their immunosuppressive functions (For review (Mauri et al 2012)). Production of a regulatory B lymphocytes results from the activation of a B cells via the CD40 receptor, the “toll like receptor” (TLR) and/or the BCR as well as CD80, CD86 and the cytokine receptors. They mainly target CD4+ T cells, CD8+ T cells and monocytes. B regs are divided into several subcategories (Mauri and Menon., 2015).

B regs were identified in several pathologies such and autoimmunity, infections and cancers especially in humans (Mauri and Menon., 2017). B regs are characterized by different phenotypes some of them are identified by the expression of immunomodulatory factor the IL-10 and their mode of action depend on IL-10. In contrast, other B cells are independent of Il-10. It was demonstrated that transitional B cells T2 are enriched in cells able to suppress the T cell responses and produce IL-10 (Blair et al., 2010). Additionally, IL10+ regulatory B cells

License CC BY-NC-ND 4.0

are considered as antibody producing cells which can be differentiate into plasma cells, this finding was observed in human as in mouse (Maseda et al., 2012).

2.6. BCR signaling

BCR is a B cell lineage specific marker, composed of three domains the extracellular, the transmembrane and the intracellular regions. Monomeric BCR is constitute of an Ig associated with two subunits Igα/Igβ (CD79a, CD79b respectively). BCR activation and signal transduction is more related the oligomer structure of the BCR (Yang et al., 2016). Activated BCR via Ag induces a cascade of signals resulted in signal transmission from the BCR oligomer to the intracellular compartment to expose the ITAM domain. ITAM is phosphorylated by LYN, a protein of the SRC family proteins, associated to the Igα/Igβ of the BCR. LYN activity contributes to the recruitment of SYK which interacts with the BCR and generates a complex of BCR/SYK (Dal Porto et al., 2004). BCR/SYK complex leads to the activation by phosphorylation of different signaling pathway in B cells such as PLC-γ2, PI3K and MAPK pathways which are very well reviewed in (Wen et al., 2019). In activated B cells, CD19 is phosphorylated and contributes to the recruitment and the activation of PI3K pathway. Activation of these pathways result in the activation of transcription factors such as NFAT, ERK and NF-κB respectively (Figure 20). These transcription factors are then translocated to the nucleus to regulate the expression of genes implicated in cell survival, proliferation and differentiation (For review (Wen et al., 2019)).

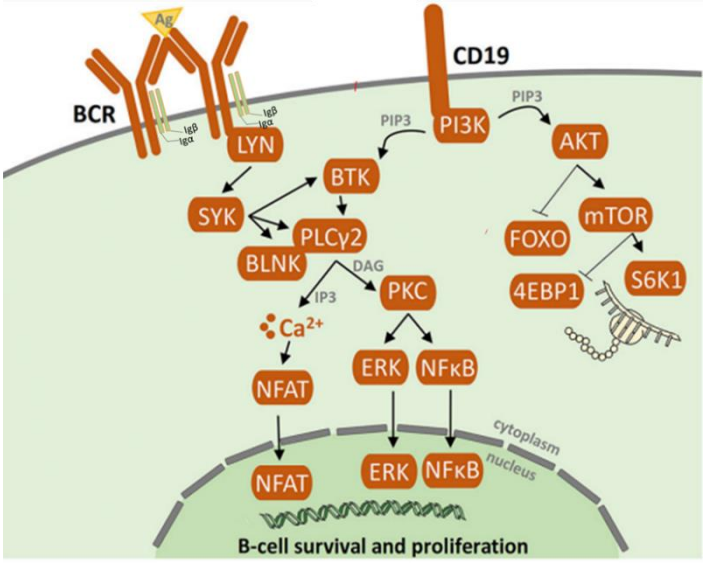

Figure 20: Signaling pathway of B cell Receptor.
Signal transduction initiates after antigen binding to the variable region of the BCR. Activation of the two subunits Igα and, Igβ. After that three kinases protein are activated: SYK, LYN and BTK. The cascade of signaling is continued via the ERK, NFAT, and NFKB signaling pathway resulting in cell survival and proliferation. Figure adapted from ((Sedlaříková et al., 2020).

License CC BY-NC-ND 4.0

License CC BY-NC-ND 4.0

Chapter II: DSB DNA Repair pathways

1. DNA and chromatin structure

Deoxyribonucleic acid (DNA) is the material element, the genome, bearing the unique and specific genetic information responsible for determination of all the functions and the phenotype in living organisms.

DNA is a double helix of a succession of nucleotides and organized as a polymer. The two strands of DNA are linked by hydrogen bonds between the bases. Four types of nucleotides (complex of sugar 'ribose' and phosphate) are present depending on the bases types, the deoxyadenosine (A), deoxycytidine (C), deoxguanine (G) and the deoxythymidine (T). DNA filament is wrapped with proteins in an organized structure called chromatin.

Our complete genome is about $6*10^9$ base pairs (bp), 2 meters in length in its unpacked form. In cellular nucleus (10µm), DNA is compacted at different scales. This compaction is a nonrandom process that relies on the presence of histones and RNA (2% of purified chromatin), each level of chromatin compaction presents an impact on genome functions.

Nucleosomes constitute the smallest scale of DNA folding (11nm). Each nucleosome is constituted of a core of four histones organized within dimers (H3-H4) and (H2A-H2B) and DNA filament about 147 bp of length. Adjacent nucleosomes are linked by the histone1 (H1). Nucleosome organization plays important function in gene expression regulation by controlling the accessibility of the DNA during DNA repair, DNA replication and transcription. Epigenetic modifications in histones and DNA such as DNA methylation are known as posttranslational modifications also and play a crucial role in gene expression regulation. An example for the epigenetic modification is histone acetylation or methylation which indicate the active or inactive transcriptional states respectively. Epigenetic regulation is implicated in other functions such as the choice of DNA repair pathways after DNA lesions as reviewed in (Caron et al., 2021) and detailed in the paragraph 7.3 of this chapter.

In larger scale of 10 kilobases (Kb), the genome has a spatial (3D) organization composed of Topologically Associating Domains (TADs) defined as self-interacting regions in the chromatin, formed of Ring-shaped complex of cohesion (Hansen et al., 2017). TAD extremities are composed of CTCF motifs able to interact among one another. Studies have demonstrated that these CTCF-CTCF interactions regulate the interactions between genes and their regulatory elements in the TAD, and the inhibition of such interactions was shown to lead to aberrant expression of genes (Wutz et al., 2017). The 3D organization of the genome plays an important role in the regulation of gene expression.

License CC BY-NC-ND 4.0

In the same scale of compaction, chromatin can be organized into two compartments, Euchromatin (A) and heterochromatin (B). The compartment A is normally enriched with active genes and DNA hypersensitive to the DNase1. In contrast, B compartment is enriched with more repressed genes (Lieberman-Aiden et al., 2009). The interactions in and with these two compartments varies and increases during the cell differentiation (Dixon et al., 2015). Finally the chromosomes in the nucleus occupy specific and proper territories and this constitutes the large scale (100 mega base 'Mb' to 3000Mb) of genome compaction (Figure 21) (Cremer and Cremer, 2001).

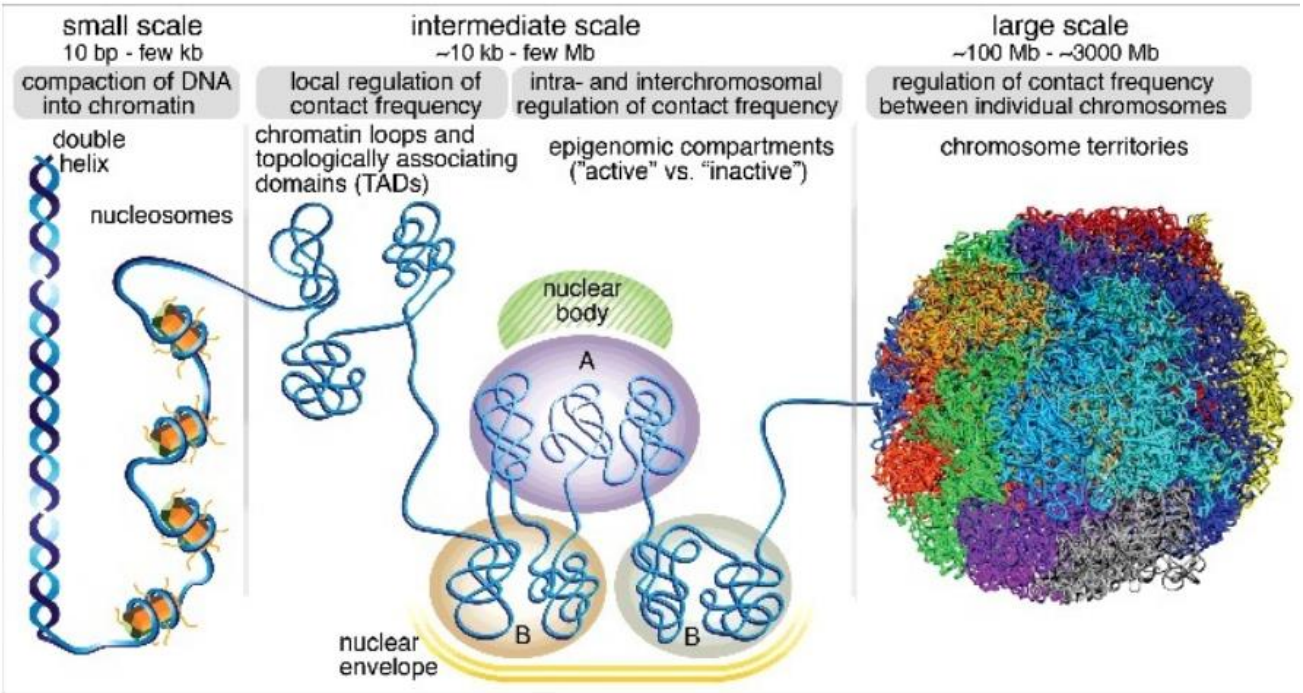

Figure 21: Schematic representation of Chromosome structure.
Nucleosomes constitute the smallest scale of DNA folding **(**11 nm) composed of 147 bp pf DNA filament and core of histones. Functionally, nucleosomes regulate gene expression by regulating the accessibility of the DNA to the binding proteins implicated in replication or transcription. Topologically Associating Domains (TADs) constitute the intermediated scale of chromatin compaction with about 100 kilobases. TADs regulate the gene expression by regulating the interaction between enhancers and the promoters. Also, TAD can be organized into two compartments A and B characterized to be active and inactive compartments respectively. At the largest scale, chromosomes associate with other chromosomes to form the stereotyped chromosome territories inside the cell nucleus (Hansen et al 2017).

2. DNA lesions agents

Many factors can threaten the genome integrity with a rate of 10^3 to 10^6 damages in the cell per day as reviewed in (Yousefzadeh et al., 2021). Maintaining the integrity of the genome is vital for conserving its function throughout the years. The factors causing these DNA damages are subdivided into two groups, the endogenous and exogenous DNA lesions agents. The endogenous mechanisms are normal metabolic activity in the cell such as alkylation,

License CC BY-NC-ND 4.0

deamination or oxidative response, DNA replication, DNA transcription and telomere shortening. The DNA lesions introduced are spontaneous DNA lesions. Physiological programmed DNA lesions also occur during meiosis, immunoglobulin diversification and affinity maturation during B cell development V (D) J recombination, CSR and SHM. In contrast, exogenous DNA damaging agents can be chemical compounds, ultraviolet rays, ionization irradiation and tobacco products (Figure 22). These different agents can lead to several types of DNA lesions such as base modification for example during SHM, single strand DNA break (SSB), double strand breaks (DSBs) such as during V (D) J and CSR or simply deletion or insertion of some nucleotides. To repair these lesions and to maintain the integrity of our genome, in our cells, several different pathways are present and able to repair specifically the different types of DNA damages (Figure 22).

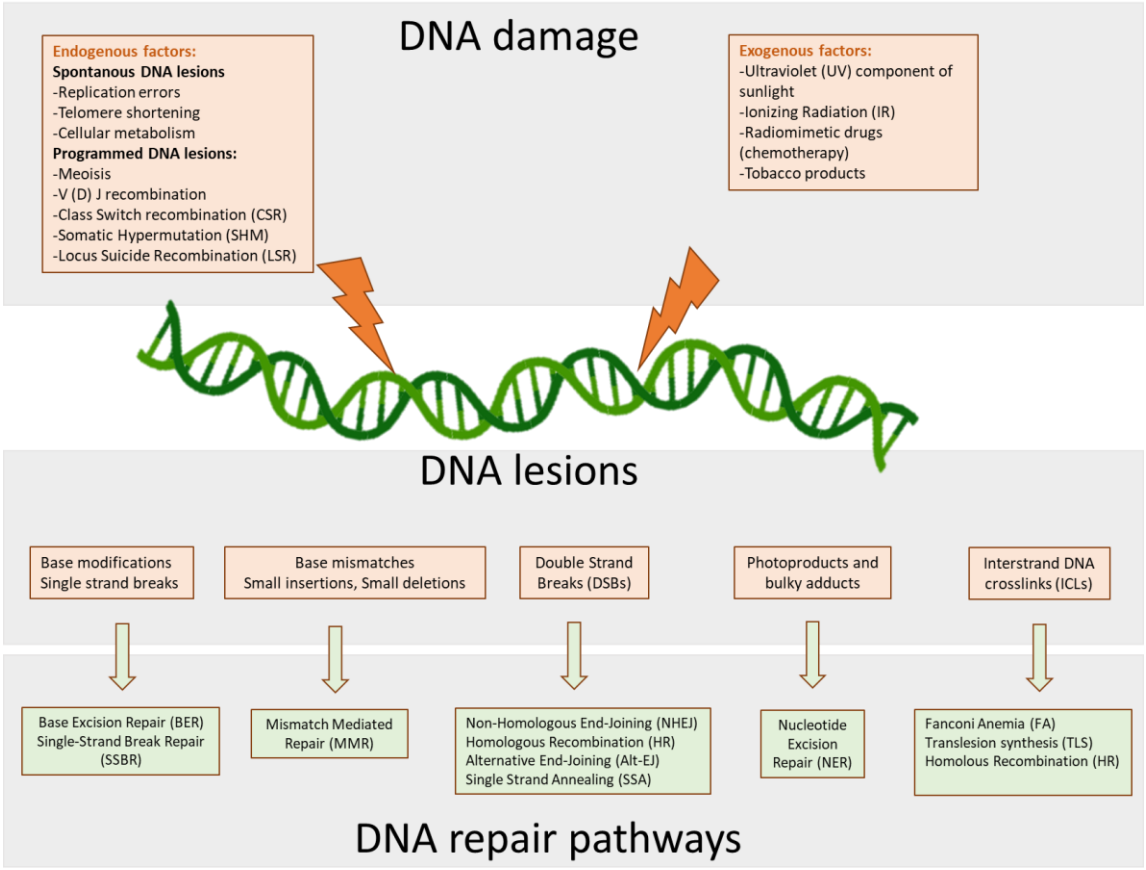

Figure 22 :Factors inducing DNA lesions and the pathways of DNA repair.
DNA damages can be caused by endogenous and exogenous factors leading to different types of DNA lesions. Each types of DNA lesions recruit the specific DNA repair pathway.

License CC BY-NC-ND 4.0

3. Pathological impact of DNA lesions

Cells display several different DNA repair pathways in order to maintain the genome integrity and stability which is a challenge for the cell. Cells are exposed to different DNA damage factors and differ by the rate of lesions occurred regarding their proliferative state. Dividing cells accumulate more DNA lesions and mutations than resting cells (Heddle, 1998). This difference result in difference in the response generated during the activation of the DNA repair pathways. Alteration in DNA repair pathways can result by failure in the DNA repair and in lesion accumulation which induce cells to enter into senescence cycle or apoptosis. On the other hand, cells which were not eliminated by apoptosis will be dangerous to the organism and lead to pathological generation resulting from alteration in the genome and mutation accumulation. In a random way, alteration in DNA repair can introduce DNA mutations in tumor suppressor genes or oncogenes, leading to lesions and mutation accumulation, and genome instability, which is considered as a hallmark of all types of cancers.

DSB constitute the most deleterious damages in the cell. Failure in DSB repair leads to cell death through apoptosis but can also affect genome integrity through chromosomal translocations and/or loss of genetic material, which are the two important causes of cancer development or lymphomagenesis (Alt et al., 2013), in addition to other pathologies like neurodegenerative disease (Rass et al., 2007). Genetic and inherited deficiency in DNA repair molecules is associated with different genetic disorder even they are rare but present the Fanconi anemia, Bloom Syndrome, Xeroderma pigmentosum and Ataxia telangiectasia syndrome as reviewed in (Machado and Menck, 1997).

In the literature, a large number of publications discuss the alterations of DNA repair and their impact in cancer and lymphoma development. This point will be detailed and discussed after in the chapter III talking about Hodgkin lymphoma and Non-Hodgkin lymphomas, the chronic lymphocytic leukemia.

License CC BY-NC-ND 4.0

4. DNA Damage Response (DDR)

To maintain the genome integrity and stability cells react to the different DNA lesions through DNA Damage Response (DDR) which in turn activates DNA repair pathways. DDR is composed of the package of damage sensors that detect the presence of lesions, transducer kinases that transmit the signals to the effectors (Derks et al., 2014). Two principal complexes of sensors are documented, the MRN complex (MRE11-RAD50-NBS1) implicated in the recognition of DSBs and the 9-1-1 complex (RAD9-RAD1-HUS1) with the replication protein A (RPA) able to recognize single strand of DNA (SSDNA) and lesions generated during the replication stress. MRN complex recruits the ataxia telangiectasia-mutated (ATM) which is able of auto phosphorylation after the dissociation of the dimeric form of ATM. The 9-1-1 and RPA recruit the Rad3-related (ATR). ATR interacting protein (ATRIP) plays the role of linker between ATR and RPA (Ünsal-Kaçmaz and Sancar, 2004). Recruited ATM and ATR phosphorylate the histones H2AX (γH2AX) present in the proximity of the DNA damage. As in the continuity of the chapter I detail only the DSBs repair pathway, here I will tackle the DDR mediated by ATM. γH2AX plays a crucial function in the recruitment of the DNA damage chechpoint1 (MDC1).

It is important to mention here that the chromatin state can influence the signaling of DDR, since heterochromatin (inactive and compacted form) is resistant to the procedure of H2AX phosphorylation and impacts the cascade of DDR pathway (For review (Sulli et al., 2012)). MDC1 implicated in the accumulation of the MRN complexes promotes the activation of ATM which is also activated by the 53 Binding protein 1 (53BP1). Activated ATM recruits and phosphorylates the checkpoint2 (CHK2). This phosphorylation leads to the activation of p53 downstream in this signaling pathway. Due to the cellular outcomes, two possibilities are possible: highly damaged cells are eliminated by apoptosis, or, with the arrest of the cell cycle, the activation of the DSB repair pathway allows the DNA repair and cells undergo their survival and proliferation. In the case of unrepaired DNA, cells enter in a senescence cycle (Figure 23). Paulson et al 1998 demonstrated that the P53 absence permits cell to continue their cell cycle phases even in the presence of incorrect DNA repair (For review (Sulli et al., 2012)).

License CC BY-NC-ND 4.0

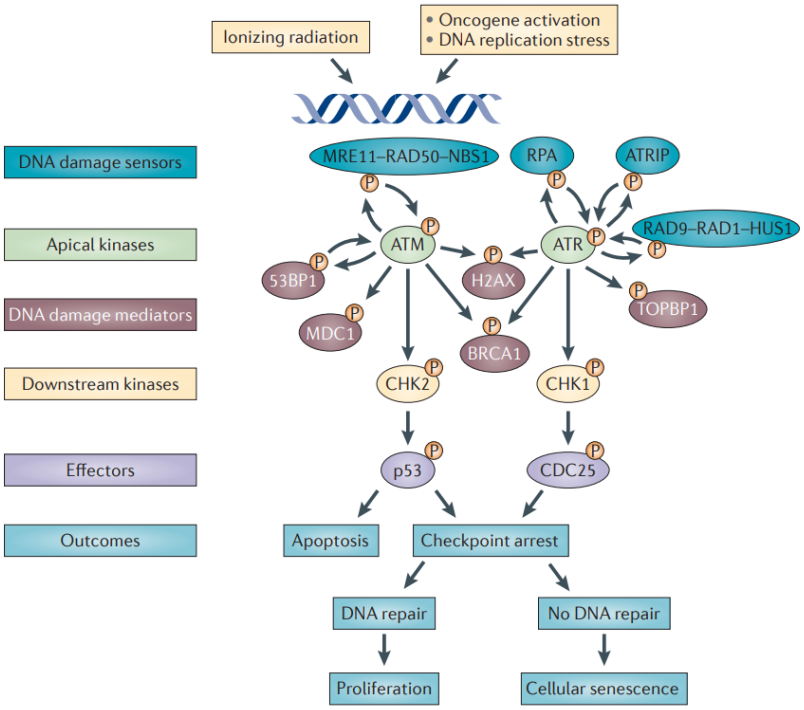

Figure 23: Signaling pathway of DNA Damage Response.
Induction of DNA lesions by ionizing radiation or during the oncogene activation and DNA replication stress, recruits the molecules of the DDR. In the case of DSB, ATM is activated by the MRN complex adn by the 53BP1 leading to the activation by phosphorylation of MDC1 and CHK2. CHK2 in his turn phosphorylates the p53 protein. In the case of ssDNA, ATR is activated by the 9-1-1 complex and RPA. This activation leads to the phosphorylation of CHK1 which in his turn activates the CDC25. At the end, activated p53 or CDC25 result in the arrest of cell cycle to activate the concerned DNA repair pathway, unrepaired DNA lead to the senescence of cells. Additionally, p53 can lead to the apoptosis of cells (Sulli et al., 2012).

5. Double Strand Break DNA repair pathways

Different DNA repair pathways are identified to repair DSBs, which are the most dangerous damages. We can identify the NHEJ, the Alt-EJ, the HR and the Single Strand Annealing (SSA). Theses pathways differ by the DNA ends that can be repaired, the molecules implicated and the structure of the junction generated after ligation. Choice of each of these pathways is regulated by several factors tackled later on in this chapter paragraph (choice of the DNA repair pathway).

5.1. Non-Homologous End Joining DNA repair pathway (NHEJ)

NHEJ and HR constitute the major DNA repair pathways of DBSs. NHEJ evolved in eukaryotes and prokaryotes to increase the possibility to repair the DSBs even in absence of sequence homology between DNA ends (Lieber, 2010a). It takes place in diploid organisms, haploid non-

License CC BY-NC-ND 4.0

dividing organisms (Stinson et al., 2020). it's the dominant DSB repair system in the G1 phase but can be activated along all cell cycle phases (Pannunzio et al., 2018).

NHEJ is characterized by the multifunctionality of the enzymes, flexibility in the mechanism and the iterative function. Enzymes and molecules can act together in any order at the DNA ends to ensure the repair in an efficacy way of diverse DSB ends in eukaryotes and prokaryotes (Lieber, 2010b).

In contrast to the high fidelity of HR, NHEJ is able to generate some insertion or deletion into the DNA (indels) (Stinson et al., 2020). However, the alteration in the junction generated by NHEJ is very limited which indicates this pathway participates in maintaining genome stability. NHEJ is a critical repair pathway not only for spontaneous DSBs generated in unattended way but also in the physiological ones generated during such V (D) J and CSR mechanisms.

5.1.1. Mechanism of NHEJ

The DNA end protection is a key regulator in the DNA repair by the NHEJ. It is ensured by the binding protein (53BP1) that inhibits the nucleolytic activity at the DNA ends. The activity of 53BP1 requires the interaction with RAP1 interacting factor 1 homolog (Rif1) and p53 protien1-Tudor interacting protein (PTIP) (Chapman et al., 2013, p. 1; Zhang et al., 2017). Recent studies demonstrate other molecules, the shieldin complex, downstream of 53BP1, Rif1 and PTIP, implicated in DNA ends protection to promote DNA repair by the NHEJ pathway. Shieldin complex is composed of SHLD1 (c20orf196), SHLD2 (FAM35A), SHLD3 (OTC-534A2.2) and Revertibility protein homologue (REV7) (Noordermeer et al., 2018). This complex was reported to localize with the DSB. Its activity is dependent of 53BP1 and RIF1. Analysis of SHLD2 showed a similarity in function with RPA, able to bind the SSDNA. Deficiency in CSR and extensive resection were observed in the absence of the shieldin complex (Noordermeer et al., 2018). Protection of the DNA ends and the presence of 0-4bp of homology between DNA ends activate the NHEJ process which can include DNA end processing steps. Blunt and compatible DNA ends can be directly joined. In contrast, DSBs presenting incompatible DNA ends or modified nucleotides requires DNA end processing.

NHEJ is initiated by symmetric fixation of the heterodimer Ku70-Ku80 proteins at the DNA ends, which forms a ring that protects the DNA ends from resection and is considered as the key player in the NHEJ pathway. Ku70-Ku80 stabilizes the DNA ends by limiting their mobility and keeping them close each other. Ku is the challenger of DNA ends binding molecules because they are characterized by high affinity to DNA ends (Ropars et al., 2011). Ku70 and Ku80 are very abundant in the cell generating competition between DNA DSB repair pathways

License CC BY-NC-ND 4.0

(For review (Zahid et al., 2021)). Fixation of the heterodimer Ku70-Ku80 on the DNA ends recruits the DNA-PKcs which binds approximately 10bp away from the DNA extremities (Figure 24).

Activity of DNA-PKcs is regulated through ATM-induced phosphorylation. Interaction of the DNA-PKcs with the Ku molecules activates the kinase activity implicated during the DNA repair (Dynan and Yoo, 1998). In addition, it has been shown that DNA-PKcs can be auto phosphorylated, which is important for the induction of the DNA end ligation (Uematsu et al., 2007). Phospho-DNA-PKcs initiates phosphorylation and recruitment of Artemis eventually necessary for hairpin structure opening at DNA ends through its endonuclease activity, XRCC4 and XLF (cernunnos) (Drouet et al., 2006).

Another factor reported is the Werner syndrome protein (WRN) which interacts with XRCC4/LIGIV complex known as (X_4L_4) by its exonuclease activity in DNA ends processing (Kusumoto et al., 2008).

Finally, after DNA end processing, DNA ligation is initiated by LIGIV enzyme, the XRCC4 and its cofactor XLF which shares similarity with XRCC4 (Riballo et al., 2009). XRCC4 stimulates the LIGIV, activates the DNA ligation and along with XLF, facilitates the filling of the broken DNA ends by its interaction with the polymerase mu and lambda (pol λ, μ) (Akopiants et al., 2009). A new factor implicated in the NHEJ DNA repair pathway identified is PAXX, which was detected to cooperate with XRCC4 (Ochi et al., 2015). This factor is activated in the case of XLF depletion, which then replaces its function (Liu et al., 2017). In the majority of cases, the junctions generated at the ligated ends by the NHEJ pathway are blunt (no insertion, no deletion) or with some indels.

License CC BY-NC-ND 4.0

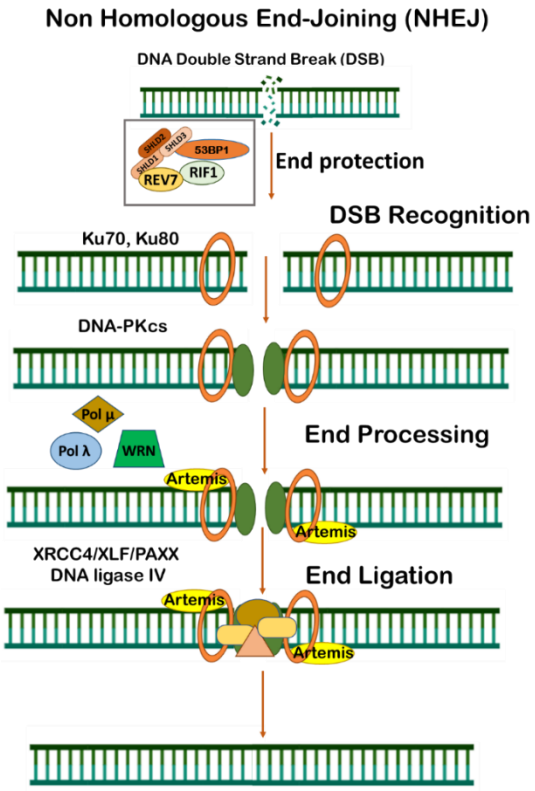

Figure 24: Schematic representation of the NHEJ repair pathway.
DNA end protection is ensured by the recruitment of 53BP1, Rif1 and the shieldin complex to the DNA ends. DSB is recognized by the heterodimer Ku70-Ku80 which form a ring on the DNA ends and leads to stabilize the DNA ends, Ku70-Ku80 recruits the DNA-PKcs. Phosphorylation of DNA-PKCS recruits the Artemis, WRN and Polμ, λ and then molecules implicated in the final step of DNA repair ligation XRCC4, XLF PAXX and the ligase IV enzyme to ligate the ends on the DSBs.

5.1.2. Alteration of NHEJ

Alteration of NHEJ activity and the defect of NHEJ components due to inherited mutations lead to pathologies development.

In human, primary immunodeficiency in Severe Combined Immunodeficiency (SCID) can result from Artemis deficiency (Moshous et al., 2001). These patients are also characterized by the increased levels of sensitivity to ionizing radiation (Michael Lieber pmc2011) and in addition they can develop other specific phenotype like stunting and microcephaly (Chinn Ik and Wt 2015).

Ligase IV syndrome, is a very rare autosomal and recessive hereditary disease, till 2009 only 28 cases reported, we can mention also a little number of patients were not reported and treated by the transplant of HSC. Patients with LIGIV deficiency are characterized by microcephaly, increased in the frequency of 7:14 translocations, immunodeficiency and sensitivity to ionizing radiation as reviewed in (Altmann and Gennery, 2016). These patients are able to develop other complications such as lymphoblastic leukemia. To more characterize

License CC BY-NC-ND 4.0

this syndrome, mouse models deficient for LIGIV were developed to reproduce the syndrome. Results showed symptoms very similar to human especially the mouse model evolved by Nijnik and Rucci (Altmann and Gennery, 2016; Nijnik et al., 2007; Rucci et al., 2010). In addition, *in vitro* human cell line of LIGIV patients showed increased sensitivity to irradiation (Altmann and Gennery, 2016). In mice, deficiency in the NHEJ molecules such as LIGIV in addition to p53 defect (LIGIV-/P53-) leads to alteration in the neurogenesis and lymphomas development and results in the death of mice due to pro-B lymphomas (Frank et al., 2000). In These mice, lymphomas develop in a RAG dependent manner and the translocation of MYC oncogene to the *IgH* locus after the usage of the Alt-EJ DNA repair pathway (Nussenzweig and Nussenzweig, 2010). Alt-EJ leads to genome instability resulting from translocations or deletions in the chromosomes (Yu et al., 2020).

XLF or cernunnos is a core factor of the NHEJ pathway. Patients with XLF deficiency, present lymphopenia with a moderate decrease in B and T cells. This phenotype was also observed in *XLF-/-* mouse model, with an accumulation of subefficient rearranged population in the thymus during the TCR repertoire generation in addition to DSBs accumulation (Roch et al., 2019).

In human, deficiency in the DNA-PKcs is characterized by classical SCID (van der Burg et al., 2009). In mice, it was shown that deficiency in the DNA-PKcs leads to immunodeficiency disease. It is important to mention that the presence of DNA-PKcs mutant unable to auto phosphorylate and to phosphorylate substrates is lethal, thereby indicating that the activity of DNA-PKcs is more important than just its presence. In addition, Cells displaying inactive DNA-PKcs are more sensitive to ionization and irradiation leading to neuronal cells apoptosis which indicate an additional function of DNA-PKcs in the cell (Jiang et al., 2015).

Ku80 is important protein during the NHEJ, it was shown that mouse model defective for Ku80 (*Ku80-/-*) is characterized by high rate of genome aberrations and DNA translocations resulting from the non-controlled high mobility of the broken DNA ends and promotes cancer development. The mouse model with *Ku80-/-* and *p53-/-* develop cancer especially at the Pro-B cell stage (Difilippantonio et al., 2000, p. 80).

5.2. Alternative End Joining DNA repair pathway (Alt-EJ)

Alternative End joining (Alt-EJ) is also known as microhomologies mediated End Joining (MMEJ) (Truong et al., 2013) and is considered as a back-up DSB DNA repair pathway (Iliakis et al., 2015). This process has been shown to be active in cells deficient for molecules implicated in NHEJ, for example deficiency of Ku and DNA ligase IV (Wang et al., 2006, p. 1).

License CC BY-NC-ND 4.0

It is characterized to be slower than NHEJ (Han and Yu, 2008) and with a low rate of efficiency (*Encyclopedia of Cancer*, 2018). This pathway is able to ligate the DNA ends thanks to the presence of microhomologies between the DNA sequences (from 2bp to 25bp in microhomology length). Alt-EJ is also described inserting some nucleotides at junction, in the most common cases, more than 10 bp (Chang et al., 2017; Iliakis et al., 2015).

The dependency of intermediate end resection of the Alt-EJ and usage of specific molecules different from those of NHEJ indicates a specific physiologic function of this DNA repair pathway in addition to its function (Sfeir and Symington, 2015). It has been demonstrated that Alt-EJ is an active pathway even in the presence of NHEJ and HR (Truong et al., 2013), also during V (D) J recombination and CSR (Corneo et al., 2007). Alt-EJ due to the usage of small microhomologies and the capacity to insert new nucleotides at the break site is not able to restore the original sequence of DNA as HR do with the usage of long homologies.

5.2.1. Mechanism of Alt-EJ

Alt-EJ is a pathway dependent on DNA end resection, it is initiated by the activity of Poly ADP-ribosylation protein (PARP1) that contributes to detection and recognition of the DNA DSB and promotes the Alt-EJ DNA repair pathway (Robert et al., 2009).

PARP1 then activates CtIP and the MRN complex which are required for resection of the DNA ends at the break sites to generate single stranded DNA (ssDNA), within 15pb to -100pb in length, on the 3' extremity (Masani et al., 2016). Using the same strategy used in HR pathway, phosphorylated CtIP recruited at DNA ends stimulates the endonuclease activity of the MRN to accomplish the resection (Anand et al., 2016). PARP1, MRN and CtIP cooperate with the Excision repair protein (ERCC1/XPF) to align and digest the tail at the DNA end to facilitate the recruitment of downstream proteins such as polymerase theta/Q/Θ (Figure 25) (For review ((Caracciolo et al., 2021)).

Polymerase Θ is a member of the polymerase A family, encoded by *POLQ* gene and implicated in replication and in DSB repair (Yousefzadeh and Wood, 2013). Studies of models characterized by polΘ mutations in addition to NHEJ protein mutations show undetectable activity of the Alt-EJ, these results denote the importance of polΘ in the Alt-EJ pathway (Chan et al., 2010). In addition, PolΘ is characterized by resulting in the insertion of more than 10 nucleotides at DSB ends during the DNA repair (Seki et al., 2004). PolΘ protein is characterized by the presence of a specific domain able to bind and block RAD51 (Ceccaldi et al., 2015). PolΘ is known to promote synapsis formation and strand annealing. The final step is the DNA end ligation by Ligase I (LIGI) and Ligase III (LIGIII) and their cofactor the XRCC1.

License CC BY-NC-ND 4.0

LIGIII have a more prominent role compared to LIGI as shown by the decrease the Alt-EJ in case of LIGIII depletion whereas the depletion of LIGI does not affect the efficiency of this DNA repair pathway (Simsek et al., 2011).

A recent study, in cell lines with DNA repair reporter system showed that 5hmC binding, embryonic stem cell specific-protein (HMCES) specifically enables DNA DSB repair through Alt-EJ pathway using microhomology sequences during CSR (Shukla et al., 2020).

Alt-EJ pathway has been shown to be associated with translocations and DNA deletions leading to the generation of tumors, especially breast cancer and leukemias (Decottignies, 2013), based on the detection of microhomologies usage in DNA repair which related with the Alt-EJ pathway (Stephens et al., 2009; Zhang and Rowley, 2006). In this sense, depletion of LIGIII in cell line showed decrease in the translocation frequency, In contrast, LIGI depletion did not show a decrease in the translocation rate (Simsek et al., 2011).

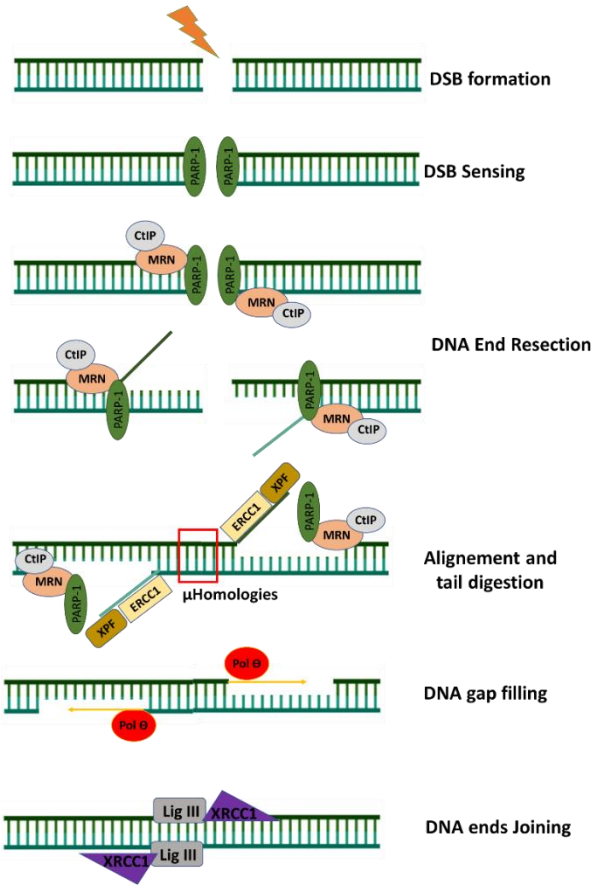

Figure 25: Schematic representation of the Alt-EJ mechanism.
DSB sensing by PARP1 leads to the recruitment of CtIP and MRN which proceed to the DNA end Resection. In the third step, tails are digested by cooperation with ERCC1 factor and gaps in the strand are then filled by the activity of PolΘ. Finally, DNA ends are ligated by the ligase III (LIGIII) and his cofactor the XRCC1 figure adapted from (Caracciolo et al., 2021).

License CC BY-NC-ND 4.0

5.2.2. Alteration of Alt-EJ

Alt-EJ is associated with chromosomal translocation (Kabotyanski et al., 1998; Simsek et al., 2011; Soulas-Sprauel et al., 2007) and genome instability (Caracciolo et al., 2021) it is particularly active in cases where NHEJ pathway is deficient (Kabotyanski et al., 1998, p. 4; Soulas-Sprauel et al., 2007) but can even be active in cells with proficient DSB DNA repair pathways (either HR or NHEJ). Data of several studies demonstrate that alteration in the levels of Alt-EJ and NHEJ molecules conduct to resistance to chemotherapy in leukemic cells (For review (Danielle Caracaloo et al 2021)).

A Study evaluating the effect of PARP1 depletion on Alt-EJ process showed its important function in this pathway. Briefly, PARP1 depletion resulted in reduction in the level of microhomology sequence usage during DSB repair (Robert et al., 2009).

LIGI and LIGIII have important and redundant function in Alt-EJ, in the condition of LIGIV depletion which abrogates the NHEJ pathway, this redundant function results in normal CSR levels even in the absence of one of these ligase (Masani et al., 2016).

CSR junctions show shorter microhomology sequences, in the absence of XRRC1, suggesting its involvement in Alt-EJ (Saribasak et al., 2011). Involvement of XRCC1 seems not crucial to Alt-EJ as CH12F3 cell lines depleted for XRCC1, in a LIGIV inactivation context, present CSR achievement at a comparable level that in the case of LIGIV depletion only. Also, defect in HMCES an Alt-EJ component leads to a CSR defect (Shukla et al., 2020).
Pol theta was shown to be upregulated in cells occurring CSR and SHM and its deletion results in 60% decrease in SHM levels (Zan et al., 2005).

5.3. Homologous Recombination DNA repair pathway (HR)

HR is active in the transient diploid stages of cell cycle from the DNA replication in the S phase cell cycle to the mitosis. HR constitutes the predominant DSB DNA repair pathway during the S and G2 cell cycle phases. It is characterized by using long homology between sequences of sister chromatids that serve as a template during the mechanism of repair. HR is known to repair DSB with a high fidelity and the minimum of incorporated errors (Thompson et al 2012). Thus, HR is the more conservative DSB DNA repair pathway illustrating its importance to be maintained at normal levels to maintain genome integrity, its alteration may lead to tumor cells generation.

License CC BY-NC-ND 4.0

5.3.1. Mechanism of HR

HR initiation and activation are dependent on extensive DNA end resection (presynaptic stage) which is accomplished by the MRN complex and CtIP. The CtIP and MRN complex activates ATM and activated ATM initiates a DDR signalization cascade and the recruitment of Exonuclease 1 (Exo1) implicated also in the DNA end resection (Tomimatsu et al., 2012, p. 1). MRN and ATM complex cooperate together and DNA resection is also done by the exonuclease activity from Mre11. Furthermore, Dna2 and BLM, characterized by their helicase activity, permit to ensure the long DNA strand resection (Nimonkar et al., 2011). The resection process generates long single strand 3' extremity (about 100bp). In the following step, the generated single stranded DNA is coated by the Replication protein A (RPA). End resection and RPA coating active the ATR complex at the DNA damage site which phosphorylates the CHK1 protein (Rhind, 2009; Shiotani and Zou, 2009). Then the coating of the single strand (RPA) need to be displaced. This displacement is ensured by RAD51 recruited to the damage site by BRCA2/PABL2. BRCA2 is recruited by BRCA1 and the BRCA1-associated RING domain protein 1 (BARD1) essential for BRCA1 stabilization. this process leads to the final step of DNA repair which consists of searching for homology of the single strand in the near chromosome, normally the sister chromatid, and leads to D-loop formation (Figure 26) (For review (Sun et al., 2020)).

The final step of the HR depends on the annealing strand. The Synthesis-dependent Strand Annealing (SDSA) results in non-crossover production and dissolves the D-Loop after short DNA synthesis. The Break Induced Replication (BIR) generates a replication fork from the D-Loop and results in the loss of heterozygosity without crossover. The Double Strand Break Repair (DSBR) of the DNA ends of DSB can results in double Holiday junction generation (dHJ) inducing crossovers or repair without induced crossover through the BLM mediated mechanism (For review (Elbakry and Löbrich, 2021)).

In somatic mammalian cells, production of crossover is rare and in the majority of cases, the DSBs are repaired by the dHJ and BLM mediated mechanisms (Plank et al., 2006).

License CC BY-NC-ND 4.0

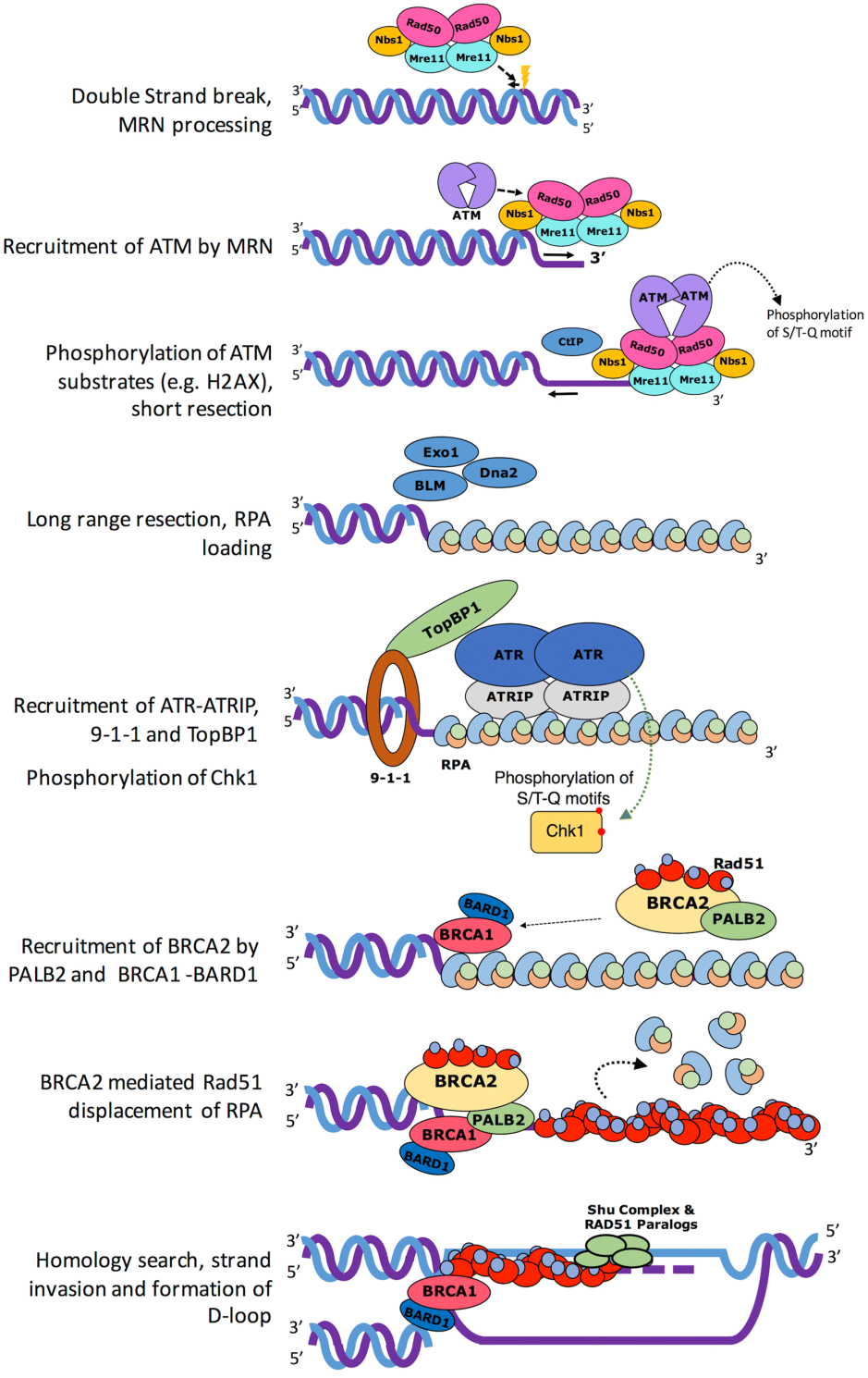

Figure 26 : Schematic representation of presynaptic step of HR pathway.
DSB sensing and recognition is achieved by the MRN complex which recruits activated ATM, phosphorylates H2AX and all together cooperate to generate short resection converted to long resection by the EXO1 Dna2, BLM activities. At this stage recruitment of ATR, ATRIP, 9-1-1 and TopBP1 results in the phosphorylation of checkpoint proteins (DDR response). Furthermore, BRCA2 is recruited to the damage by PALB2, and BRCA1-BARD1 with the Rad51. RAD51 contributes to the displacement of RPA with BRCA2, resulting in D-Loop formation with homology sequences repair the DSB, Shu complex is the equivalent of RAD51 and present in yeast (Sun et al., 2020).

License CC BY-NC-ND 4.0

5.3.2. Alteration of HR

It is a very well controlled mechanism due to its importance and his characteristic of high fidelity especially during cell replication in the S and G2 phases to maintain genome integrity. Alteration in the levels and molecules of HR mechanism can lead to cell death or can contribute to cancer development. Additionally, deficiency in HR molecules especially BRCA1/2, the most studied proteins, can be detected in diverse cancer types (Wen et al., 2022). Deficiency in HR pathway leads to the activation of the other DNA repair pathways such as NHEJ and Alt-EJ (Scully et al., 2019).

In multiple myeloma, HR was showed to be detected at high levels due to the Ikaros Zinc Finger protein 1 (IKZF1) which has been demonstrated to play an important role in promoting the HR in this cancer by interacting with CtIP (Liu et al., 2022).

5.4. Single Strand Annealing DNA repair pathway (SSA)

Repair of resected DNA ends can occur by SSA in presence of intermediate DNA end resection in contrast to HR that requires long single strand extremity.

Presence of repeated motif sequences on the DNA end in absence of donor sequence activates repair by SSA. Repeated sequences constitute the substrate to the SSA molecules. SSA is independent from the RAD51 activity (Deng et al 2014). DNA repair can be supported by SSA when RAD51 or BRCA1 are nonfunctional and RPA on the DNA end inhibits the microhomology interaction required for the Alt-EJ (Scully et al., 2019).

As in HR, DNA ends are processed by nucleases and helicases such as WRN/BLM/Dna2 to generate 3’ single strand at DNA extremity. RPA coat the single strand which lead to the activation of RAD52 for RPA displacement and recruitment of the endonucleases like ERCC1 and XPF. These latter form a complex to eliminate the single strand. RAD52 protein mediates the activity of the DNA end cleavage complex which gives the accessibility to synthetize and ligate the complementary sequence via LIGIII (Figure 27) (Motycka et al., 2004).

SSA is considered as a mutagenic DNA DSB repair system because the repeated and the intervening sequences are partially eliminated during the cleavage step (Blasiak, 2021). Mutations introduced by SSA lead to cancer development as reviewed in (Blasiak, 2021). In 2019, Scully et al demonstrated that SSA can be an error free repair pathway when its activity occurred in a blocked replication fork with DNA segment duplication. In this situation, usage of SSA allows the deletion of one segment copy (Scully et al., 2019).

License CC BY-NC-ND 4.0

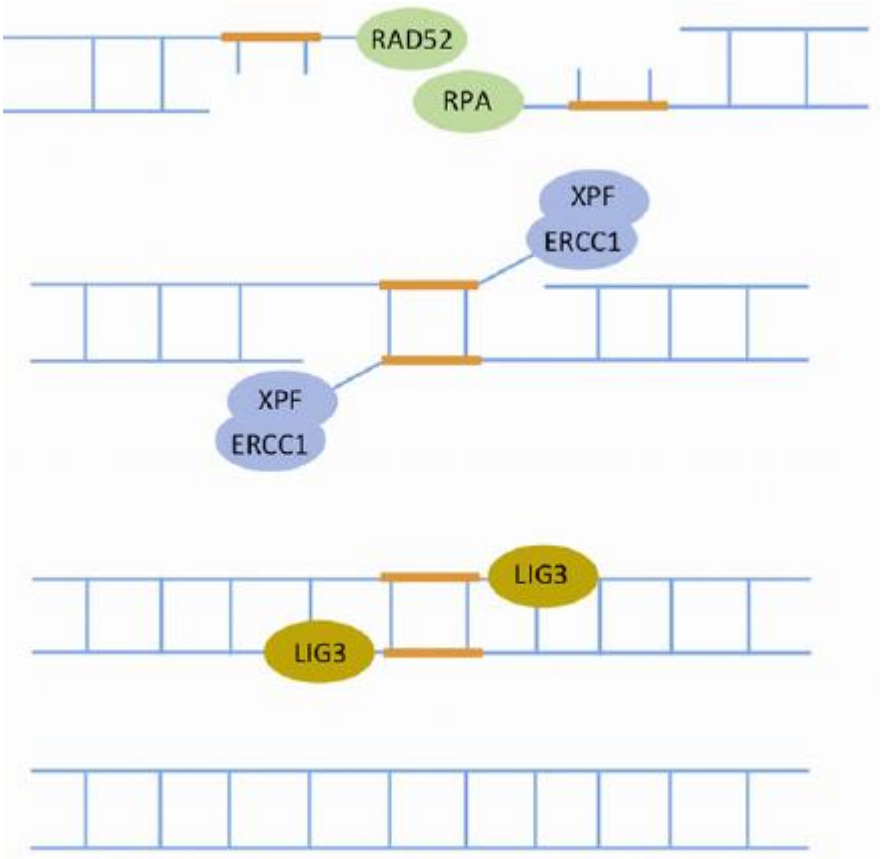

Figure 27: Schematic representation of the SSA pathway.
Generation of DSBs flanked by homologous repeats (orange boxes) activate the repair via SSA pathway. Recruitment of the RAD52 is the key in SSA, RAD52 cooperates with RPA by their nuclease and helicase activities to generate single stranded DNA which is cleaved by the ERCC1/XPF complex. Finally, DNA ends are ligated by the LIG3 (LIGIII) activity resulting in shorter DNA compared to the original sequence with loss of some region.

License CC BY-NC-ND 4.0

6. Junction structure after DNA ligation

DNA end ligation generates a junction and DNA structure at the junction depends on the employed DSB repair pathway. Analysis of junction structure can reveal the usage of a particular DSB system rather the others (Figure 28).

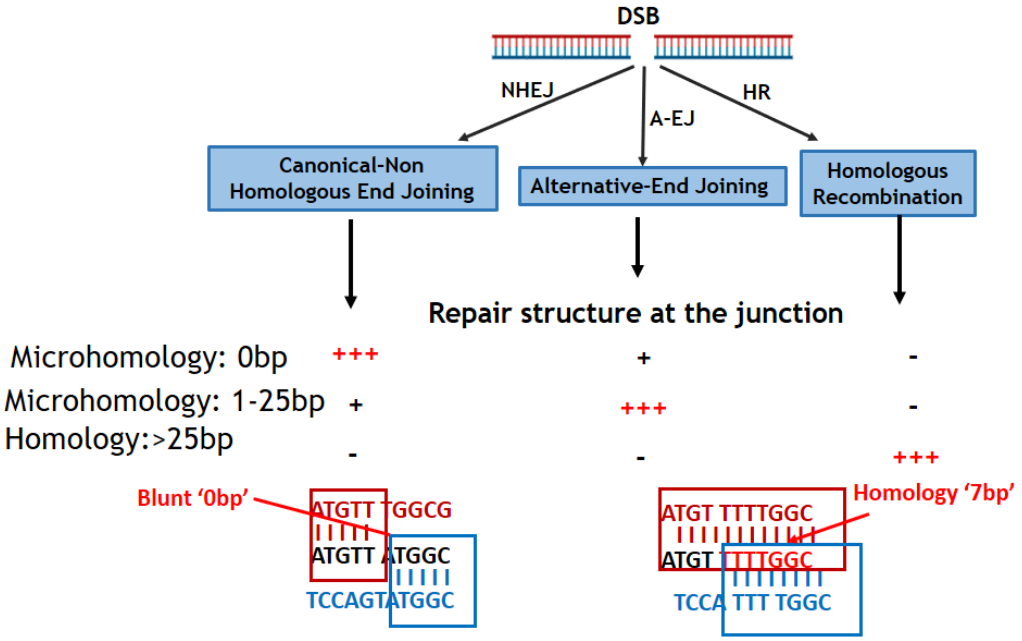

Figure 28 : Schematic representation of the junction structure generated by DSB repair.
DSBs activate DNA repair pathways (NHEJ, A-EJ or HR) characterized by the size of homology in the resulting repair junction. NHEJ-produced junctions are in the majority blunt (with non-homology), the Alt-EJ system produces junctions with more homology usage (1-25bp) called μhomologies, and finally the HR generates junctions with long homology longer than 25bp.

7. Choice of the DSB DNA repair pathway in the cell

Choice of the DSB DNA repair pathway can be influenced by different factors: sequence and structure of the DNA ends, DNA end resection, which constitutes an important factor regulating the choice of DSB repair, the cell cycle phase and the chromatin marks at the DSB.

The DSB inducing mechanism itself can also influence the DNA repair choice. For example, in normal situation V (D) J is restricted to be repaired by NHEJ. Even in the presence of HR or the Alt-EJ, even the predominance of molecules (G1 phase) of this repair pathway. In addition, the structure of at the coding DNA ends, hairpin structure, orient the NHEJ usage due to the requirement of Artemis.

In some cases, alteration of the DSB inducing mechanism itself can affect the choice of DSB DNA repair pathway. For example, DSB during V (D) J mechanism can be repaired by

License CC BY-NC-ND 4.0

unconventional ways due to the mutation of the post cleavage complex which destabilizes this complex and promotes the DNA repair via HR and Alt-EJ. Also, when the RAG activity is not sufficient for the NHEJ activation, it leads to Alt-EJ activation and usage (For review (Deriano and Roth, 2013)).

7.1. DNA end resection modulates the DSB repair pathway choice

DNA end resection process define two major groups of DNA DSB repair, and it can be considered as an important factor regulating the choice of the DNA repair pathway. As detailed before, NHEJ pathway is independent of the end resection and implicates molecules that protect the DNA ends. In contrast, Alt-EJ, SSA and HR depend on DNA end resection from the intermediated stage to the extensive one respectively. This resection is accomplished by the presence of specific molecules. To orient the choice of DNA repair pathway, a real competition exists between these complexes allowing DNA end protection or resection (Figure 29).

First, 53BP1 recruited by the γH2AX to the DSB site, constitutes the major protein contributing to DNA end protection and stimulating the NHEJ DNA repair in DSB foci. In this context, deficiency in both 53BP1 and γH2AX in the presence of KAP1 protein leads to microhomologies ends formation and promotes DNA end resection (Tubbs et al., 2014).

The predominance of Ku can be considered as a repressor of the Alt-EJ pathway during G0/G1 cell cycle phases. In other words, the restriction of resection proteins expression in cells in the G0/G1 phases contributes to favoring NHEJ.

Alt-EJ activity can be reduced by the BLM and EXO1 factors, which are related to the generation of long extension that promotes the HR pathway rather than Alt-EJ in the S/G2 cell cycle phases (Tomimatsu et al., 2014).

DNA end protection can occur via the activity of some complexes downstream of 53BP1. Recently, the Shieldin complex, composed of MAD2L2/REV7 and the three shieldin components SHLD1, SHLD2, SHLD3, was identified. This complex is characterized to be active downstream of 53BP1-Rif1 and has been shown to cooperate and to protect the DNA ends to favor the NHEJ and limit the HR mechanism (de Krijger et al., 2021; Mirman and Lange, 2020; “Shieldin – the protector of DNA ends,” 2019). Shieldin complex binds the single stranded DNA and physically hinds more than 50bp of nucleotides thus inhibiting the access of other molecules to carry out end resection (Noordermeer et al., 2018).

License CC BY-NC-ND 4.0

Additionally, shieldin complex was identified to promote the recruitment of Asteroid homolog 1 (ASTE1), acting downstream of shieldin complex in the NHEJ pathway. ASTE1 is characterized by its endonuclease activity that eliminates the single strand present on the 3' extremity. Defect in CSR mechanism was detected in the absence of ASTE1 (Zhao et al., 2021).

Also, proximity of the DNA ends in DSB site constitutes another factor regulating and influencing the DNA repair pathway choice, since repair by NHEJ requires not distant DNA ends ensured by the activity of Ku70-Ku80 (Chang et al., 2017).

On the other hand, absence of end resection complex actors leads to decrease in HR DNA repair and favors the NHEJ pathway (Liu and Kong, 2021) .

License CC BY-NC-ND 4.0

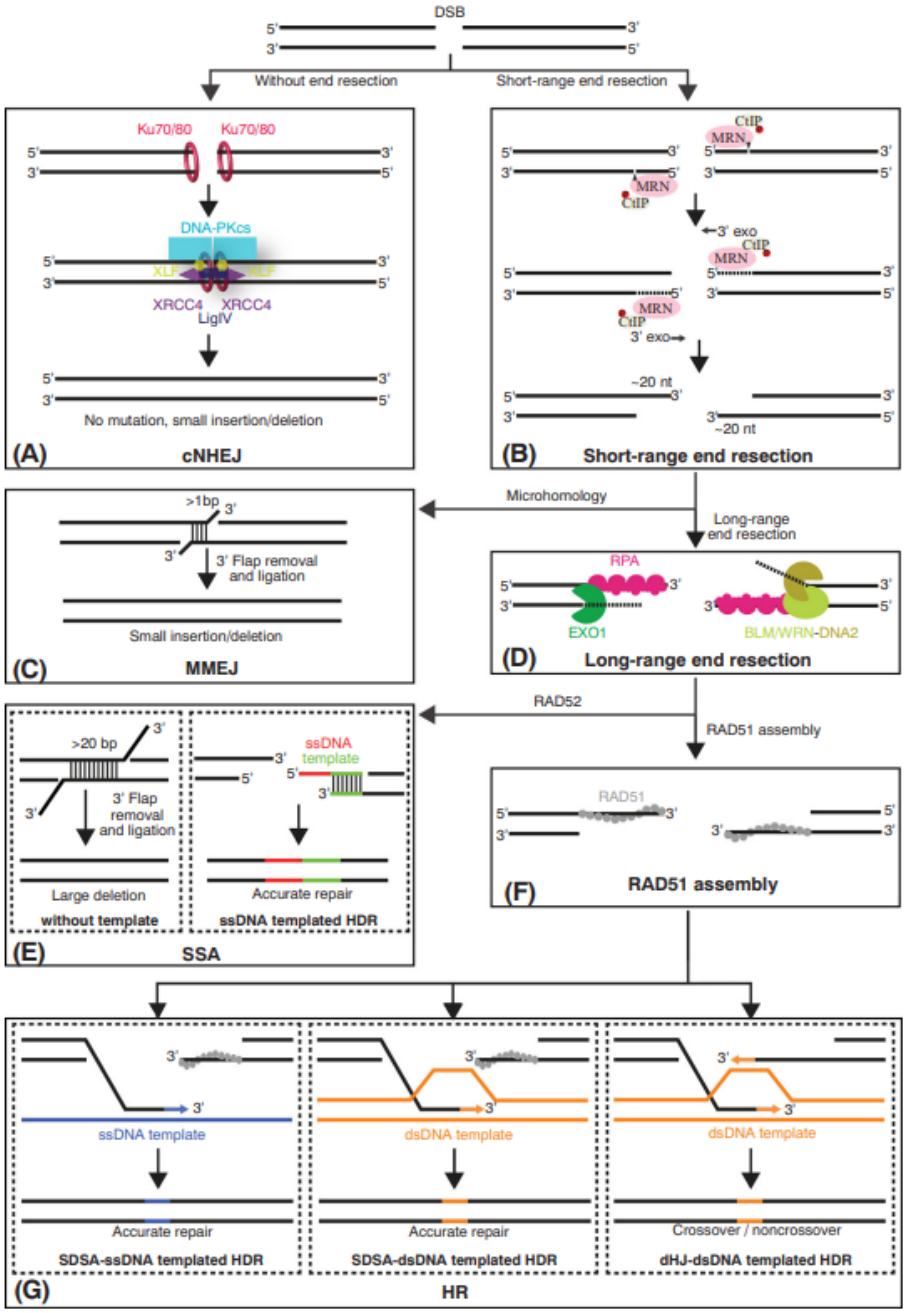

Figure 29: ***representation of how end resection influences the choice of DSB repair pathway choice.***

License CC BY-NC-ND 4.0

7.2. Effect of the cell cycle phases on the DSB repair choice

Cell cycle regulates the DNA repair choice by regulating the levels of expression of concerned molecules (Figure 30). HR activity is restricted to the S/G2 cell cycle phases, when homologous chromosomes are in proximity thereby facilitating the HR pathway. In contrast, in G1 phase and outside of S/G2, NHEJ constitutes the predominant DSB repair pathway in human cells even that 80% of ionized radiation can be repaired by NHEJ in the G2 phase (Zhao et al., 2017).

Activity of HR is regulated during the cell cycle phases in response to several factors. CtIP, the implicated protein in DNA end resection, is predominant in the S/G2 phase I compared to G1 phase (Yun and Hiom, 2009). On the other hand, BRCA1, BRCA2 and RAD51, proteins implicated in the HR pathway, are absent during the G0/G1 cell cycle due to the LIN37, a transcriptional repressor factor of the DREAM family, which regulates their expression level (B.-R. Chen et al., 2021). In addition, ATM is able to promote the HR repair in S/G2 cell cycles due to the presence of a switch from ATM to ATR activity (For review (Shibata and Jeggo, 2021)).

In the S/G2 phases, the Cdk2 protein able to activate and to phosphorylate CtIP and BRCA1 that favors the recruitment of HR molecules rather than NHEJ by its capacity to eliminate the heterodimer Ku70-Ku80 from the DNA ends (Isono et al., 2017, p. 1; Yun and Hiom, 2009).

In addition, the competition between the initiating molecules of each DNA repair pathway (Ku in NHEJ and RAD51/52 in HR) regarding their abundance in the cell can also affect the choice.

The modulator of retrovirus infection (MRI), considered as a DNA repair choice regulator, has the capability to interact with heterodimer Ku70-Ku80 and inhibits the NHEJ pathway to favor HR in the S and G2 cell cycle phases (Hung et al., 2018). In contrast, during the G1 phase this interaction favors the NHEJ pathway (Arnoult et al., 2017; Hung et al., 2018). Contradictory results obtained from the knockdown versus the deletion of the MRI gene indicated that the determination of the MRI function is still a problematic area (Wahsner et al., 2019).

On the other hand, the polϴ enzyme implicated in the Alt-EJ DNA repair pathway is not detected during the G0/G1, in pro-B cells leading to the predominance of NHEJ pathway (Yu et al., 2020).

Other studies showed that transition from one cycle phase to another phase with unrepaired DNA ends can activate the Alt-EJ depending on the presence of the Alt-EJ critical protein pol ϴ. B cells at the pro-B cell stage with a triple deficiency in P53/pol ϴ/XRCC4 are unable to pass from one cell cycle phase to another resulting in accumulation of cells in the G1 phase

License CC BY-NC-ND 4.0

with breaks in the chromosomes which eventually leads to lethality in the coming mitosis (Yu et al., 2020).

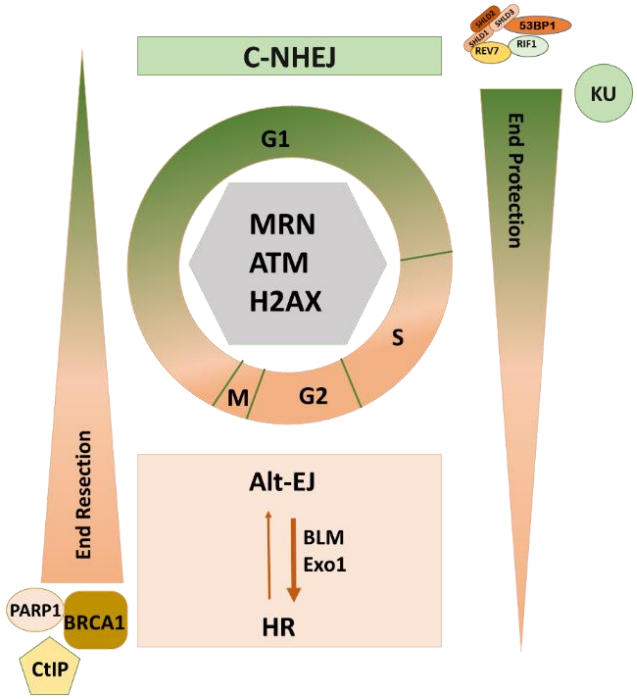

Figure 30: ***Schematic representation of cell cycle effect on DNA repair choice.***
Cell cycle phases affect the choice of DSB DNA repair. DNA end protection molecules (53BP1, RIF1, REV7, shieldin) are predominant especially in the G1 phase lead to the predominance of the NHEJ in this phase. In contrast, molecules of end resection like BRCA1 PARP1 CtIP are predominant in the S and G2 phases and lead to the predominance of HR and Alt-EJ. Orientation of the choice between Alt-EJ and HR is conducted by BLM and EXO1 proteins predominance.

7.3. Effect of chromatin state on DNA DSB repair pathway choice

Chromatin structure plays an important role and strongly influences the orientation of the DSB repair pathway as well as in the signaling of DDR. It was shown that, the heterochromatin form is less sensitive to the H2AX phosphorylation which is limited to the periphery of heterochromatin. γH2AX is detected normally in the euchromatin structure (Figure 31). The reduction of the chromatin compaction levels by inhibiting the deacetylase enzyme (HDAC) of histones results in increase of DDR singling and then H2AX phosphorylation. Studies showed that DSBs in the heterochromatin (packed and inactive form of the chromatin) are mostly repaired by the HR pathway (Goodarzi et al., 2008; Sulli et al., 2012).

License CC BY-NC-ND 4.0

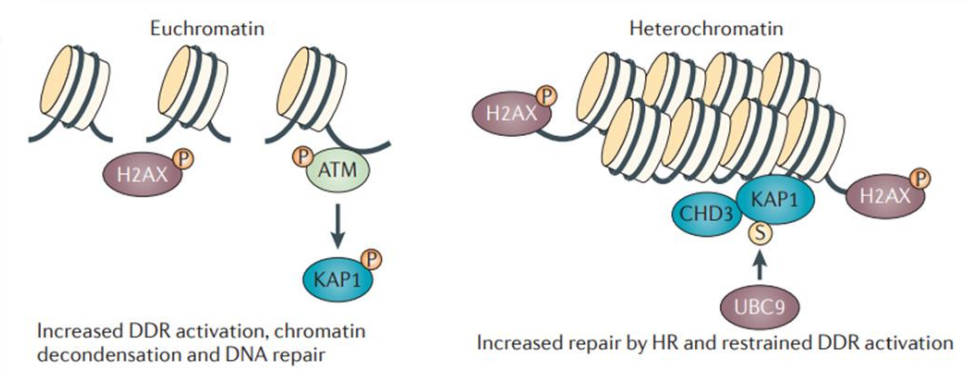

Figure 31: Schematic representation of the influence of the chromatin state and γH2AX and DDR. Euchromatin is sensitive to the phosphorylation of H2AX upon DDR. In contrast γH2AX is limited to the extremity of heterochromatin and affects the DDR and the DNA repair (Sulli et al., 2012).

Additionally, epigenetic marks such as histone acetylation or methylation, influence DNA DSB repair system choice.

The mono and demethylated form of H4K20 (H4K20me1/2) play an important role in the orientation of the DNA repair choice. 53BP1 is a protein playing an important role in the promotion of NHEJ as DSB DNA repair. 53BP1 presents a domain which is able to interact with the H4K20me2. H4K20me2 is a constitutive mark present in the genome formed from H4K20me1 by the activity of the methyltransferase KMT5 (Simonetta et al 2018). Addition of new histones during replication in the S phase results in the dilution of H4K20me2 which explains the efficiency recruitment of 53BP1 in the G1 in contrast to S and G2, the cell cycle phases characterized by the predominance of HR pathway. Binding of 53BP1 is also promoted by the H2AK15ub, ubiquitylation of H2AK is ensured by the RNF8 and RNF168 recruited to the damage site during the DDR by MDC1. 53BP1 binding and Rif1 cooperate to inhibit binding of resection such as CtIP, BRCA1, Dna2 and EXO1 promoting the end resection and then the NHEJ pathway (Figure 32 a) (For review (Fontana et al., 2018).

Histones can also be in an acetylated form, acetylation occurs by two important enzymes, hMOF and KAT5. H4K16ac presence is associated to an active transcriptional state of the chromatin. Its function in influencing and orienting the DSB is not well established. A recent study demonstrated that in the S cell cycle phase, preexisting H4K16ac in the active form of chromatin (euchromatin) functions to increase the recruitment of HR to DSB sites (Horikoshi et al., 2019). H4K16ac promotes the HR response by stimulating the BRCA1 on the DSB site and, on the other hand, it inhibits the 53BP1 binding which in turn, inhibiting end protection, inhibits NHEJ pathway (Figure 32 b) (Tang et al., 2013).

License CC BY-NC-ND 4.0

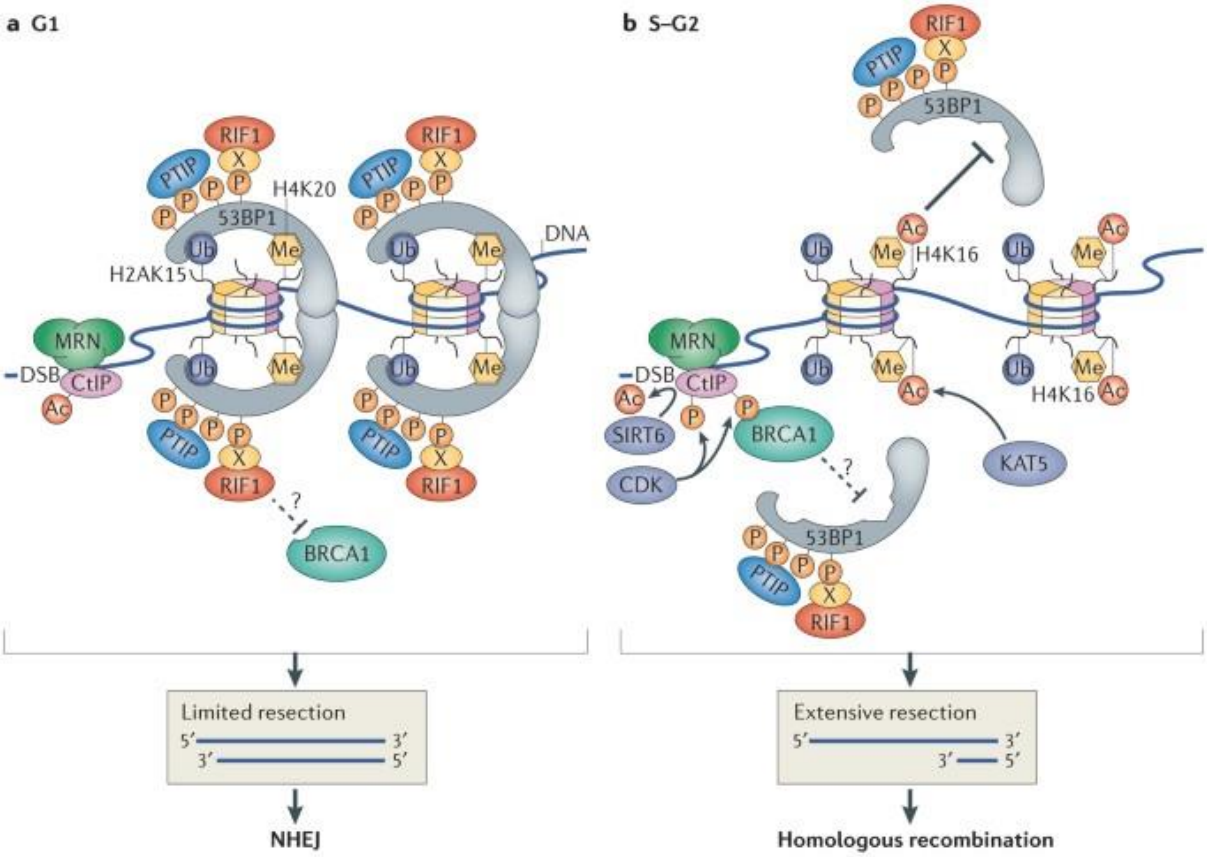

Figure 32: Histone modification impact the DSB repair choice.
A- During the G1 cell cycle methylation of the H4K20 promotes the recruitment of 53BP1 and then the actors of DNA end resection which favor the repair by NHEJ pathway. B- the chromatin in the S-G2 cell cycle is different with enrichment of H4K16ac that inhibit the 53BP1 and favor the recruitment of the actors implicated in DNA end resection favoring the HR pathway (Panier and Boulton, 2014).

Additionally, Trimethylation of the lysine 36 in the histone 3 (H3K36me3) presents at the DSB site leads to RAD51 accumulation and then orients the repair of the DNA end by the HR pathway (Daugaard et al., 2012). H3K36me3 also known to enable recruitment of CtIP molecule via LEDGF reinforcing the HR response (Daugaard et al., 2012). Recently it was shown that a cross talk exists between H4K16ac and H3K36me3 and promotes the DNA repair to HR, H3K36me3 induced by the DNA damage promotes the interaction of LEDGF with KAT5 which lead to the H4K16ac generation (Figure 33) (Li and Wang, 2017).

License CC BY-NC-ND 4.0

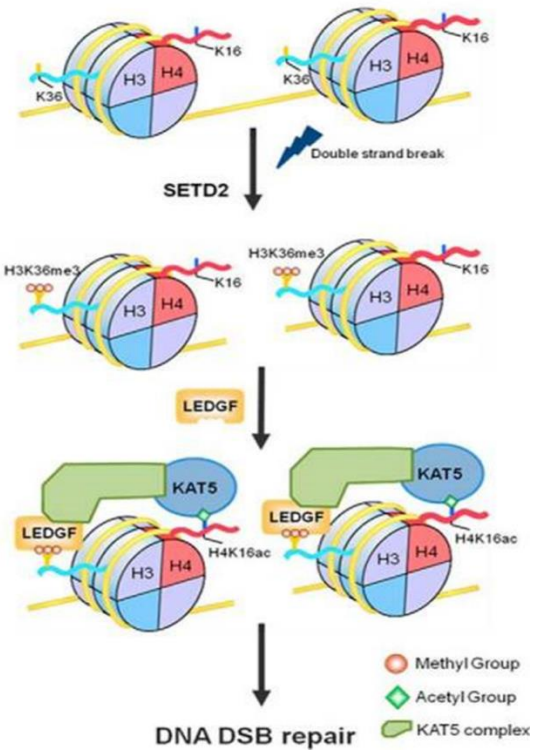

Figure 33: A cross talk exist between H3K36me3 and H4k16ac.
DNA damage induces the trimethylation of H3K36 by the SETD2 enzyme. This methylation recruits the LEDGF. LEDGF able to interact with KAT5 that acetylates the H4K16. Together, they promote HR repair by inhibiting of the DNA end resection (Li and Wang, 2017).

License CC BY-NC-ND 4.0

Chapter III: B Lymphomas

B Lymphomas are divided into two major groups, the Hodgkin Lymphoma (HL) and Non-Hodgkin Lymphomas (NHL). This latter represent majority of B cell cancers and about 3% of all cancers worldwide (Thandra et al., 2021). NHL include Chronic Lymphocytic Leukemia (CLL). NHL account also for follicular Lymphoma (FL), marginal zone Lymphoma (MZL), Burkitt's Lymphoma (BL), hairy cell leukemia, etc...

A. Chronic Lymphocytic Leukemia (CLL)

1. Overview on CLL

CLL is an incurable malignant blood disease, and known as the most common leukemia with an incidence of 4.9/100000 person per year using the lasted update of SEER ("Chronic Lymphocytic Leukemia - Cancer Stat Facts," 2021). CLL represents in United States from 25% to 30% of cancers ("Chronic Lymphocytic Leukemia - Cancer Stat Facts," 2021) and very recurrent in western countries.

CLL affects males more than females with a rate of 1.7/1. Most common in elderly persons with an age average of 72 year (70 years in men and 74 years in females). CLL is rare in person under the age 50 years (Molica, 2006), however CLL detection in younger population is increasing due to the raise in the routine blood testing (Mauro et al., 1999). Based on the World Health Organization 'WHO', CLL can be divided into three subtypes: typical CLL, prolymphocytic Leukemia 'PL' and 50% of cases are combined CLL/PL.

CLL is characterized by the proliferation of mature clonal CD5+ malignant B cells and their accumulation in the bone marrow, peripheral blood and SLO such as lymph nodes and spleen.

Clinical evolution of this pathology is very heterogeneous, it can be variable from months to decades. Some patients with CLL are asymptomatic, in contrast, other patients develop an alteration in their general health and need to be treated.

2. Clinical and biological characteristics

2.1. Diagnostic

CLL patients in the majority of cases are asymptomatic and CLL is detected during routine blood testing, in contrast, some of patients can develop one or more symptoms (Figure 34).

License CC BY-NC-ND 4.0

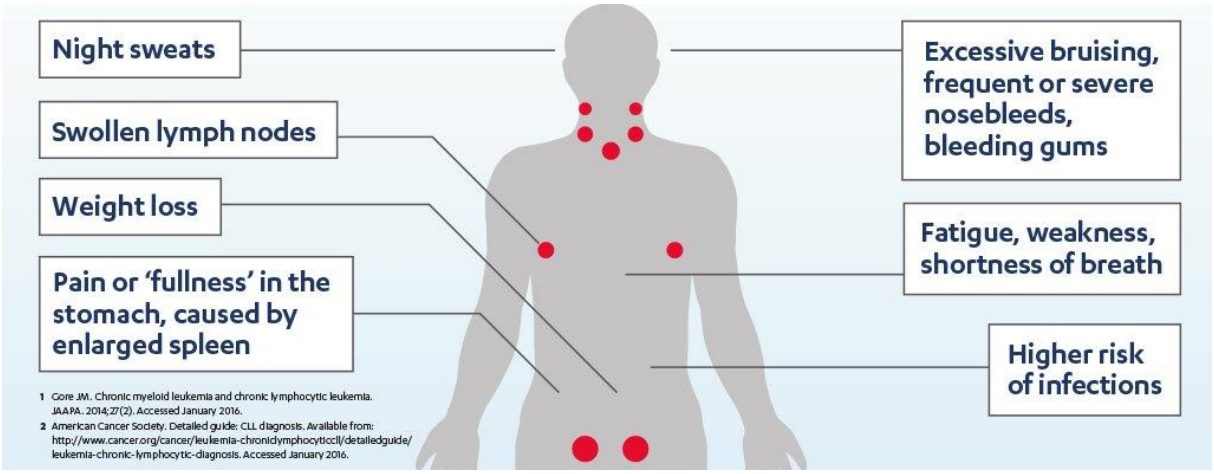

Figure 34: Signs and symptoms of chronic Lymphocytic leukemia.

To confirm the CLL diagnosis, different criteria are measured:

-Blood cell count with hyperlymphocytosis ≥ 5000 B cells /µl and during three months at least.

-Blood smear characterized by the presence of cytopenia. Morphological examination of the blood smear is an important step and shows small mature lymphocytes very close to the normal lymphocytes. These lymphocytes have nevertheless atypia, such as a less dense chromatin, arranged in large clumps and without a visible nucleolus. Gumprecht nuclear shadows or smudge cells, found as cell debris, are other characteristic morphologic features found in CLL (for review (Hallek and Al-Sawaf, 2021).

-Immunophenotyping of cancer cells using a dedicated panel of markers brings out cells CD5+, CD23+, CD20+ and CD19+, FMC7- (Rawstron et al., 2018). Clonality of B cells can be confirmed by flow cytometry using antibody targeting the κ or λ light chain of Ig.

CD5 marker is normally expressed on T cells and the rare B1 population of B cells in adult. It is important to mention that CD5 marker can be expressed in another lymphoma type such as mantle lymphoma. CD23, a marker for activated B cells and it is characterized by the low affinity receptor for IgE. CD20 is found at lower level in CLL cells compared to the level of expression on normal B cells.

Presence of cytopenia induced by bone marrow infiltrate reinforce the CLL diagnosis even the count of B cell detected is lower than 5000 cells/µl. Absence of cytopenia with low number of B cells <5000 cells/µl is diagnosed as Monoclonal B-lymphocytosis (MBL). It was shown that MBL can develop into CLL with a rate of 1-2% per year (Rawstron et al., 2008). Other markers can be used in order to refine the diagnosis CLL such as CD79b, CD81, CD43, CD200, CD10, or ROR1 (Rawstron et al., 2018).

License CC BY-NC-ND 4.0

To facilitate the confirmation of CLL diagnosis, it was established a score system: Royal Marsden Hospital (Matutes score). According to this system 1 point is given to each marker CD5 and CD23 when they are positive. In contrast, 1 point is given to each of FMC7 and CD22 when they are negative (Table 3). A total score ≥ 4 points define CLL disease, NHL is diagnosed with a score obtained from 0-3.

Table 3: Matutes score in in CLL diagnosis.

Antibody	1 point	0 point
Surface Ig	Low expression	High expression
CD5	+	-
CD23	+	-
FMC 7	-	+
CD79b or CD22	- Or low expression	+ Or high expression

The National Cancer Institute-Working Group (NCI-WG) updated the Matutes score in CLL diagnosis. With this new updated CLL diagnosis, CLL is confirmed when blood count ≥5000 B cells/µl, co-expression of CD19, CD5, CD23 and low levels of CD79b and Igκ or Igλ.

2.2. Prognostic

Mutational status of *IgHV* genes

CLL cells express low level of Ig on their membrane, in the vast majority of cases, Ig are IgM co-expressed with IgD. Based on the mutational status of the IgHV two groups of CLL are defined: the mutated and the unmutated IgHV CLL patients. This status obtained by comparison of the IgHV sequence of tumoral CLL B cell clone with the reference germline sequence. IgHV is considered mutated (M-IgHV) when the difference between the sequences is ≥ 2%. When the difference between the sequence is <2% IgHV is considered as unmutated (UM-IgHV). M-IgHV is associated with more favorable prognosis than UM-IgHV (Döhner et al., 2000).

ZAP-70

ZAP-70 is an intracellular protein implicated in the signal transduction in T lymphocytes an NK cells after antigen encounter (Lanier et al., 1998). Expression of ZAP-70 in B cells of CLL patients was demonstrated by qPCR and its expression was associated to UM-IgHV and poor prognosis. But in routine, the flow cytometry constitutes the technique of reference used for

License CC BY-NC-ND 4.0

the assessment of ZAP-70 expression using a precise protocol as described in the paper from Rizzo (Rizzo et al., 2013). ZAP-70 promotes the transmission of signals in CLL cells resulted from antigen encounter (Dürig et al., 2003, p. 70; Wiestner et al., 2003). The implication of ZAP-70 in the prognosis prediction is still controversial as studies did not correlate the level of ZAP-70 with the IgHV status (Morabito et al., 2015). The mechanism by which ZAP-70 contributes to an aggressive disease is not clear, but recently, it was shown in primary cells low levels of ZAP-70 result in reducing MYC expression. Furthermore, ZAP-70 promotes cell survival in the absence of over BCR signaling. In addition, ZAP-70 was identified to constitute the link with the microenvironment of malignant B cells by regulating the recruitment and activation of T cells (J. Chen et al., 2021). All these data suggest that ZAP-70 is implicated in the regulation of tumor CLL cell survival, the expression of MYC and also contributes to the regulation of the microenvironment of CLL cells (J. Chen et al., 2021).

CD38

CD38 identified as an activation maker implicated in the differentiation of T cells (Reinherz et al., 1980)**.** The expression of CD38 is not restricted to T cells**,** several studies have shown CD38 expression in non-hematopoietic cells such as endothelial cells, neurons, prostatic and pancreatic cells (Kato et al., 1995; Kramer et al., 1995, p. 38; Mizuguchi et al., 1995)**.** CD38 is also expressed in the different subpopulations of B cells from the earliest stage CLP to mature B cells. The level of CD38 expression differs depending on the maturation and activation stage of cells (Howard et al., 1993). Studies showed the expression of CD38 on CLL cells and identified this positive marker expression as a prognosis indicator (Ibrahim et al., 2001, p. 38). Increased levels of CD38 is associated with aggressive disease in CLL. In contrast to ZAP-70, increased expression of CD38 is not correlated to the mutational status of IgHV in CLL patients (Ibrahim et al., 2001).

Altogether, and based on these indicators, CLL patients are divided into two groups. A group with poor prognosis characterized by UM-IgHV status, high levels of ZAP-70 and CD38. The second group associated with more favorable prognosis characterized by the M-IgHV, low levels of ZAP-70 and CD38.

License CC BY-NC-ND 4.0

BCR signaling

In CLL as well as in other B lymphomas, BCR plays an important role through the activation of survival and proliferation signaling pathways. BCR signaling was found increased in CLL cells with high levels of ZAP-70. Increased ZAP-70 and BCR signaling are associated with poor prognosis (Chen et al., 2002, p. 7). In addition to the BCR signaling induced by autoantigens present in the microenvironment of CLL cells. It is also observed BCR autonomous signaling (Dühren-von Minden et al., 2012). BCR with UM-IgHV are polyreactive able to react with molecules present in the microenvironment of CLL such as myosin, vimentin or rheumatoid factors (Figure 35) (Hoogeboom et al., 2013). This signaling results in activation of proliferation and survival of tumoral cells. Inhibition of BCR signaling constitute a target for CLL treatment.

30% of CLL patients are characterized by the expression of a restricted BCR repertoire with skewed IgHV repertoire, called as stereotyped BCR. These BCR is classified into subsets regarding the similarity in the amino acid sequence of CDR3 domain in V_H. To define a stereotyped BCR an identity of 50% is required. About hundreds of subset are defined, but there is 19 subsets predominant and represent 10% of all BCR of CLL (Agathangelidis et al., 2012). It was shown that subsets #1 and #2 are associated with the aggressive and poor prognosis of CLL patients. Subset #1 is characterized by the presence of poor prognosis indicators such as NOTCH1 mutation and autonomous signaling of BCR via cross-linking of IgM which induce cell survival and proliferation. Subset #2 also characterized by the presence of poor prognosis indicators of CLL such as high levels of MYC, UM-IgHV, *SF3B1* mutation and autonomous signaling of BCR, in addition to the predominance of subsets #4,#6 and #8 which also associated with poor outcomes in CLL patients (For review (Hacken et al., 2019).

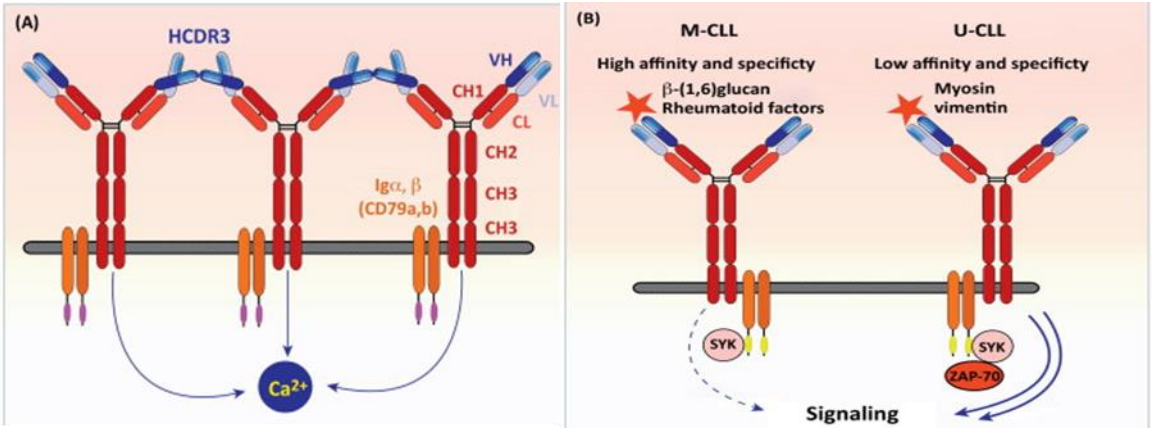

Figure 35: BCR signaling in CLL.
In CLL cells, BCR signaling can be activated by autonomous signal resulted from oligomer generation (A.) or by molecules produced by the microenvironment (B.) of CLL such as myosin, vimentin and rheumatoid factors. The affinity of the BCR is lower in UM-IgHV.(Burger and Chiorazzi, 2013).

License CC BY-NC-ND 4.0

Recurrent mutations

The predominant mutated gene in CLL is the Splicing Factor 3B subunit1 (***SF3B1)*** gene. Its mutation is detected in 10 % to 15 % of CLL patients (Wang et al., 2011, p. 3). Due to the importance in the splicing mechanism, mutations in SF3B1 lead to the alteration in splicing machinery. SF3B1 mutation affects the telomere maintenance, the NOCH1 signaling pathway and alter the DDR (For review (Wan and Wu, 2013, p. 3).

In addition to *SF3B1* mutations, in CLL other mutations into the RNA splicing machinery are detected such as Exportin1 (XPO1). Recently, it was shown that mutation of XPO1 is detected in a cohort of CLL patients, and mutated XPO1 is associated with shorter time to the first treatment and poor prognosis.

Presence of more than one mutated gene implicated in the RNA splicing machinery reveals that the RNA processing pathway is the most pathological pathway implicated during the development of CLL (Moia et al., 2020).

The second predominant mutation detected in 10% of CLL is the mutation of *Notch homolog 1* ***(NOTCH1)*** gene (Puente et al., 2015). NOTCH1 is a heterodimeric, single-pass transmembrane receptor implicated in the transactivation of genes implicated in cell proliferation and survival as the proto-oncogene MYC. Frequently found mutation of *NOTCH1* consists on a frameshift deletion resulting in the alteration of the domain for the proteasomal cleavage of activated NOTCH1. This mutation leads to an increase in the NOTCH1 stability and results in continuous activity and MYC overexpression (Rosati et al., 2018).

A relationship was suggested between *NOTCH1* mutation and trisomy 12 in CLL development, since 40% of CLL with NOTCH1 activating mutation present trisomy 12 (Del Giudice et al., 2012). Also, 80% of CLL patients with *NOTCH1* mutations are characterized by UM-IgHV leading to the association with poor prognosis and increased risk in Richter transformation (For review (Bosch and Dalla-Favera, 2019).

Protection of Telomere **(POT1)** protein is implicated in the maintenance of the telomeres and the protection of the chromosomes ends. POT1 is found mutated in 3 to 7% in CLL patients. POT1 mutations increase the aberrations of telomere structure and fusion of the chromosome ends favoring the evolution and progression of the disease. POT1 mutations is associated with aggressive clinical stage of CLL, the presence of POT1 mutations was found correlated with *SF3B1* mutation and UM-IgHV (Ramsay et al., 2013).

License CC BY-NC-ND 4.0

Cytogenetic alterations

Deletion 13q14 (del13q14) is detected in approximately 60% of CLL cases (Landau et al., 2015); Its deletion constitutes the most frequent chromosomal abnormality in CLL. Del13q14 is more frequent in mutated IgHV in comparison to UM-IgHV and is associated with more favorable prognosis and prolonged time of survival (Rossi et al., 2013). When the deletion affects the retinoblastoma gene (*RB1*) gene located on the longer arm of chromosome 13, it results in acceleration in the clinical courses of patients (Ouillette et al., 2011). 13q14 also contains genes coding for micro-RNA such as MIR15-A and MIR16-1 shown to be implicated in the regulation of expression of apoptosis and cell cycle regulating genes (Cimmino et al., 2005). Longevity of CLL cells is due to the alteration in the pro-survival and pro-apoptotic factors of the family of B cell leukemia/lymphoma 2 (Bcl-2) and is considered as a hallmark of CLL (Packham and Stevenson, 2005). It was shown that the pro-survival factors such as Bcl-2 and Mcl-1 are increased in CLL cells (Saxena et al., 2004). MIR15-A and MIR16-1 are negatively correlated to the anti-apoptotic factor Bcl-2 expression, deletion of these microRNA results in increased levels of Bcl-2. This activity is regulated in the posttranscriptional level of Bcl-2 (Cimmino et al., 2005).

Deletion 11q22–q23 (del11q) is detected in 15% of CLL cases and constitutes the second common chromosomal abnormality in CLL (Döhner et al., 2000). In 25% of cases, this deletion affects ATM, a tumor suppressor gene encoding implicated in the DDR. Alterations of ATM are associated with poor prognosis (Shiloh and Ziv, 2013; Skowronska et al., 2012).

Trisomy 12 constitutes the third chromosomal abnormality observed in CLL and is detected in 15% of CLL cases (Döhner et al., 2000). Combined trisomy 12 with *NOTCH1* mutations decreases the survival of CLL patients (Del Giudice et al., 2012). Additionally, trisomy 12 increases the Richter Syndrome (RS) transformation risk.

Deletion 17p13 (del17p) is detected in 10% of patients with CLL (Döhner et al., 2000). This deletion affects normally the total p arm of the chromosome 17 and results in the deletion of the tumor suppressor gene *TP53*. Deletion of *TP53* is observed in 80% of CLL cells with del17p (Zenz et al., 2008). Del17p is more frequently detected in *UM-IGHV* CLL patients than in patients with *M-IGHV status*.

2p gain (2p+) : short arm gain of the chromosome 2 is detected in 15% of CLL patients and is recurrent in advanced stages of CLL with the evolution of the disease and probably promotes Richter transformation (Chapiro et al., 2010; Rinaldi et al., 2011). This chromosomal abnormality is also detected in other lymphomas such FL and DLBCL (Ferreira et al., 2008). This gain is variable and can be concern a part of 2p or the totality of 2p. It is associated with

License CC BY-NC-ND 4.0

the markers of poor prognosis such as del11q and UM-IgHV status. The XPO1 gene is localized on the 2p. XPO1 mutation is implicated in drug resistance during CLL patient treatment. In addition, 2p contains the loci of proto-oncogenes *REL*, *BCL11A* and *MYCN*. These three genes play a role in the resistance of CLL cells to treatment (Cosson et al., 2017; Kostopoulou et al., 2019; Miller et al., 2021).

MYCN is a member of MYC family known to be amplified in CLL cells and associated with poor prognosis. MYCN was detected overexpressed in patients with 2p gain, this overexpression is related to short survival (Deambrogi et al., 2010).

REL is a subunit of Nuclear Factor Kappa B (NFκB), it was shown that the subunit RELA of REL family is implicated in disease progression of CLL *in vitro* (Hewamana et al., 2008) which suggests that RELA can be used as a prognostic marker and it can be a therapeutic target in CLL (Hewamana et al., 2009).

2.3. Classification

Binet and RAI staging are used to classify the CLL patients into different stages related to their time of survival, and clinical characteristics and their need to treatment (Table 4). This classification cannot predict the prognosis of patients while the majority of them are diagnosed at early stages (Shanafelt, 2009). Additionally, this classification does not include the status of some indicators of prognosis such as zeta chain-associated protein ZAP-70, CD38, the mutational status of IgHV and the chromosomal abnormalities. A third classification system was described the international prognostic index (CLL-IPI). This system includes five parameters of CLL patients the age, IgHV status, clinical stage, TP53 status (normal, mutation or del17p) and serum-β2 microglobulin. This system classifies CLL patients into four groups regarding their score. Group one with a score (0-1) characterized by low risk and longer treatment to first treatment (TTFT), the second (2-3) with an intermediate risk and TTFT, the third with a score (4-6) characterized by the high risk and short TTFT and the last group with poorer prognosis (7-10) with very high risk (International CLL-IPI working group, 2016). Score attributed for each parameter to predict the global score is represented in the (Table5).

License CC BY-NC-ND 4.0

Table 4: Characteristics of RAI and Binet classification.

RAI			
Stages	RISK	Characteristics	Global Survival (years)
0	Low	lymphocytosis	> 15
I/II	Intermediate	Lymphadenopathy	7-8
III/IV	High	Anemia/thrombocytopenia	5-6
BINET			
A	Low	< 3 lymphoid areas enlarged	> 15
B	Intermediate	≥ 3 lymphoid areas enlarged	7-8
C	High	Anemia/thrombocytopenia	5-6

Table 5: International prognostic Index of CLL (CLL-IPI).

	Adverse Factor	Grade
Age	>65 years	1
Clinical Stage	Rai I-IV or Binet B-C	1
β_2-microglobulin level	>3.5 mg/L	2
IGHV mutation status	Unmutated (>98% homology with germline)	2
Del(17p) and/or *TP53* mutation	Present	4

Risk	Score	5-year Overall Survival (p<0.001 for all)
Low	0-1	93%
Intermediate	2-3	79%
High	4-6	63%
Very High	7-10	23%

2.4. Treatments of CLL

Treatment is not required for all CLL patients, it is applicable to patients presenting symptoms and with advanced stage in RAI or Binet classification, some of the targets in CLL treatment are visualized in the (Figure 36). For several decades, the monotherapy using alkylating agent, the chlorambucil (low coast, low toxicity) was used first to treat CLL ("Chemotherapeutic options in chronic lymphocytic leukemia," 1999).

In addition, three analogues of purine are used to treat the CLL patients such as fludarabine that induces the p53 related gene, cladribine targeting the polβ and the pentostatin, which

License CC BY-NC-ND 4.0

inhibit the adenosine deaminase, and lead to the inhibition of DNA synthesis. The most beneficial of these three treatments is the fludarabine which is able to induce the high remission percentage compared to other types of treatment. The efficacity of the fludarabine cannot be observed if it applicated as a single treatment and need to be combined with other agents. Fludarabine was used combined with cyclophosphamide and the rituximab (monoclonal antibody to CD20), this combination is considered as the reference for CLL treatment (Hallek, 2019). Another cytostatic agent was known to treat various type of cancers, the Bendamustine. Studies were done to test the efficacity of this agent on CLL cells and to compare it with other agent such as fludarabine+chlorambucil and the results showed more efficiency of Bendamustine suggesting that the it is a potential CLL treatment using single agent (For review (Hallek, 2019)).

In addition to the cytostatic agents used to treat CLL, the development of biotechnology technics enables synthesis of monoclonal antibodies and the increase in the understanding of the CLL physiopathology and development, led the use of specific monoclonal antibodies targeting molecules implicated in the CLL development. CLL cells express the CD20, a calcium channel that doesn't have natural ligand. Targeting the CD20 by a monoclonal antibody has emerged in 1998 to treat NHL including CLL. Three important anti-CD20 are known the ofatumumab, obinutuzumab and Rituximab which was the first monoclonal antibody described to target CD20. Another monoclonal antibody was developed to target the CD52 present on the surface of all lymphoid populations. Efficiency and function of each of these treatments is reviewed in (Hallek and Al-Sawaf, 2021).

As the BCR signal is implicated in CLL cells development, it was developed molecules targeting this pathway. The most common molecules targeting the BCR signaling are:

Fostamatinib, which targets the SYK. Inhibition of SYK decreases the activation and proliferation molecules in CLL cells such as CD69 and CD86, CD38, Ki67 respectively (Herman et al., 2013).

Idelasib (CAL101), is used in a second line in CLL treatment in the cases with highly aggressive and progressive disease. This treatment is characterized by a long and durable response without increase in the toxicity on normal cells. It targets the PI3K and inhibits the phosphorylation of AKT and MAPK in B cells leading to their apoptosis (Khan et al., 2014).

Ibrutinib (PCI-32765), which is an inhibitor of BTK downstream in the signaling pathway of BCR. Ibrutinib binds BTK leading to its inhibition in an irreversible way. This molecule is used as first line of treatment in aggressive form of CLL in combination with the inhibitor of SYK (Young and Staudt, 2014) or with the inhibitor of Bcl-2, the venetoclax (Jain et al., 2019).

License CC BY-NC-ND 4.0

Dasatinib, an inhibitor of LYN, was shown to have an activity even as a single agents in relapsed CLL patients (P. C. Amrein et al., 2011).

As mentioned before, molecules targeting cell survival and proliferation were developed to increase the range of CLL treatment by inducing the death of cancer cells. Other strategies targeting the microenvironment cells had been developed to improve the immune system vis a vis of the CLL tumor cells. The CAR T cells treatment is based on the reinjection of patient autologous T cells modified by lentivirus to target CLL cells. These cells are able to target the CD19 expressed on tumor cells but also have an impact on normal B cells (Mancikova and Smida, 2021). In contrast, it was shown that CAR T cells targeting specifically the light chain Ig of the tumor cells present a minimal level on normal B cells, and this type of CAR T cell can be used as an alternative to CD19 CAR T cells (Ranganathan et al., 2021).

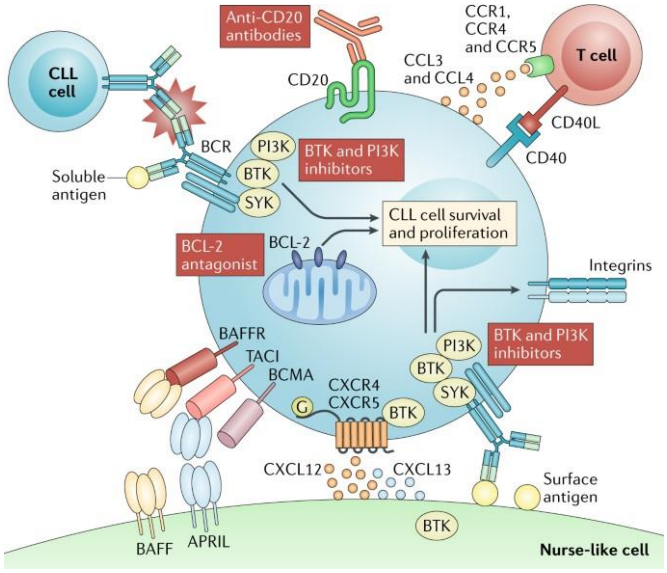

Figure 36 : Schematic representation of the inhibitors and their targets in CLL treatment.
Several inhibitors are used during the CLL treatment such as anti-CD20, the targeting of the pathways activated by the BCR such as BTK and PI3k inhibitors , and the inhibitors targeting the anti-apoptotic factor like BCL-2 (Burger and O'Brien, 2018).

3. Cell of origin in CLL

Identification of the cell of origin, the original normal cell that transformed to malignant cell, is important point in understanding the emergence of the malignant disease. Determination of cell of origin permits the identification of the alteration events occurred during the transformation. Different B cell subpopulations were suggested over the years to be a putative for the origin cell of CLL. This was done based on the evolution of biological technics and the understanding of the mechanisms regulating differentiation of B cells (For review (Bosch and Dalla-Favera, 2019). Two hypotheses concerned the cell of origin in CLL are present.

License CC BY-NC-ND 4.0

First, CLL cells were suggested to be originate from HSC due to the presence of genetic methylation and epigenetic modification normally present in HSC and detected in 80 to 98% of CLL B cell patients (Gahn et al., 1997). In 2011, it was again suggested the HSC is the origin of CLL after HSC xenografts in immunodeficient mice. These mice developed B cells expressing CD5 marker with a MBL/CLL phenotype (Kikushige et al., 2011). The HSC as CLL cell of origin hypothesis is still controversial and needs confirmation (Husby and Grønbæk, 2017).

Secondly, CLL B cells were suggested to derived from mature B cells due to the detection of Ig clonal rearrangements in addition to the expression of CD23, a B cell activation marker, of CD5, of weak levels of CD20 and of membrane Ig (Sabattini et al., 2010). Expression of CD5 on CLL cells oriented the hypothesis to the B1 cells (expressing CD5 and implicated in the innate immunity) as the cell of origin in CLL. The two subsets of CLL patients regarding the mutational status of IgHV gene suggest that UM-IgHV is most probably derived from naïve B cells in the pre-GC formation. In contrast the M-IgHV status suggests the progression of these CLL cells from post-GC (Klein et al., 2001; Rosenwald et al., 2001).

Finally, the origin of CLL cells is still a debate due to the heterogeneity observed in this disease and the hypothesis that CLL originates from HSC or mature B cells, also the second hypothesis that CLL originate from mature B cells (pre-GC, post-GC and GC independent (B1) cells) need to be confirmed.

4. Evolution of CLL

4.1. Clinical complications of CLL

Several complications can be observed due to CLL. CLL patients are more vulnerable to opportunist infections, 10 to 20% of CLL patients are likely to develop auto-immune diseases due to the production of monoclonal antibodies by non-leukemic cells. This latter point is observed in 90% of cases. These antibodies target the blood cells resulting in anemia or thrombocytopenia (Dearden, 2008; Morrison, 2010; Visco et al., 2014). Additionally, CLL patients are able to develop solid cancers such as skin cancer, and rarely breast, lung and prostate cancers. Finally, CLL disease can be progress to Richter Syndrome (RS).

RS is the transformation of CLL to an aggressive phenotype of lymphomas, especially to diffuse large B cell lymphoma DLBCL and rarely to Hodgkin lymphoma (HL). RS is observed in CLL patients with a rate of 3 et 10% (Parikh et al., 2014) . RS emerged from CLL shares histological similarities with DLBCL but still has distinct profile. The most common indicators

License CC BY-NC-ND 4.0

that increase the risk of Richter transformation is NOTCH1 mutation, TP53 deletion or alteration, UM-IgHV, abnormalities in c-MYC, increased expression level of CD38 as reviewed in (Jain and O'Brien, 2012).

4.2. Microenvironmental factors

The tumor microenvironment (TME) cells accounts for macrophages, T cells, FDC, mesenchymal Stroma Cells (MSC), and natural killer cells. TME ensures a protective niche for CLL cells and plays an important role influencing the survival of CLL cells by giving stimuli that activate cell survival and proliferation (Burger et al., 2009). These functions accomplished by molecules such as cytokines or chemokines produced by the microenvironment that interact with CLL cells via their specific receptors (Figure 37). In addition, direct contacts between CLL cells and MSC were observed via the adhesion molecules expressed on both MSC and CLL cells (Figure 38). Also, the crosstalk between MSC and CLL cells can be ensured by soluble factors or via the newly identified way represented by the extracellular vesicles (Dubois et al., 2020). This TME constitutes a new theme for targeting the CLL using different treatments (Figure 37) (For review (Svanberg et al., 2021). Effector CD8+ T cells that control the tumor development by their effector function was showed to be decrease in CLL TME. Additionally, present CD8+ are characterized by exhaustion marks such as PD-1 inhibitory receptor expression, and these CD8+ present in LL blood are unable to generate a synapse with CLL cells (Roessner and Seiffert, 2020).

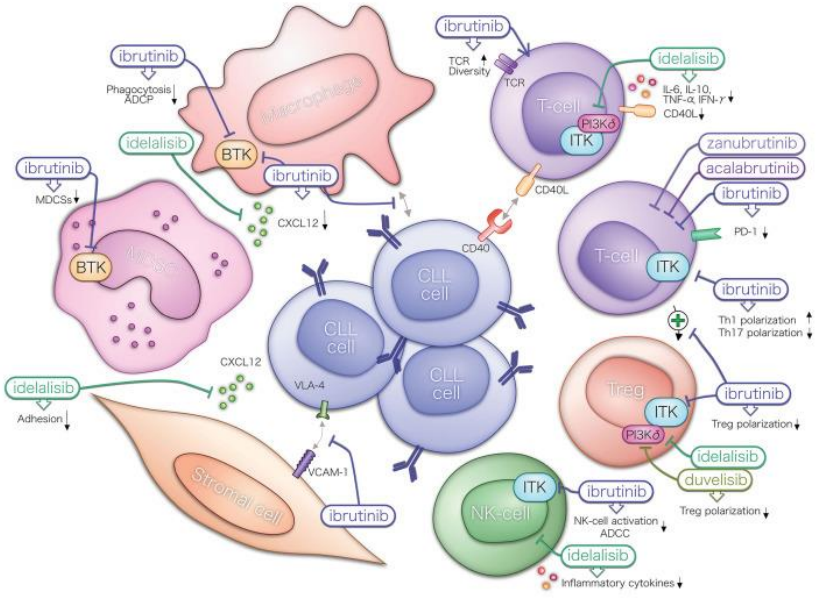

Figure 37: Tumor microenvironment in CLL.
Microenvironment of CLL is composed of different cell type such as T cells, natural killer cells, stromal cells, mesenchymal cells and macrophages. These cells contribute to the survival maintenance and proliferation of CLL by producing cytokines and chemokines. These cells constitute a target to treat CLL (Svanberg et al., 2021).

License CC BY-NC-ND 4.0

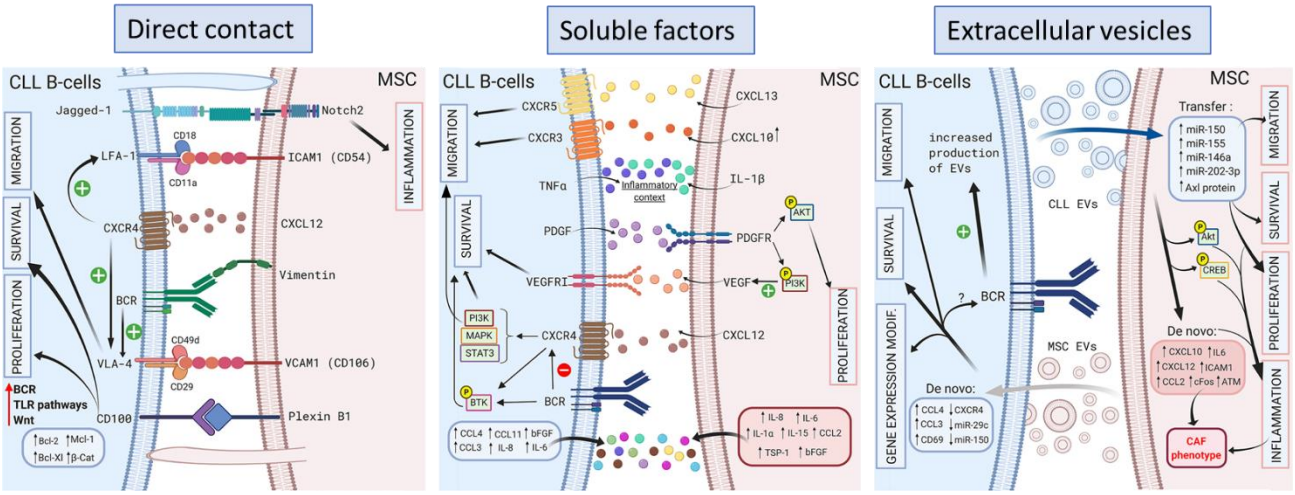

Figure 38: Crosstalk between CLL and MSC cells.
MSC play an important role in the CLL microenvironment. Three types of crosstalk exist between the MSC and CLL cells via direct contact, soluble factors or via the extracellular vesicles. Figure adapted from (Dubois et al., 2020).

4.3. AID in CLL

In normal condition, in B lymphocytes, AID expression is restricted to activated B cells. In contrast, AID can be expressed in cancers including the CLL cells (McCarthy et al., 2003). It was shown that AID is expressed in a proliferative and activated, and on-going CSR subset of CLL cells in correlation with the overexpression of survival and proliferative markers such as c-MYC, ki-67, Bcl-2 (Palacios et al., 2010).

AID seems to play a role in the early stages of tumoral evolution since CLL patients with AID expressing cells are associated with poor prognosis and increased cytogenetic complications such as del11q and del17p (Gelmez et al., 2017, 2014).

In CLL cells, as well as in normal B cells, AID can be detected in spliced variant forms, but only the full length of mRNA is expressed. These splice variants are deficient for CSR domain and can activate or inactivate the SHM. In CLL cells, four AID transcript variants were observed in high levels in contrast to normal B cells occurring normally the CSR and SHM. These variants are implicated in decrease in SHM and CSR but in the increase in the DSB generation. Also these variants were correlated with trisomy 12 as reviewed in (Oppezzo et al., 2021). Full length AID was reported to mutate in efficient way the V and S regions of the *IgH* locus in CLL cells. Detection of AID protein in UM-IgHV cell and the presence of switched IgG suggest that the function of AID in CSR and SHM is not linked in CLL cells. AID can mutate the switch regions without affection of the V region.

License CC BY-NC-ND 4.0

In addition to its mutational function, AID was reported to play a role in DNA demethylation during the generation of GC (Dominguez et al., 2015). A study was conducted to evaluate the DNA methylation induced by AID in CLL cells expressing or not AID. In these cells, a small difference in the global methylation profile was detected without determination for any specific implicated target or gene. This difference in DNA methylation did not affect the level of gene expression (Schubert et al., 2018). More studies are required to determine the impact of AID DNA methylation in CLL.

4.4. DSBs repair alteration

The Histone H2AX is phosphorylated on his serine 139 (γH2AX) in response to the presence of DSB. This γH2AX accumulates around the DSB forming foci and its labeling indicates the presence of DNA damages. These foci are responsible for the recruitment of proteins implicated in the repair pathway such as 53BP1. Accumulation of DNA lesions was shown to be increased in CLL comparing to healthy cells. This was demonstrated by increased immunofluorescence labeling of γH2AX in CLL compared to normal cells. In addition, γH2AX was observed increased in CLL compared to MBL indicating that the accumulation of DNA damages contributes to the disease evolution (Popp et al., 2019).

A study was conducted in primary CLL cells to explore the DNA repair mechanism predominant in CLL cells and to determine if there is an alteration in DNA repair usage. This study was done using DNA repair reporter system via plasmids and showed that DSBs are mainly repaired by Alt-EJ pathway compared to NHEJ pathway after the analysis of repair junction structure in CLL cells. Assessment of the level of expression of the different molecules of each DNA repair pathway (Alt-EJ and NHEJ) by qPCR reveals that XRCC1, LIGIII and PARP-1 (Alt-EJ) molecules are highly expressed in CLL cells rather than NHEJ molecules compared to normal B cells (Gassner et al., 2018).

In cancer cells, alteration of DNA repair can influence the sensitivity to the treatment by increasing the cell resistance and can contribute to the disease evolution without any treatment. Concerning the treatment of CLL it was shown that inhibition of HR an NHEJ increases the cell sensitivity to the chlorambucil (L. Amrein et al., 2011).

B. Hodgkin Lymphoma (HL)

Hodgkin lymphoma (HL) is a cancer of the lymphatic system, it represents 10% of all lymphomas types (Piris et al., 2020). HL is divided into two types, the classical Hodgkin lymphoma (CHL) which represents 95% of all HL and the nodular Lymphocytes Predominant Hodgkin Lymphoma (NLPHL) which accounts for 5% of HL (Cuceu et al., 2018b). CHL can be

License CC BY-NC-ND 4.0

divided into four subtypes: Nodular Sclerosis (NSHL), Mixed Cellularity (MCHL), Lymphocyte-Depleted (LDHL), and Lymphocyte-Rich (LR-HL) (Buettner et al., 2005). Two groups of age are more affected by HL then others. It is affect persons with 20-40 years and those with more than 75 years ("Hodgkin lymphoma," 2018).

Hodgkin lymphoma is a curable disease depending on the stage of diagnosis. The main cure used is chemotherapy combined or not with irradiation in adults patients (Rinaldi, 2018).

All Hodgkin lymphomas types are characterized by the presence of a mononuclear and large multinucleated cell named Hodgkin and Reed Sternberg cells respectively (H/RS). H/RS are transformed cells characterized by their capacity to escape the apoptosis mechanisms (Benharroch et al., 1996). Presence of these cells are useful for the diagnosis of HL and to differentiated from non-Hodgkin lymphoma.

Hodgkin and Reed Sternberg cells are non-abundant elements since they are representing only about 1% of all tumor mass making study of these cells and tumor characteristics difficult and allowing to require sensitive approaches to isolate and analyze tumoral cells. H/RS cells are present in an inflammatory microenvironment which represent about 99% of the tumor mass and constituted from: B cells, eosinophils, T cells macrophages, and plasma cells (Lee et al., 2003; Opinto et al., 2021).

H/RS are clonal based on the V genes rearrangements studies as demonstrated by Küppers et al in 1998 ("Clonality and Germinal Centre B-cell Derivation of Hodgkin/Reed-Sternberg Cells in Hodgkin's Disease - PubMed,"). Histological studies, detection of SHM and CSR mechanisms in the *IgH* locus of this cell type demonstrated that H/RS in the majority of cases derived from germinal center cells. In addition, more than 40% of H/RS cells are positive to Epstein Barr Virus 'EBV'. This observation consolidates that H/RS derived from GC since EBV infect naïve B cells in the pre- GC step. EBV infection increases the risk to develop Hodgkin Lymphoma.

H/RS express on their surface the marker of lymphoid cell activation CD30, and the CD15, known as a marker for myeloid/monocyte cells. In some cases, H/RS cells may be negative for the CD15 marker ("CD15 Antigen - an overview | ScienceDirect Topics," n.d.). H/RS cells are negative for CD45, CD3 or CD247, CD14, CD20, and CD138 , the marker of plasma cells, (Buettner et al., 2005). These cell markers are used to select, isolate, and study H/RS cells. Characterization of H/RS markers allow the development of new treatment strategy in adults patients targeting the marker CD30 with an anti-CD30 antibody, the Brentuximab vedotin (Gravanis et al., 2016).

License CC BY-NC-ND 4.0

Several studies have demonstrated that H/RS cell centers are characterized by the presence of genetic instability like chromosomal instability, microsatellite instability, telomere dysfunction and altered DNA repair. Genome instability observed in HL results from the alteration of expression levels of TRF1, TRF2, Ku80 factors implicated in DSB DNA repair and genome stability (Cuceu et al., 2018a).

In addition, breakpoints are frequent in HL, and the Ig loci specifically in the *IgH* locus in H/RS cells. This latter breakpoint can result in deletion of part of the constant region, alteration in class switch recombination with production of some immunoglobulin such as IgG4 and IgA in favors to others (Irsch et al., 2001).

Although, Absence of BCR expression on the surface of H/RS cells suggests their apoptosis since BCR is responsible for cell survival signaling. In contrast, H/RS cells escape show to apoptosis due to the presence of crippled mutation. Several mechanisms are reported to explain the absence of BCR and since LSR conduced to BCR loss in B cells, study of the LSR as a potential cause for the BCR loss represents an objective of our study.

License CC BY-NC-ND 4.0

License CC BY-NC-ND 4.0

Thesis objectives

License CC BY-NC-ND 4.0

License CC BY-NC-ND 4.0

Thesis objectives

Locus suicide recombination is a genetic rearrangement in activated B cells (Péron et al., 2012). LSR occurs between the Sμ and the 3'RR of the *IgH* locus leading to the excision of all constant genes, which conducts to the abrogation of IgH expression and loss of the BCR at the B cell surface. BCR plays a crucial role in the transmission of survival signals, its absence leads to the death of the B cells (Lam et al., 1997). Characterization of LSR and the determination of its biological function is an important subject to understand. My thesis work has interrogated whether LSR is implicated in normal B cell physiology and in pathological conditions of B cells.

Tumoral B cells of Chronic Lymphocytic Leukemia (CLL) express Ig on their surface, which is, in the vast majority of cases, unswitched Ig (IgM) and this raises the question of Ig recombination process alteration in this B cell cancer. In the first objective of my thesis, we have examined the occurrence of LSR in CLL (**Article 1**). We detected LSR junctions in CLL patients and based on the LSR counts we distinguished two groups of CLL patients, one group with high count of LSR junctions (LSR^{High}) and the other group with low count of LSR junctions (LSR^{Low}). Clinical and molecular analysis of these two groups allowed us to conclude that high LSR count in CLL associated with poor prognosis and is induced by MYC independently of AID, these results constitute my first article (Al Jamal et al., 2022).

In addition, analysis of LSR junctions in CLL patients showed difference junctions structure profile between the two groups with an alteration of the structure in the LSR^{Low} group. This observation leads to the main objective of the second part of my thesis work questioning the alteration in DNA double strand break repair in CLLs with low LSR junction counts. An alternative explanation is LSR repair structure is an indicator of the cell origin of the CLL LSR^{Low} condition. This is suggested by similarity in LSR repair with those observed in normal B cells from healthy tonsils. These results conduct to my second article (**Article 2 in preparation**).

Additionally, I worked on Hodgkin lymphoma (HL). In HL, the tumoral cells called Reed Sternberg H/RS cells do not express a BCR on their membrane. So, we aimed to analyze if the LSR mechanism can contribute to the loss of BCR in HL samples and especially in sorted RS cells (**Preliminary data**).

License CC BY-NC-ND 4.0

License CC BY-NC-ND 4.0

Results

License CC BY-NC-ND 4.0

License CC BY-NC-ND 4.0

Article I: Increased IgH locus suicide recombination in Chronic Lymphocytic Leukemia denotes MYC driven IgH rearrangements

Our work in the first part of my thesis explores the *IgH* locus recombination mechanisms in chronic lymphocytic leukemia (CLL). In normal condition, activated B cells express Activation Induced cytidine Deaminase (AID). AID introduces DNA lesions on *IgH* locus leading to the formation of double strand breaks (DSB). Junction of DNA ends and DNA repair result in CSR that allows immunoglobulin isotypes diversification. CSR is required for the B cell receptor (BCR) expression and immune responses. AID can also target the 3'RR of the *IgH* locus during the locus suicide recombination (LSR). LSR leads to the deletion of the constant region of IgH and conducts to cell death through loss of BCR expression.

In CLL, an indolent non-Hodgkin B cell lymphoma, tumor B cells express BCR at low level. In the vast majority of cases IgM is the expressed Ig and class-switched CLLs are rare. This latter observation questions the alteration in *IgH* locus recombination machinery. First, we used DNA samples from 47 CLL patients and 9 or 5 healthy donors to count LSR and CSR events per sample. To do so, we amplified by nested PCR CSR and LSR junctions and we did high throughput sequencing and data were analyzed using a specific bioinformatics tool the CSReport.

As expected CSR junction counts were lower in CLLs. In contrast, LSR junction counts were at comparable levels between healthy PBMC and patients. Thus, we defined two groups of CLLs: LSR^{Low} CLLs and LSR^{High} CLLs using the mean of LSR junction counts obtained in healthy PBMC as a cut off.

We performed study of IgHV mutation status and we observed that LSR^{High} CLLs were enriched in IgHV unmutated cases which is associated with poor prognosis in CLL. In accord with this result we observed that LSR^{High} group is characterized by shorter time free survival without treatment as shown in the Kaplan Meyer curves of Treatment Free Survival (TFS).

We analyzed the diversity of LSR junctions using Shannon diversity index. We observed higher diversity of LSR junctions in LSR^{High} group. This raised the question of an on-going process so, we determined the level of AID expression. Weak levels of AID transcripts were detected by qPCR analysis in both CLL groups. Moreover, low mutation rate of PIM1, an AID off target gene, was observed in LSR^{High} CLLs.

Altogether, these results suggest that LSR is an active process in LSR^{High} CLL cells but in these cells, AID seems not to be induced. We also assessed cell proliferation in these two groups of CLL patients: we have measured the telomere length by specific qPCR on genomic DNA, and we observed shorter telomeres in LSR^{High} group compared to LSR^{Low} and healthy

License CC BY-NC-ND 4.0

PBMC reflecting an increased proliferation cycle. Moreover, shorter telomeres in LSR^{High} CLLs were associated with increased *MYC* expression in LSR^{High} group.

As IgH recombination requires DNA accessibility though transcription, we analyzed IgH transcription. We found higher levels of non-coding and coding transcripts in LSR^{High} when compared to LSR^{Low} CLLs meaning that *IgH* locus DNA was accessible to the recombination machinery in these patients.

As *IgH* locus recombination occurs physiologically in proliferating cells, we hypothesized that *MYC* overexpression in LSR^{High} CLLs potentiates IgH recombination. This was examined on the murine lymphoma cell line, CH12F3, which able to undergo CSR and LSR after stimulation. CH12F3 subclones expressing or not AID in presence or not of *MYC* overexpression were showed that *MYC* overexpression tends to increase the LSR junctions count, even in presence or in absence of AID.

Our results indicate that in LSR^{High} CLLs cells, the accessibility of *IgH* locus could be increased in a MYC dependent manner resulting in shorter survival and implying an additional MYC driven AID independent mechanism of *IgH* recombination. Also, LSR^{High} and ^{Low} CLLs appear to be characterized by different features certainly due to different CLL tumoral transformation mechanisms.

License CC BY-NC-ND 4.0

Increased *IgH* locus suicide recombination in Chronic Lymphocytic Leukemia denotes MYC driven IgH rearrangements

Israa Al Jamal[1,2], Milène Parquet[1], Said Aoufouchi[3], Morwenna Le Guillou[3], Kenza Guiyedi[1], David Rizzo[1,4], Marine Dupont[1,4], Mélanie Boulin[1,4], Hend Boutouil[1], Chahrazed El Hamel[5], Justine Lerat[6], Samar Al Hamaoui[2], Nehman Makdissy[2], Jean Feuillard[1,4], Nathalie Gachard[1,4], Sophie Peron[1]*.

[1] Centre National de la Recherche Scientifique (CNRS) Unité Mixte de Recherche (UMR) 7276/INSERM U1262, Université de Limoges, Limoges, France.

[2] Faculty of Sciences, GSBT Genomic Surveillance and Biotherapy Team, Mont Michel Campus, Lebanese University, Tripoli, Lebanon.

[3] CNRS UMR9019, Gustave Roussy, B Cell and Genome Plasticity Team, Villejuif, France and Université Paris-Saclay, Orsay, France.

[4] Laboratoire d'Hématologie Biologique, Centre Hospitalier Universitaire de Limoges, Limoges, France.

[5] Collection Biologique Hôpital de la Mère et de l'Enfant (CB-HME), Department of pediatric, Limoges University Hospital, Limoges, France.

[6] Department of Otorinolaryngology, Limoges University Hospital, Limoges, France.

*Corresponding author.

Correspondence should be addressed to:

Sophie Peron

CRIBL – Contrôle de la réponse immune B et des lymphoprolifération - UMR CNRS 7276 INSERM1262.

Centre de biologie et de recherche en santé, 2 rue du Pr Bernard Descottes, 87 000 Limoges, France.

Phone: (+33) 519 564 210; Email: sophie.peron@unilim.fr

License CC BY-NC-ND 4.0

KEY POINT

MYC high expression and increased accessibility of *IgH* locus could promote AID-independent *IgH* rearrangements in poor prognosis CLL patients.

ABSTRACT

Chronic lymphocytic leukemia (CLL) is an indolent non-Hodgkin lymphoma characterized by tumor B-cells that weakly express a B-cell receptor (BCR). Activation Induced-cytidine deaminase (AID) is required for Ig class switch recombination (CSR) and is implicated in Ig heavy chain (*IgH*) Locus Suicide Recombination (LSR) inducing BCR loss. The great majority of CLL B-cells have not-switched and express mu/delta Ig isotypes. This suggests abnormalities in Ig gene recombination in CLL. Studying both CSR and LSR, we found that CLL patients could be separated into two groups, LSR^{Low} and LSR^{High}, based on LSR counts. Although both groups express low levels of AID, the detection of LSR^{High} tumor cells indicates an ongoing high rate LSR process. However, these cells display low *IGHV* and *PIM1* (an AID off-target) mutation rates. *MYC* overexpression, increased *IgH* locus accessibility and decreased telomere length were associated with shorter treatment free survival. *In vitro* experiments with the CH12F3 cell model indicated that MYC potentiated CSR and LSR and could drive some LSR in *AID* knocked out cells.

Altogether, our results indicate that MYC could promote AID-independent *IgH* rearrangements in poor prognosis CLL patients.

License CC BY-NC-ND 4.0

INTRODUCTION

In normal activated B-cells, Activation Induced-cytidine deaminase (AID) is the key enzyme for class switch recombination (CSR) and IGHV somatic hypermutation (SHM)[1,2]. It is also implicated in another *IgH* rearrangement, Locus Suicide Recombination (LSR). LSR recombines the *IgH* locus between the switch μ (Sμ) region and one 3'α2 regulatory region (3'α2RR) of the *IgH* locus. This region contains enhancers (HS3, HS1.2, and HS4) and like-switch (LS) regions and controls *IgH* locus transcription necessary for *IgH* expression[3]. When LSR hits the active *IgH* locus, it induces the loss of BCR expression and B-cell death [4–6].

Chronic lymphocytic leukemia (CLL) is an incurable indolent non-Hodgkin B-cell lymphoma of the elderly characterized by the expansion of malignant CD5+ B cells. CLL BCR is composed, in most cases, of the mu (μ) and delta (δ) immunoglobulin (Ig) isotypes (IgM^+IgD^+)[7]. Ig class-switched CLLs are rare[8] and were shown to express AID at higher levels[9–12]. However, class-switched CLLs are predominantly IGHV-unmutated[10], an indication that the CSR and SHM functions of AID are uncoupled in these tumor cells. More broadly, increased AID expression in CLL is not only associated with unmutated IGHV genes but also with unfavorable cytogenetic aberrations and poor prognosis[13]. This raises the question of abnormalities in the Ig gene recombination machinery in this B-cell cancer.

PATIENTS AND METHODS

Detailed information on CLL patients and healthy samples, clinical correlations, DNA and RNA extractions, *IgH* recombination junction amplification and high throughput sequencing, qRT-PCR, telomere length assay, immunophenotyping, *PIM1* targeted sequencing are detailed in Supplemental methods.

All sequencing data has been deposited in the National Center for Biotechnology Information's BioProject (PRJNA830327).

License CC BY-NC-ND 4.0

RESULTS AND DISCUSSION

To investigate the *IgH* recombination machinery, we analyzed both CSR and LSR in DNA samples collected at CLL diagnosis from patients (N=47) with more than 98% blood tumor cell infiltration (Sup figure 1). Controls consisted of healthy volunteers (HV) (N=5 for CSR and N=9 for LSR). As expected in this IgM^+ IgD^+ B-cell cancer, CSR levels were much lower in CLL than in HV samples and no CLLs exhibited increased CSR counts (Figure 1A). Even if at low levels, LSR was found at comparable levels in both HV and CLL (Figure 1B), being undetectable in only 3/47 (6.3%) CLL patients. However, some patients had increased LSR counts when compared to HVs (Figure 1B). Distribution of LSR counts was bimodal with a valley at 27. That value being also the mean of LSR counts in HVs (Sup figure 2), we separated CLL patients into two groups called LSR^{High} (12/47 patients = 26%), and LSR^{Low} (35/47 patients = 74%) (Sup table 1). CSR counts were not significantly different in both groups (Figure 1C). According to the same methodology, a threshold of 800 CSR counts was selected to separate CLL patients into CSR^{Low} and CSR^{High} groups. As shown in supplementary table 2, LSR^{High} status did not seem to be related to CSR^{High} status. Consistently, the correlation between CSR count and LSR count was poor (correlation coefficient r=0.2, not shown). This indicates that increased LSR was poorly or not related to class-switching in CLL.

To further study LSR^{High} CLLs, we analyzed LSR junction diversity in both groups and in HVs using the Shannon Index (Figure 1D). This index was significantly higher in LSR^{High} CLL samples than in LSR^{Low} CLLs and HVs, indicating increased junction diversity. However, LSR^{High} samples exhibited a stronger homology to IGHV reference sequences (Figure 1E). With a threshold of 95% homology, 10/12 (83%) LSR^{High} CLLs were not or only weakly mutated while 20/35 (57%) LSR^{Low} CLLs were highly mutated (Fischer test, p=0.02). Consistently, we found that LSR^{High} patients exhibited low rates of AID off-target *PIM1* mutations (Figure 1F, p=0.01). When compared to centroblasts and naïve B-cells sorted from benign reactive tonsils, AID expression was at comparable levels in both LSR^{Low} and LSR^{High} CLL, being as low as in naïve B-cells (Figure 1G). Therefore, LSR was poorly or not related to AID expression level in these patients.

Because diversity of LSR junctions in LSR^{High} CLLs is evocative of an on-going process, we analyzed the expression of non-coding and coding transcripts of the constant part of *IgH* locus. We found higher levels in LSR^{High} when compared to LSR^{Low} CLLs (Figure 2A and 2B), meaning that *IgH* locus DNA was accessible to the recombination machinery in these patients. As *IgH* locus recombination occurs physiologically in proliferating cells[14], we measured the relative telomere length. While being homogeneous in HVs, with a mean of 2.14, telomere lengths were very heterogeneous in LSR^{Low} patients, 13 (40%) had long or very long telomeres, indicating that the cells underwent a few

License CC BY-NC-ND 4.0

proliferation cycles. In contrast, all but one LSR^{High} patient homogeneously exhibited telomeres that were shorter than HVs, reflecting an increased proliferation cycles (Figure 2C). Moreover, shorter telomeres in LSR^{High} CLLs were associated with increased *MYC* expression (Figure 2D). Most likely reflecting increased proliferation and in agreement with the fact that decreased telomere length is a poor prognosis factor associated with genomic instability and TP53 mutations[15], the Kaplan Meyer curves of Treatment Free Survival (TFS) showed that TFS for LSR^{High} CLLs was significantly shorter than for LSR^{Low} CLLs (≈14 months compared to ≈71 months; P<0.001) (Figure 2E).

To functionally evaluate the impact of *MYC* expression on *IgH* locus recombination, we used the murine B-cell lymphoma CH12F3 cell line and its AID knock-out (ko) counterpart stably transfected or not with a *MYC* overexpression vector and *in vitro* stimulated to undergo CSR and LSR. As shown in figure 2F and 2G for LSR, and in supplemental figure 4 for CSR, levels of both CSR and LSR were increased when *MYC* was overexpressed ($AID^{+}MYC^{+}$). In the absence of AID (AID^{-}), CSR was undetectable while some LSR junctions could be found. When MYC was overexpressed ($AID^{-}MYC^{+}$), CSR remained undetectable but number of LSR junctions was increased. A contamination could be ruled out because the sequence of these LSR junctions was unique, some of them harboring sequence fragments of Sx region in between of Sμ and 3'α2RR, which suggests that these LSR events were preceded by a sequential CSR event.

These results show that MYC potentiated both CSR and LSR when AID was expressed. Even if rare, LSR was possible in the absence of AID and was increased in the presence of MYC. Keeping in mind the recently reported residual CSR in the absence of AID[16], the very unusual sequence of some LSR junctions with Sx insertion could also indicate that a CSR event is possible in the absence of AID.

CLL is known to harbor DNA repair alterations and to accumulate DSB across the genome[17–19]. In our patients, AID was expressed at the same levels as in tonsil naïve B-cells. Therefore, we can hypothesize that, when AID is weakly or not expressed, high expression of *MYC* and increased proliferation in LSR^{high} CLLs would favor random DNA breaks and inaccurate DSB repair, promoting in turn genetic instability. This MYC driven-AID independent *IgH* locus recombination would explain why IGHV and *PIM*1 mutation rates were low in LSR^{High} CLLs. Whether these MYC driven-*IgH* rearrangements occur in CLL proliferation centers of secondary lymphoid organs remains to be determined.

Altogether, our results strongly indicate that in LSR^{High} CLLs cells, the accessibility of *IgH* locus could be increased in a MYC dependent manner resulting in shorter survival and implying an additional MYC driven AID-independent mechanism of *IgH* recombination.

License CC BY-NC-ND 4.0

ACKNOWLEDGEMENTS

This work was supported by grants from la Ligue Contre le Cancer (Comité de la Haute-Vienne, CD87) and by grants from INCa-Cancéropôle GSO (Emergence program N°2019-E11). We are grateful to Dr. Villéger at the CRBioLim and to Dr. Vallejo and the INSERM CIC 1435, Dupuytren Hospital, Limoges, France, for providing human samples. *We thank* Dr. *Jeanne Cook Moreau* (UMR CNRS 7276 INSERM 1276) for careful English editing. IAJ is supported by Fondation pour la Recherche Medicale (FRM) and Lebanese associations (AZM and Saade, LASeR). MP is supported by Région Nouvelle Aquitaine and Université de Limoges. KG is supported by Région Nouvelle Aquitaine and Délégation INSERM Nouvelle Aquitaine. SP is a National Institute of Health and Medical Research (INSERM) investigator.

AUTHORSHIP CONTRIBUTIONS

IAL performed experiments and participated in writing of the original draft.

MP, SA, MLG, KG, MB and MD participated in experiments.

DR, MD and NG participated in data curation.

CEH and JL provided tonsils from patients undergoing tonsillectomies performed in Limoges Dupuytren hospital.

SA, SAH and NM participated in writing the original draft.

JF, NG and SP led the conceptualization, data curation, funding acquisition, manuscript writing.

DISCLOSURE OF CONFLICTS OF INTEREST

The authors declare no competing interests.

License CC BY-NC-ND 4.0

FIGURE LEGENDS

Figure 1: LSR is detectable in CLL patients and suggests that increased LSR rate is not related to AID. **A.** CSR junction counts analyzed by NGS and CSReport in CLL patients (N=47, 32986 junctions) are lower than in HV PBMCs (N=5, 10301 CSR junctions). **B**: LSR junctions were at comparable levels in both CLL samples (N=47, 1060 LSR junctions) and HV PBMCs (N=9, 239 LSR junctions). **C.** CSR counts were not significantly different in both LSR^{Low} (N=35, 22247 junctions) and LSR^{High} (N=11, 10739 junctions). **D.** Shannon diversity index indicates higher LSR junction diversity in LSR^{High} CLL samples (N=11) than in LSR^{Low} (N=35) CLLs and healthy PBMCs (N=9). **E.** Graph represents percentage of identity in IgHV segments: in LSR^{Low} (N=34) low % of identity detected compared to the high homology of IgHV segments in LSR^{High} (N=12) groups. The mean frequency of Somatic Hyper Mutation (SHM) in both groups of CLL is represented in the box. **F.** NGS of *PIM*1, AID off-target gene, and mutation frequency analysis show high level of mutation frequency in LSR^{Low} (N=8) compared to healthy PBMCs (N=8) and LSR^{High} (N=7). **G**. Quantification of AID transcripts, relative to CD19 transcripts, is low in LSR^{Low} CLLs (N=7) and LSR^{High} CLLs (N=6) compared to normal B-centroblasts (N=4) used as positive controls and comparable to AID transcript levels in sorted naïve B-cells (N=4) used as negative controls. Graphs represent mean ± SEM. Statistical analyses were performed using Unpaired T test ns: non-significant, *P<0, 05, **P<0.01, ***P<0.001 and ****P<0.0001**.**

Figure 2: LSR in LSR^{High} CLL patients may be an AID independent MYC driven *IgH* locus rearrangement. Quantification of *IgH* non-coding transcripts (Sμ, Sγ1, Sγ3, HS1.2 and HS4) (**A**) and coding transcripts (Cμ and surface IgM (sIgM)) (**B)** in CLL LSR^{Low} (N=4 to 7) and LSR^{High} (N=3 to 5) CLLs. LSR^{High} exhibited high levels of *IgH* locus transcription in both productive and non-productive transcripts. **C.** Relative telomere length (RTL) measured by specific qRT-PCR relative to human beta globin gene (LSR^{Low}, N=33; LSR^{High}, N=12; healthy PBMCs, N=6). Telomere length was significantly shorter in LSR^{High} compared to LSR^{Low} and healthy PBMCs. **D.** MYC expression was higher in LSR^{High} (N=6) compared to CLL LSR^{Low} (N=7). **E.** Cumulative survival time (days) without treatment (TFS) for patients indicated shorter TFS in LSR^{High} CLLs. **F.** Detection of LSR junctions in activated CH12F3 clones overexpressing or not *MYC* in the presence of AID (AID^{+}, N=1 ; AID^{+} MYC^{+}, N=3) suggested MYC tends to increase the LSR junction count. This was also observed in the absence of AID (**G.**), as LSR junctions, even if rare, were detectable in CH12F3 AID^{-} clones (N=2) and their appeared to increase with the MYC overexpression (AID^{-} MYC^{+}, N=2). Graphs represent mean ± SEM. Statistical analyses were performed using Unpaired T test (A., B., C., D.,) or Chi2 test (E.) ns: non-significant, *P<0, 05, **P<0.01, and ***P<0.001**.**

License CC BY-NC-ND 4.0

REFERENCES

1. Revy, P. *et al.* Activation-induced cytidine deaminase (AID) deficiency causes the autosomal recessive form of the Hyper-IgM syndrome (HIGM2). *Cell* **102**, 565–575 (2000).

2. Muramatsu, M. *et al.* Class switch recombination and hypermutation require activation-induced cytidine deaminase (AID), a potential RNA editing enzyme. *Cell* **102**, 553–563 (2000).

3. Pinaud, E. *et al.* The IgH locus 3' regulatory region: pulling the strings from behind. *Adv Immunol* **110**, 27–70 (2011).

4. Péron, S. *et al.* AID-Driven Deletion Causes Immunoglobulin Heavy Chain Locus Suicide Recombination in B Cells. *Science* **336**, 931–934 (2012).

5. Boutouil, H., Boyer, F., Cook-Moreau, J., Cogné, M. & Péron, S. IgH locus suicide recombination does not depend on NHEJ in contrast to CSR in B cells. *Cell. Mol. Immunol.* **16**, 201–202 (2019).

6. Dalloul, I. *et al.* Locus suicide recombination actively occurs on the functionally rearranged IgH allele in B-cells from inflamed human lymphoid tissues. *PLoS Genet* **15**, e1007721 (2019).

7. Katayama, Y., Sakai, A., Katsutani, S., Takimoto, Y. & Kimura, A. Lack of allelic exclusion and isotype switching in B cell chronic lymphocytic leukemia. *American Journal of Hematology* **68**, 295–297 (2001).

8. Geisler, C. H. *et al.* Prognostic Importance of Flow Cytometric Immunophenotyping of 540 Consecutive Patients With B-Cell Chronic Lymphocytic Leukemia. *Blood* **78**, 1795–1802 (1991).

9. Oppezzo, P. *et al.* Do CLL B cells correspond to naive or memory B-lymphocytes? Evidence for an active Ig switch unrelated to phenotype expression and Ig mutational pattern in B-CLL cells. *Leukemia* **16**, 2438–2446 (2002).

10. Oppezzo, P. *et al.* Chronic lymphocytic leukemia B cells expressing AID display dissociation between class switch recombination and somatic hypermutation. *Blood* **101**, 4029–4032 (2003).

11. Efremov, D. G., Ivanovski, M., Batista, F. D., Pozzato, G. & Burrone, O. R. IgM-producing chronic lymphocytic leukemia cells undergo immunoglobulin isotype-switching without acquiring somatic mutations. *J Clin Invest* **98**, 290–298 (1996).

12. Fais, F. *et al.* Examples of in vivo isotype class switching in IgM+ chronic lymphocytic leukemia B cells. *J Clin Invest* **98**, 1659–1666 (1996).

13. Heintel, D. *et al.* High expression of activation-induced cytidine deaminase (AID) mRNA is associated with unmutated IGVH gene status and unfavourable cytogenetic aberrations in patients with chronic lymphocytic leukaemia. *Leukemia* **18**, 756–762 (2004).

14. Stavnezer, J., Guikema, J. E. J. & Schrader, C. E. Mechanism and Regulation of Class Switch Recombination. *Annu Rev Immunol* **26**, 261–292 (2008).

15. Véronèse, L. *et al.* Telomeres and chromosomal instability in chronic lymphocytic leukemia. *Leukemia* **27**, 490–493 (2013).

16. Dalloul, I. *et al.* UnAIDed Class Switching in Activated B-Cells Reveals Intrinsic Features of a Self-Cleaving IgH Locus. *Frontiers in Immunology* **12**, 4488 (2021).

License CC BY-NC-ND 4.0

17. Deriano, L. *et al.* Human chronic lymphocytic leukemia B cells can escape DNA damage-induced apoptosis through the nonhomologous end-joining DNA repair pathway. *Blood* **105**, 4776–4783 (2005).

18. Bouley, J. *et al.* A new phosphorylated form of Ku70 identified in resistant leukemic cells confers fast but unfaithful DNA repair in cancer cell lines. *Oncotarget* **6**, 27980–28000 (2015).

19. Popp, H. D. *et al.* Accumulation of DNA damage and alteration of the DNA damage response in monoclonal B-cell lymphocytosis and chronic lymphocytic leukemia. *Leuk Lymphoma* **60**, 795–804 (2019).

License CC BY-NC-ND 4.0

FIGURES

Figure 1

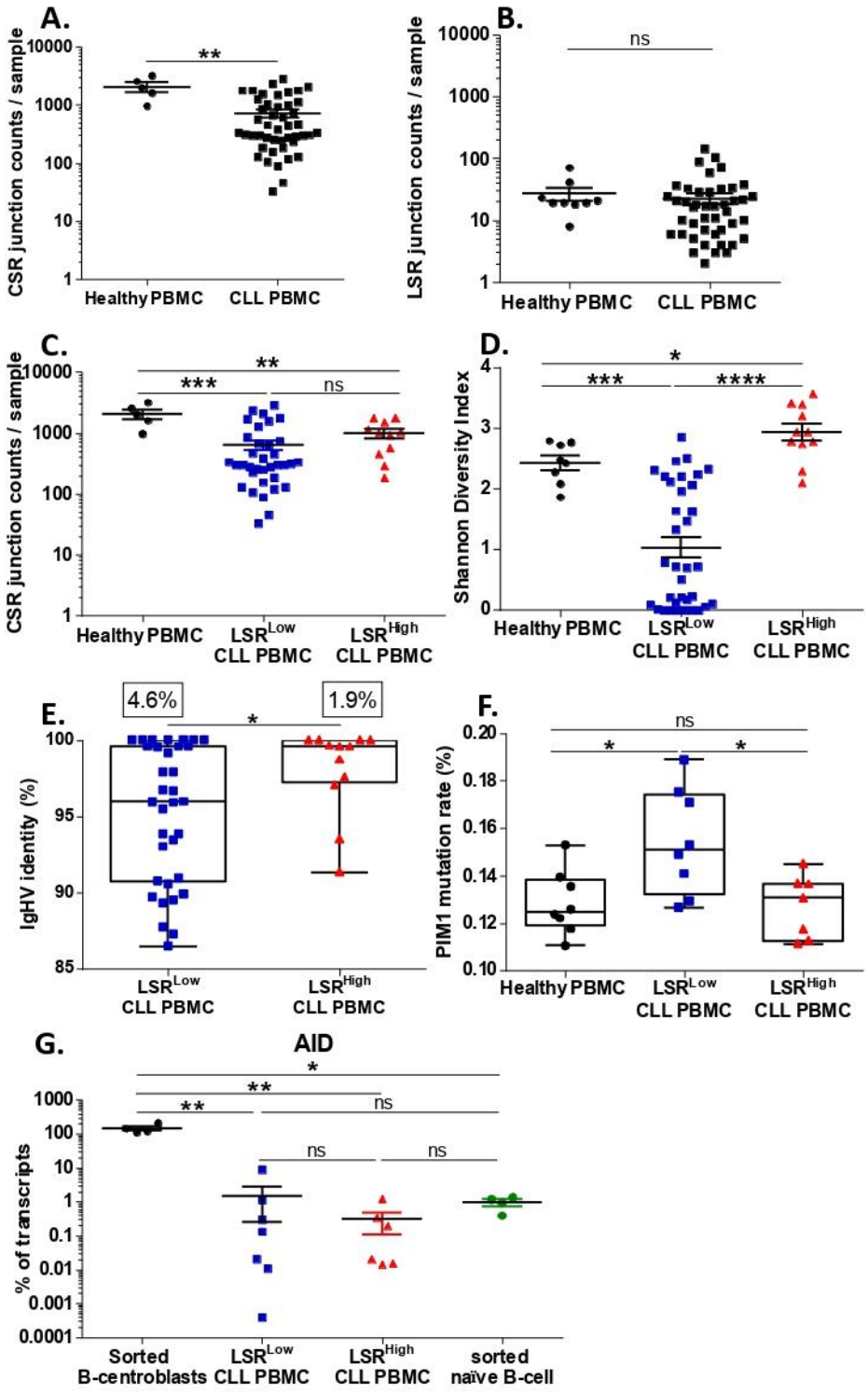

License CC BY-NC-ND 4.0

Figure 2

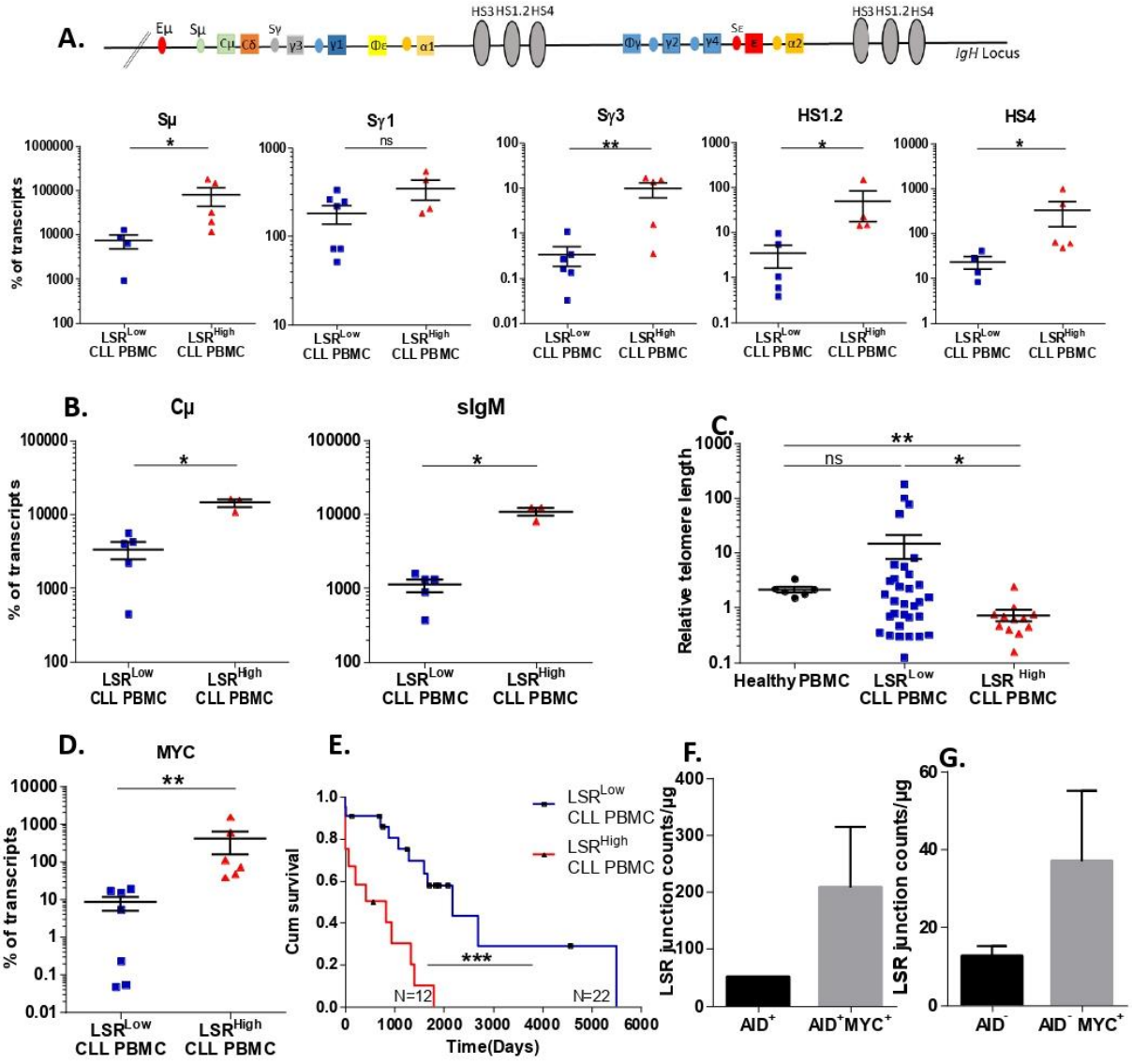

License CC BY-NC-ND 4.0

SUPPLEMENTAL DATA

METHODS

Human materials and ethics

The project was conducted according to the guidelines of the Declaration of Helsinki. CLL Peripheral Blood Mononuclear Cells (PBMCs) were from CRBioLim from Limoges Hospital, CHU Dupuytren (authorization: DC-2008-604, AC-2016-2758, and AC-2019-3418). Tonsils were obtained from children scheduled for elective tonsillectomy and were obtained from CRBioLim (authorization: DC-2008-604, AC-2018-3157). PBMCs from healthy volunteers (HV) were collected through the research project approved by CPP Sud Méditerranée I (N°. 2021-A00778-33).

DNA extraction:

PBMC DNA were extracted using phenol/chloroform method. CLL DNA were extracted using kit QiAmp DNA Blood (51104 Qiagen).

Human CSR and LSR junction counts:

Human CSR and LSR junctions were amplified as previously described[1] and used to prepare next generation sequencing (NGS) libraries (Ion Xpress™ Plus Fragment Library Kit, Life technologies, Thermofisher, 447269) sequenced with ion proton or S5 chip (Life Technologies). Results were collected in the FastQ format and then analyzed using CSReport [2]. Shannon diversity index (H) was used to estimate sample diversity and was calculated considering the number of reads (ni) for each particular LSR junction and the total read number (N) of LSR junctions: $H = -\sum_{i=1}^{s} Pi \ln(pi)$ with $pi = \frac{ni}{N}$ .The H value ranges from 0 when LSR junction diversity shrinks due to clonal dominance to high values for samples with higher diversity.

CH12F3 CSR and LSR junction count:

The murine CH12F3 cell line was transfected or not by *MYC* expression vector (pCDNA3-HA-HA-humanC-MYC, Plasmid#74164, Addgene). Cells were cultured in RPMI 1640 with Ultra Glutamine, 10% FCS (Lonza), sodium pyruvate (Lonza), penicillin/ streptomycin (Lonza), nonessential amino acids (Lonza), and β2-ME. Cells were stimulated for CSR toward IgA for 72 hours with murine IL-4 (5 ng/ml; PeproTech), human TGF-β1 (1 ng/ml; R&D Systems), and murine antiCD40 Ab (1µg/ml; eBioscience). CSR and LSR Junctions were amplified by nested PCR using specific primers (sup table 3) as described[2].

License CC BY-NC-ND 4.0

IGHV sequence analysis:

Amplification of V, D, and J rearranged genes was performed using the Biomed-2 strategy with FR1 and FR2 primers and sequence analysis were performed as previously described [3].

Flow cytometry analysis:

Immunophenotyping was done on a Navios-flow cytometer from Beckman Coulter using the protocol for routine CLL diagnosis using: CD5-APC (Beckman coulter PN a60790, clone BL1a), CD19-ECD (Beckman coulter A07770, clone J3-119) and Anti-human Kappa light chain/Anti-Human Lambda light chains/RPE (Dako, FR481 X0935). Results were analyzed with Kaluza software version 2.1 (Beckman Coulter).

RNA extraction, cDNA synthesis and quantitative real time PCR:

Total RNA was isolated using TRIZOL reagent (TRIzol™ Reagent, 15596018) and reverse transcribed (Advantage RT-for-PCR kit Applied Biosystems™, Thermofisher 4368814/10400745). qRT-PCR was performed with the SYBR Green PCR mix (SensiFast hi ROX Syber Green BIO820025) for different targets of interest (Supplemental table 3) or with Taqman PCR mix (SensiFast Probe Hi-Rox kit BIO820025) and MYC probe (4331182 Hs00905030_m1, Thermofisher). Normal centroblasts and naïve B-cells were sorted as described[4] from tonsils.

Relative Telomere length assay (RTL):

Twenty five nanograms of DNA extracted from PBMCs or HV were used in triplicate to assess the RTL by qPCR as described previously[5].

Mutation analysis of PIM1:

We amplified the PIM1 exon 4 DNA segment with specific primers (Supplemental table 3) as this exon contains a base pair shown to be AID-targeted in the mouse model of CLL and in human CLL [6] using Phusion High fidelity Taq polymerase (Thermo Scientific, F-530XL) Productswere used to build libraries and were submitted to NGS as described above. For each library analysis was done by alignment of sequenced reads with the reference sequence NM_002648.4 using the Torrent Mapping Alignment Program (TMAP) for Ion Torrent Data and Super-maximal Exact Matching algorithm [7]. The resulting BAM files were processed to generate per-base nucleotide count table files consisting of matrices with *n* lines × 4 columns (*n* is the length of the sequenced DNA) and the columns correspond to nucleotides (A, C, G, and T). The consensus sequence is the most frequently read nucleotide and corresponds to the sequence reference. Counts of mutated bases were calculated by addition of numbers of sequenced bases different from the nucleotide that was sequenced the most frequently.

Statistical analysis:

Graphs, histograms, curves, and statistical analysis were designed using graph pad 6-prism software.

License CC BY-NC-ND 4.0

SUPPLEMENTAL TABLES

Count of LSR using CSReport	Healthy PBMC	LSR^{Low} CLL PBMC	LSR^{High} CLL PBMC
LSR positive samples / total samples (%)	9/9 (100)	32/35 (91)	12/12 (100)
Mean of LSR junction (min-max)	26.6 (8-71)	10.2 (0-24)	58.5 (29-145)

Supplemental table 1. Numbers of healthy volunteers and CLL patients tested and LSR junction counts and intervals (minimum-maximum) obtained for each group. Based on the mean of junction counts obtained in healthy PBMCs we divided the CLL cohort into two groups the first: LSR^{Low} ≤27 junctions and LSR^{High} > 27 junctions per sample.

Samples * (P=0,05)	LSR^{Low} CLL PBMC	LSR^{High} CLL PBMC
CSR^{Low} CLL PBMC	27	5
CSR^{High} CLL PBMC	8	7

Supplemental table 2. Repartition of patients between the two groups of LSR ($LSR^{Low\ and}$ LSR^{High}) and CSR (CSR^{Low}, ≤800 CSR junctions per sample, and CSR^{High}, >800 CSR junctions per sample). Statistical analysis was performed using Fisher's Exact Test *P<0.05.

License CC BY-NC-ND 4.0

Target and segment		Primer name	Sequence 5'-3'
CSR Junctions (CH12F3)	PCR1	Sμ1	F:TAGTAAGCGAGGCTCTAAAAAGCA
		Sα1	R:CAGCAGTGAGTTTAACAATCC
	PCR2	Sμ2	F:GCTTGAGCCAAAATGAAGTAGACT
		Sα2	R:CCTCAGTGCAACTCTATCTAGGTCT
LSR Junctions (CH12F3)	PCR1	Sμ1	F:TAGTAAGCGAGGCTCTAAAAAGCA
		LS2-R3	R:AACAAGAGGTGGGGAGTGTG
		LS4-R3	R:CTATAGCCATGTGGGGCTGT
		LS10-R3	R:GGGAGTGCCAGTGTCAACTT
	PCR2	Sμ2	F:GCTTGAGCCAAAATGAAGTAGACT
		LS2-R2	R:TGTCCAGGCTGAGCTACCTT
		LS4-R2	R:TTTACCAATCTCCCCCACTG
		LS10-R2	R:GTGAGTGTGTGGGGTTTGTG
IgH locus Transcription	Sμ	Sμg	F:GGTGTGGGTTTTCACAGCTT
			R:CCTCACCAAGTCCACCAAGT
	Sγ1	Sγ1-3	F:CTGGGATGGAGAAGGGAAGG
			R:CTGGTCTCAAGCACACGTTC
	HS	HS1,2	F:GAGTTTTCGGCATCTCTGGG
			R:ACAGATCAGAGCCCTCACAC
		HS4	F:GTGTGTCTGAGGGTGAGTGA
			R:ACACTGTCACACACTCCACA
	Sγ3	Sγ3	F:AGCTGTGCAACTGGAGTCCT
			R:TGAGCCACCTAATCCAAACC
	IgM total (Cμ)	hIgM CH1	F :CAGAATGCGTCCTCCATGTG
			R :GGTGGACTTGGTGAGGAAGA
	Surface IgM	hsIgM-CH4-For	F: AAGAGGAATGGAACACGGGG
		hsIgM-MB-Rev	R :ACAAGGTGACGGTGGTACTG
Telomere length	Telomere	Telomere A	CGGTTTGTTTGGGTTTGGGTTTGGGTTT GGGTTTGGGTT
		Telomere B	GGCTTGCCTTACCCTTACCCTTACCCTTAC CCTTACCCT
AICDA transcription	AID		F :GAGGCAAGAAGACACTCTGG
			R :GTGACATTCCTGGAAGTTGC
PIM1 mutation	PIM1		F :ATGAGTGGGTGGGGTGAGG
			R :ATCGAGCCAGGCGGCCC
Internal control	CD19		F:AGACTCCTTCTCCAACGGTA
			R:GGTCAGCTCTTCATCCTCGT
	Human Beta globin (hbg)	Hbg1	GCTTCTGACACAACTGTGTTCACTAGC
		Hbg2	CACCAACTTCATCCACGTTCACC

Supplemental Table 3. Primers used in this study.

SUPPLEMENTAL FIGURES

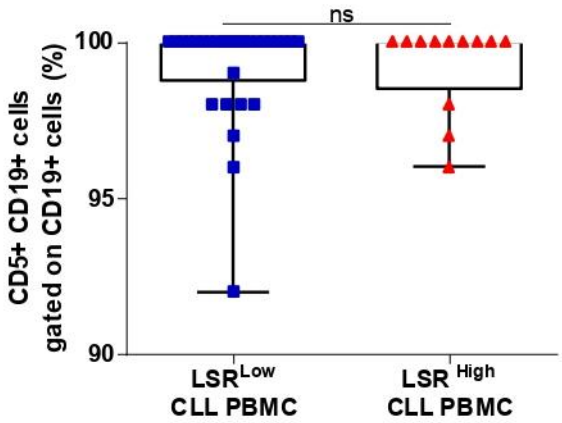

Supplemental figure 1. Blood tumor infiltration in CLL groups indicated by the percentage of CD5+ CD19+ B cells gated on total CD19+ B cells. Statistical analysis was performed using the Unpaired T test, ns: no significant difference.

License CC BY-NC-ND 4.0

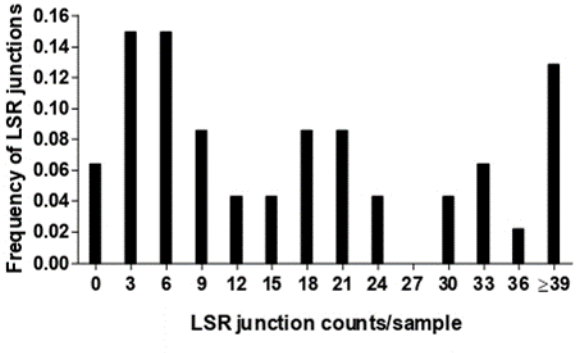

Supplemental figure 2. Distribution of LSR junction counts in CLL patients is bimodal with a valley at 27.

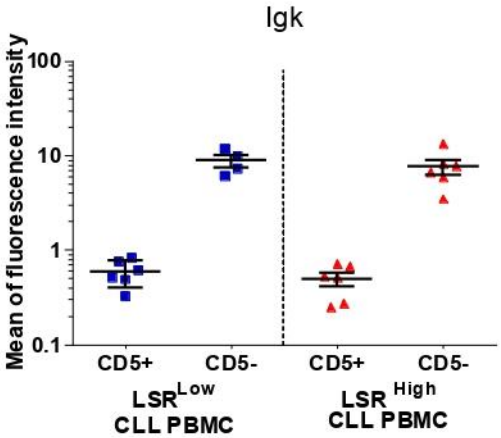

Supplemental figure 3. Mean fluorescence intensity (MFI) of Ig kappa light chains (Igk) is indicative of the level of B-cell receptor (BCR) expression at the B-cell surface. IgK MFI appears comparable for $CD5^{+}CD19^{+}$ tumor cells from both CLL groups (LSR^{Low}, N= 4 to 6; LSR^{High}, N=6) and decreased compared to normal $CD5^{-}CD19^{+}$ B-cells. Statistical analysis was performed using Unpaired T test, ns: no significant difference.

License CC BY-NC-ND 4.0

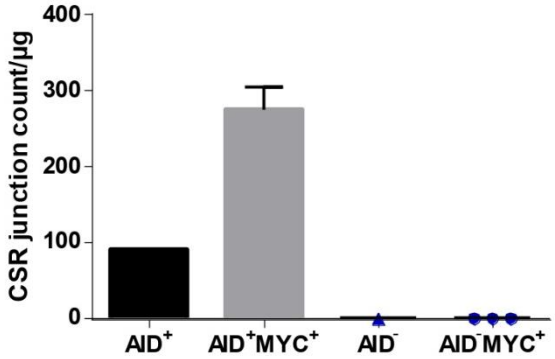

Supplemental figure 4. CSR junction counts in CH12F3 cell line.

CSR were detectable in AID^+ clone as expected (AID^+, N= 1). Overexpression of *MYC* in the presence of AID seemed to result in increased CSR junctions (AID^+MYC^+, N=3). No CSR junctions were detected in the absence of AID (AID^-, N=1), even with MYC overexpression (AID^-MYC^+, N=3).

ADDITIONAL REFERENCES

1. Dalloul, I. *et al.* Locus suicide recombination actively occurs on the functionally rearranged IgH allele in B-cells from inflamed human lymphoid tissues. *PLoS Genet* **15**, e1007721 (2019).
2. Boyer, F. *et al.* CSReport: A New Computational Tool Designed for Automatic Analysis of Class Switch Recombination Junctions Sequenced by High-Throughput Sequencing. *J. Immunol.* **198**, 4148–4155 (2017).
3. Gachard, N. *et al.* IGHV gene features and MYD88 L265P mutation separate the three marginal zone lymphoma entities and Waldenström macroglobulinemia/lymphoplasmacytic lymphomas. *Leukemia* **27**, 183–189 (2013).
4. Wohlford, E. M. *et al.* Changes in Tonsil B Cell Phenotypes and EBV Receptor Expression in Children Under 5-Years-Old. *Cytometry B Clin Cytom* **94**, 291–301 (2018).
5. Joglekar, M. V. *et al.* An Optimised Step-by-Step Protocol for Measuring Relative Telomere Length. *Methods Protoc* **3**, E27 (2020).
6. Morande, P. E. *et al.* AID overexpression leads to aggressive murine CLL and nonimmunoglobulin mutations that mirror human neoplasms. *Blood* **138**, 246–258 (2021).
7. Li, H. & Durbin, R. Fast and accurate short read alignment with Burrows–Wheeler transform. *Bioinformatics* **25**, 1754–1760 (2009).

License CC BY-NC-ND 4.0

License CC BY-NC-ND 4.0

Article II: LSR as an indicator of cellular origin in CLL cases with superior outcomes?

In the first part of my work, we amplified LSR junctions from PBMC from CLL patients. We divided the CLL cohort into two groups LSR^{High} with >27 junctions per sample and LSR^{Low} ≤ 27 junctions per sample based on the cut off as the mean of LSR junctions obtained in healthy PBMC. These two groups exhibit different molecular characteristics and LSR^{Low} group was associated with more favorable prognosis. Thanks to the CSReport software developed in our laboratory (Boyer et al., 2017), we analyzed LSR and CSR junction structures in these two groups of CLL patients as well as in healthy PBMC.

LSR junction's structure in LSR^{High} CLL cells were comparable to that of LSR junctions from healthy PBMC B cells. LSR junctions were characterized by a decrease in the junctions with blunt or µhomology of 1-2bp in length in favor of junctions with microhomologies 3-6bp and insertions longer than 4bp compared to CSR junctions. In contrast, we observed differential junction structures in LSR^{Low} group compared to LSR^{High} CLL and healthy PBMC. LSR junctions exhibited more few microhomologies (1-2bp) and blunt structures at the detriment of junctions with long insertions (≥4bp). CSR junctions were comparable between patients and controls.

As junction's structure reflects the DNA repair machinery, our observation raised the question of an alteration in DNA repair pathway during LSR in LSR^{Low} group. As shown previously in our laboratory (Boutouil et al., 2019), in murine B cells, LSR does not seem to depend of NHEJ pathway but rather seems to implicate the Alt-EJ pathway. LSR junction's structure obtained in normal human B cells and in LSR^{High} CLL group was coherent with the implication of Alt-EJ during LSR in human as suggested (Dalloul et al., 2019) and as described in mice.

We tried to decipher whether differential DSB repair can account for our observation and in first intend we interrogated the recruitment of proteins implicated in DSB reparation but also the chromatin status at the *IgH* locus, looking for epigenetic marks known to orient the way of DSB repair. Chromatin immunoprecipitation (ChIP) on stimulated naïve B cells from peripheral blood from healthy donors with antibodies directed against different actors of DSB repair pathways showed significant recruitment for XRCC4 (NHEJ) to the donor and acceptor segments of CSR on *IgH* locus. In contrast, PARP-1 and Pol~~Θ~~ (Alt-EJ) were significantly recruited to the donor/acceptor segments of LSR on *IgH* locus. Additionally, we performed analysis of the enrichment at the *IgH* segments of H4K20me1 epigenetic mark favoring NHEJ recruitment at the DSB and the H4K16ac known to rather inhibit the NHEJ. Results in healthy *in vitro* activated PBMC showed that H4K20me1 is more enriched on the CSR donor/acceptor

License CC BY-NC-ND 4.0

segments and H4K16ac was more enriched on LSR acceptor segments. Confirming that LSR repair in human as in mice is dependent of Alt-EJ pathway. Nevertheless, these results were not retrieved in CLLs who showed similar profile with enrichment of H4K20me1 on the whole of *IgH* locus which different from activated B cells and similar to resting B cells. In parallel, we did the quantification of transcripts of genes implicated in NHEJ and Alt-EJ in CLL PBMC cells and we did not detect difference between CLL LSR^{Low} and CLL LSR^{High} groups.

Observation of *IgH* locus with H4K20me1 and H4K16ac chromatin status in CLL similar to that of resting B cells appears in concordance with the *in vivo* occurrence of LSR in activated B cells. These latter are found in germinal centers within the secondary organs. Also, in CLL, LSR has been certainly achieved in CLL proliferation centers in secondary lymphoid organs. Indeed, we performed the analysis of LSR junction's structure from secondary lymphoid organs (healthy tonsils). LSR junction's structure of LSR^{Low} group was comparable to those obtained from healthy tonsils with a structural feature at the repair joint reminiscent to repair structure observed in the case of NHEJ employment. So, the recruitment of NHEJ to *IgH* locus in CD19+ B cells from tonsils was subsequently questioned. ChIP experiment on tonsils cells showed enriched recruitment of NHEJ actors on the LSR acceptor segments.

Obtained results point on the similarity of LSR junctions between CLL LSR^{Low} samples and healthy tonsils. We propose tumoral cells, in LSR^{Low} CLL, emerge from B cell population which is normally restricted to the compartments of B cell activation achievement. This hypothesis raises questions on the cellular characteristics of the normal B cells undergoing LSR in normal condition and on the processes implicated in the persistence of this population with in-turn a tumoral phenotype in LSR^{Low} CLL.

License CC BY-NC-ND 4.0

LSR as an indicator of cellular origin in CLL cases with superior outcomes?

Israa Al Jamal[1,3], Kenza Guiyedi[1], Milène Parquet[1], David Rizzo[1,2], Mélanie Boulin[1,2], Samar Al Hamaoui[3], Nehman Makdissy[3], Jean Feuillard[1,2], Nathalie Gachard[1,2], Sophie Peron[1]*.

[1] Centre National de la Recherche Scientifique (CNRS) Unité Mixte de Recherche (UMR) 7276/INSERM U1262, Université de Limoges, Limoges, France.

[2] Laboratoire d'Hématologie Biologique, Centre Hospitalier Universitaire de Limoges, Limoges, France

[3] Faculty of Sciences, GSBT Genomic Surveillance and Biotherapy Team, Mont Michel Campus, Lebanese University, Beirut, Lebanon.

*Corresponding author.

ABSTRACT

Chronic Lymphocytic Leukemia (CLL) in an indolent and still incurable lymphoma. Tumor cells are CD5+ CD23+ CD19+ B cells. Locus Suicide Recombination (LSR) is a rare genetic rearrangement of *IgH* locus that can occur during the terminal maturation of B cells in addition to Class Switch Recombination (CSR) and Somatic hypermutation (SHM) upon B cell activation. We previously showed that CLL cells in a cohort of 47 patients are positive for LSR and we divided the CLL cohort into two groups LSR^{Low} and LSR^{High} based on the mean count of LSR junctions in healthy PBMC. LSR^{Low} group is associated with superior outcome in CLL patients and present different molecular characteristics compared to LSR^{High}. Further analysis performed on LSR junctions from LSR^{Low} patients showed an abnormal formation of the LSR junctions characterized by microhomology. In addition, LSR junction's structure profile was skewed toward those observed in cells from healthy tonsils. Overall, these findings suggest that CLL LSR^{Low} cells with unique structural LSR features could be related to an as-yet-uncharacterized tonsil normal B cell subpopulation involved in LSR-induced B cell deletion.

INTRODUCTION

CLL is the clonal expansion of small CD19+ CD23+ CD5+ B cells (Caligaris-Cappio and Hamblin, 1999). Being still incurable, CLL evolution is highly variable, with an overall survival ranging from few years to decades (Kajüter et al., 2021). Normal counterpart of malignant CLL B cells remains undetermined and controversial (Scully et al., 2019). If CLL B cells are characterized by remarkable phenotype homogeneity and common gene expression profile, patients show a marked genetic heterogeneity allowing patient stratification (Rai/Binet staging systems). Among CLL genetic landscape specificity as important prognosis indicator, mutational status of the variable region (IgHV) on the immunoglobulin

License CC BY-NC-ND 4.0

(Ig) heavy-chain (IgH) locus is used to divide CLL cases into two groups with significantly disparate outcome and reflects the importance of the B cell receptor (BCR) (Döhner et al., 2000). Others major prognosis factors are chromosomal abnormalities such del17p, del11q, trisomy 12, isolated del13q or complex karyotype evidence the genomic instability in the CLL pathogenesis (Baliakas et al., 2019). In the vast majority of CLL cases, BCR at the tumor B cell surface is constituted by an IgM associated or not with the IgD and Ig-switched CLL is rare (Katayama et al., 2001). Surprisingly, AID, absolutely required for CSR in B cells, has been repeatedly detected in CLL B cells independently of the IgHV mutational status (Palacios et al., 2010). AID likely contributes to CLL evolution and seems to generate intraclonal diversity targeting *IgH* locus and non-Ig targets (off-targets)(Morande et al., 2021). LSR is another IgH rearrangement. LSR proceeds in activated B cells between the Sμ region and one of the like-switch (LS) repetitive regions, within one of the two 3'α regulatory region (3'αRR) of the *IgH* locus (Péron et al., 2012). LSR results in complete deletion of the cluster of *IgH* constant genes (from Cμ to Cα2) and when LSR hits the active *IgH* locus, it induces the loss of BCR expression and the death of the concerned B cell. Questioning the LSR occurrence in CLL, we highlighted that it could be represent an additional prognosis indicator and we assigned patient samples with low LSR frequency to a superior outcome compared to ones enriched for LSR junctions (Al Jamal et al., 2022). Going deeper in the molecular study of LSR junctions, obtained results suggest the LSR-on going activated B cells in tonsils from healthy controls can represent the normal counterpart of the LSR^{Low} CLL cases.

METHODS

Human materials and ethics

The project was conducted according to the guidelines of the Declaration of Helsinki. CLL Peripheral Blood Mononuclear Cells (PBMCs) were obtained from CRBioLim from Limoges Hospital, CHU Dupuytren (authorization: DC-2008-604, AC-2016-2758, and AC-2019-3418). Tonsils were obtained from children scheduled for elective tonsillectomy and were obtained from CRBioLim (authorization: DC-2008-604, AC-2018-3157). PBMCs from healthy volunteers (HV) were collected through the research project approved by CPP Sud Méditerranée I (N°. 2021-A00778-33).

DNA extraction

PBMC and tonsils DNA were extracted using phenol/chloroform method. CLL DNA were extracted using kit QiAmp DNA Blood (51104 Qiagen).

License CC BY-NC-ND 4.0

Amplification of Human Sμ/Sγ CSR junctions

CSR junctions were amplified in triplicate using 200 ng of genomic DNA of extracted from fresh peripheral blood of Human Healthy donors, tonsils and peripheral blood of CLL patients. Amplification of target junctions was performed by nested PCR using two couples of primers and the Herculase II fusion DNA polymerase (Agilent 60067). For the first nested PCR we used these primers : **Forward:** Sμh1a: ACCAGGTAGTGGAGGGTGGTA and a **Reverse** consensus primer Reverse: IgGa cons GGTCACCACGCTGCTGAG that can amplify the four type of IgG (IgG1, IgG2, IgG3 and IgG4) with the following conditions: 98°C/30sec, 2cycles of 98°C/10sec, 64°C/30sec,68°C/4min, 3 cycles of 98°C/10sec, 62°C/30sec,68°C/4min, 25 cycles of 98°C/10sec, 60°C/30sec, 68°C/4min and 68°C/5min. and The second nested PCR with these couple of primers was **Forward:** Sμh1b: (CAGGGAACTGGGGTATCAAG) and **Reverse:** IgGb cons: (CTTGACCAGGCAGCCCAG) with the following program: 98°C/30sec, 30 cycles of 98°C/10sec, 58°C/30sec, 68°C/4min, and 68°C/5min.

Amplification of Human Sμ/3'RR LSR junctions

LSR junctions were amplified in triplicate using 200 ng of genomic DNA extracted from peripheral blood of Human Healthy donors, tonsils and peripheral blood of C. Amplification of target junctions was performed by nested PCR using six couples of primers and the Herculase II fusion DNA polymerase (Agilent 60067). These primers amplify LSR junctions produced on HS1.2, HS4 and HS3. For the first nested PCR we used these primers: Eμh1 **Forward:** (AGGCTGACCGAAACTGAAAA) and 3'farhhs4 **Reverse** (CAAGCGTCAAGGTGTGGAC) with the following program: 98°C/30sec, 2cycles of 98°C/10sec, 64°C/30sec,68°C/4min, 3 cycles of 98°C/10sec, 62°C/30sec,68°C/4min, 25 cycles of 98°C/10sec, 60°C/30sec, 68°C/4min and 68°C/5min. and the second nested PCR with the 2 primers Sμ1b **Forward** (CAGGGAACTGGGGTATCAAG) and Probe 3'hhs4 **Reverse** (GGACGCGGTTTGCTTTTAT) with the following program 98°C/30sec, 30 cycles of 98°C/10sec, 58°C/30sec, 68°C/4min, and 68°C/5min.

High Throughput Sequencing (HTS) of CSR and LSR junctions

Triplicates Amplicons of LSR or CSR junctions from nested PCR were mixed. DNA is quantified by Qubit high sensitivity kit (Qubit® dsDNA HS Assay Kits nos. Q32851, Q32854) with the Qubit® Fluorometer machine. 100ng of DNA are used for library preparation with Ion Xpress™ Plus Fragment Library Kit (Thermo fisher, life technology, no. 4471269). DNA of each library were dosed by Qubit high sensitivity then diluted to 22ng/ml. Pool of all prepared barcoded libraries (5µl/library) sequenced with ion proton or S5 chip (1-96 samples/chip). Bio analyzer analysis chip 2100 expert (11 samples/chip) verifies the Length of each prepared library fragment; from 250bp to 300bp. Results are collects as Fastq format then proceeds to the bioinformatics analysis.

License CC BY-NC-ND 4.0

Primary B cell activation

Naïve B cells are isolated from peripheral blood of Human Healthy donors after Ficoll gradient lymphocytes separation (CMSMSL01-01) using naïve B Cell Isolation kit II (no. 130-091-150). Naïve B cells were cultured in RPMI 1640 media, supplemented with Non-Essential Amino Acids (NEAA 1%), antibiotics: Streptomycin, penicillin (SP 1%), Ultra glutamine (1%), fetal bovine serum (FBS 10%), Sodium Pyruvate (1%). Cells were activated with 1µl (250ng/ml) of cross-linked CD40 ligand (Human CD40-Ligands Multimer kits 100µg, no. 130-098-775), 1.6µl/ml (200U/ml) of Interleukin 4 IL-4 (Human IL-4 premium grade 25µg, no.130-093-921). CD40-ligand, IL-4 Stimulate the class switch from IgM to IgG1 (ɣ1) and Locus Suicide Recombination (LSR) *in vitro* in human cells. These cells were stimulated for 96 hours. Cells are collected after stimulation for DNA and RNA studies.

Chromatin immunoprecipitation 'ChIP'

Activated B Cells, tonsils cells and CLL cells were counted using cell counter (cellometer), diluted to 2*10^6cells/ml. Cells were fixed by formaldehyd 37% (1% final concentration) 15' at room temperature (RT) under agitation, glycine 2.125M (0.125M final concentration) 5' at RT under agitation, washed with cold PBS(1X). Nucleus were isolated by cellular lysis buffer, then chromatin extraction by nuclear lysis buffer, chromatins were sonicated using ultrasound sonicator 10 series of 10 pulses/ 4 second for each pulse, amplitude 80. Solutions used are represented in the (Supplemental table 1) (Legube et al., 2006).

Chromatins were dosed by Nano drop, diluted 10 times incubated with 1ml of 50% A/G Proteins (A agarose no. P-1925-5ML, Roche, G sepharose, no. P-3296-5ML, Roche) over night at 4°C under agitation. After a series of washing, DNA is incubated 5 hours at 4°C under rock with 1µg of specific antibodies targeting different DNA repair pathway: Non-Homologous end joining (NHEJ), Alternative End Joining (Alt-EJ) and Homologous Recombination (HR) and epigenetic marks. Antibodies and their references are cited in the supplemental information (Supplemental table 2). After we incubated 1hour30' at 4°C with 100µlof 50% A/G beads and washed 5 times by the wash buffer, suspend in TE (10.1, PH 8.1) incubated at 37°C, 15' with 1µl of RNase cocktail (500U/ml, AM2286), and with SDS10% overnight at 70°C, with proteinase 1 hour45' at 65°C. DNA is extracted with the classic method of phenol/chloroform, eluted with 100 µl/H2O quality molecular biology. ChIP followed by qPCR on genomic DNA.

Protease inhibitor cocktail were added to all Buffer used in this protocol (cOmpleteTM, Mini, EDTA-free Protease inhibitor cocktail, no. 11836170001, Roche, Sigma Aldrich) and (cOmpleteTM, Protease Inhibitor Cocktail, no.11697498001, Roche, Sigma Aldrich).

License CC BY-NC-ND 4.0

RNA extraction and cDNA synthesis and real time PCR:

Total RNA was isolated from cultured cells or cells from CLL samples using TRIZOL reagent (TRIzol™ Reagent, 15596018). To verify cell activation, we quantified the Activation Induced Cytidine Deaminase (AID) enzyme expression. Equal amount of cDNA was synthesized using the Advantage RT-for-PCR kit (Advantage RT-for-PCR kit Applied Biosystems™, Thermofisher 4368814/10400745) and mixed with the Power SYBR Green PCR master mix (SensiFast Hi ROX syber green BIO920025) using forward and reverse specific primers, or with SensiFast Probe Hi ROX kit BIO820025 using specific probes (LIG3: HS00242692-m1, LIG4: HS01866071-u1, PolΘ: HS00981375-m1, 53BP1: HS00996818-m1, Rif1: HS00871714-m1). qPCR on genomic DNA of ChIP experiments were done using the syber mix and primers of different targets (supplemental table 3). CD19 used as an internal control.

Bioinformatics analysis

To analyze repartition of junction structure and DNA repair of LSR and CSR after high throughput sequencing we used a software dedicated for class switch junction analysis named CSReport.

Statistical analysis

Graphs, histograms and statistical analysis are designed using graph pad 6 prism software.

RESULTS AND DISCUSSION

CLL LSR^{Low} and CLL LSR^{High} present distinct structure profiles of LSR junctions

LSR product is a recombined *IgH* locus junction between a donor S region and the 3'RR as the recombination acceptor region. During the recombinational process, donor and acceptor sequences are targets of DNA lesions leading to DNA double strand breaks (DSB). Repair of DNA DSB is a highly ordered, robust and constitutive process in mammalian cells. Study of structure at the repair junction is common in studies of genetic rearrangement molecular mechanisms, especially to get information on DNA repair machinery. Repair structure analysis is based on identification of nucleotide insertion, expressed in length in base pairs (bp), between donor and acceptor DNA segments of the recombination. Junctions are also structurally defined by sequence homology between recombined sequences. Results shown in figure 1 were obtained from CLL PBMC and healthy volunteer PBMC. The LSR^{Low} CLL group appears to differ from others samples in LSR structure profile. LSR junctions exhibited more few microhomologies (1-2bp) and blunt structures at the detriment of junctions with long insertions (≥4bp) (Figure 1A). These latter appear similar to structure profiles observed in normal B cells (Figure 1A). In contrast, no difference was observed between CSR structure profile between normal and pathological samples whatever the LSR^{Low} or LSR^{High} status (Figure 1B).

License CC BY-NC-ND 4.0

DSB are extremely harmful DNA lesions and inaccurate repair is directly implicated in chromosome translocations, fortunately this is a rare event thanks to the DNA damage response. Several pathways are solicited for DSB reparation. The two major ones are NHEJ (non-homologous end Joining) and homologous recombination (HR), but there is also the Alt-EJ (Alternative End-joining) pathway. NHEJ and Alt-EJ, due to their capacity to ligate DNA ends from independent molecular origins, are good candidate processes for DNA rearrangement. During CSR repair, the joining of DSB ends results mainly from the NHEJ (Soulas-Sprauel et al., 2007). We already observed in murine B cells that the repair structure of LSR differs from those of CSR (Boutouil et al., 2019). Also, in normal human B cells isolated from peripheral blood, repair signature for LSR is highly different from those of CSR (Figure 1A and 1B). Chromatin immunoprecipitation experiments on activated B cells from peripheral blood of healthy donors using antibodies raised against proteins specific to NHEJ (XRCC4) or Alt-EJ (PARP1 and POLθ) pathways showed that XRCC4, PARP-1 and POLθ are significantly recruited to Sμ region. Only XRCC4 is recruited to Sγ1 while PARP1 and POLθ are recruited on HS1.2 and HS4 (Figure 1C). These results imply NHEJ and Alt-EJ usage during DSB repair at the *IgH* locus with a specific recruitment of the NHEJ at the CSR donor/acceptor DNA segments and the Alt-EJ at the LSR donor/acceptor segments. This could be explained by the chromatin context with the great enrichment of H4K20me1, known to promote NHEJ via the 53BP1 accumulation at DSB (Hartlerode et al., 2012) on CSR segment and the enrichment of H4K16ac, which is no favorable to promote NHEJ at the DSB (Horikoshi et al., 2019) on the 3'RR HS1.2 and HS4 DNA (Figure1D). Activation of B cells was verified by quantification of AID transcripts in activated and resting B cells (Supplemental figure 1A). Absence of HR recruitment to the *IgH* locus was observed by negative recruitment of Rad52 (Supplemental figure 1B).

LSR^{Low} CLL exhibit different DNA repair during LSR compared to LSR^{High} CLL and healthy PBMC?

LSR junction's structure profile observed in the LSR^{Low} CLLs questions the DNA repair process employed in this condition. Observed junction structure profile reveals an increase in the frequency of blunt junctions and 1-2bp microhomology junctions. This profile is reminiscent of the usage of NHEJ. To evaluate whether an unbalanced DSB repair could explain the differential LSR junction structure observed in CLL we analyzed the expression levels of DSB response actors in both groups LSR^{High} and LSR^{Low}. qRT-PCR allowing quantification of transcripts coding for actors implicated in the protection of DSB DNA ends from resection and favoring NHEJ (53BP1, Rif1 and Rev7), NHEJ actors (LIGIV) and Alt-EJ actors (PARP-1, POLθ and LIGIII) were performed. As shown in the figure 2A, we did not detected any significant difference on the transcription level for all tested transcripts of NHEJ implicated proteins between LSR^{High} and LSR^{Low}. Similarly, the level of Alt-EJ actors' transcription as comparable in LSR^{Low} and LSR^{High} (Figure 2B). Results did not reveal differential expression for tested candidate genes

License CC BY-NC-ND 4.0

between CLL groups. Nevertheless, as LSR is normally occuring in activated B cell, PBMC DNA are not the more appropriate samples for our analysis.

LSR^{Low} and LSR^{High} CLL PBMC appears as resting cells

In the previous data no difference was observed at the transcription levels between the NHEJ and Alt-EJ actors between LSR^{Low} and LSR^{High}. We analyzed the chromatin context on the *IgH* locus on PBMC from the two groups of CLL patients. ChIP experiments against the epigenetic marks H4K20me1 and H4K16ac were performed. qPCR on the Sμ (LSR donor segment) and HS1.2, HS4 (LSR acceptor segments) showed an enrichment of H4K20me1 on the whole *IgH* locus. H4K16ac was observed to be not recruited (Figure 2C). This profile was similar between LSR^{Low} and LSR^{High} cells and we do not observed difference in chromatin context at the *IgH* locus (Figure 2C). This is in accord with previous results of no difference between both groups on quantification of expression of Alt-EJ and NHEJ proteins. Furthermore, ChIP results on CLLs correlate with results from resting B cells isolated PBMC of healthy donors rather than with in vitro activated B cells. The predominance of H4K20me1 epigenetic mark enriched on the whole *IgH* locus including the 3'RR (Figure 2D) is retrieved on CLL PBMC as in healthy peripheral blood B cells. This suggests that CLL PBMC are in a global resting state, LSR junctions are stigmata products of the recombination mechanism and LSR has been achieved in CLL proliferation centers in secondary lymphoid organs (Ghia et al., 2002).

LSR^{Low} CLL cells share similarities in LSR DSB repair with tonsil cells

LSR, in CLL cells, may occur in secondary lymphoid organs as suggested above and this is consistent with the normal condition of LSR occurrence in activated B cells (Dalloul et al., 2019; Péron et al., 2012). To get insights in LSR in B cells from secondary lymphoid organs in physiological condition, we studied the LSR junction structure in normal B cells from tonsils from healthy volunteers. As shown in figure 3A, LSR junction structure in normal cells from tonsils is comparable to those of CLL LSR^{Low} cells with the decrease of junctions with insertions ≥4bp in favor of increase blunt junctions and junctions with 1-2 bp microhomology. Repair junctions harboring blunt structure and structure with very short microhomology (1-2bp) is highly reminiscent of that seen in the case of NHEJ-employed DSB repair (Lieber, 2010), so, the recruitment of NHEJ to *IgH* locus in CD19+ B cells from tonsils was subsequently questioned. ChIP experiments using antibodies raised against XRCC4 and PARP-1 were performed as previously and a significant enrichment of XRCC4 was observed on Sμ, Sγ and Hs1.2 segments. PARP-1 was observed to be not recruited to these segments. This is in accord with LSR junction structure observed in tonsils and collectively our results suggest that CLL LSR^{Low} B cells share common LSR junction features with normal B cells from tonsils. Whereas, CLL LSR^{High} samples share with healthy

License CC BY-NC-ND 4.0

PBMC same LSR junction structure profile. Indeed, LSR junctions amplified from secondary lymphoid organs (tonsils) reflect “on-going” LSR in activated B cells, the small number of LSR junctions detected in PBMC is certainly amplified from non-functional IgH allele (Dalloul et al., 2019) from circulating memory B cells in blood after their activation in secondary lymphoid organs. Data obtained here concerning LSR in normal PBMC and tonsils suggest LSR-deletion of B cell population in memory B cells compared to activated B cells. For instance, no data have been obtained concerning which B cell sub-population is prone to LSR in vivo, thanks to our results we can suppose the targeted B cells harbor LSR with repair junctions enriched in blunt and with short microhomology junctions.

Finally, if LSR regulates B cells homeostasis, it would not be surprising that LSR participates in the elimination of pathological B cells. There are many situations where it is necessary to exercise control of B cells, CLL is a condition in which B cell homeostasis dysregulation occurs. As observed in our manuscript, activated B cells in secondary lymphoid organs can represent the cell of origin of the LSR^{Low} CLLs, anomalies participating in the emergence of this pathological condition remain to be determined. CLL LSR^{High} B cells appear to be note related to activation on-going B cells and the normal B cell counterpart in this CLL sub-group seems to be differ from that of LSR^{Low} CLL.

ACKNOWLEDGEMENTS

This work was supported by grants from la Ligue Contre le Cancer (Comité de la Haute-Vienne, CD87) and by grants from INCa-Cancéropôle GSO (Emergence program N°2019-E11). We are grateful to Dr. Villéger and to Dr. Al Hamel at the CRBioLim, Dupuytren Hospital, Limoges, to Dr. Vallejo and the INSERM CIC 1435, Dupuytren Hospital, Limoges, and to Dr. Lerat, Dupuytren Hospital, Limoges, France, for providing human samples. This work was supported by grants from la Ligue Contre le Cancer (Comité de la Haute-Vienne, CD87). IAJ is supported by Fondation pour la Recherche Medicale (FRM) and Association Libanaise. KG is supported by Région Nouvelle Aquitaine and Délégation INSERM Nouvelle Aquitaine. MP is supported by Région Nouvelle Aquitaine and Université de Limoges.

AUTHORSHIP CONTRIBUTIONS

IAL performed experiments and participated in writing of the original draft.

KG, MP and MB participated in experiments.

DR and NG participated in data curation.

SAH and NM participated in writing the original draft.

JF, NG and SP led the conceptualization, data curation, funding acquisition, manuscript writing.

DISCLOSURE OF CONFLICTS OF INTEREST

The authors declare no competing interests.

License CC BY-NC-ND 4.0

FIGURE LEGENDS

Figure 1: CLL LSR^{Low} and CLL LSR^{High} present distinct structure profile of LSR junctions.

Different structures of LSR and CSR junctions (insertions, blunt or µhomologies) are represented based on high throughput sequencing and analysis by CSReport software. **A.** Structure of LSR junctions in CLL groups and healthy PBMC (healthy PBMC N=9, 239 junctions; LSR^{Low} N= 35, 703 junctions; LSR^{High} N=12, 703 junctions). No difference observed between healthy PBMC and LSR^{High} group. In contrast, the LSR junction's structure are significantly different in LSR^{Low} group in comparison with both healthy or LSR^{High} group. A decrease of junctions with insertions ≥4bp and the increase in blunt junctions and junctions with 1-2bp µhomology were observed. **B.** Structure of CSR junctions in CLL groups and healthy PBMC (healthy PBMC N=5, 10301junctions; LSR^{Low} N=35, 22247 junctions; LSR^{High} N=11, 10739 junctions). All CSR junctions in the different group are similar with no significant difference. **C.** Immunoprecipitation (ChIP) experiments were performed in naïve B cells isolated from peripheral blood of healthy donors and stimulated with IL-4 and CD40L for 96hours with antibodies raised against: XRCC4 (NHEJ DNA repair pathway molecule) and PARP-1, POLϴ (Alt-EJ DNA repair pathway molecules). **D.** ChIP of two epigenetic marks H4K20me1 and H4K16ac, using the same strategy on stimulated naïve B cells. qPCR were performed on the genomic DNA extracted after ChIP using specific primers for Sµg, Sµd(CSR/LSR donor segments), Sɣ1-3,Sɣ1-a(CSR acceptor segments), HS1.2, HS4(LSR acceptor segments) and Sγ3,CD19 (negative controls). This graph shows results of qPCR with fold enrichment method compared to mock condition (N=3 to 5). **C.** XRCC4, PARP-1 and POLϴ were significantly recruited to Sµ donor region, XRCC4 was more recruited to Sɣ1 than PARP-1 and POLϴ. On 3'RR (HS1.2, HS4) there was a significant recruitment of PARP-1, POLϴ and not XRCC4 compared to mock. No significant recruitment was observed on the negative controls. **D.** H4k20me1 was more enriched on Sµ region than on Sɣ1 and on 3'RR in contrast to H4K16ac which was more enriched on 3'RR than on Sµ and Sɣ1. No significant enrichment was detected on the negative controls. H4K20me1 was significantly enriched on CD19 as expected as it's transcription activator marker. All these results suggest that DSBs of LSR are prone to be repaired by Alt-EJ rather than NHEJ in normal B cells. Graph designed with prism6 graph pad with mean±SEM, statistical analysis using Chisq test (A and B) unpaired non-parametric T test (C and D), ns: no significant difference, * P<0.05, **P<0,001, ***P<0.001.

Figure 2: LSR repair in LSR^{Low} seems to be promoted by NHEJ. Quantitative RT-PCR were performed on cDNA obtained on total RNA extracted from LSR^{Low} (N=9 to 11) and LSR^{High} (N=4 to 10) CLL PBMC using different probes targeting actors of the NHEJ DNA repair pathway: 53BP1, Rif1, Rev7 and LLIGIV **(A)** and the Alt-EJ system: PARP-1, Polϴ and LIGIII **(B)**. Results represented here are normalized to the CD19 transcripts level. No difference in the transcripts level was observed between the two groups. **C.** Analysis of chromatin epigenetic context of the *IgH* Locus in the CLL groups (LSR^{Low} N=4, LSR^{High} N=4)

License CC BY-NC-ND 4.0

was done to establish which DNA repair pathway is promoted, result showed significant enrichment of H4K20me1 on the Sμ and 3'RR region and no enrichment of H4K16ac in CLL LSR^{Low} group and this group exhibits similar chromatin profile, concerning these particular marks, to resting B cells with. **D.** Chromatin context analysis in resting B cells (N=4) by ChIP experiments show a significant enrichment of H4K20me1 on the targeted regions of *IgH* locus. In contrast, H4K16ac was negative and not enriched on the *IgH* locus and CD19 (negative control) of resting B cells. Graphs are represented using the graph pad prism 6, statistical analysis was performed using the unpaired non-parametric T test, ns: no significance difference, *P<0.05.

Figure 3: CLL LSR^{Low} present LSR structure profile similar to LSR junctions detected in normal tonsils. A. LSR junction's structure of healthy PBMC (N=9, 239 junctions), tonsils (N=24, 701 junctions) and LSR^{Low} CLL (N=35, 357 junctions). A significant difference in the LSR junction structure was observed in LSR^{Low} compared to healthy PBMC. In contrast this profile was similar to LSR junction structure in healthy tonsils with a decreased in junctions with insertions ≥4bp and the increase in blunt junctions and junctions with 1-2 μhomologies. B. Study of the DNA repair pathway of *IgH* locus in normal tonsils by chip experiments using XRCC4 and PARP-1 antibodies. Result shows significative recruitment of XRCC4 on Sμg (CSR/LSR donor segment), on Sγ1-a, Sγ1-3 (CSR acceptor segments) and Hs1.2 (LSR acceptor segment) PARP-1 is not recruited on all these segments. These results suggest that LSR^{Low} CLL cells share similarities with tonsils cells. Graphs are represented using the graph pad prism6, statistical analysis was performed using Chisq test, ns: no significance difference, ****P<0.0001 (A) and unpaired non-parametric T test ns: no significance, *P<0.05, **P<0.01 (B).

License CC BY-NC-ND 4.0

REFERENCES

Al Jamal, I., Parquet, M., Boutouil, H., Guiyedi, K., Rizzo, D., Dupont, M., Boulin, M., El Hamel, C., Lerat, J., Aoufouchi, S., al Hamaoui, S., Makdissy, N., Feuillard, J., Gachard, N., Peron, S., 2022. Increased frequencies of IgH locus suicide recombination points on Chronic Lymphocytic Leukemia with low rate of AID related somatic mutations, cMYC overexpression and short telomeres. bioRxiv 2022.03.06.482661. https://doi.org/10.1101/2022.03.06.482661

Baliakas, P., Jeromin, S., Iskas, M., Puiggros, A., Plevova, K., Nguyen-Khac, F., Davis, Z., Rigolin, G.M., Visentin, A., Xochelli, A., Delgado, J., Baran-Marszak, F., Stalika, E., Abrisqueta, P., Durechova, K., Papaioannou, G., Eclache, V., Dimou, M., Iliakis, T., Collado, R., Doubek, M., Calasanz, M.J., Ruiz-Xiville, N., Moreno, C., Jarosova, M., Leeksma, A.C., Panayiotidis, P., Podgornik, H., Cymbalista, F., Anagnostopoulos, A., Trentin, L., Stavroyianni, N., Davi, F., Ghia, P., Kater, A.P., Cuneo, A., Pospisilova, S., Espinet, B., Athanasiadou, A., Oscier, D., Haferlach, C., Stamatopoulos, K., ERIC, the European Research Initiative on CLL, 2019. Cytogenetic complexity in chronic lymphocytic leukemia: definitions, associations, and clinical impact. Blood 133, 1205–1216. https://doi.org/10.1182/blood-2018-09-873083

Boutouil, H., Boyer, F., Cook-Moreau, J., Cogné, M., Péron, S., 2019. IgH locus suicide recombination does not depend on NHEJ in contrast to CSR in B cells. Cell. Mol. Immunol. 16, 201. https://doi.org/10.1038/s41423-018-0172-2

Caligaris-Cappio, F., Hamblin, T.J., 1999. B-cell chronic lymphocytic leukemia: a bird of a different feather. J. Clin. Oncol. Off. J. Am. Soc. Clin. Oncol. 17, 399–408. https://doi.org/10.1200/JCO.1999.17.1.399

Dalloul, I., Boyer, F., Dalloul, Z., Pignarre, A., Caron, G., Fest, T., Chatonnet, F., Delaloy, C., Durandy, A., Jeannet, R., Lereclus, E., Boutouil, H., Aldigier, J.-C., Péron, S., Le Noir, S., Cook-Moreau, J., Cogné, M., 2019. Locus suicide recombination actively occurs on the functionally rearranged IgH allele in B-cells from inflamed human lymphoid tissues. PLoS Genet. 15, e1007721. https://doi.org/10.1371/journal.pgen.1007721

Döhner, H., Stilgenbauer, S., Benner, A., Leupolt, E., Kröber, A., Bullinger, L., Döhner, K., Bentz, M., Lichter, P., 2000. Genomic aberrations and survival in chronic lymphocytic leukemia. N. Engl. J. Med. 343, 1910–1916. https://doi.org/10.1056/NEJM200012283432602

Ghia, P., Granziero, L., Chilosi, M., Caligaris-Cappio, F., 2002. Chronic B cell malignancies and bone marrow microenvironment. Semin. Cancer Biol. 12, 149–155. https://doi.org/10.1006/scbi.2001.0423

Hartlerode, A.J., Guan, Y., Rajendran, A., Ura, K., Schotta, G., Xie, A., Shah, J.V., Scully, R., 2012. Impact of Histone H4 Lysine 20 Methylation on 53BP1 Responses to Chromosomal Double Strand Breaks. PLoS ONE 7, e49211. https://doi.org/10.1371/journal.pone.0049211

Horikoshi, N., Sharma, D., Leonard, F., Pandita, R.K., Charaka, V.K., Hambarde, S., Horikoshi, N.T., Gaur Khaitan, P., Chakraborty, S., Cote, J., Godin, B., Hunt, C.R., Pandita, T.K., 2019. Pre-existing H4K16ac levels in euchromatin drive DNA repair by homologous recombination in S-phase. Commun. Biol. 2, 1–12. https://doi.org/10.1038/s42003-019-0498-z

Kajüter, H., Wellmann, I., Khil, L., Jöckel, K.-H., Zhang, C., Fink, A.-M., Hallek, M., Stang, A., 2021. Survival of patients with chronic lymphocytic leukemia before and after the introduction of chemoimmunotherapy in Germany. Blood Cancer J. 11, 1–4. https://doi.org/10.1038/s41408-021-00556-7

Katayama, Y., Sakai, A., Katsutani, S., Takimoto, Y., Kimura, A., 2001. Lack of allelic exclusion and isotype switching in B cell chronic lymphocytic leukemia. Am. J. Hematol. 68, 295–297. https://doi.org/10.1002/ajh.10042

Legube, G., McWeeney, S.K., Lercher, M.J., Akhtar, A., 2006. X-chromosome-wide profiling of MSL-1 distribution and dosage compensation in Drosophila. Genes Dev. 20, 871–883. https://doi.org/10.1101/gad.377506

License CC BY-NC-ND 4.0

Lieber, M.R., 2010. The Mechanism of Double-Strand DNA Break Repair by the Nonhomologous DNA End Joining Pathway. Annu. Rev. Biochem. 79, 181–211. https://doi.org/10.1146/annurev.biochem.052308.093131

Morande, P.E., Yan, X.-J., Sepulveda, J., Seija, N., Marquez, M.E., Sotelo, N., Abreu, C., Crispo, M., Fernández-Graña, G., Rego, N., Bois, T., Methot, S.P., Palacios, F., Remedi, V., Rai, K.R., Buschiazzo, A., Di Noia, J.M., Navarrete, M.A., Chiorazzi, N., Oppezzo, P., 2021. AID overexpression leads to aggressive murine CLL and nonimmunoglobulin mutations that mirror human neoplasms. Blood 138, 246–258. https://doi.org/10.1182/blood.2020008654

Palacios, F., Moreno, P., Morande, P., Abreu, C., Correa, A., Porro, V., Landoni, A.I., Gabus, R., Giordano, M., Dighiero, G., Pritsch, O., Oppezzo, P., 2010. High expression of AID and active class switch recombination might account for a more aggressive disease in unmutated CLL patients: link with an activated microenvironment in CLL disease. Blood 115, 4488–4496. https://doi.org/10.1182/blood-2009-12-257758

Péron, S., Laffleur, B., Denis-Lagache, N., Cook-Moreau, J., Tinguely, A., Delpy, L., Denizot, yves, Pinaud, E., Cogné, M., 2012. AID-Driven Deletion Causes Immunoglobulin Heavy Chain ”Locus Suicide Recombination” in B Cells. Science epub ahead of print. https://doi.org/10.1126/science.1218692

Scully, R., Panday, A., Elango, R., Willis, N.A., 2019. DNA double strand break repair pathway choice in somatic mammalian cells. Nat. Rev. Mol. Cell Biol. 20, 698–714. https://doi.org/10.1038/s41580-019-0152-0

Soulas-Sprauel, P., Le Guyader, G., Rivera-Munoz, P., Abramowski, V., Olivier-Martin, C., Goujet-Zalc, C., Charneau, P., de Villartay, J.-P., 2007. Role for DNA repair factor XRCC4 in immunoglobulin class switch recombination. J. Exp. Med. 204, 1717–1727. https://doi.org/10.1084/jem.20070255

License CC BY-NC-ND 4.0

FIGURES

Figure 1

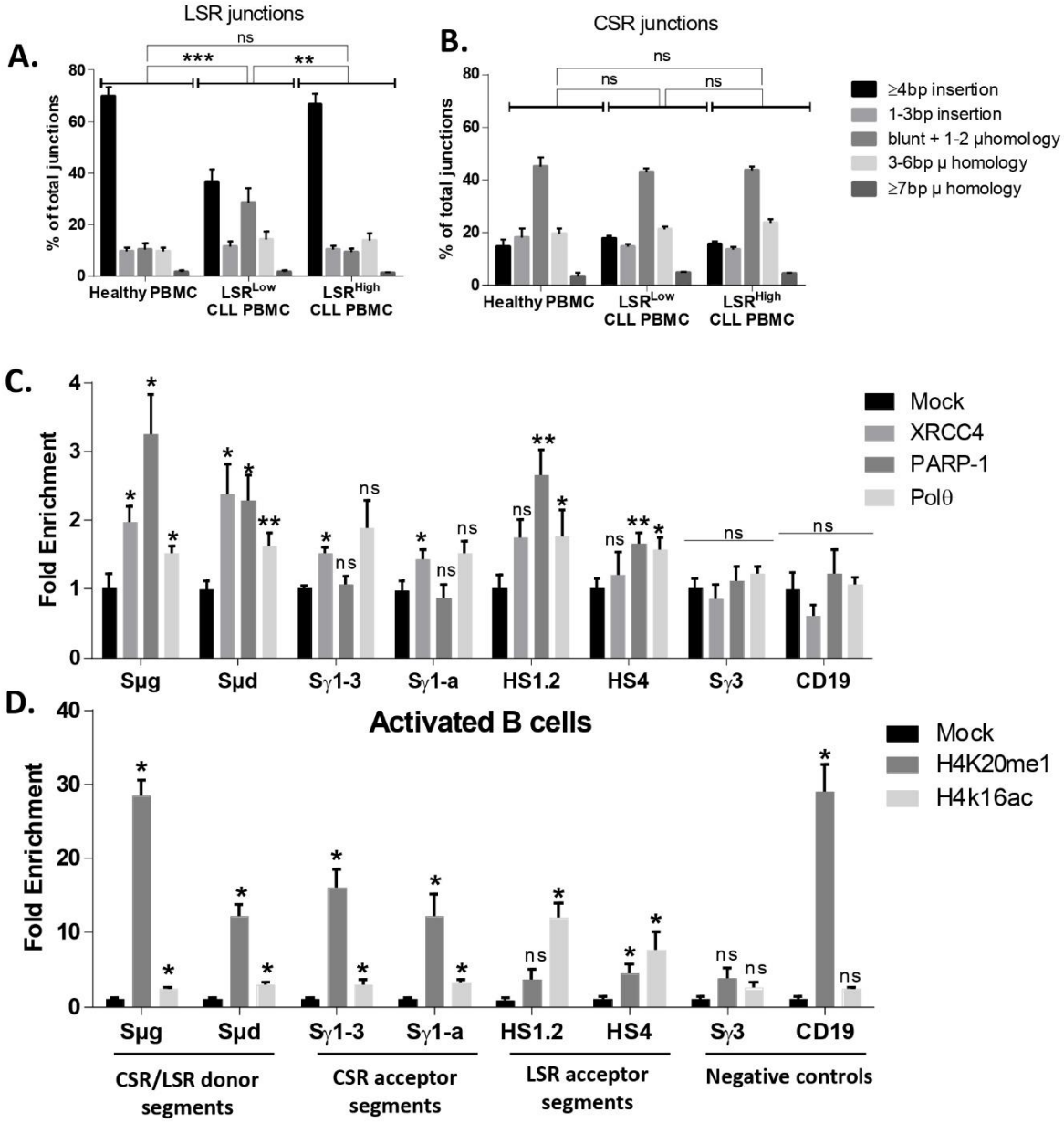

License CC BY-NC-ND 4.0

Figure 2

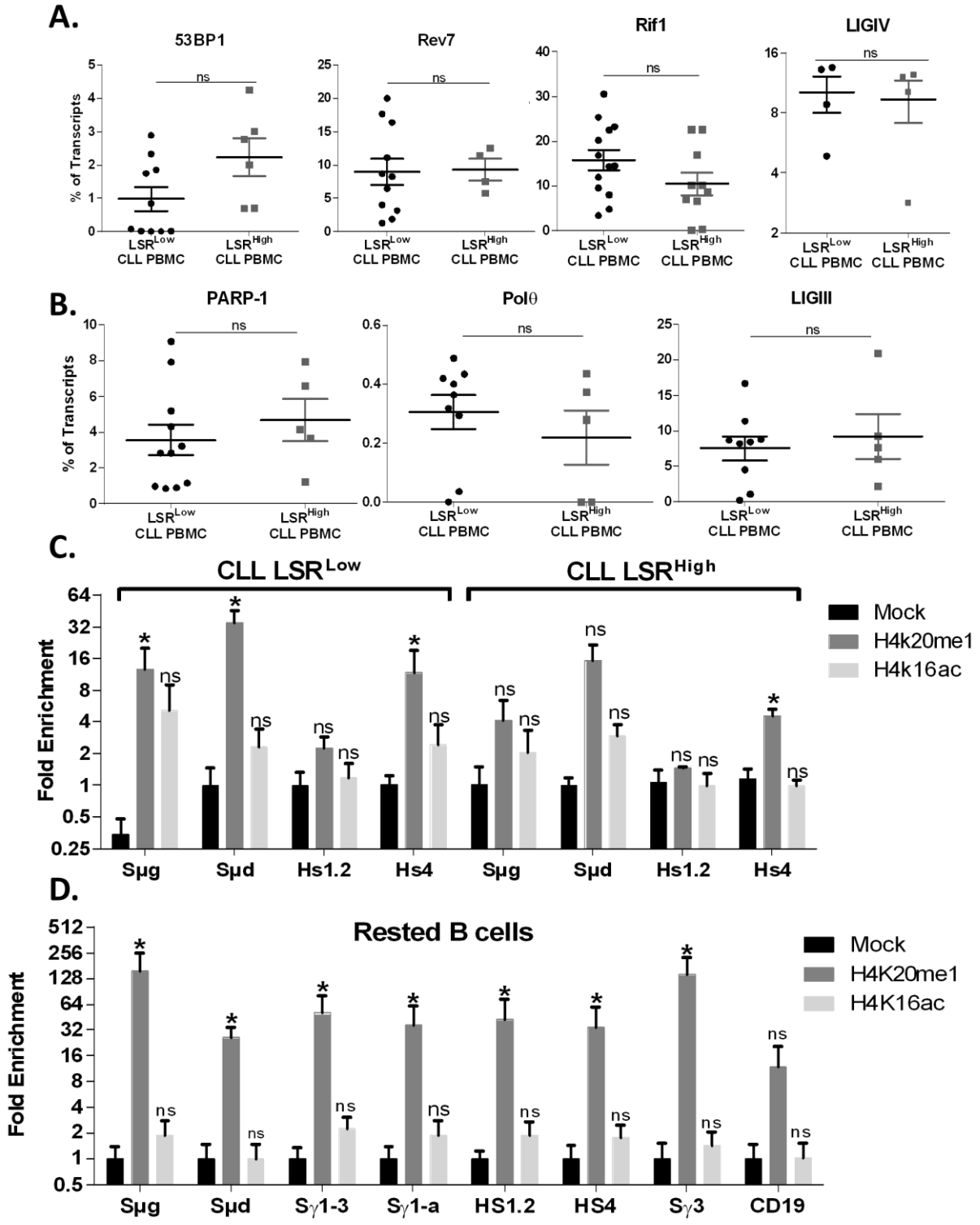

License CC BY-NC-ND 4.0

Figure 3

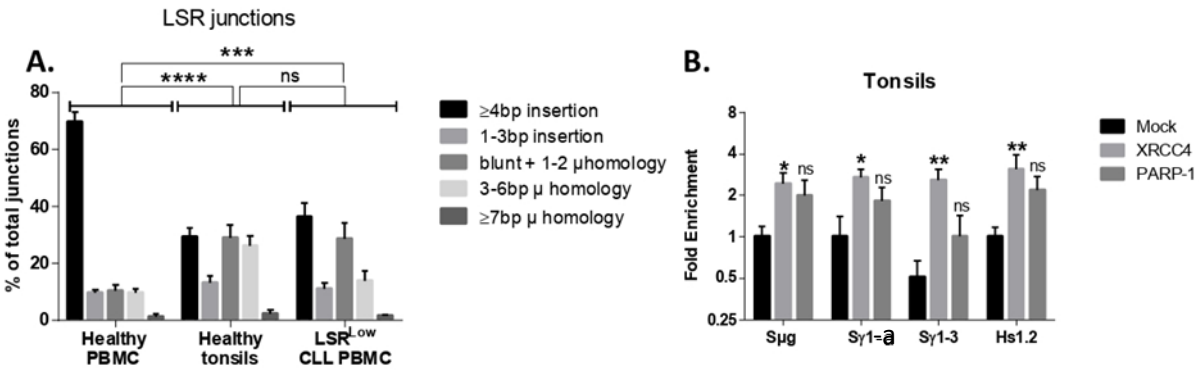

License CC BY-NC-ND 4.0

SUPPLEMENTAL DATA

Supplemental figure 1

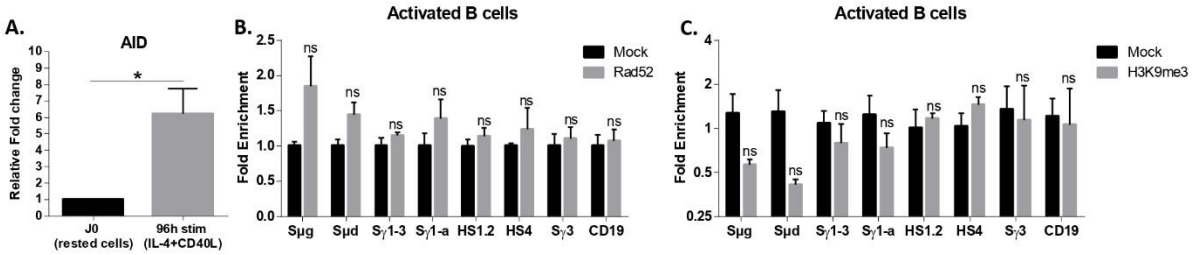

Supplemental figure 1: controls of the experiments. A. Validation of naive B cell activation by AID transcript quantification. After 96 hours of stimulation with IL-4 and CD40L, a significant increase in AID transcripts was observed in stimulated B cells compared to not stimulated B cells (J0). **B.** ChIP experiments on activated B cells using antibody raised against HR pathway (Rad52) (N=4). Rad52 is not recruited to any segment of *IgH* locus and allow to exclude the activity of HR in LSR and CSR. **C.** ChIP experiments on activated B cells targeting H3K9me3 epigenetic mark as negative control (transcription insulator) (N=4). Results of qPCR showed a no enrichment of H3K9me3 on the different segment of *IgH* locus. Graphs are represented using the graph pad prism6. Statistical analysis was performed using the unpaired non-parametric T test: ns: no significance, *P<0.05.

SUPPLEMENTAL TABLES

Supplemental table 1: Solutions used in ChIP experiment

Solutions	Constituants
Cellular Lysis Buffer (CLP)	200µl pipes (aliquotes a –20°C) 850µl KCL 2M 1ml NP-40 10% H2O QSP 20 ml 2 tablets protease inhibitor « complète mini EDTA free »
Nuclear Lysis Buffer (NLB):	1 ml Tris 1M PH8.1 400µl EDTA 0.5M PH8 2ml SDS 10% H2O QSP 20ml 2 tablets protease inhibitor "complete mini EDTA free".
Dilution Buffer:	50µl SDS 10% 5.5ml triton X100-10% 120µl EDTA 0.5M PH8 835µl Tris 1m PH 8.1 1670µl NaCl 5M H2O QSP 50 ml 1 tablet protease inhibitor « complete EDTA free ».
IP Buffer:	1V Nuclear Lysis Buffer 9V Dilution Buffer
Dialysis Buffer:	80µl EDTA 0.5M 999µl Tris 1M PH8.1 200µl Sarkosyl 20% H2O QSP 20ml 2 tablets protease inhibitor « complete mini EDTA free »
Wash Buffer:	1.66 ml Tris 3M PH8.8 5ml LiCl 5M 5ml NP-40 10% 5ml NaDoc 10% H2O QSP 50 ml 1 tablet protease inhibitor « complete »
TE 10.1 PH 8.1	500µL de Tris 1M 100µL de EDTA 0.5M H2O QSP 50ml

License CC BY-NC-ND 4.0

Supplemental table 2: Antibodies used in ChIP experiments

Antibodies	Reference	Concentration
XRCC4	ab97351 Rb pAb to XRCC4	50µl(1mg/ml)
PARP-1	Ab227244 Rb pAb to PARP1	100µl (0,23mg/ml)
POLϴ	Ab111218 Rb pAb to DNA polymerase theta	100µg (1mg/ml)
RAD52	Sc-36531 (F-7) lot #F1116 Mouse monoclonal IgG1	200µg/ml
H4K20me1	Ab9051 Rb pAb to histone H4mono methyl K20	100µg (1mg/ml)
H4K16ac	EMD millipore 07-329 Anti-acetyl-histone H4(lys16) Rb lot 2960455	100µl (1mg/ml)
H3K9me3	EMD millipore 05-1242 Anti-trimethyl histone H3 lys9 clone 6f12-h4 lot 2992005	200µl (1mg/ml)

Supplemental table 3: Primers used in this study

Target segment	Primer name	Sequence 5'-3'
Sµ	Sµg	F:GGTGTGGGTTTTCACAGCTT
		R:CCTCACCAAGTCCACCAAGT
	Sµd	F:GGGGCTTGGTATGTTCTCAA
		R:AGCCCATTTGAAGGAGAGGT
Sγ1	Sγ1-3	F:CTGGGATGGAGAAGGGAAGG
		R:CTGGTCTCAAGCACACGTTC
	Sγ1-a	F:TGCTCTGCTGGGTCAGTTC
		R:GGGAGAAGGGAAGAGTCCAG
HS	HS1,2	F:GAGTTTTCGGCATCTCTGGG
		R:ACAGATCAGAGCCCTCACAC
	HS4	F:GTGTGTCTGAGGGTGAGTGA
		R:ACACTGTCACACACTCCACA
Sγ3	Sγ3	F:AGCTGTGCAACTGGAGTCCT
		R:TGAGCCACCTAATCCAAACC
AID	AID	F:GAGGCAAGAAGACACTCTGG
		R:GTGACATTCCTGGAAGTTGC
CD19	CD19	F:AGACTCCTTCTCCAACGGTA
		R:GGTCAGCTCTTCATCCTCGT

License CC BY-NC-ND 4.0

License CC BY-NC-ND 4.0

Preliminary data of Hodgkin Lymphoma

In my thesis work, I had the opportunity to participate to a project centered on the LSR mechanism as a potential cause of loss of BCR expression in Hodgkin lymphoma (HL) tumor cells.

INTRODUCTION

Hodgkin lymphoma (HL) is a cancer of the lymphatic system, it represents 10% of all lymphomas types (Piris et al., 2020). Tumor cells in HL called H/RS are present with the CD15+, CD30+ phenotype and these cells represent 1-10% of the tumor mass. H/RS cells does not express a BCR on their surface. In H/RS cells, down regulation of B cell transcriptomic profile was observed (Küppers et al., 2012). These cells represent transformed B cells, lineage link was confirmed by the expression of Pax-5. H/RS cells were identified to carry crippled mutations in the light and heavy chains of Ig resulting in the absence of BCR expression on cell surface (Marafioti et al., 2000). Since LSR conducts to the loss of BCR in B cells. We raised the question of the LSR as an additional explanation for BCR loss in HL and especially in H/RS cells.

METHODS

Human materials

The project was conducted according to the guidelines of the Declaration of Helsinki. HL patients were obtained from CRBioLim from Limoges Hospital, CHU Dupuytren. Tonsils were obtained from children scheduled for elective tonsillectomy and were obtained from CRBioLim (authorization: DC-2008-604, AC-2018-3157).

H/RS and CD20+ Cell sorting

Frozen HL samples were used to isolate H/RS and normal B cells using the same protocol and antibodies as described in (Reichel et al., 2017) and using ARIA II.

DNA extraction

DNA was extracted from HL samples cells and sorted H/RS, CD20+ B cells using the classical phenol/chloroform method.

CSR and LSR junction's sequencing

200 ng of genomic DNA of HL samples or from sorted CD20+ and H/RS cells are used for amplification of CSR and LSR junctions by nested PCR as described in the article 1 and 2.

License CC BY-NC-ND 4.0

CSR and LSR junctions were sequenced by NGS (ion proton and S5) and analyzed using the CSReport software.

Bioinformatics and statistical analysis

Junction counts and structure were analyzed using the CSReport software. Graphs are represented using the graph pad prism6 and statistical analysis was preformed using the chi-square or non-parametric T test.

RESULTS

HL samples exhibits LSR junctions.

In the first step we looked on the LSR junction count per sample, the number of LSR junctions in HL samples was lower than in healthy tonsils and in CLL samples. We obtained 8 among 11 patients negative for the LSR. The positive samples exhibit LSR junctions within the range of 1 to 108 junctions per sample.

Analysis of LSR and CSR junction's structure in the positive HL samples reveals a global profile different compared to healthy tonsils with a significant decrease of junctions with insertions ≥4bp and junctions with 0-2bp of microhomology suggesting an alteration in the DNA repair in HL samples (Figure 39A). CSR junction's structure was comparable in count and structure to those obtained in healthy tonsil cells (Figure 39B).

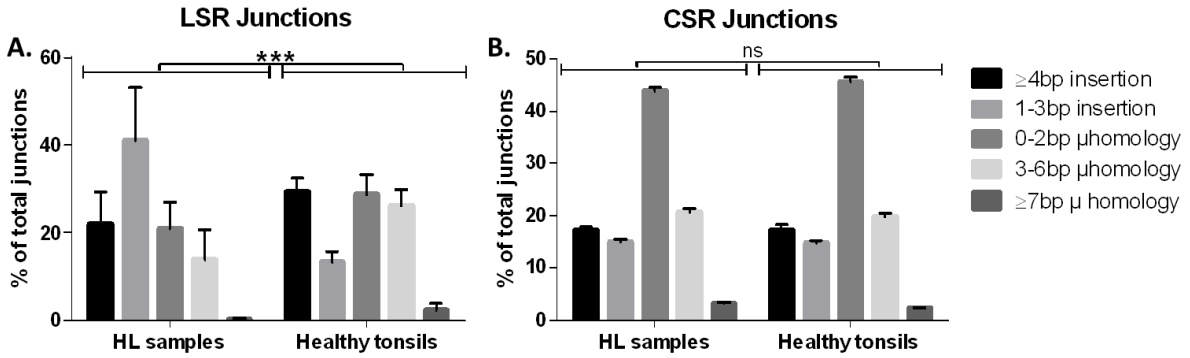

Figure 39: Structure of LSR and CSR junctions in HL and healthy tonsils samples.
A. LSR junctions amplified form HL samples (N=19, only 11 was positive with (193 junctions), and from tonsils samples (N =24, 701 junctions). A significant difference was observed in the structure of LSR junctions between HL and healthy tonsils. HL samples are enriched with junctions with small insertions more the tonsils samples are. **B.** CSR junctions amplified from HL samples (N=19, 76631 junctions) and healthy tonsils (N=14, 75951 junctions). No difference was observed in the structure of LSR junctions between HL and healthy tonsils. Graphs are represented with (mean±SEM). Statistical analysis was performed using Chisq test: ns: no significance difference, ***P<0.001.

License CC BY-NC-ND 4.0

H/RS are defective to CSR

As shown in the first part, HL samples carrying LSR junctions, this observation did not allow us to conclude on the implication of LSR in the loss of BCR since we amplified the LSR junctions from all cells of HL tumor samples. Indeed H/RS represent only 1-10% of the tumor mass, and we analyzed the LSR junctions and the CSR junctions on sorted B cells and H/RS cells. The cell sorting was based on the phenotypic differences between B cells present in the TME of HL (CD20+) and the H/RS (CD15+, CD30+). We isolated these two different populations from four DMSO cryopreserved cells from HL lymph nodes.

As Ig of H/RS is enriched with chromosomal break points, we searched for abnormalities during *IgH* locus rearrangement, we amplified the CSR junctions in these sorted cells using equal amount of extracted DNA. CSR count analysis showed a significant decrease in the count in three of these four patients with a tendency to a decrease in the fourth patient (Table 6).

Table 6: CSR junction counts in HL sorted cells.
Asterix indicate presence of significative difference between CD20+ and H/RS of HL samples.

HL samples	CD20+ B cells	H/RS cells
	CSR junctions count/200ng of gDNA	
#1	1484	399 *
#2	796	91 *
#3	231	20 *
#4	162	149

H/RS cells present alteration in CSR DNA repair machinery

We continued our analysis on the structure of CSR junctions. As shown in the (Figure 40A), analysis of CSR junction between sorted CD20+ B cells and sorted H/RS cells from 4 HL samples reveals a skewed structure profile in H/RS cells but without statistically significance. In contrast, the detailed analysis on each single sample alone as shown in the (Figure 40B) highlights alteration in the structure in H/RS cells compared to CD20+. It is important to note that these latter retain the expected CSR structure profile.

License CC BY-NC-ND 4.0

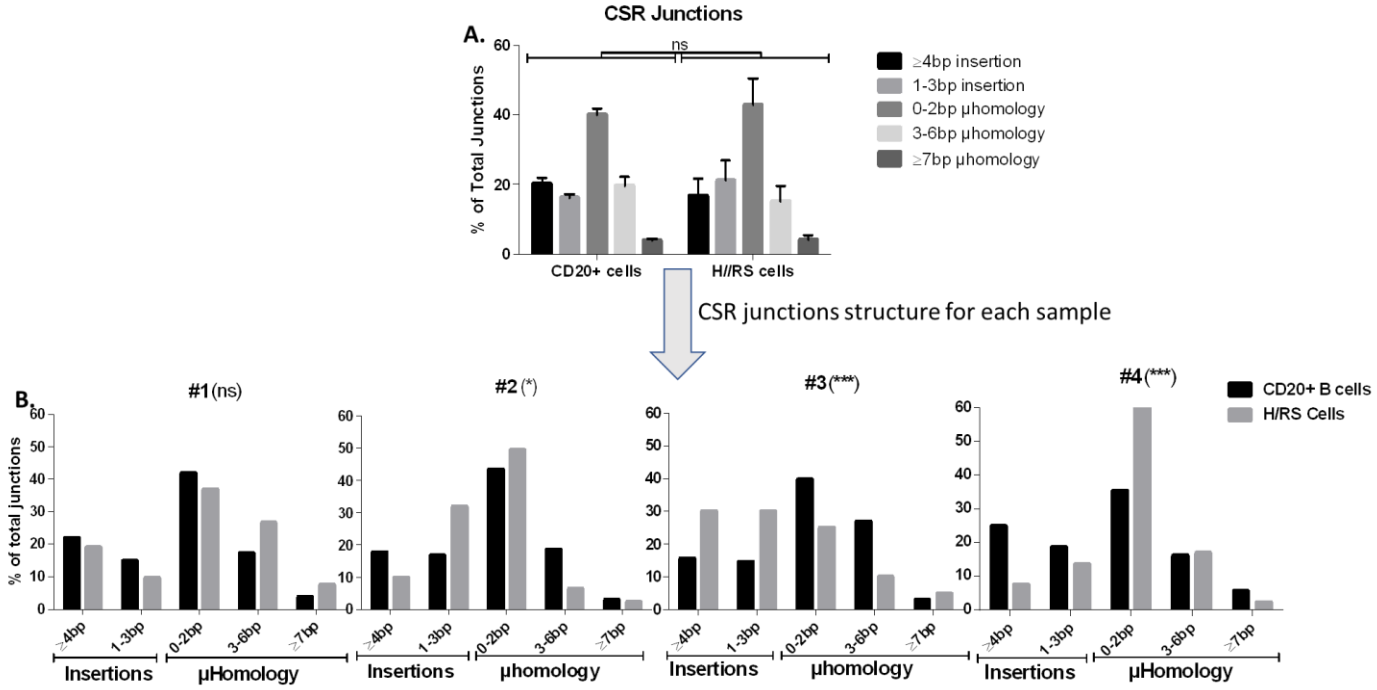

Figure 40: CSR junction structure in HL sorted cells (CD20+ and H/RS cells).
A. CSR junction structure of total obtained junctions. No significant difference was observed in the global analysis between H/RS cells and the CD20+ B cells. **B.** Analysis of CSR junctions in CD20+ B cells and H/RS cells for individual samples. We observed a heterogeneous alteration in the CSR junctions of H/RS compared to those of CD20+ B cells. Graphs are represented using graph pad prism 6 (mean±SEM). Statistical analysis was performed using the chisq test: ns: no significant difference, *P<0.05, ***P<0.001.

DISCUSSION

In these preliminary data, we observed that LSR is poorly amplified from HL samples since we detected it in 11 among 19 HL DNA whereas CSR is detected broadly in the same range of that in healthy samples. Global analysis showed LSR junctions in HL presented an altered structure profile while CSR junctions appeared structurally similar to those of healthy tonsils. As the bulk analysis cannot allow to differentiate LSR and CSR junctions from tumor cells and CD20+ B cells present in the TME, we performed the same methodology to sorted populations. Material obtained after cell sorting didn't allow to amplify LSR junctions but was sufficient to detect CSR joints.

We first noticed that H/RS exhibits low rate of CSR compared to CD20+ B cells. In addition, an alteration of structure of CSR junctions was observed in purified H/RS cells compared to CD20+ cells. These results suggest a DNA DSB repair alteration restricted to the H/RS cells. It remains to determine whether LSR structure is altered or not in H/RS cells.

Finally, we are not able for the moment to definitively conclude whether LSR can cause the BCR loss in H/RS cells. Nevertheless, our results evidence a DNA repair default in H/RS which

License CC BY-NC-ND 4.0

can potentiates defect in IgH recombination and loss of the BCR in H/RS cells. To go further, additional HL samples are required to repeat CSR and LSR analysis in sorted H/RS cells and normal counterpart B cells. If results are confirmed, the DNA repair defect will remain to be elucidated.

License CC BY-NC-ND 4.0

License CC BY-NC-ND 4.0

Discussion and Future Perspectives

License CC BY-NC-ND 4.0

License CC BY-NC-ND 4.0

Discussion and Future Perspectives

The main theme of research in our laboratory is the fundamental research concerning the B cells and the mechanisms implicated in the lymphoproliferative diseases including the Ig rearrangement processes. In 2012, it was described a novel mechanism of Ig rearrangement, the locus suicide recombination, that occurs in B cells between the Sμ and the 3'RR of *IgH* locus conducting to the excision of all constant region and then promotes alteration in the BCR expression. LSR mechanism constitutes the main center of my thesis work.

To sum up, during my thesis, I worked on the locus suicide recombination (LSR) mechanism in human B cells in pathological conditions, chronic lymphocytic leukemia (CLL) and Hodgkin lymphoma (HL), and also in B cells from healthy volunteers, peripheral blood and tonsils, secondary lymphoid organs. As well detailed in the result part, two main objectives were studied in order to improve the knowledge about LSR mechanism.

CLL is an indolent and still incurable lymphoma, recurrent in western countries. CLL tumor cells are CD5+, CD23+, CD19+ and CD20+ (Caligaris-Cappio and Hamblin, 1999). CLL cells express Ig on their surface, an IgM co-expressed with IgD in the vast majority of cases (Klein et al., 2001). Presence of unswitched Ig on CLL cells raised the question of abnormalities in Ig rearrangement.

First, we quantified CSR and LSR junctions from DNA extracted from peripheral blood of cohort of 47 CLL patients and from 9 healthy donors. CSR junction count in CLL was, as expected, less than in PBMC from healthy volunteers. CLL cells were positive for LSR junction, and in the first global view the LSR count was similar to healthy PBMC, but deeper analysis of the count allowed us to distinguish two groups of CLL patients called LSR^{High} and LSR^{Low} using the mean of LSR junction obtained in healthy PBMC as cut off. We continued our study in order to delineate the differences of these two groups and to establish if the count of LSR junctions can correlate with the prognosis of CLL patients. It is well documented that the mutational status of IgHV genes is related to the prognosis of patients. UM-IgHV, mutational status associated with aggressive disease, was found increased in the LSR^{High} CLL patients of our cohort. In coherent way, LSR^{High} group was associated with the shorter TFS. LSR^{High} patients were enriched in B and C Binet stages reinforcing the association of LSR^{High} with poorer prognosis (data not shown in the manuscript). Amplified LSR junctions can't be derived from B cell normal counterpart as CLL samples are taken at the diagnosis with very high tumor infiltration. In peripheral blood, detection of LSR junctions has been assigned to the non-functional IgH allele (Dalloul et al., 2019). Difference in the LSR count obtained between both groups isn't consecutive to different in B cell richness (not shown) and results from LSR

License CC BY-NC-ND 4.0

amplification from CLL cells since tumoral infiltration in B cell population is higher than 98%. Additionally, we estimated the LSR junction diversity by Shannon index calculation, which is influenced by the diversity and the abundance of each LSR junction, and as mentioned in our results, LSR^{High} group was more diversified than LSR^{Low}. Increased count of LSR junctions raised the question of on-going process. As reviewed in (Oppezzo et al., 2021), AID can be expressed in proliferative subpopulation of CLL cells, accounting for around 1% of the CLL cells. Since LSR was described induced by AID (Péron et al., 2012a), we quantified the AID transcripts from cDNA extracted from PBMC of CLL patients. However, AID was similarly and at very weak levels in both groups compared to the positive controls, sorted centroblasts from tonsils, without difference with AID expression from sorted naïve B cells. Lack of detection of AID expression in CLL PBMC can be due to the very low frequency of CLL cells supposed to express AID. We cannot exclude AID-induced LSR in CLL samples is achieved abroad the peripheral blood compartment. In normal condition, AID is expressed in activated B cells in the secondary lymphoid organs. Analysis and quantification of AID from CLL cells from secondary lymphoid organs will be realized in the short-term perspectives of this project.

Nevertheless, analysis of PIM1, an AID off target gene, reveals an increased mutation rate in the CLL LSR^{Low} group. In contrast, the CLL LSR^{High} group present normal low level of PIM1 mutation suggesting absence of AID expression and an AID-independent LSR in LSR^{High} CLL. To explore the AID activity in CLL patient's additional works on the short and long terms of this project will be achieved. AID activity is not restricted to the CSR and LSR, AID is also required in generating the diversity of the variable region of *IgH* locus during the Somatic hypermutation. Analysis of the VDJ diversity to detect de novo mutations in CLL patients will allow to determine a reactivation of AID in samples. In addition, the analysis of other AID off target genes such as Mcl-1 which found mutated in aggressive CLL will be assessed (Morande et al., 2021).

In parallel, because *IgH* recombination take place in proliferating cells, we examined the proliferation state of the cells by measuring the telomere length and quantifying *MYC* expression. Telomere length was shorter and associated with high levels of *MYC* expression in LSR^{High} group indicating several rounds of cell divisions in the cells of this group. In addition, we tested the accessibility of *IgH* locus by quantifying the transcription levels of coding and non-coding transcripts which were detected at high levels in LSR^{High} group indicating higher locus accessibility.

High IgM levels expression has been assigned to poor prognosis CLL patients (Mazzarello et al., 2022). In this article, authors showed that CLL cells co-express IgM and IgD and that high level of IgM expression is associated with poor prognosis and excessive signaling of the BCR,

License CC BY-NC-ND 4.0

in contrast to patients with CLL cells expressing high levels of IgD. In our study, we compared, and found similar within CLL patients, the level of surface BCR. This was done by Igk labelling and fluorescence flow cytometry analysis. The IgM expression was assessed at the transcription level. In the continuing work, analysis of IgM expression at the protein level and its localization at the cell surface, and the BCR signaling by western blot and /or flow cytometry will be done. In our CLL cohort, these analyses are on-going using western blot analysis on proteins extracted from dry pellet of cells. In long term, during the recruitment of supplemental CLL patients in collaboration with the CHU of Limoges and the CRBioLim, we will proceed systematically to IgM expression at the CLL cell surface.

Additionally, high IgM expression on the CLL cells suggests a defect in the CSR mechanism. It was shown in the literature that deletion in the switch region results in the resistance to CSR mechanism even in the presence of mutated variable region (Pham-Ledard et al., 2017). Detection of intra-Sμ deletions will be interesting since these cells of LSR^{High} group express high level of IgM transcripts.

Increased *MYC* expression, weak AID expression levels and accessible *IgH* locus questions the implication of MYC in the high LSR count independently of AID activity. Recently it was shown that CSR junctions can be detected even at low level in AID-/- conditions (Dalloul et al., 2021b). We addressed this question in murine cell line CH12F3 known to undergo CSR and LSR upon stimulation. Clones of CH12F3 wt or AID KO were generated. These clones were transfected by vector overexpressing *MYC* and stimulated for 72 hours. High throughput sequencing of PCR amplified CSR and LSR junctions from these clones reveals increase in the count of LSR in condition of overexpression of *MYC* even in the AID wt of AID KO.

Our results indicate that in LSR^{High} CLLs cells, the high transcription of the *IgH* locus, probably increased in a MYC dependent manner results in an additional MYC driven AID independent mechanism of *IgH* recombination.

Our data raise the question of the alteration of AID activity by *MYC* overexpression with a shift of AID action toward IgH recombination rather than its mutator activity on VDJ and non *Ig* target genes. This can be assessed on activated B cells from mouse model overexpressing MYC (kovalchuk J exp med 2000) invalidates or not for AID.
In the future, simple quantification of MYC and telomere length measurement will be helpful to classify the CLL patients.
LSR^{High} and ^{Low} CLLs appear to be characterized by different features certainly due to different CLL tumoral transformation mechanisms. DNA double strand breaks generated during the CSR and LSR mechanisms seem repaired by distinct DNA DSB repair pathways. Three DSB

License CC BY-NC-ND 4.0

repair pathways are described the NHEJ, Alt-EJ and HR. It is well documented that during the CSR mechanism, DSB are repaired mainly by the NHEJ pathway, and in case of NHEJ defect, DSB are repaired, in a lesser efficiency, by Alt-EJ. Analysis of the junction structure gives information on the DSB repair system used. NHEJ is able to directly ligate ends (blunt junctions) or ends sharing small µhomologies (1-2 bp). Alt-EJ is defined to ligate ends harboring longer µhomologies than NHEJ and presents the capability to introduce insertions at the junctions.

Based on the characteristic differences observed in LSR junctions between LSR^{High} and LSR^{Low} CLL groups, we analyzed the LSR and CSR junction's structure to evaluate if it's relevant of an alteration of the DNA repair. Indeed, LSR^{High} group exhibits the same profile of LSR junctions compared to those obtained from PBMC of healthy donors. This repair profile reflects the usage of Alt-EJ, in coherence with previous data published in our lab on the DNA repair during LSR in murine cells (Boutouil et al., 2019b). ChIP experiments on *in vitro* activated B cells isolated from peripheral blood against DNA repair pathway actors showed expected results suggesting the employment of Alt-EJ pathway on the 3'RR of the *IgH* locus. To explore the difference in DNA repair recruitment on *IgH* locus, characterization of the chromatin context on the CSR and LSR donor segments was performed. Choices of the epigenetic marks studied in our manuscript was based on previous studies from the literature showing that methylation of the lysine 20 of H4 (H4K20me) promotes the recruitment of 53BP1 to the DSB break site, protects the DNA ends from resection and favors the repair via NHEJ pathway (Hartlerode et al., 2012). On the other hand, we choose the H4K16ac known to inhibit the 53BP1 recruitment and to favor DNA DSB repair pathways other than NHEJ (Horikoshi et al., 2019, p. 16). In accord with our previous results we observed H4K20me1 enrichment on the CSR donor and acceptor segments. H4k16ac in activated cells was enriched on the LSR donor and acceptor segments.

Difference in the LSR junction's structure observed in LSR^{Low} group suggests employment of NHEJ in DNA repair step. This suggestion was difficult to confirm by qPCR quantification of NHEJ and Alt-EJ actors in the two groups of CLL groups. Results did not reveal differential expression for tested candidate genes between CLL groups. Nevertheless, as LSR is normally occurring in activated B cell, PBMC DNA are not the more appropriate samples for our analysis.

Since LSR occurs in the secondary lymphoid organs we analyzed LSR junction's structure in tonsils cells. We observed a difference in the LSR profile emerged from tonsils compared to PBMC cells, in normal conditions.

License CC BY-NC-ND 4.0

This profile was characterized by the decrease in the junctions with ≥4bp insertions and increase in blunt junctions or with 1-2bp microhomology. LSR^{Low} exhibits the same profile as tonsils. The fact that same junction features are sharing by CLL LSR^{Low} and cells from tonsils suggests CLL tumor cells can originate from B cells normally restricted to secondary lymphoid organs. This latter population appears to be associated with LSR employing a DSB repair step achieved presumably through NHEJ as confirmed by ChIP experiments against NHEJ and Alt-EJ actors revealing the significant recruitment of NHEJ molecule on the whole of *IgH* locus including the 3'RR region.

Indeed, we suggest that a subpopulation of B cell is deleted in tonsils before they emerge in the peripheral blood. This population is not yet characterized. I started the characterization of this subpopulation but due to the limit time of thesis all objectives are difficult to be enriched and this subject will be continued by the current PhD students.

We planed to sort different B cell subpopulations from healthy tonsils accordingly to described specific phenotypes (Wohlford et al., 2018). The gating strategy represented in the (Figure 41).

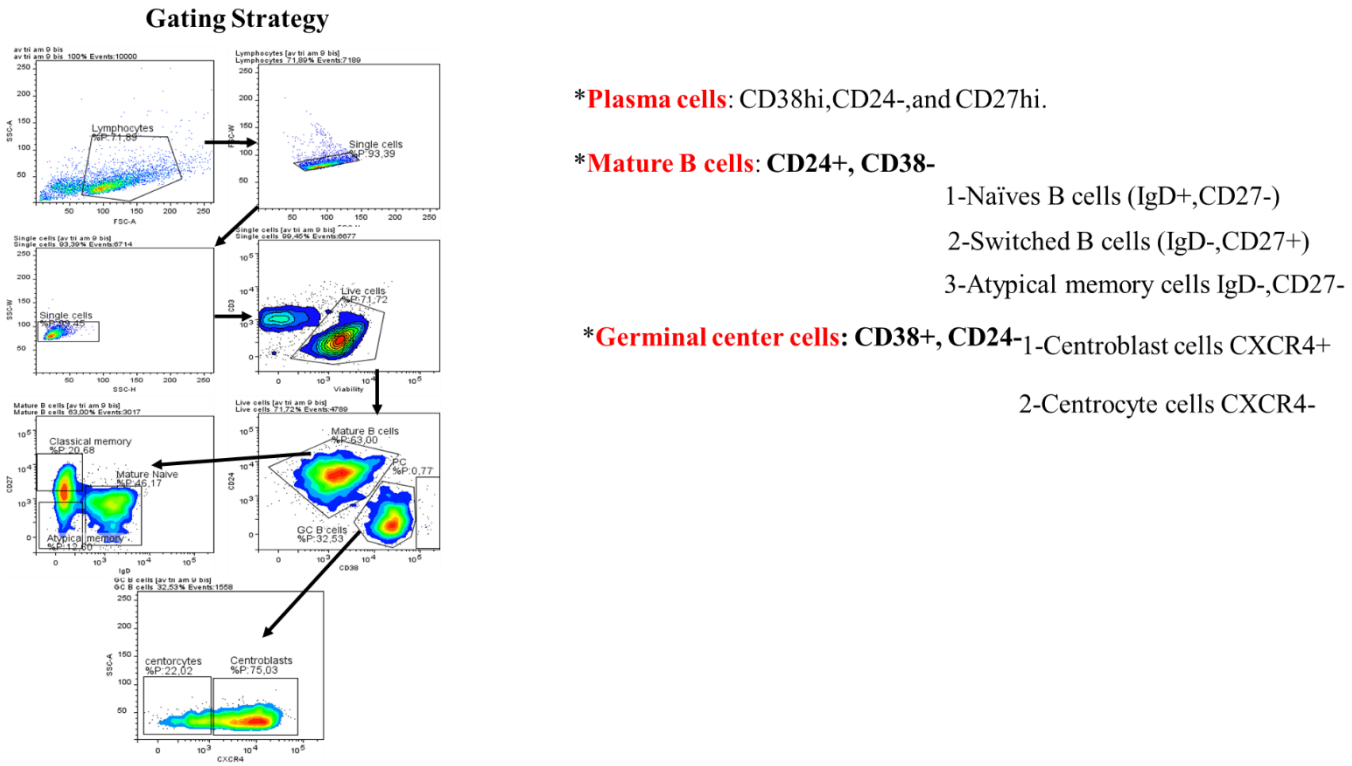

Figure 41: Gating strategy to isolate the different subpopulation of tonsils B cells.

On sorted cells, RNA and DNA extraction will be done to analyze the transcriptomic as well as the LSR junction count and characteristics of each population. Detection of population with LSR junctions harboring enrichment in blunt junctions and junctions with little microhomology will be privileged for transcriptomic, epigenetic and DNA mutation analysis. Data obtained will

License CC BY-NC-ND 4.0

be compared to those of CLL LSR^{Low} samples. This will also assign the LSR mechanism to a physiological role in the homeostasis of B cells by eliminating pathological B cells.

License CC BY-NC-ND 4.0

Conclusions

My thesis work has allowed us to use the LSR mechanism to differentiate CLL patients in two subtypes characterized by distinct outcomes and unrelated origins: LSR^{High} and LSR^{Low}. This work highlights the contribution of the knowledge in physiological mechanisms for a better understanding of pathological conditions. However, several questions remain to be elucidated.

In the first part, our findings of LSR indicate that high LSR count is associated with poor prognosis indicators. These CLL cells has entered in several rounds of proliferation with a high expression of *MYC* and an open and accessible *IgH* locus. We have hypothesized that overexpression of *MYC*, inducing high rate of mitosis in CLL cells, renders these cells more susceptible to DNA lesions during replication, transcription and/or due to reactive oxygen species. *IgH* locus, highly transcribed in CLL LSR^{High} cells, may be prone to be targeted by DNA lesions and LSR recombination as a hazardous event. In confirmation of this hypothesis, we showed that high LSR count is detected after *MYC* overexpression and in absence of AID in activated murine B cell lymphoma line cells (CH12F3). Results of this work question the AID activity in CLL:

1- Is AID activity restricted to secondary lymphoid organs and CLL proliferation centers?
2- Can AID activities in IgH recombination, mutation of Ig and off-target genes be dissociated?
3- Does MYC account for the orientation of AID activity towards recombination or mutation?
4- We observed increases transcription of the entire constant part of the *IgH* locus, why we do not observe an increase in CSR junctions in CLL LSR^{High} samples?
5- Is LSR an event participating in the CLL pathogenesis or an unrelated consequence?

In the second part, study of LSR^{Low} CLL interrogated the DSB repair employed during LSR. Since, these patients harbor specific LSR junction structural profile, we searched for a DSB repair alteration in this condition. This led to observe LSR^{Low} CLLs and cells from tonsils from healthy volunteers share the same LSR junction structure distribution and suggested LSR^{Low} CLL cells can originate from tonsil B cells.

In addition, several questions are pending:

1- Why our results on LSR DSB repair on *in viv*o activated human B cells are not concordant with results obtained after *in vitro* stimulation (Boutouil et al., 2019b; Dalloul et al., 2019)?

License CC BY-NC-ND 4.0

2- LSR-induced B cell population in tonsils, with blunt and with 1-2bp microhomology LSR junction enrichment, has to be identified to allow their characterization.
3- What are the dysregulated mechanisms implicated in emergence of tumoral CLL LSR^{Low} cells from their normal counterpart in tonsils.

Finally, concerning the work of HL, if we are not able to confirm that LSR is an additional cause for the BCR loss on the surface of these tumor cells, we observed CSR defect in tumor cells. CSR can probably related to the alteration in the DSB repair in H/RS. Indeed, these latter can participate in abrogation of IgH expression and the absence of BCR at the H/RS cell membrane.

License CC BY-NC-ND 4.0

Bibliographic References

License CC BY-NC-ND 4.0

License CC BY-NC-ND 4.0

Bibliographic References

Abarrategui, I., Krangel, M.S., 2009. Germline transcription: a key regulator of accessibility and recombination. Adv Exp Med Biol 650, 93–102. https://doi.org/10.1007/978-1-4419-0296-2_8

Agathangelidis, A., Darzentas, N., Hadzidimitriou, A., Brochet, X., Murray, F., Yan, X.-J., Davis, Z., van Gastel-Mol, E.J., Tresoldi, C., Chu, C.C., Cahill, N., Giudicelli, V., Tichy, B., Pedersen, L.B., Foroni, L., Bonello, L., Janus, A., Smedby, K., Anagnostopoulos, A., Merle-Beral, H., Laoutaris, N., Juliusson, G., di Celle, P.F., Pospisilova, S., Jurlander, J., Geisler, C., Tsaftaris, A., Lefranc, M.-P., Langerak, A.W., Oscier, D.G., Chiorazzi, N., Belessi, C., Davi, F., Rosenquist, R., Ghia, P., Stamatopoulos, K., 2012. Stereotyped B-cell receptors in one-third of chronic lymphocytic leukemia: a molecular classification with implications for targeted therapies. Blood 119, 4467–4475. https://doi.org/10.1182/blood-2011-11-393694

Akopiants, K., Zhou, R.-Z., Mohapatra, S., Valerie, K., Lees-Miller, S.P., Lee, K.-J., Chen, D.J., Revy, P., de Villartay, J.-P., Povirk, L.F., 2009. Requirement for XLF/Cernunnos in alignment-based gap filling by DNA polymerases lambda and mu for nonhomologous end joining in human whole-cell extracts. Nucleic Acids Res 37, 4055–4062. https://doi.org/10.1093/nar/gkp283

Al Jamal, I., Parquet, M., Boutouil, H., Guiyedi, K., Rizzo, D., Dupont, M., Boulin, M., El Hamel, C., Lerat, J., Aoufouchi, S., al Hamaoui, S., Makdissy, N., Feuillard, J., Gachard, N., Peron, S., 2022. Increased frequencies of IgH locus suicide recombination points on Chronic Lymphocytic Leukemia with low rate of AID related somatic mutations, cMYC overexpression and short telomeres. bioRxiv 2022.03.06.482661. https://doi.org/10.1101/2022.03.06.482661

Alt, F.W., Zhang, Y., Meng, F.-L., Guo, C., Schwer, B., 2013. Mechanisms of programmed DNA lesions and genomic instability in the immune system. Cell 152, 417–429. https://doi.org/10.1016/j.cell.2013.01.007

Altmann, T., Gennery, A.R., 2016. DNA ligase IV syndrome; a review. Orphanet Journal of Rare Diseases 11, 137. https://doi.org/10.1186/s13023-016-0520-1

Amrein, L., Davidson, D., Shawi, M., Petruccelli, L.A., Miller, W.H., Aloyz, R., Panasci, L., 2011. Dual inhibition of the homologous recombinational repair and the nonhomologous end-joining repair pathways in chronic lymphocytic leukemia therapy. Leuk Res 35, 1080–1086. https://doi.org/10.1016/j.leukres.2011.01.004

Amrein, P.C., Attar, E.C., Takvorian, T., Hochberg, E.P., Ballen, K.K., Leahy, K.M., Fisher, D.C., Lacasce, A.S., Jacobsen, E.D., Armand, P., Hasserjian, R.P., Werner, L., Neuberg, D., Brown, J.R., 2011. Phase II study of dasatinib in relapsed or refractory chronic lymphocytic leukemia. Clin Cancer Res 17, 2977–2986. https://doi.org/10.1158/1078-0432.CCR-10-2879

Anand, R., Ranjha, L., Cannavo, E., Cejka, P., 2016. Phosphorylated CtIP Functions as a Co-factor of the MRE11-RAD50-NBS1 Endonuclease in DNA End Resection. Mol Cell 64, 940–950. https://doi.org/10.1016/j.molcel.2016.10.017

Arnoult, N., Correia, A., Ma, J., Merlo, A., Garcia-Gomez, S., Maric, M., Tognetti, M., Benner, C.W., Boulton, S.J., Saghatelian, A., Karlseder, J., 2017. Regulation of DNA repair pathway choice in S and G2 phases by the NHEJ inhibitor CYREN. Nature 549, 548–552. https://doi.org/10.1038/nature24023

Baum, C.M., Weissman, I.L., Tsukamoto, A.S., Buckle, A.M., Peault, B., 1992. Isolation of a candidate human hematopoietic stem-cell population. Proc Natl Acad Sci U S A 89, 2804–2808.

Bébin, A.-G., Carrion, C., Marquet, M., Cogné, N., Lecardeur, S., Cogné, M., Pinaud, E., 2010. In vivo redundant function of the 3' IgH regulatory element HS3b in the mouse. J Immunol 184, 3710–3717. https://doi.org/10.4049/jimmunol.0901978

Benharroch, D., Prinsloo, I., Goldstein, J., Brousset, P., Kachko, L., Gopas, J., 1996. A comparison of distinct modes of tumor cell death in Hodgkin's disease using morphology and in situ DNA fragmentation. Ultrastruct Pathol 20, 497–505. https://doi.org/10.3109/01913129609016354

Birshtein, B.K., 2014. Epigenetic Regulation of Individual Modules of the immunoglobulin heavy chain locus 3' Regulatory Region. Front Immunol 5, 163. https://doi.org/10.3389/fimmu.2014.00163

License CC BY-NC-ND 4.0

Blasiak, J., 2021. Single-Strand Annealing in Cancer. International Journal of Molecular Sciences 22, 2167. https://doi.org/10.3390/ijms22042167

Bosch, F., Dalla-Favera, R., 2019. Chronic lymphocytic leukaemia: from genetics to treatment. Nat Rev Clin Oncol 16, 684–701. https://doi.org/10.1038/s41571-019-0239-8

Boutouil, H., Boyer, F., Cook-Moreau, J., Cogné, M., Péron, S., 2019a. IgH locus suicide recombination does not depend on NHEJ in contrast to CSR in B cells. Cell Mol Immunol 16, 201–202. https://doi.org/10.1038/s41423-018-0172-2

Boutouil, H., Boyer, F., Cook-Moreau, J., Cogné, M., Péron, S., 2019b. IgH locus suicide recombination does not depend on NHEJ in contrast to CSR in B cells. Cellular and Molecular Immunology 16, 201. https://doi.org/10.1038/s41423-018-0172-2

Brezski, R.J., Georgiou, G., 2016. Immunoglobulin isotype knowledge and application to Fc engineering. Current Opinion in Immunology, Antigen processing * Special section: New concepts in antibody therapeutics 40, 62–69. https://doi.org/10.1016/j.coi.2016.03.002

Buettner, M., Greiner, A., Avramidou, A., Jäck, H.-M., Niedobitek, G., 2005. Evidence of abortive plasma cell differentiation in Hodgkin and Reed-Sternberg cells of classical Hodgkin lymphoma. Hematol Oncol 23, 127–132. https://doi.org/10.1002/hon.764

Burger, J.A., Chiorazzi, N., 2013. B cell receptor signaling in chronic lymphocytic leukemia. Trends in Immunology 34, 592–601. https://doi.org/10.1016/j.it.2013.07.002

Burger, J.A., Ghia, P., Rosenwald, A., Caligaris-Cappio, F., 2009. The microenvironment in mature B-cell malignancies: a target for new treatment strategies. Blood 114, 3367–3375. https://doi.org/10.1182/blood-2009-06-225326

Burger, J.A., O'Brien, S., 2018. Evolution of CLL treatment — from chemoimmunotherapy to targeted and individualized therapy. Nat Rev Clin Oncol 15, 510–527. https://doi.org/10.1038/s41571-018-0037-8

Caligaris-Cappio, F., Hamblin, T.J., 1999. B-cell chronic lymphocytic leukemia: a bird of a different feather. J Clin Oncol 17, 399–408. https://doi.org/10.1200/JCO.1999.17.1.399

Caracciolo, D., Riillo, C., Di Martino, M.T., Tagliaferri, P., Tassone, P., 2021. Alternative Non-Homologous End-Joining: Error-Prone DNA Repair as Cancer's Achilles' Heel. Cancers (Basel) 13, 1392. https://doi.org/10.3390/cancers13061392

Caron, P., Pobega, E., Polo, S.E., 2021. DNA Double-Strand Break Repair: All Roads Lead to HeterochROMAtin Marks. Front Genet 12, 730696. https://doi.org/10.3389/fgene.2021.730696

CD15 Antigen - an overview | ScienceDirect Topics [WWW Document], n.d. URL https://www.sciencedirect.com/topics/medicine-and-dentistry/cd15-antigen (accessed 4.23.20).

Ceccaldi, R., Liu, J.C., Amunugama, R., Hajdu, I., Primack, B., Petalcorin, M.I.R., O'Connor, K.W., Konstantinopoulos, P.A., Elledge, S.J., Boulton, S.J., Yusufzai, T., D'Andrea, A.D., 2015. Homologous-recombination-deficient tumours are dependent on Polθ-mediated repair. Nature 518, 258–262. https://doi.org/10.1038/nature14184

Chan, S.H., Yu, A.M., McVey, M., 2010. Dual roles for DNA polymerase theta in alternative end-joining repair of double-strand breaks in Drosophila. PLoS Genet 6, e1001005. https://doi.org/10.1371/journal.pgen.1001005

Chang, H.H.Y., Pannunzio, N.R., Adachi, N., Lieber, M.R., 2017. Non-homologous DNA end joining and alternative pathways to double-strand break repair. Nat Rev Mol Cell Biol 18, 495–506. https://doi.org/10.1038/nrm.2017.48

Chao, M.P., Seita, J., Weissman, I.L., 2008. Establishment of a normal hematopoietic and leukemia stem cell hierarchy. Cold Spring Harb Symp Quant Biol 73, 439–449. https://doi.org/10.1101/sqb.2008.73.031

Chapiro, E., Leporrier, N., Radford-Weiss, I., Bastard, C., Mossafa, H., Leroux, D., Tigaud, I., De Braekeleer, M., Terré, C., Brizard, F., Callet-Bauchu, E., Struski, S., Veronese, L., Fert-Ferrer, S., Taviaux, S., Lesty, C., Davi, F., Merle-Béral, H., Bernard, O.A., Sutton, L., Raynaud, S.D., Nguyen-

License CC BY-NC-ND 4.0

Khac, F., 2010. Gain of the short arm of chromosome 2 (2p) is a frequent recurring chromosome aberration in untreated chronic lymphocytic leukemia (CLL) at advanced stages. Leuk Res 34, 63–68. https://doi.org/10.1016/j.leukres.2009.03.042

Chapman, J.R., Barral, P., Vannier, J.-B., Borel, V., Steger, M., Tomas-Loba, A., Sartori, A.A., Adams, I.R., Batista, F.D., Boulton, S.J., 2013. RIF1 Is Essential for 53BP1-Dependent Nonhomologous End Joining and Suppression of DNA Double-Strand Break Resection. Mol Cell 49, 858–871. https://doi.org/10.1016/j.molcel.2013.01.002

Chauveau, C., Cogné, M., 1996. Palindromic structure of the IgH 3'locus control region. Nat Genet 14, 15–16. https://doi.org/10.1038/ng0996-15

Chemotherapeutic options in chronic lymphocytic leukemia: a meta-analysis of the randomized trials. CLL Trialists' Collaborative Group, 1999. . J Natl Cancer Inst 91, 861–868. https://doi.org/10.1093/jnci/91.10.861

Chen, B.-R., Wang, Y., Tubbs, A., Zong, D., Fowler, F.C., Zolnerowich, N., Wu, W., Bennett, A., Chen, C.-C., Feng, W., Nussenzweig, A., Tyler, J.K., Sleckman, B.P., 2021. LIN37-DREAM prevents DNA end resection and homologous recombination at DNA double-strand breaks in quiescent cells. Elife 10, e68466. https://doi.org/10.7554/eLife.68466

Chen, J., Sathiaseelan, V., Moore, A., Tan, S., Chilamakuri, C.S.R., Roamio Franklin, V.N., Shahsavari, A., Jakwerth, C.A., Hake, S.B., Warren, A.J., Mohorianu, I., D'Santos, C., Ringshausen, I., 2021. ZAP-70 constitutively regulates gene expression and protein synthesis in chronic lymphocytic leukemia. Blood 137, 3629–3640. https://doi.org/10.1182/blood.2020009960

Chen, L., Widhopf, G., Huynh, L., Rassenti, L., Rai, K.R., Weiss, A., Kipps, T.J., 2002. Expression of ZAP-70 is associated with increased B-cell receptor signaling in chronic lymphocytic leukemia. Blood 100, 4609–4614. https://doi.org/10.1182/blood-2002-06-1683

Chen, Z., Xiao, Y., Zhang, J., Li, J., Liu, Y., Zhao, Y., Ma, C., Luo, J., Qiu, Y., Huang, G., Korteweg, C., Gu, J., 2011. Transcription Factors E2A, FOXO1 and FOXP1 Regulate Recombination Activating Gene Expression in Cancer Cells. PLoS One 6, e20475. https://doi.org/10.1371/journal.pone.0020475

Chi, X., Li, Y., Qiu, X., 2020. V(D)J recombination, somatic hypermutation and class switch recombination of immunoglobulins: mechanism and regulation. Immunology 160, 233–247. https://doi.org/10.1111/imm.13176

Chronic Lymphocytic Leukemia - Cancer Stat Facts [WWW Document], n.d. . SEER. URL https://seer.cancer.gov/statfacts/html/clyl.html (accessed 6.25.22).

Cimmino, A., Calin, G.A., Fabbri, M., Iorio, M.V., Ferracin, M., Shimizu, M., Wojcik, S.E., Aqeilan, R.I., Zupo, S., Dono, M., Rassenti, L., Alder, H., Volinia, S., Liu, C.-G., Kipps, T.J., Negrini, M., Croce, C.M., 2005. miR-15 and miR-16 induce apoptosis by targeting BCL2. Proc Natl Acad Sci U S A 102, 13944–13949. https://doi.org/10.1073/pnas.0506654102

Clonality and Germinal Centre B-cell Derivation of Hodgkin/Reed-Sternberg Cells in Hodgkin's Disease - PubMed [WWW Document], n.d. URL https://pubmed.ncbi.nlm.nih.gov/9926232/ (accessed 4.22.20).

Clybouw, C., Fischer, S., Auffredou, M., Hugues, P., Alexia, C., Bouillet, P., Raphael, M., Leca, G., Strasser, A., Tarlinton, D., Vazquez, A., 2011. Regulation of memory B-cell survival by the BH3-only protein Puma. Blood 118, 4120–8. https://doi.org/10.1182/blood-2011-04-347096

Corneo, B., Wendland, R.L., Deriano, L., Cui, X., Klein, I.A., Wong, S.-Y., Arnal, S., Holub, A.J., Weller, G.R., Pancake, B.A., Shah, S., Brandt, V.L., Meek, K., Roth, D.B., 2007. Rag mutations reveal robust alternative end joining. Nature 449, 483–486. https://doi.org/10.1038/nature06168

Cosson, A., Chapiro, E., Bougacha, N., Lambert, J., Herbi, L., Cung, H.-A., Algrin, C., Keren, B., Damm, F., Gabillaud, C., Brunelle-Navas, M.-N., Davi, F., Merle-Béral, H., Le Garff-Tavernier, M., Roos-Weil, D., Choquet, S., Uzunov, M., Morel, V., Leblond, V., Maloum, K., Lepretre, S., Feugier, P., Lesty, C., Lejeune, J., Sutton, L., Landesman, Y., Susin, S.A., Nguyen-Khac, F., 2017. Gain in the short arm of chromosome 2 (2p+) induces gene overexpression and drug resistance in chronic

License CC BY-NC-ND 4.0

lymphocytic leukemia: analysis of the central role of XPO1. Leukemia 31, 1625–1629. https://doi.org/10.1038/leu.2017.100

Cremer, T., Cremer, C., 2001. Chromosome territories, nuclear architecture and gene regulation in mammalian cells. Nat Rev Genet 2, 292–301. https://doi.org/10.1038/35066075

Cuceu, C., Colicchio, B., Jeandidier, E., Junker, S., Plassa, F., Shim, G., Mika, J., Frenzel, M., AL Jawhari, M., Hempel, W.M., O'Brien, G., Lenain, A., Morat, L., Girinsky, T., Dieterlen, A., Polanska, J., Badie, C., Carde, P., M'Kacher, R., 2018a. Independent Mechanisms Lead to Genomic Instability in Hodgkin Lymphoma: Microsatellite or Chromosomal Instability. Cancers (Basel) 10. https://doi.org/10.3390/cancers10070233

Cuceu, C., Hempel, W.M., Sabatier, L., Bosq, J., Carde, P., M'kacher, R., 2018b. Chromosomal Instability in Hodgkin Lymphoma: An In-Depth Review and Perspectives. Cancers (Basel) 10. https://doi.org/10.3390/cancers10040091

Dalloul, I., Boyer, F., Dalloul, Z., Pignarre, A., Caron, G., Fest, T., Chatonnet, F., Delaloy, C., Durandy, A., Jeannet, R., Lereclus, E., Boutouil, H., Aldigier, J.-C., Péron, S., Le Noir, S., Cook-Moreau, J., Cogné, M., 2019. Locus suicide recombination actively occurs on the functionally rearranged IgH allele in B-cells from inflamed human lymphoid tissues. PLoS Genet 15, e1007721. https://doi.org/10.1371/journal.pgen.1007721

Dalloul, I., Laffleur, B., Dalloul, Z., Wehbi, B., Jouan, F., Brauge, B., Derouault, P., Moreau, J., Kracker, S., Fischer, A., Durandy, A., Le Noir, S., Cogné, M., 2021a. UnAIDed Class Switching in Activated B-Cells Reveals Intrinsic Features of a Self-Cleaving IgH Locus. Frontiers in Immunology 12.

Dalloul, I., Laffleur, B., Dalloul, Z., Wehbi, B., Jouan, F., Brauge, B., Derouault, P., Moreau, J., Kracker, S., Fischer, A., Durandy, A., Le Noir, S., Cogné, M., 2021b. UnAIDed Class Switching in Activated B-Cells Reveals Intrinsic Features of a Self-Cleaving IgH Locus. Front Immunol 12, 737427. https://doi.org/10.3389/fimmu.2021.737427

Daugaard, M., Baude, A., Fugger, K., Povlsen, L.K., Beck, H., Sørensen, C.S., Petersen, N.H.T., Sorensen, P.H.B., Lukas, C., Bartek, J., Lukas, J., Rohde, M., Jäättelä, M., 2012. LEDGF (p75) promotes DNA-end resection and homologous recombination. Nat Struct Mol Biol 19, 803–810. https://doi.org/10.1038/nsmb.2314

de Krijger, I., Föhr, B., Pérez, S.H., Vincendeau, E., Serrat, J., Thouin, A.M., Susvirkar, V., Lescale, C., Paniagua, I., Hoekman, L., Kaur, S., Altelaar, M., Deriano, L., Faesen, A.C., Jacobs, J.J.L., 2021. MAD2L2 dimerization and TRIP13 control shieldin activity in DNA repair. Nat Commun 12, 5421. https://doi.org/10.1038/s41467-021-25724-y

Deambrogi, C., De Paoli, L., Fangazio, M., Cresta, S., Rasi, S., Spina, V., Gattei, V., Gaidano, G., Rossi, D., 2010. Analysis of the REL, BCL11A, and MYCN proto-oncogenes belonging to the 2p amplicon in chronic lymphocytic leukemia. Am J Hematol 85, 541–544. https://doi.org/10.1002/ajh.21742

Dearden, C., 2008. Disease-specific complications of chronic lymphocytic leukemia. Hematology. American Society of Hematology. Education Program. https://doi.org/10.1182/asheducation-2008.1.450

Decottignies, A., 2013. Alternative end-joining mechanisms: a historical perspective. Front Genet 4, 48. https://doi.org/10.3389/fgene.2013.00048

Del Giudice, I., Rossi, D., Chiaretti, S., Marinelli, M., Tavolaro, S., Gabrielli, S., Laurenti, L., Marasca, R., Rasi, S., Fangazio, M., Guarini, A., Gaidano, G., Foà, R., 2012. NOTCH1 mutations in +12 chronic lymphocytic leukemia (CLL) confer an unfavorable prognosis, induce a distinctive transcriptional profiling and refine the intermediate prognosis of +12 CLL. Haematologica 97, 437–441. https://doi.org/10.3324/haematol.2011.060129

Deriano, L., Roth, D.B., 2013. Modernizing the nonhomologous end-joining repertoire: alternative and classical NHEJ share the stage. Annu Rev Genet 47, 433–455. https://doi.org/10.1146/annurev-genet-110711-155540

Derks, K.W.J., Hoeijmakers, J.H.J., Pothof, J., 2014. The DNA damage response: the omics era and its impact. DNA Repair (Amst) 19, 214–220. https://doi.org/10.1016/j.dnarep.2014.03.008

License CC BY-NC-ND 4.0

Difilippantonio, M.J., Zhu, J., Chen, H.T., Meffre, E., Nussenzweig, M.C., Max, E.E., Ried, T., Nussenzweig, A., 2000. DNA repair protein Ku80 suppresses chromosomal aberrations and malignant transformation. Nature 404, 510–514. https://doi.org/10.1038/35006670

Dixon, J.R., Jung, I., Selvaraj, S., Shen, Y., Antosiewicz-Bourget, J.E., Lee, A.Y., Ye, Z., Kim, A., Rajagopal, N., Xie, W., Diao, Y., Liang, J., Zhao, H., Lobanenkov, V.V., Ecker, J.R., Thomson, J.A., Ren, B., 2015. Chromatin architecture reorganization during stem cell differentiation. Nature 518, 331–336. https://doi.org/10.1038/nature14222

Döhner, H., Stilgenbauer, S., Benner, A., Leupolt, E., Kröber, A., Bullinger, L., Döhner, K., Bentz, M., Lichter, P., 2000. Genomic aberrations and survival in chronic lymphocytic leukemia. N Engl J Med 343, 1910–1916. https://doi.org/10.1056/NEJM200012283432602

Dominguez, P.M., Teater, M., Chambwe, N., Kormaksson, M., Redmond, D., Ishii, J., Vuong, B., Chaudhuri, J., Melnick, A., Vasanthakumar, A., Godley, L.A., Papavasiliou, F.N., Elemento, O., Shaknovich, R., 2015. DNA Methylation Dynamics of Germinal Center B Cells Are Mediated by AID. Cell Rep 12, 2086–2098. https://doi.org/10.1016/j.celrep.2015.08.036

Dranoff, G., 2004. Cytokines in cancer pathogenesis and cancer therapy. Nat Rev Cancer 4, 11–22. https://doi.org/10.1038/nrc1252

Drouet, J., Frit, P., Delteil, C., de Villartay, J.-P., Salles, B., Calsou, P., 2006. Interplay between Ku, Artemis, and the DNA-dependent Protein Kinase Catalytic Subunit at DNA Ends*. Journal of Biological Chemistry 281, 27784–27793. https://doi.org/10.1074/jbc.M603047200

Dubois, N., Crompot, E., Meuleman, N., Bron, D., Lagneaux, L., Stamatopoulos, B., 2020. Importance of Crosstalk Between Chronic Lymphocytic Leukemia Cells and the Stromal Microenvironment: Direct Contact, Soluble Factors, and Extracellular Vesicles. Frontiers in Oncology 10.

Dühren-von Minden, M., Übelhart, R., Schneider, D., Wossning, T., Bach, M.P., Buchner, M., Hofmann, D., Surova, E., Follo, M., Köhler, F., Wardemann, H., Zirlik, K., Veelken, H., Jumaa, H., 2012. Chronic lymphocytic leukaemia is driven by antigen-independent cell-autonomous signalling. Nature 489, 309–312. https://doi.org/10.1038/nature11309

Dürig, J., Nückel, H., Cremer, M., Führer, A., Halfmeyer, K., Fandrey, J., Möröy, T., Klein-Hitpass, L., Dührsen, U., 2003. ZAP-70 expression is a prognostic factor in chronic lymphocytic leukemia. Leukemia 17, 2426–2434. https://doi.org/10.1038/sj.leu.2403147

Dynan, W.S., Yoo, S., 1998. Interaction of Ku protein and DNA-dependent protein kinase catalytic subunit with nucleic acids. Nucleic Acids Res 26, 1551–1559.

Elantak, L., Espeli, M., Boned, A., Bornet, O., Bonzi, J., Gauthier, L., Feracci, M., Roche, P., Guerlesquin, F., Schiff, C., 2012. Structural basis for galectin-1-dependent pre-B cell receptor (pre-BCR) activation. J Biol Chem 287, 44703–44713. https://doi.org/10.1074/jbc.M112.395152

Elbakry, A., Löbrich, M., 2021. Homologous Recombination Subpathways: A Tangle to Resolve. Frontiers in Genetics 12.

Encyclopedia of Cancer, 2018. . Academic Press.

Ferreira, B., García, J., Suela, J., Mollejo, M., Camacho, F., Carro, A., Montes, S., Piris, M., Cigudosa, J., 2008. Comparative genome profiling across subtypes of low-grade B-cell lymphoma identifies type-specific and common aberrations that target genes with a role in B-cell neoplasia. Haematologica 93, 670–9. https://doi.org/10.3324/haematol.12221

Fontana, G.A., Reinert, J.K., Thomä, N.H., Rass, U., n.d. Shepherding DNA ends: Rif1 protects telomeres and chromosome breaks. Microb Cell 5, 327–343. https://doi.org/10.15698/mic2018.07.639

Frank, K.M., Sharpless, N.E., Gao, Y., Sekiguchi, J.M., Ferguson, D.O., Zhu, C., Manis, J.P., Horner, J., DePinho, R.A., Alt, F.W., 2000. DNA Ligase IV Deficiency in Mice Leads to Defective Neurogenesis and Embryonic Lethality via the p53 Pathway. Molecular Cell 5, 993–1002. https://doi.org/10.1016/S1097-2765(00)80264-6

Gahn, B., Schäfer, C., Neef, J., Troff, C., Feuring-Buske, M., Hiddemann, W., Wörmann, B., 1997. Detection of trisomy 12 and Rb-deletion in CD34+ cells of patients with B-cell chronic lymphocytic leukemia. Blood 89, 4275–4281.

License CC BY-NC-ND 4.0

Galloway, A., Saveliev, A., Łukasiak, S., Hodson, D.J., Bolland, D., Balmanno, K., Ahlfors, H., Monzón-Casanova, E., Mannurita, S.C., Bell, L.S., Andrews, S., Díaz-Muñoz, M.D., Cook, S.J., Corcoran, A., Turner, M., 2016. RNA-binding proteins ZFP36L1 and ZFP36L2 promote cell quiescence. Science 352, 453–459. https://doi.org/10.1126/science.aad5978

Gassner, F.J., Schubert, M., Rebhandl, S., Spandl, K., Zaborsky, N., Catakovic, K., Blaimer, S., Hebenstreit, D., Greil, R., Geisberger, R., 2018. Imprecision and DNA Break Repair Biased Towards Incompatible End Joining in Leukemia. Mol Cancer Res 16, 428–438. https://doi.org/10.1158/1541-7786.MCR-17-0373

Gatto, D., Brink, R., 2013. B cell localization: regulation by EBI2 and its oxysterol ligand. Trends Immunol 34, 336–341. https://doi.org/10.1016/j.it.2013.01.007

Gelmez, M.Y., Coskunpinar, E., Saracoglu, B., Deniz, G., Aktan, M., 2017. Investigation of AID, Dicer, and Drosha Expressions in Patients with Chronic Lymphocytic Leukemia. Immunol Invest 46, 433–446. https://doi.org/10.1080/08820139.2017.1288241

Gelmez, M.Y., Teker, A.B.A., Aday, A.D., Yavuz, A.S., Soysal, T., Deniz, G., Aktan, M., 2014. Analysis of activation-induced cytidine deaminase mRNA levels in patients with chronic lymphocytic leukemia with different cytogenetic status. Leuk Lymphoma 55, 326–330. https://doi.org/10.3109/10428194.2013.803225

Goodarzi, A.A., Noon, A.T., Deckbar, D., Ziv, Y., Shiloh, Y., Löbrich, M., Jeggo, P.A., 2008. ATM Signaling Facilitates Repair of DNA Double-Strand Breaks Associated with Heterochromatin. Molecular Cell 31, 167–177. https://doi.org/10.1016/j.molcel.2008.05.017

Gravanis, I., Tzogani, K., van Hennik, P., de Graeff, P., Schmitt, P., Mueller-Berghaus, J., Salmonson, T., Gisselbrecht, C., Laane, E., Bergmann, L., Pignatti, F., 2016. The European Medicines Agency Review of Brentuximab Vedotin (Adcetris) for the Treatment of Adult Patients With Relapsed or Refractory CD30+ Hodgkin Lymphoma or Systemic Anaplastic Large Cell Lymphoma: Summary of the Scientific Assessment of the Committee for Medicinal Products for Human Use. Oncologist 21, 102–109. https://doi.org/10.1634/theoncologist.2015-0276

Guo, C., Yoon, H.S., Franklin, A., Jain, S., Ebert, A., Cheng, H.-L., Hansen, E., Despo, O., Bossen, C., Vettermann, C., Bates, J.G., Richards, N., Myers, D., Patel, H., Gallagher, M., Schlissel, M.S., Murre, C., Busslinger, M., Giallourakis, C.C., Alt, F.W., 2011. CTCF-binding elements mediate control of V(D)J recombination. Nature 477, 424–430. https://doi.org/10.1038/nature10495

Haberman, A.M., Gonzalez, D.G., Wong, P., Zhang, T.-T., Kerfoot, S.M., 2019. Germinal center B cell initiation, GC maturation, and the coevolution of its stromal cell niches. Immunol Rev 288, 10–27. https://doi.org/10.1111/imr.12731

Hacken, E. ten, Gounari, M., Ghia, P., Burger, J.A., 2019. The importance of B cell receptor isotypes and stereotypes in Chronic Lymphocytic Leukemia. Leukemia 33, 287–298. https://doi.org/10.1038/s41375-018-0303-x

Hallek, M., 2019. Chronic lymphocytic leukemia: 2020 update on diagnosis, risk stratification and treatment. Am J Hematol 94, 1266–1287. https://doi.org/10.1002/ajh.25595

Hallek, M., Al-Sawaf, O., 2021. Chronic lymphocytic leukemia: 2022 update on diagnostic and therapeutic procedures. American Journal of Hematology 96, 1679–1705. https://doi.org/10.1002/ajh.26367

Han, L., Yu, K., 2008. Altered kinetics of nonhomologous end joining and class switch recombination in ligase IV-deficient B cells. J Exp Med 205, 2745–2753. https://doi.org/10.1084/jem.20081623

Hansen, A.S., Cattoglio, C., Darzacq, X., Tjian, R., 2017. Recent evidence that TADs and chromatin loops are dynamic structures. Nucleus 9, 20–32. https://doi.org/10.1080/19491034.2017.1389365

Hartlerode, A.J., Guan, Y., Rajendran, A., Ura, K., Schotta, G., Xie, A., Shah, J.V., Scully, R., 2012. Impact of Histone H4 Lysine 20 Methylation on 53BP1 Responses to Chromosomal Double Strand Breaks. PLoS One 7, e49211. https://doi.org/10.1371/journal.pone.0049211

HAWLEY, R.G., RAMEZANI, A., HAWLEY, T.S., 2006. Hematopoietic Stem Cells. Methods Enzymol 419, 149–179. https://doi.org/10.1016/S0076-6879(06)19007-2

License CC BY-NC-ND 4.0

Heddle, J.A., 1998. The role of proliferation in the origin of mutations in mammalian cells. Drug Metab Rev 30, 327–338. https://doi.org/10.3109/03602539808996316

Herman, S., Barr, P., McAuley, E., Liu, D., Wiestner, A., Friedberg, J., 2013. Fostamatinib inhibits B-cell receptor signaling, cellular activation and tumor proliferation in patients with relapsed and refractory chronic lymphocytic leukemia. Leukemia 27, 1769–1773. https://doi.org/10.1038/leu.2013.37

Hewamana, S., Alghazal, S., Lin, T.T., Clement, M., Jenkins, C., Guzman, M.L., Jordan, C.T., Neelakantan, S., Crooks, P.A., Burnett, A.K., Pratt, G., Fegan, C., Rowntree, C., Brennan, P., Pepper, C., 2008. The NF-kappaB subunit Rel A is associated with in vitro survival and clinical disease progression in chronic lymphocytic leukemia and represents a promising therapeutic target. Blood 111, 4681–4689. https://doi.org/10.1182/blood-2007-11-125278

Hewamana, S., Lin, T.T., Rowntree, C., Karunanithi, K., Pratt, G., Hills, R., Fegan, C., Brennan, P., Pepper, C., 2009. Rel a is an independent biomarker of clinical outcome in chronic lymphocytic leukemia. J Clin Oncol 27, 763–769. https://doi.org/10.1200/JCO.2008.19.1114

Hodgkin lymphoma [WWW Document], 2018. . nhs.uk. URL https://www.nhs.uk/conditions/hodgkin-lymphoma/ (accessed 7.10.22).

Hoogeboom, R., Wormhoudt, T.A., Schipperus, M.R., Langerak, A.W., Dunn-Walters, D.K., Guikema, J.E.J., Bende, R.J., van Noesel, C.J.M., 2013. A novel chronic lymphocytic leukemia subset expressing mutated IGHV3-7-encoded rheumatoid factor B-cell receptors that are functionally proficient. Leukemia 27, 738–740. https://doi.org/10.1038/leu.2012.238

Horikoshi, N., Sharma, D., Leonard, F., Pandita, R.K., Charaka, V.K., Hambarde, S., Horikoshi, N.T., Gaur Khaitan, P., Chakraborty, S., Cote, J., Godin, B., Hunt, C.R., Pandita, T.K., 2019. Pre-existing H4K16ac levels in euchromatin drive DNA repair by homologous recombination in S-phase. Commun Biol 2, 1–12. https://doi.org/10.1038/s42003-019-0498-z

Howard, M., Grimaldi, J.C., Bazan, J.F., Lund, F.E., Santos-Argumedo, L., Parkhouse, R.M., Walseth, T.F., Lee, H.C., 1993. Formation and hydrolysis of cyclic ADP-ribose catalyzed by lymphocyte antigen CD38. Science 262, 1056–1059. https://doi.org/10.1126/science.8235624

Huang, C., 2020. Germinal Center Reaction, in: Wang, J.-Y. (Ed.), B Cells in Immunity and Tolerance, Advances in Experimental Medicine and Biology. Springer, Singapore, pp. 47–53. https://doi.org/10.1007/978-981-15-3532-1_4

Hung, P.J., Johnson, B., Chen, B.-R., Byrum, A.K., Bredemeyer, A.L., Yewdell, W.T., Johnson, T.E., Lee, B.J., Deivasigamani, S., Hindi, I., Amatya, P., Gross, M.L., Paull, T.T., Pisapia, D.J., Chaudhuri, J., Petrini, J.J.H., Mosammaparast, N., Amarasinghe, G.K., Zha, S., Tyler, J.K., Sleckman, B.P., 2018. MRI is a DNA Damage Response Adaptor during Classical Non-Homologous End Joining. Mol Cell 71, 332-342.e8. https://doi.org/10.1016/j.molcel.2018.06.018

Husby, S., Grønbæk, K., 2017. Mature lymphoid malignancies: origin, stem cells, and chronicity. Blood Adv 1, 2444–2455. https://doi.org/10.1182/bloodadvances.2017008854

Ibrahim, S., Keating, M., Do, K.-A., O'Brien, S., Huh, Y.O., Jilani, I., Lerner, S., Kantarjian, H.M., Albitar, M., 2001. CD38 expression as an important prognostic factor in B-cell chronic lymphocytic leukemia. Blood 98, 181–186. https://doi.org/10.1182/blood.V98.1.181

Iliakis, G., Murmann, T., Soni, A., 2015. Alternative end-joining repair pathways are the ultimate backup for abrogated classical non-homologous end-joining and homologous recombination repair: Implications for the formation of chromosome translocations. Mutat Res Genet Toxicol Environ Mutagen 793, 166–175. https://doi.org/10.1016/j.mrgentox.2015.07.001

IMGT Repertoire (IG and TR) 1. Locus and genes [WWW Document], n.d. URL https://www.imgt.org/IMGTrepertoire/LocusGenes/locusdesc/human/IGH/Hu_IGHdesc.html#refs (accessed 3.9.22).

Immunoglobulin Kappa Chain - an overview | ScienceDirect Topics [WWW Document], n.d. URL https://www.sciencedirect.com/topics/medicine-and-dentistry/immunoglobulin-kappa-chain (accessed 3.14.22).

License CC BY-NC-ND 4.0

Inlay, M.A., Lin, T., Gao, H.H., Xu, Y., 2006. Critical roles of the immunoglobulin intronic enhancers in maintaining the sequential rearrangement of IgH and Igk loci. J Exp Med 203, 1721–1732. https://doi.org/10.1084/jem.20052310

International CLL-IPI working group, 2016. An international prognostic index for patients with chronic lymphocytic leukaemia (CLL-IPI): a meta-analysis of individual patient data. Lancet Oncol 17, 779–790. https://doi.org/10.1016/S1470-2045(16)30029-8

Irsch, J., Wolf, J., Tesch, H., Diehl, V., Radbruch, A., Staratschek-Jox, A., 2001. Class switch recombination was specifically targeted to immunoglobulin (Ig)G4 or IgA in Hodgkin's disease-derived cell lines. British Journal of Haematology 113, 785–793. https://doi.org/10.1046/j.1365-2141.2001.02818.x

Isono, M., Niimi, A., Oike, T., Hagiwara, Y., Sato, H., Sekine, R., Yoshida, Y., Isobe, S.-Y., Obuse, C., Nishi, R., Petricci, E., Nakada, S., Nakano, T., Shibata, A., 2017. BRCA1 Directs the Repair Pathway to Homologous Recombination by Promoting 53BP1 Dephosphorylation. Cell Rep 18, 520–532. https://doi.org/10.1016/j.celrep.2016.12.042

Jain, N., Keating, M., Thompson, P., Ferrajoli, A., Burger, J., Borthakur, G., Takahashi, K., Estrov, Z., Fowler, N., Kadia, T., Konopleva, M., Alvarado, Y., Yilmaz, M., DiNardo, C., Bose, P., Ohanian, M., Pemmaraju, N., Jabbour, E., Sasaki, K., Kanagal-Shamanna, R., Patel, K., Jorgensen, J., Garg, N., Wang, X., Sondermann, K., Cruz, N., Wei, C., Ayala, A., Plunkett, W., Kantarjian, H., Gandhi, V., Wierda, W., 2019. Ibrutinib and Venetoclax for First-Line Treatment of CLL. New England Journal of Medicine 380, 2095–2103. https://doi.org/10.1056/NEJMoa1900574

Jain, P., O'Brien, S., 2012. Richter's transformation in chronic lymphocytic leukemia. Oncology (Williston Park) 26, 1146–1152.

Jiang, W., Crowe, J.L., Liu, X., Nakajima, S., Wang, Y., Li, C., Lee, B.J., Dubois, R.L., Liu, C., Yu, X., Lan, L., Zha, S., 2015. Differential phosphorylation of DNA-PKcs regulates the interplay between end-processing and end-ligation during non-homologous end-joining. Mol Cell 58, 172–185. https://doi.org/10.1016/j.molcel.2015.02.024

Jung, D., Giallourakis, C., Mostoslavsky, R., Alt, F.W., 2006. Mechanism and control of V(D)J recombination at the immunoglobulin heavy chain locus. Annu Rev Immunol 24, 541–570. https://doi.org/10.1146/annurev.immunol.23.021704.115830

Kabotyanski, E.B., Gomelsky, L., Han, J.O., Stamato, T.D., Roth, D.B., 1998. Double-strand break repair in Ku86- and XRCC4-deficient cells. Nucleic Acids Res 26, 5333–5342. https://doi.org/10.1093/nar/26.23.5333

Kassambara, A., Rème, T., Jourdan, M., Fest, T., Hose, D., Tarte, K., Klein, B., 2015. GenomicScape: an easy-to-use web tool for gene expression data analysis. Application to investigate the molecular events in the differentiation of B cells into plasma cells. PLoS Comput Biol 11, e1004077. https://doi.org/10.1371/journal.pcbi.1004077

Kato, I., Takasawa, S., Akabane, A., Tanaka, O., Abe, H., Takamura, T., Suzuki, Y., Nata, K., Yonekura, H., Yoshimoto, T., 1995. Regulatory role of CD38 (ADP-ribosyl cyclase/cyclic ADP-ribose hydrolase) in insulin secretion by glucose in pancreatic beta cells. Enhanced insulin secretion in CD38-expressing transgenic mice. J Biol Chem 270, 30045–30050. https://doi.org/10.1074/jbc.270.50.30045

Khan, M., Saif, A., Sandler, S., Mirrakhimov, A.E., 2014. Idelalisib for the Treatment of Chronic Lymphocytic Leukemia. ISRN Oncology 2014, e931858. https://doi.org/10.1155/2014/931858

Khatri, I., Berkowska, M.A., van den Akker, E.B., Teodosio, C., Reinders, M.J.T., van Dongen, J.J.M., 2021. Population matched (pm) germline allelic variants of immunoglobulin (IG) loci: Relevance in infectious diseases and vaccination studies in human populations. Genes Immun 22, 172–186. https://doi.org/10.1038/s41435-021-00143-7

Kikushige, Y., Ishikawa, F., Miyamoto, T., Shima, T., Urata, S., Yoshimoto, G., Mori, Y., Iino, T., Yamauchi, T., Eto, T., Niiro, H., Iwasaki, H., Takenaka, K., Akashi, K., 2011. Self-renewing hematopoietic stem cell is the primary target in pathogenesis of human chronic lymphocytic leukemia. Cancer Cell 20, 246–259. https://doi.org/10.1016/j.ccr.2011.06.029

License CC BY-NC-ND 4.0

Kishi, H., Jin, Z.-X., Wei, X.-C., Nagata, T., Matsuda, T., Saito, S., Muraguchi, A., 2002. Cooperative binding of c-Myb and Pax-5 activates the RAG-2 promoter in immature B cells. Blood 99, 576–583. https://doi.org/10.1182/blood.v99.2.576

Klein, U., Tu, Y., Stolovitzky, G.A., Mattioli, M., Cattoretti, G., Husson, H., Freedman, A., Inghirami, G., Cro, L., Baldini, L., Neri, A., Califano, A., Dalla-Favera, R., 2001. Gene Expression Profiling of B Cell Chronic Lymphocytic Leukemia Reveals a Homogeneous Phenotype Related to Memory B Cells 〉. J Exp Med 194, 1625–1638.

Kostopoulou, F., Gabillaud, C., Chapiro, E., Grange, B., Tran, J., Bouzy, S., Degaud, M., Ghamlouch, H., Le Garff-Tavernier, M., Maloum, K., Choquet, S., Leblond, V., Gabarre, J., Lavaud, A., Morel, V., Roos-Weil, D., Uzunov, M., Guieze, R., Bernard, O.A., Susin, S.A., Tournilhac, O., Nguyen-Khac, F., 2019. Gain of the short arm of chromosome 2 (2p gain) has a significant role in drug-resistant chronic lymphocytic leukemia. Cancer Med 8, 3131–3141. https://doi.org/10.1002/cam4.2123

Kramer, G., Steiner, G., Födinger, D., Fiebiger, E., Rappersberger, C., Binder, S., Hofbauer, J., Marberger, M., 1995. High expression of a CD38-like molecule in normal prostatic epithelium and its differential loss in benign and malignant disease. J Urol 154, 1636–1641.

Kudithipudi, S., Schuhmacher, M.K., Kebede, A.F., Jeltsch, A., 2017. The SUV39H1 Protein Lysine Methyltransferase Methylates Chromatin Proteins Involved in Heterochromatin Formation and VDJ Recombination. ACS Chem. Biol. 12, 958–968. https://doi.org/10.1021/acschembio.6b01076

Küppers, R., Engert, A., Hansmann, M.-L., 2012. Hodgkin lymphoma. J Clin Invest 122, 3439–3447. https://doi.org/10.1172/JCI61245

Kusumoto, R., Dawut, L., Marchetti, C., Lee, J.W., Vindigni, A., Ramsden, D., Bohr, V., 2008. Werner protein cooperates with the XRCC4-DNA ligase IV complex in end-processing. Biochemistry. https://doi.org/10.1021/bi702325t

Lam, K.P., Kühn, R., Rajewsky, K., 1997. In vivo ablation of surface immunoglobulin on mature B cells by inducible gene targeting results in rapid cell death. Cell 90, 1073–1083. https://doi.org/10.1016/s0092-8674(00)80373-6

Landau, D.A., Tausch, E., Taylor-Weiner, A.N., Stewart, C., Reiter, J.G., Bahlo, J., Kluth, S., Bozic, I., Lawrence, M., Böttcher, S., Carter, S.L., Cibulskis, K., Mertens, D., Sougnez, C., Rosenberg, M., Hess, J.M., Edelmann, J., Kless, S., Kneba, M., Ritgen, M., Fink, A., Fischer, K., Gabriel, S., Lander, E., Nowak, M.A., Döhner, H., Hallek, M., Neuberg, D., Getz, G., Stilgenbauer, S., Wu, C.J., 2015. Mutations driving CLL and their evolution in progression and relapse. Nature 526, 525–530. https://doi.org/10.1038/nature15395

Lanier, L.L., Corliss, B.C., Wu, J., Leong, C., Phillips, J.H., 1998. Immunoreceptor DAP12 bearing a tyrosine-based activation motif is involved in activating NK cells. Nature 391, 703–707. https://doi.org/10.1038/35642

Leandro, M.J., 2013. B-cell subpopulations in humans and their differential susceptibility to depletion with anti-CD20 monoclonal antibodies. Arthritis Res Ther 15 Suppl 1, S3. https://doi.org/10.1186/ar3908

LeBien, T.W., Tedder, T.F., 2008. B lymphocytes: how they develop and function. Blood 112, 1570–1580. https://doi.org/10.1182/blood-2008-02-078071

Ledesma-Soto, Y., Blanco-Favela, F., Fuentes-Pananá, E.M., Tesoro-Cruz, E., Hernández-González, R., Arriaga-Pizano, L., Legorreta-Haquet, M.V., Montoya-Diaz, E., Chávez-Sánchez, L., Castro-Mussot, M.E., Chávez-Rueda, A.K., 2012. Increased levels of prolactin receptor expression correlate with the early onset of lupus symptoms and increased numbers of transitional-1 B cells after prolactin treatment. BMC Immunol 13, 11. https://doi.org/10.1186/1471-2172-13-11

Lee, I.-S., Kim, S.H., Song, H.G., Park, S.H., 2003. The molecular basis for the generation of Hodgkin and Reed-Sternberg cells in Hodgkin's lymphoma. Int. J. Hematol. 77, 330–335. https://doi.org/10.1007/bf02982639

License CC BY-NC-ND 4.0

Leeman-Neill, R.J., Lim, J., Basu, U., 2018. The Common Key to Class-Switch Recombination and Somatic Hypermutation: Discovery of AID and Its Role in Antibody Gene Diversification. The Journal of Immunology 201, 2527–2529. https://doi.org/10.4049/jimmunol.1801246

Lefranc, M.-P., Giudicelli, V., Ginestoux, C., Jabado-Michaloud, J., Folch, G., Bellahcene, F., Wu, Y., Gemrot, E., Brochet, X., Lane, J., Regnier, L., Ehrenmann, F., Lefranc, G., Duroux, P., 2009. IMGT, the international ImMunoGeneTics information system. Nucleic Acids Res 37, D1006-1012. https://doi.org/10.1093/nar/gkn838

Le Noir, S., Boyer, F., Lecardeur, S., Brousse, M., Oruc, Z., Cook-Moreau, J., Denizot, Y., Cogné, M., 2017. Functional anatomy of the immunoglobulin heavy chain 3′ super-enhancer needs not only core enhancer elements but also their unique DNA context. Nucleic Acids Res 45, 5829–5837. https://doi.org/10.1093/nar/gkx203

Li, L., Wang, Y., 2017. Cross-talk between the H3K36me3 and H4K16ac histone epigenetic marks in DNA double-strand break repair. J Biol Chem 292, 11951–11959. https://doi.org/10.1074/jbc.M117.788224

Lieber, M.R., 2010a. The Mechanism of Double-Strand DNA Break Repair by the Nonhomologous DNA End Joining Pathway. Annu Rev Biochem 79, 181–211. https://doi.org/10.1146/annurev.biochem.052308.093131

Lieber, M.R., 2010b. The Mechanism of Double-Strand DNA Break Repair by the Nonhomologous DNA End Joining Pathway. Annu Rev Biochem 79, 181–211. https://doi.org/10.1146/annurev.biochem.052308.093131

Lieberman-Aiden, E., van Berkum, N.L., Williams, L., Imakaev, M., Ragoczy, T., Telling, A., Amit, I., Lajoie, B.R., Sabo, P.J., Dorschner, M.O., Sandstrom, R., Bernstein, B., Bender, M.A., Groudine, M., Gnirke, A., Stamatoyannopoulos, J., Mirny, L.A., Lander, E.S., Dekker, J., 2009. Comprehensive mapping of long range interactions reveals folding principles of the human genome. Science 326, 289–293. https://doi.org/10.1126/science.1181369

Lin, D., Ippolito, G.C., Zong, R.-T., Bryant, J., Koslovsky, J., Tucker, P., 2007. Bright/ARID3A contributes to chromatin accessibility of the immunoglobulin heavy chain enhancer. Molecular Cancer 6, 23. https://doi.org/10.1186/1476-4598-6-23

Liu, M., Zhang, Ying, Wu, Yunzhao, Jin, J., Cao, Y., Fang, Z., Geng, L., Yang, L., Yu, M., Bu, Z., Ji, Y., Shan, H., Zou, Z., Liu, L., Wang, Y., Zhang, Youping, Tong, Y., Xu, H., Lei, H., Liu, W., Gao, F., Wu, Yingli, 2022. IKZF1 selectively enhances homologous recombination repair by interacting with CtIP and USP7 in multiple myeloma. Int J Biol Sci 18, 2515–2526. https://doi.org/10.7150/ijbs.70960

Liu, S., Kong, D., 2021. End resection: a key step in homologous recombination and DNA double-strand break repair. GENOME INSTAB. DIS. 2, 39–50. https://doi.org/10.1007/s42764-020-00028-5

Liu, X., Shao, Z., Jiang, W., Lee, B.J., Zha, S., 2017. PAXX promotes KU accumulation at DNA breaks and is essential for end-joining in XLF-deficient mice. Nat Commun 8, 13816. https://doi.org/10.1038/ncomms13816

Machado, C.R., Menck, C.F.M., 1997. Human DNA repair diseases: From genome instability to cancer. Braz. J. Genet. 20, 755–762. https://doi.org/10.1590/S0100-84551997000400032

Mahony, C.B., Bertrand, J.Y., 2019. How HSCs Colonize and Expand in the Fetal Niche of the Vertebrate Embryo: An Evolutionary Perspective. Frontiers in Cell and Developmental Biology 7.

Mancikova, V., Smida, M., 2021. Current State of CAR T-Cell Therapy in Chronic Lymphocytic Leukemia. Int J Mol Sci 22, 5536. https://doi.org/10.3390/ijms22115536

Marafioti, T., Hummel, M., Foss, H.D., Laumen, H., Korbjuhn, P., Anagnostopoulos, I., Lammert, H., Demel, G., Theil, J., Wirth, T., Stein, H., 2000. Hodgkin and reed-sternberg cells represent an expansion of a single clone originating from a germinal center B-cell with functional immunoglobulin gene rearrangements but defective immunoglobulin transcription. Blood 95, 1443–1450.

Marquet, M., Garot, A., Bender, S., Carrion, C., Rouaud, P., Lecardeur, S., Denizot, Y., Cogné, M., Pinaud, E., 2014. The Eμ enhancer region influences H chain expression and B cell fate without

License CC BY-NC-ND 4.0

impacting IgVH repertoire and immune response in vivo. J Immunol 193, 1171–1183. https://doi.org/10.4049/jimmunol.1302868

Marshall, J.S., Warrington, R., Watson, W., Kim, H.L., 2018. An introduction to immunology and immunopathology. Allergy, Asthma & Clinical Immunology 14, 49. https://doi.org/10.1186/s13223-018-0278-1

Maruyama, M., Lam, K.-P., Rajewsky, K., 2001. Memory B-cell persistence is independent of persisting immunizing antigen. Nature 409. https://doi.org/10.1038/35053144

Masani, S., Han, L., Meek, K., Yu, K., 2016. Redundant function of DNA ligase 1 and 3 in alternative end-joining during immunoglobulin class switch recombination. Proc Natl Acad Sci U S A 113, 1261–1266. https://doi.org/10.1073/pnas.1521630113

Matsumoto, M.L., 2022. Molecular Mechanisms of Multimeric Assembly of IgM and IgA. Annual Review of Immunology 40, null. https://doi.org/10.1146/annurev-immunol-101320-123742

Mauro, F.R., Foa, R., Giannarelli, D., Cordone, I., Crescenzi, S., Pescarmona, E., Sala, R., Cerretti, R., Mandelli, F., 1999. Clinical characteristics and outcome of young chronic lymphocytic leukemia patients: a single institution study of 204 cases. Blood 94, 448–454.

Mazzarello, A.N., Gentner-Göbel, E., Dühren-von Minden, M., Tarasenko, T.N., Nicolò, A., Ferrer, G., Vergani, S., Liu, Y., Bagnara, D., Rai, K.R., Burger, J.A., McGuire, P.J., Maity, P.C., Jumaa, H., Chiorazzi, N., n.d. B cell receptor isotypes differentially associate with cell signaling, kinetics, and outcome in chronic lymphocytic leukemia. J Clin Invest 132, e149308. https://doi.org/10.1172/JCI149308

McCarthy, H., Wierda, W.G., Barron, L.L., Cromwell, C.C., Wang, J., Coombes, K.R., Rangel, R., Elenitoba-Johnson, K.S.J., Keating, M.J., Abruzzo, L.V., 2003. High expression of activation-induced cytidine deaminase (AID) and splice variants is a distinctive feature of poor-prognosis chronic lymphocytic leukemia. Blood 101, 4903–4908. https://doi.org/10.1182/blood-2002-09-2906

Melchers, F., 2015. Checkpoints that control B cell development. J Clin Invest 125, 2203–2210. https://doi.org/10.1172/JCI78083

Mikocziova, I., Greiff, V., Sollid, L.M., 2021. Immunoglobulin germline gene variation and its impact on human disease. Genes Immun 22, 205–217. https://doi.org/10.1038/s41435-021-00145-5

Miller, C.R., Huang, Y., Ruppert, A.S., Labanowska, J., Jaglowski, S.M., Maddocks, K.J., Rogers, K.A., Bhat, S., Kittai, A.S., Grever, M., Lapalombella, R., Abruzzo, L.V., Heerema, N.A., Byrd, J.C., Hertlein, E.K., Woyach, J.A., 2021. Significance of chromosome 2p gain in ibrutinib-treated chronic lymphocytic leukemia patients. Leukemia 35, 3287–3290. https://doi.org/10.1038/s41375-021-01237-x

Mirman, Z., Lange, T. de, 2020. 53BP1: a DSB escort. Genes Dev. 34, 7–23. https://doi.org/10.1101/gad.333237.119

Mizuguchi, M., Otsuka, N., Sato, M., Ishii, Y., Kon, S., Yamada, M., Nishina, H., Katada, T., Ikeda, K., 1995. Neuronal localization of CD38 antigen in the human brain. Brain Res 697, 235–240. https://doi.org/10.1016/0006-8993(95)00885-t

Moia, R., Favini, C., Ferri, V., Bomben, R., Sagiraju, S., Bittolo, T., Scarfo, L., Bonfiglio, S., Maffei, R., Baldoni, S., Raponi, S., Spina, V., Bruscaggin, A., Terzi di Bergamo, L., De Paoli, L., Margiotta Casaluci, G., Deambrogi, C., Rasi, S., Condoluci, A., Kodipad, A.A., Adhinaveni, R., Mokabari, K., Mahmoud, A.M., Patriarca, A., Olivieri, J., D'Arena, G., Zaja, F., Chiarenza, A., Del Poeta, G., Zucchetto, A., Rossi, F.M., Del Giudice, I., Sportoletti, P., Marasca, R., Ghia, P., Foà, R., Gaidano, G., Rossi, D., Gattei, V., 2020. Mutations of the Exportin 1 (XPO1) Gene Predict Shorter Time to First Treatment in 1092 Early Stage Chronic Lymphocytic Leukemia Patients. A Training/Validation Study. Blood 136, 31–32. https://doi.org/10.1182/blood-2020-136389

Molica, S., 2006. Sex differences in incidence and outcome of chronic lymphocytic leukemia patients. Leuk Lymphoma 47, 1477–1480. https://doi.org/10.1080/10428190600555819

Morabito, F., Cutrona, G., Gentile, M., Fabris, S., Matis, S., Vigna, E., Todoerti, K., Colombo, M., Recchia, A.G., Bossio, S., Stefano, L.D., Ilariucci, F., Cortelezzi, A., Consoli, U., Vincelli, I., Pesce, E.A.,

License CC BY-NC-ND 4.0

Musolino, C., Molica, S., Raimondo, F.D., Neri, A., Ferrarini, M., 2015. Is ZAP70 still a key prognostic factor in early stage chronic lymphocytic leukaemia? Results of the analysis from a prospective multicentre observational study. British journal of haematology 168, 455–459. https://doi.org/10.1111/bjh.13117

Morande, P.E., Yan, X.-J., Sepulveda, J., Seija, N., Marquez, M.E., Sotelo, N., Abreu, C., Crispo, M., Fernández-Graña, G., Rego, N., Bois, T., Methot, S.P., Palacios, F., Remedi, V., Rai, K.R., Buschiazzo, A., Di Noia, J.M., Navarrete, M.A., Chiorazzi, N., Oppezzo, P., 2021. AID overexpression leads to aggressive murine CLL and nonimmunoglobulin mutations that mirror human neoplasms. Blood 138, 246–258. https://doi.org/10.1182/blood.2020008654

Morrison, V.A., 2010. Infectious complications of chronic lymphocytic leukaemia: Pathogenesis, spectrum of infection, preventive approaches. Best Practice and Research in Clinical Haematology 23, 145–153. https://doi.org/10.1016/j.beha.2009.12.004

Moshous, D., Callebaut, I., de Chasseval, R., Corneo, B., Cavazzana-Calvo, M., Le Deist, F., Tezcan, I., Sanal, O., Bertrand, Y., Philippe, N., Fischer, A., de Villartay, J.P., 2001. Artemis, a novel DNA double-strand break repair/V(D)J recombination protein, is mutated in human severe combined immune deficiency. Cell 105, 177–186. https://doi.org/10.1016/s0092-8674(01)00309-9

Motycka, T.A., Bessho, T., Post, S.M., Sung, P., Tomkinson, A.E., 2004. Physical and functional interaction between the XPF/ERCC1 endonuclease and hRad52. J Biol Chem 279, 13634–13639. https://doi.org/10.1074/jbc.M313779200

Muramatsu, M., Sankaranand, V.S., Anant, S., Sugai, M., Kinoshita, K., Davidson, N.O., Honjo, T., 1999. Specific expression of activation-induced cytidine deaminase (AID), a novel member of the RNA-editing deaminase family in germinal center B cells. J Biol Chem 274, 18470–18476. https://doi.org/10.1074/jbc.274.26.18470

Nijnik, A., Woodbine, L., Marchetti, C., Dawson, S., Lambe, T., Liu, C., Rodrigues, N.P., Crockford, T.L., Cabuy, E., Vindigni, A., Enver, T., Bell, J.I., Slijepcevic, P., Goodnow, C.C., Jeggo, P.A., Cornall, R.J., 2007. DNA repair is limiting for haematopoietic stem cells during ageing. Nature 447, 686–690. https://doi.org/10.1038/nature05875

Nimonkar, A.V., Genschel, J., Kinoshita, E., Polaczek, P., Campbell, J.L., Wyman, C., Modrich, P., Kowalczykowski, S.C., 2011. BLM-DNA2-RPA-MRN and EXO1-BLM-RPA-MRN constitute two DNA end resection machineries for human DNA break repair. Genes Dev 25, 350–362. https://doi.org/10.1101/gad.2003811

Noordermeer, S.M., Adam, S., Setiaputra, D., Barazas, M., Pettitt, S.J., Ling, A.K., Olivieri, M., Álvarez-Quilón, A., Moatti, N., Zimmermann, M., Annunziato, S., Krastev, D.B., Song, F., Brandsma, I., Frankum, J., Brough, R., Sherker, A., Landry, S., Szilard, R.K., Munro, M.M., McEwan, A., Goullet de Rugy, T., Lin, Z.-Y., Hart, T., Moffat, J., Gingras, A.-C., Martin, A., van Attikum, H., Jonkers, J., Lord, C.J., Rottenberg, S., Durocher, D., 2018. The shieldin complex mediates 53BP1-dependent DNA repair. Nature 560, 117–121. https://doi.org/10.1038/s41586-018-0340-7

Nussenzweig, A., Nussenzweig, M.C., 2010. Origin of chromosomal translocations in lymphoid cancer. Cell 141, 27–38. https://doi.org/10.1016/j.cell.2010.03.016

Ochi, T., Blackford, A.N., Coates, J., Jhujh, S., Mehmood, S., Tamura, N., Travers, J., Wu, Q., Draviam, V.M., Robinson, C.V., Blundell, T.L., Jackson, S.P., 2015. DNA repair. PAXX, a paralog of XRCC4 and XLF, interacts with Ku to promote DNA double-strand break repair. Science 347, 185–188. https://doi.org/10.1126/science.1261971

Ochiai, K., Maienschein-Cline, M., Simonetti, G., Chen, J., Rosenthal, R., Brink, R., Chong, A.S., Klein, U., Dinner, A.R., Singh, H., Sciammas, R., 2013. Transcriptional regulation of germinal center B and plasma cell fates by dynamical control of IRF4. Immunity 38, 918–929. https://doi.org/10.1016/j.immuni.2013.04.009

Odegard, V.H., Schatz, D.G., 2006. Targeting of somatic hypermutation. Nat Rev Immunol 6, 573–583. https://doi.org/10.1038/nri1896

License CC BY-NC-ND 4.0

Opinto, G., Agostinelli, C., Ciavarella, S., Guarini, A., Maiorano, E., Ingravallo, G., 2021. Hodgkin Lymphoma: A Special Microenvironment. J Clin Med 10, 4665. https://doi.org/10.3390/jcm10204665

Oppezzo, P., Navarrete, M., Chiorazzi, N., 2021. AID in Chronic Lymphocytic Leukemia: Induction and Action During Disease Progression. Front Oncol 11, 634383. https://doi.org/10.3389/fonc.2021.634383

Ouillette, P., Collins, R., Shakhan, S., Li, J., Li, C., Shedden, K., Malek, S.N., 2011. The prognostic significance of various 13q14 deletions in chronic lymphocytic leukemia. Clin Cancer Res 17, 6778–6790. https://doi.org/10.1158/1078-0432.CCR-11-0785

Packham, G., Stevenson, F.K., 2005. Bodyguards and assassins: Bcl-2 family proteins and apoptosis control in chronic lymphocytic leukaemia. Immunology 114, 441–449. https://doi.org/10.1111/j.1365-2567.2005.02117.x

Palacios, F., Moreno, P., Morande, P., Abreu, C., Correa, A., Porro, V., Landoni, A.I., Gabus, R., Giordano, M., Dighiero, G., Pritsch, O., Oppezzo, P., 2010. High expression of AID and active class switch recombination might account for a more aggressive disease in unmutated CLL patients: link with an activated microenvironment in CLL disease. Blood 115, 4488–4496. https://doi.org/10.1182/blood-2009-12-257758

Palm, A.-K.E., Henry, C., 2019. Remembrance of Things Past: Long-Term B Cell Memory After Infection and Vaccination. Frontiers in Immunology 10.

Panier, S., Boulton, S.J., 2014. Double-strand break repair: 53BP1 comes into focus. Nat Rev Mol Cell Biol 15, 7–18. https://doi.org/10.1038/nrm3719

Pannunzio, N.R., Watanabe, G., Lieber, M.R., 2018. Nonhomologous DNA end-joining for repair of DNA double-strand breaks. J Biol Chem 293, 10512–10523. https://doi.org/10.1074/jbc.TM117.000374

Parikh, S.A., Kay, N.E., Shanafelt, T.D., 2014. How we treat Richter syndrome. Blood 123, 1647–1657. https://doi.org/10.1182/blood-2013-11-516229

Pavri, R., 2017. R Loops in the Regulation of Antibody Gene Diversification. Genes (Basel) 8, E154. https://doi.org/10.3390/genes8060154

Peperzak, V., Vikström, I., Walker, J., Glaser, S.P., LePage, M., Coquery, C.M., Erickson, L.D., Fairfax, K., Mackay, F., Strasser, A., Nutt, S.L., Tarlinton, D.M., 2013. Mcl-1 is essential for the survival of plasma cells. Nat Immunol 14, 290–297. https://doi.org/10.1038/ni.2527

Pereira, J., Kelly, L., Xu, Y., Cyster, J., 2009. EBI2 mediates B cell segregation between the outer and centre follicle. Nature 460, 1122–6. https://doi.org/10.1038/nature08226

Perlot, T., Alt, F.W., 2008. Cis-regulatory elements and epigenetic changes control genomic rearrangements of the IgH locus. Adv Immunol 99, 1–32. https://doi.org/10.1016/S0065-2776(08)00601-9

Péron, S., Laffleur, B., Denis-Lagache, N., Cook-Moreau, J., Tinguely, A., Delpy, L., Denizot, yves, Pinaud, E., Cogné, M., 2012a. AID-Driven Deletion Causes Immunoglobulin Heavy Chain "Locus Suicide Recombination" in B Cells. Science epub ahead of print. https://doi.org/10.1126/science.1218692

Péron, S., Laffleur, B., Denis-Lagache, N., Cook-Moreau, J., Tinguely, A., Delpy, L., Denizot, Y., Pinaud, E., Cogné, M., 2012b. AID-driven deletion causes immunoglobulin heavy chain locus suicide recombination in B cells. Science 336, 931–934. https://doi.org/10.1126/science.1218692

Pham-Ledard, A., Prochazkova-Carlotti, M., Deveza, M., Laforet, M.-P., Beylot-Barry, M., Vergier, B., Parrens, M., Feuillard, J., Merlio, J.-P., Gachard, N., 2017. Molecular analysis of immunoglobulin variable genes supports a germinal center experienced normal counterpart in primary cutaneous diffuse large B-cell lymphoma, leg-type. Journal of Dermatological Science 88, 238–246. https://doi.org/10.1016/j.jdermsci.2017.07.008

Pinaud, E., Marquet, M., Fiancette, R., Péron, S., Vincent-Fabert, C., Denizot, Y., Cogné, M., 2011. The IgH locus 3' regulatory region: pulling the strings from behind. Adv Immunol 110, 27–70. https://doi.org/10.1016/B978-0-12-387663-8.00002-8

License CC BY-NC-ND 4.0

Piris, M.A., Medeiros, L.J., Chang, K.-C., 2020. Hodgkin lymphoma: a review of pathological features and recent advances in pathogenesis. Pathology, Lymphoma 2020: morphology, markers, molecules, WHO knows what next? 52, 154–165. https://doi.org/10.1016/j.pathol.2019.09.005

Plank, J.L., Wu, J., Hsieh, T., 2006. Topoisomerase IIIα and Bloom's helicase can resolve a mobile double Holliday junction substrate through convergent branch migration. Proc Natl Acad Sci U S A 103, 11118–11123. https://doi.org/10.1073/pnas.0604873103

Popp, H.D., Flach, J., Brendel, S., Ruppenthal, S., Kleiner, H., Seifarth, W., Schneider, S., Schulze, T.J., Weiss, C., Wenz, F., Hofmann, W.-K., Fabarius, A., 2019. Accumulation of DNA damage and alteration of the DNA damage response in monoclonal B-cell lymphocytosis and chronic lymphocytic leukemia. Leukemia & Lymphoma 60, 795–804. https://doi.org/10.1080/10428194.2018.1498494

Puente, X.S., Beà, S., Valdés-Mas, R., Villamor, N., Gutiérrez-Abril, J., Martín-Subero, J.I., Munar, M., Rubio-Pérez, C., Jares, P., Aymerich, M., Baumann, T., Beekman, R., Belver, L., Carrio, A., Castellano, G., Clot, G., Colado, E., Colomer, D., Costa, D., Delgado, J., Enjuanes, A., Estivill, X., Ferrando, A.A., Gelpí, J.L., González, B., González, S., González, M., Gut, M., Hernández-Rivas, J.M., López-Guerra, M., Martín-García, D., Navarro, A., Nicolás, P., Orozco, M., Payer, Á.R., Pinyol, M., Pisano, D.G., Puente, D.A., Queirós, A.C., Quesada, V., Romeo-Casabona, C.M., Royo, C., Royo, R., Rozman, M., Russiñol, N., Salaverría, I., Stamatopoulos, K., Stunnenberg, H.G., Tamborero, D., Terol, M.J., Valencia, A., López-Bigas, N., Torrents, D., Gut, I., López-Guillermo, A., López-Otín, C., Campo, E., 2015. Non-coding recurrent mutations in chronic lymphocytic leukaemia. Nature 526, 519–524. https://doi.org/10.1038/nature14666

Rajewsky, K., 1996. Clonal selection and learning in the antibody system. Nature 381, 751–758. https://doi.org/10.1038/381751a0

Ramsay, A.J., Quesada, V., Foronda, M., Conde, L., Martínez-Trillos, A., Villamor, N., Rodríguez, D., Kwarciak, A., Garabaya, C., Gallardo, M., López-Guerra, M., López-Guillermo, A., Puente, X.S., Blasco, M.A., Campo, E., López-Otín, C., 2013. POT1 mutations cause telomere dysfunction in chronic lymphocytic leukemia. Nat Genet 45, 526–530. https://doi.org/10.1038/ng.2584

Ranganathan, R., Shou, P., Ahn, S., Sun, C., West, J., Savoldo, B., Dotti, G., 2021. CAR T cells Targeting Human Immunoglobulin Light Chains Eradicate Mature B-cell Malignancies While Sparing a Subset of Normal B Cells. Clin Cancer Res 27, 5951–5960. https://doi.org/10.1158/1078-0432.CCR-20-2754

Rass, U., Ahel, I., West, S.C., 2007. Defective DNA repair and neurodegenerative disease. Cell 130, 991–1004. https://doi.org/10.1016/j.cell.2007.08.043

Rawstron, A.C., Bennett, F.L., O'Connor, S.J.M., Kwok, M., Fenton, J.A.L., Plummer, M., de Tute, R., Owen, R.G., Richards, S.J., Jack, A.S., Hillmen, P., 2008. Monoclonal B-cell lymphocytosis and chronic lymphocytic leukemia. N Engl J Med 359, 575–583. https://doi.org/10.1056/NEJMoa075290

Rawstron, A.C., Kreuzer, K.-A., Soosapilla, A., Spacek, M., Stehlikova, O., Gambell, P., McIver-Brown, N., Villamor, N., Psarra, K., Arroz, M., Milani, R., de la Serna, J., Cedena, M.T., Jaksic, O., Nomdedeu, J., Moreno, C., Rigolin, G.M., Cuneo, A., Johansen, P., Johnsen, H.E., Rosenquist, R., Niemann, C.U., Kern, W., Westerman, D., Trneny, M., Mulligan, S., Doubek, M., Pospisilova, S., Hillmen, P., Oscier, D., Hallek, M., Ghia, P., Montserrat, E., 2018. Reproducible diagnosis of chronic lymphocytic leukemia by flow cytometry: An European Research Initiative on CLL (ERIC) & European Society for Clinical Cell Analysis (ESCCA) Harmonisation project. Cytometry B Clin Cytom 94, 121–128. https://doi.org/10.1002/cyto.b.21595

Reichel, J.B., McCormick, J., Fromm, J.R., Elemento, O., Cesarman, E., Roshal, M., 2017. Flow-sorting and Exome Sequencing of the Reed-Sternberg Cells of Classical Hodgkin Lymphoma. JoVE (Journal of Visualized Experiments) e54399. https://doi.org/10.3791/54399

License CC BY-NC-ND 4.0

Reinherz, E.L., Kung, P.C., Goldstein, G., Levey, R.H., Schlossman, S.F., 1980. Discrete stages of human intrathymic differentiation: analysis of normal thymocytes and leukemic lymphoblasts of T-cell lineage. Proc Natl Acad Sci U S A 77, 1588–1592. https://doi.org/10.1073/pnas.77.3.1588

Rhind, N., 2009. Changing of the guard: how ATM hands off DNA double-strand break signaling to ATR. Mol Cell 33, 672–674. https://doi.org/10.1016/j.molcel.2009.03.004

Riballo, E., Woodbine, L., Stiff, T., Walker, S.A., Goodarzi, A.A., Jeggo, P.A., 2009. XLF-Cernunnos promotes DNA ligase IV-XRCC4 re-adenylation following ligation. Nucleic Acids Res 37, 482–492. https://doi.org/10.1093/nar/gkn957

Rinaldi, A., Mian, M., Kwee, I., Rossi, D., Deambrogi, C., Mensah, A.A., Forconi, F., Spina, V., Cencini, E., Drandi, D., Ladetto, M., Santachiara, R., Marasca, R., Gattei, V., Cavalli, F., Zucca, E., Gaidano, G., Bertoni, F., 2011. Genome-wide DNA profiling better defines the prognosis of chronic lymphocytic leukaemia. Br J Haematol 154, 590–599. https://doi.org/10.1111/j.1365-2141.2011.08789.x

Rinaldi, I., 2018. The Role of Reed-Sternberg CD30 Receptor and Lymphocytes in Pathogenesis of Disease and Its Implication for Treatment. Acta Med Indones 50, 93–95.

Rizzo, D., Bouvier, G., Youlyouz-Marfak, I., Guerin, E., Trimoreau, F., Bordessoule, D., Jaccard, A., Gachard, N., Feuillard, J., 2013. T/B ratio does not reflect levels of ZAP70 expression in clonal CLL B-cells due to ZAP70 overexpression in patient T-cells. Cytometry B Clin Cytom 84, 125–132. https://doi.org/10.1002/cyto.b.21055

Robert, I., Dantzer, F., Reina-San-Martin, B., 2009. Parp1 facilitates alternative NHEJ, whereas Parp2 suppresses IgH/c-myc translocations during immunoglobulin class switch recombination. J Exp Med 206, 1047–1056. https://doi.org/10.1084/jem.20082468

Roch, B., Abramowski, V., Chaumeil, J., de Villartay, J.-P., 2019. Cernunnos/Xlf Deficiency Results in Suboptimal V(D)J Recombination and Impaired Lymphoid Development in Mice. Frontiers in Immunology 10.

Roco, J.A., Mesin, L., Binder, S.C., Nefzger, C., Gonzalez-Figueroa, P., Canete, P.F., Ellyard, J., Shen, Q., Robert, P.A., Cappello, J., Vohra, H., Zhang, Y., Nowosad, C.R., Schiepers, A., Corcoran, L.M., Toellner, K.-M., Polo, J., Meyer-Hermann, M., Victora, G., Vinuesa, C.G., 2019. Class Switch Recombination Occurs Infrequently in Germinal Centers. Immunity 51, 337-350.e7. https://doi.org/10.1016/j.immuni.2019.07.001

Roessner, P.M., Seiffert, M., 2020. T-cells in chronic lymphocytic leukemia: Guardians or drivers of disease? Leukemia 34, 2012–2024. https://doi.org/10.1038/s41375-020-0873-2

Romanow, W.J., Langerak, A.W., Goebel, P., Wolvers-Tettero, I.L., van Dongen, J.J., Feeney, A.J., Murre, C., 2000. E2A and EBF act in synergy with the V(D)J recombinase to generate a diverse immunoglobulin repertoire in nonlymphoid cells. Mol Cell 5, 343–353. https://doi.org/10.1016/s1097-2765(00)80429-3

Ropars, V., Drevet, P., Legrand, P., Baconnais, S., Amram, J., Faure, G., Márquez, J.A., Piétrement, O., Guerois, R., Callebaut, I., Le Cam, E., Revy, P., de Villartay, J.-P., Charbonnier, J.-B., 2011. Structural characterization of filaments formed by human Xrcc4–Cernunnos/XLF complex involved in nonhomologous DNA end-joining. Proceedings of the National Academy of Sciences 108, 12663–12668. https://doi.org/10.1073/pnas.1100758108

Rosati, E., Baldoni, S., De Falco, F., Del Papa, B., Dorillo, E., Rompietti, C., Albi, E., Falzetti, F., Di Ianni, M., Sportoletti, P., 2018. NOTCH1 Aberrations in Chronic Lymphocytic Leukemia. Front Oncol 8, 229. https://doi.org/10.3389/fonc.2018.00229

Rosenwald, A., Alizadeh, A.A., Widhopf, G., Simon, R., Davis, R.E., Yu, X., Yang, L., Pickeral, O.K., Rassenti, L.Z., Powell, J., Botstein, D., Byrd, J.C., Grever, M.R., Cheson, B.D., Chiorazzi, N., Wilson, W.H., Kipps, T.J., Brown, P.O., Staudt, L.M., 2001. Relation of Gene Expression Phenotype to Immunoglobulin Mutation Genotype in B Cell Chronic Lymphocytic Leukemia. J Exp Med 194, 1639–1648.

Rossi, D., Rasi, S., Spina, V., Bruscaggin, A., Monti, S., Ciardullo, C., Deambrogi, C., Khiabanian, H., Serra, R., Bertoni, F., Forconi, F., Laurenti, L., Marasca, R., Dal-Bo, M., Rossi, F.M., Bulian, P.,

License CC BY-NC-ND 4.0

Nomdedeu, J., Del Poeta, G., Gattei, V., Pasqualucci, L., Rabadan, R., Foà, R., Dalla-Favera, R., Gaidano, G., 2013. Integrated mutational and cytogenetic analysis identifies new prognostic subgroups in chronic lymphocytic leukemia. Blood 121, 1403–1412. https://doi.org/10.1182/blood-2012-09-458265

Rouaud, P., Saintamand, A., Saad, F., Carrion, C., Lecardeur, S., Cogné, M., Denizot, Y., 2014. Elucidation of the enigmatic IgD class-switch recombination via germline deletion of the IgH 3' regulatory region. Journal of Experimental Medicine 211, 975–985. https://doi.org/10.1084/jem.20131385

Rouaud, P., Vincent-Fabert, C., Fiancette, R., Cogné, M., Pinaud, E., Denizot, Y., 2012. Enhancers located in heavy chain regulatory region (hs3a, hs1,2, hs3b, and hs4) are dispensable for diversity of VDJ recombination. J Biol Chem 287, 8356–8360. https://doi.org/10.1074/jbc.M112.341024

Rouaud, P., Vincent-Fabert, C., Saintamand, A., Fiancette, R., Marquet, M., Robert, I., Reina-San-Martin, B., Pinaud, E., Cogné, M., Denizot, Y., 2013. The IgH 3' regulatory region controls somatic hypermutation in germinal center B cells. Journal of Experimental Medicine 210, 1501–1507. https://doi.org/10.1084/jem.20130072

Rucci, F., Notarangelo, L.D., Fazeli, A., Patrizi, L., Hickernell, T., Paganini, T., Coakley, K.M., Detre, C., Keszei, M., Walter, J.E., Feldman, L., Cheng, H.-L., Poliani, P.L., Wang, J.H., Balter, B.B., Recher, M., Andersson, E.-M., Zha, S., Giliani, S., Terhorst, C., Alt, F.W., Yan, C.T., 2010. Homozygous DNA ligase IV R278H mutation in mice leads to leaky SCID and represents a model for human LIG4 syndrome. Proc Natl Acad Sci U S A 107, 3024–3029. https://doi.org/10.1073/pnas.0914865107

Sabattini, E., Bacci, F., Sagramoso, C., Pileri, S.A., 2010. WHO classification of tumours of haematopoietic and lymphoid tissues in 2008: an overview. Pathologica 102, 83–87.

Saintamand, A., Vincent-Fabert, C., Marquet, M., Ghazzaui, N., Magnone, V., Pinaud, E., Cogné, M., Denizot, Y., 2017. Eμ and 3'RR IgH enhancers show hierarchic unilateral dependence in mature B-cells. Sci Rep 7, 442. https://doi.org/10.1038/s41598-017-00575-0

Saribasak, H., Maul, R., Cao, Z., McFleder, R., Yang, W., McNeill, D., Wilson III, D., Gearhart, P., 2011. XRCC1 suppresses somatic hypermutation and promotes alternative nonhomologous end joining in Igh genes. The Journal of experimental medicine 208, 2209–16. https://doi.org/10.1084/jem.20111135

Saxena, A., Viswanathan, S., Moshynska, O., Tandon, P., Sankaran, K., Sheridan, D.P., 2004. Mcl-1 and Bcl-2/Bax ratio are associated with treatment response but not with Rai stage in B-cell chronic lymphocytic leukemia. Am J Hematol 75, 22–33. https://doi.org/10.1002/ajh.10453

Schatz, D.G., Ji, Y., 2011. Recombination centres and the orchestration of V(D)J recombination. Nat Rev Immunol 11, 251–263. https://doi.org/10.1038/nri2941

Schroeder, H.W., Cavacini, L., 2010. Structure and Function of Immunoglobulins. J Allergy Clin Immunol 125, S41–S52. https://doi.org/10.1016/j.jaci.2009.09.046

Schubert, M., Hackl, H., Gassner, F.J., Greil, R., Geisberger, R., 2018. Investigating epigenetic effects of activation-induced deaminase in chronic lymphocytic leukemia. PLoS One 13, e0208753. https://doi.org/10.1371/journal.pone.0208753

Scully, R., Panday, A., Elango, R., Willis, N.A., 2019. DNA double strand break repair pathway choice in somatic mammalian cells. Nat Rev Mol Cell Biol 20, 698–714. https://doi.org/10.1038/s41580-019-0152-0

Sedlaříková, L., Petrackova, A., Papajik, T., Turcsányi, P., Kriegova, E., 2020. Resistance-Associated Mutations in Chronic Lymphocytic Leukemia Patients Treated With Novel Agents. Frontiers in Oncology 10, 894. https://doi.org/10.3389/fonc.2020.00894

Seki, M., Masutani, C., Yang, L.W., Schuffert, A., Iwai, S., Bahar, I., Wood, R.D., 2004. High-efficiency bypass of DNA damage by human DNA polymerase Q. EMBO J 23, 4484–4494. https://doi.org/10.1038/sj.emboj.7600424

License CC BY-NC-ND 4.0

Sepulveda, M.A., Garrett, F.E., Price-Whelan, A., Birshtein, B.K., 2005. Comparative analysis of human and mouse 3' Igh regulatory regions identifies distinctive structural features. Mol Immunol 42, 605–615. https://doi.org/10.1016/j.molimm.2004.09.006

Sfeir, A., Symington, L.S., 2015. Microhomology-Mediated End Joining: A Back-up Survival Mechanism or Dedicated Pathway? Trends Biochem Sci 40, 701–714. https://doi.org/10.1016/j.tibs.2015.08.006

Shanafelt, T.D., 2009. Predicting clinical outcome in CLL: how and why. Hematology 2009, 421–429. https://doi.org/10.1182/asheducation-2009.1.421

Shang, J., Zha, H., Sun, Y., 2020. Phenotypes, Functions, and Clinical Relevance of Regulatory B Cells in Cancer. Frontiers in Immunology 11.

Shibata, A., Jeggo, P.A., 2021. ATM's Role in the Repair of DNA Double-Strand Breaks. Genes (Basel) 12, 1370. https://doi.org/10.3390/genes12091370

Shieldin – the protector of DNA ends, 2019. . EMBO reports 20, e47560. https://doi.org/10.15252/embr.201847560

Shiloh, Y., Ziv, Y., 2013. The ATM protein kinase: regulating the cellular response to genotoxic stress, and more. Nat Rev Mol Cell Biol 14, 197–210. https://doi.org/10.1038/nrm3546

Shiotani, B., Zou, L., 2009. Single-stranded DNA orchestrates an ATM-to-ATR switch at DNA breaks. Mol Cell 33, 547–558. https://doi.org/10.1016/j.molcel.2009.01.024

Shukla, V., Halabelian, L., Balagere, S., Samaniego-Castruita, D., Feldman, D.E., Arrowsmith, C.H., Rao, A., Aravind, L., 2020. HMCES Functions in the Alternative End-Joining Pathway of the DNA DSB Repair during Class Switch Recombination in B Cells. Molecular Cell 77, 384-394.e4. https://doi.org/10.1016/j.molcel.2019.10.031

Simsek, D., Brunet, E., Wong, S.Y.-W., Katyal, S., Gao, Y., McKinnon, P.J., Lou, J., Zhang, L., Li, J., Rebar, E.J., Gregory, P.D., Holmes, M.C., Jasin, M., 2011. DNA Ligase III Promotes Alternative Nonhomologous End-Joining during Chromosomal Translocation Formation. PLoS Genet 7, e1002080. https://doi.org/10.1371/journal.pgen.1002080

Skowronska, A., Parker, A., Ahmed, G., Oldreive, C., Davis, Z., Richards, S., Dyer, M., Matutes, E., Gonzalez, D., Taylor, A.M.R., Moss, P., Thomas, P., Oscier, D., Stankovic, T., 2012. Biallelic ATM inactivation significantly reduces survival in patients treated on the United Kingdom Leukemia Research Fund Chronic Lymphocytic Leukemia 4 trial. J Clin Oncol 30, 4524–4532. https://doi.org/10.1200/JCO.2011.41.0852

Soulas-Sprauel, P., Rivera-Munoz, P., Malivert, L., Le Guyader, G., Abramowski, V., Revy, P., de Villartay, J.-P., 2007. V(D)J and immunoglobulin class switch recombinations: a paradigm to study the regulation of DNA end-joining. Oncogene 26, 7780–7791. https://doi.org/10.1038/sj.onc.1210875

Stavnezer, J., Guikema, J.E.J., Schrader, C.E., 2008. Mechanism and regulation of class switch recombination. Annu Rev Immunol 26, 261–292. https://doi.org/10.1146/annurev.immunol.26.021607.090248

Stebegg, M., Kumar, S.D., Silva-Cayetano, A., Fonseca, V.R., Linterman, M.A., Graca, L., 2018. Regulation of the Germinal Center Response. Frontiers in Immunology 9.

Stephens, P.J., McBride, D.J., Lin, M.-L., Varela, I., Pleasance, E.D., Simpson, J.T., Stebbings, L.A., Leroy, C., Edkins, S., Mudie, L.J., Greenman, C.D., Jia, M., Latimer, C., Teague, J.W., Lau, K.W., Burton, J., Quail, M.A., Swerdlow, H., Churcher, C., Natrajan, R., Sieuwerts, A.M., Martens, J.W., Silver, D.P., Langerod, A., Russnes, H.E., Foekens, J.A., Reis-Filho, J.S., van 't Veer, L., Richardson, A.L., Børreson-Dale, A.-L., Campbell, P.J., Futreal, P.A., Stratton, M.R., 2009. COMPLEX LANDSCAPES OF SOMATIC REARRANGEMENT IN HUMAN BREAST CANCER GENOMES. Nature 462, 1005–1010. https://doi.org/10.1038/nature08645

Stilgenbauer, S., Schnaiter, A., Paschka, P., Zenz, T., Rossi, M., Döhner, K., Bühler, A., Böttcher, S., Ritgen, M., Kneba, M., Winkler, D., Tausch, E., Hoth, P., Edelmann, J., Mertens, D., Bullinger, L., Bergmann, M., Kless, S., Mack, S., Jäger, U., Patten, N., Wu, L., Wenger, M.K., Fingerle-Rowson, G., Lichter, P., Cazzola, M., Wendtner, C.M., Fink, A.M., Fischer, K., Busch, R., Hallek,

License CC BY-NC-ND 4.0

M., Döhner, H., 2014. Gene mutations and treatment outcome in chronic lymphocytic leukemia: results from the CLL8 trial. Blood 123, 3247–3254. https://doi.org/10.1182/blood-2014-01-546150

Stinson, B.M., Moreno, A.T., Walter, J.C., Loparo, J.J., 2020. A Mechanism to Minimize Errors during Non-homologous End Joining. Molecular Cell 77, 1080-1091.e8. https://doi.org/10.1016/j.molcel.2019.11.018

Sulli, G., Di Micco, R., di Fagagna, F. d'Adda, 2012. Crosstalk between chromatin state and DNA damage response in cellular senescence and cancer. Nat Rev Cancer 12, 709–720. https://doi.org/10.1038/nrc3344

Sun, Y., McCorvie, T.J., Yates, L.A., Zhang, X., 2020. Structural basis of homologous recombination. Cell. Mol. Life Sci. 77, 3–18. https://doi.org/10.1007/s00018-019-03365-1

Svanberg, R., Janum, S., Patten, P.E.M., Ramsay, A.G., Niemann, C.U., 2021. Targeting the tumor microenvironment in chronic lymphocytic leukemia. Haematologica 106, 2312–2324. https://doi.org/10.3324/haematol.2020.268037

Tang, J., Cho, N.W., Cui, G., Manion, E.M., Shanbhag, N.M., Botuyan, M.V., Mer, G., Greenberg, R.A., 2013. Acetylation limits 53BP1 association with damaged chromatin to promote homologous recombination. Nat Struct Mol Biol 20, 317–325. https://doi.org/10.1038/nsmb.2499

Taylor, J.J., Pape, K.A., Jenkins, M.K., 2012. A germinal center-independent pathway generates unswitched memory B cells early in the primary response. J Exp Med 209, 597–606. https://doi.org/10.1084/jem.20111696

Thandra, K.C., Barsouk, Adam, Saginala, K., Padala, S.A., Barsouk, Alexander, Rawla, P., 2021. Epidemiology of Non-Hodgkin's Lymphoma. Med Sci (Basel) 9, 5. https://doi.org/10.3390/medsci9010005

Timblin, G.A., Schlissel, M.S., 2013. Ebf1 and c-Myb repress Rag transcription downstream of Stat5 during early B cell development. J Immunol 191, 10.4049/jimmunol.1301675. https://doi.org/10.4049/jimmunol.1301675

Tomimatsu, N., Mukherjee, B., Catherine Hardebeck, M., Ilcheva, M., Vanessa Camacho, C., Louise Harris, J., Porteus, M., Llorente, B., Khanna, K.K., Burma, S., 2014. Phosphorylation of EXO1 by CDKs 1 and 2 regulates DNA end resection and repair pathway choice. Nat Commun 5, 3561. https://doi.org/10.1038/ncomms4561

Tomimatsu, N., Mukherjee, B., Deland, K., Kurimasa, A., Bolderson, E., Khanna, K.K., Burma, S., 2012. Exo1 plays a major role in DNA end resection in humans and influences double-strand break repair and damage signaling decisions. DNA Repair (Amst) 11, 441–448. https://doi.org/10.1016/j.dnarep.2012.01.006

Townsend, C.L., Laffy, J.M.J., Wu, Y.-C.B., Silva O'Hare, J., Martin, V., Kipling, D., Fraternali, F., Dunn-Walters, D.K., 2016. Significant Differences in Physicochemical Properties of Human Immunoglobulin Kappa and Lambda CDR3 Regions. Frontiers in Immunology 7.

Truong, L.N., Li, Y., Shi, L.Z., Hwang, P.Y.-H., He, J., Wang, H., Razavian, N., Berns, M.W., Wu, X., 2013. Microhomology-mediated End Joining and Homologous Recombination share the initial end resection step to repair DNA double-strand breaks in mammalian cells. Proc Natl Acad Sci U S A 110, 7720–7725. https://doi.org/10.1073/pnas.1213431110

Tubbs, A.T., Dorsett, Y., Chan, E., Helmink, B., Lee, B.-S., Hung, P., George, R., Bredemeyer, A.L., Mittal, A., Pappu, R.V., Chowdhury, D., Mosammaparast, N., Krangel, M.S., Sleckman, B.P., 2014. KAP-1 Promotes Resection of Broken DNA Ends Not Protected by γ-H2AX and 53BP1 in G1-Phase Lymphocytes. Mol Cell Biol 34, 2811–2821. https://doi.org/10.1128/MCB.00441-14

Uematsu, N., Weterings, E., Yano, K., Morotomi-Yano, K., Jakob, B., Taucher-Scholz, G., Mari, P.-O., van Gent, D.C., Chen, B.P.C., Chen, D.J., 2007. Autophosphorylation of DNA-PKCS regulates its dynamics at DNA double-strand breaks. J Cell Biol 177, 219–229. https://doi.org/10.1083/jcb.200608077

License CC BY-NC-ND 4.0

Ünsal-Kaçmaz, K., Sancar, A., 2004. Quaternary Structure of ATR and Effects of ATRIP and Replication Protein A on Its DNA Binding and Kinase Activities. Molecular and Cellular Biology 24, 1292–1300. https://doi.org/10.1128/MCB.24.3.1292-1300.2003

van der Burg, M., van Dongen, J.J., van Gent, D.C., 2009. DNA-PKcs deficiency in human: long predicted, finally found. Current Opinion in Allergy and Clinical Immunology 9, 503–509. https://doi.org/10.1097/ACI.0b013e3283327e41

Victora, G.D., Dominguez-Sola, D., Holmes, A.B., Deroubaix, S., Dalla-Favera, R., Nussenzweig, M.C., 2012. Identification of human germinal center light and dark zone cells and their relationship to human B-cell lymphomas. Blood 120, 2240–2248. https://doi.org/10.1182/blood-2012-03-415380

Vincent-Fabert, C., Fiancette, R., Pinaud, E., Truffinet, V., Cogné, N., Cogné, M., Denizot, Y., 2010. Genomic deletion of the whole IgH 3' regulatory region (hs3a, hs1,2, hs3b, and hs4) dramatically affects class switch recombination and Ig secretion to all isotypes. Blood 116, 1895–1898. https://doi.org/10.1182/blood-2010-01-264689

Visco, C., Barcellini, W., Maura, F., Neri, A., Cortelezzi, A., Rodeghiero, F., 2014. Autoimmune cytopenias in chronic lymphocytic leukemia. Am J Hematol 89, 1055–1062. https://doi.org/10.1002/ajh.23785

Wahsner, J., Gale, E.M., Rodríguez-Rodríguez, A., Caravan, P., 2019. Chemistry of MRI Contrast Agents: Current Challenges and New Frontiers. Chem Rev 119, 957–1057. https://doi.org/10.1021/acs.chemrev.8b00363

Wan, Y., Wu, C.J., 2013. SF3B1 mutations in chronic lymphocytic leukemia. Blood 121, 4627–4634. https://doi.org/10.1182/blood-2013-02-427641

Wang, L., Lawrence, M.S., Wan, Y., Stojanov, P., Sougnez, C., Stevenson, K., Werner, L., Sivachenko, A., DeLuca, D.S., Zhang, L., Zhang, W., Vartanov, A.R., Fernandes, S.M., Goldstein, N.R., Folco, E.G., Cibulskis, K., Tesar, B., Sievers, Q.L., Shefler, E., Gabriel, S., Hacohen, N., Reed, R., Meyerson, M., Golub, T.R., Lander, E.S., Neuberg, D., Brown, J.R., Getz, G., Wu, C.J., 2011. SF3B1 and Other Novel Cancer Genes in Chronic Lymphocytic Leukemia. N Engl J Med 365, 2497–2506. https://doi.org/10.1056/NEJMoa1109016

Wang, M., Wu, Weizhong, Wu, Wenqi, Rosidi, B., Zhang, L., Wang, H., Iliakis, G., 2006. PARP-1 and Ku compete for repair of DNA double strand breaks by distinct NHEJ pathways. Nucleic Acids Res 34, 6170–6182. https://doi.org/10.1093/nar/gkl840

Wen, H., Feng, Z., Ma, Y., Liu, R., Ou, Q., Guo, Q., Shen, Y., Wu, Xue, Shao, Y., Bao, H., Wu, Xiaohua, 2022. Homologous recombination deficiency in diverse cancer types and its correlation with platinum chemotherapy efficiency in ovarian cancer. BMC Cancer 22, 550. https://doi.org/10.1186/s12885-022-09602-4

Wen, Y., Jing, Y., Yang, L., Kang, D., Jiang, P., Li, N., Cheng, J., Li, J., Li, X., Peng, Z., Sun, X., Miller, H., Sui, Z., Gong, Q., Ren, B., Yin, W., Liu, C., 2019. The regulators of BCR signaling during B cell activation. Blood Science 1, 119–129. https://doi.org/10.1097/BS9.0000000000000026

Wiestner, A., Rosenwald, A., Barry, T.S., Wright, G., Davis, R.E., Henrickson, S.E., Zhao, H., Ibbotson, R.E., Orchard, J.A., Davis, Z., Stetler-Stevenson, M., Raffeld, M., Arthur, D.C., Marti, G.E., Wilson, W.H., Hamblin, T.J., Oscier, D.G., Staudt, L.M., 2003. ZAP-70 expression identifies a chronic lymphocytic leukemia subtype with unmutated immunoglobulin genes, inferior clinical outcome, and distinct gene expression profile. Blood 101, 4944–4951. https://doi.org/10.1182/blood-2002-10-3306

Wohlford, E.M., Baresel, P.C., Wilmore, J.R., Mortelliti, A.J., Coleman, C.B., Rochford, R., 2018. Changes in Tonsil B Cell Phenotypes and EBV Receptor Expression in Children Under 5-Years-Old. Cytometry B Clin Cytom 94, 291–301. https://doi.org/10.1002/cyto.b.21589

Wutz, G., Várnai, C., Nagasaka, K., Cisneros, D.A., Stocsits, R.R., Tang, W., Schoenfelder, S., Jessberger, G., Muhar, M., Hossain, M.J., Walther, N., Koch, B., Kueblbeck, M., Ellenberg, J., Zuber, J., Fraser, P., Peters, J., 2017. Topologically associating domains and chromatin loops depend on

License CC BY-NC-ND 4.0

cohesin and are regulated by CTCF, WAPL, and PDS5 proteins. EMBO J 36, 3573–3599. https://doi.org/10.15252/embj.201798004

Xu, Z., Zan, H., Pone, E.J., Mai, T., Casali, P., 2012. Immunoglobulin class-switch DNA recombination: induction, targeting and beyond. Nat Rev Immunol 12, 517–531. https://doi.org/10.1038/nri3216

Young, R.M., Staudt, L.M., 2014. Ibrutinib treatment of CLL – the cancer fights back. Cancer Cell 26, 11–13. https://doi.org/10.1016/j.ccr.2014.06.023

Yousefzadeh, M., Henpita, C., Vyas, R., Soto-Palma, C., Robbins, P., Niedernhofer, L., 2021. DNA damage—how and why we age? eLife 10, e62852. https://doi.org/10.7554/eLife.62852

Yousefzadeh, M.J., Wood, R.D., 2013. DNA polymerase POLQ and cellular defense against DNA damage. DNA Repair (Amst) 12, 1–9. https://doi.org/10.1016/j.dnarep.2012.10.004

Yu, W., Lescale, C., Babin, L., Bedora-Faure, M., Lenden-Hasse, H., Baron, L., Demangel, C., Yelamos, J., Brunet, E., Deriano, L., 2020. Repair of G1 induced DNA double-strand breaks in S-G2/M by alternative NHEJ. Nat Commun 11, 5239. https://doi.org/10.1038/s41467-020-19060-w

Yun, M.H., Hiom, K., 2009. CtIP-BRCA1 modulates the choice of DNA double-strand-break repair pathway throughout the cell cycle. Nature 459, 460–463. https://doi.org/10.1038/nature07955

Zahid, S., Seif El Dahan, M., Iehl, F., Fernandez-Varela, P., Le Du, M.-H., Ropars, V., Charbonnier, J.B., 2021. The Multifaceted Roles of Ku70/80. Int J Mol Sci 22, 4134. https://doi.org/10.3390/ijms22084134

Zan, H., Casali, P., 2013. Regulation of Aicda expression and AID activity. Autoimmunity 46, 83–101. https://doi.org/10.3109/08916934.2012.749244

Zan, H., Shima, N., Xu, Z., Al-Qahtani, A., Evinger III, A.J., Zhong, Y., Schimenti, J.C., Casali, P., 2005. The translesion DNA polymerase θ plays a dominant role in immunoglobulin gene somatic hypermutation. EMBO J 24, 3757–3769. https://doi.org/10.1038/sj.emboj.7600833

Zenz, T., Kröber, A., Scherer, K., Häbe, S., Bühler, A., Benner, A., Denzel, T., Winkler, D., Edelmann, J., Schwänen, C., Döhner, H., Stilgenbauer, S., 2008. Monoallelic TP53 inactivation is associated with poor prognosis in chronic lymphocytic leukemia: results from a detailed genetic characterization with long-term follow-up. Blood 112, 3322–3329. https://doi.org/10.1182/blood-2008-04-154070

Zhang, A., Peng, B., Huang, P., Chen, J., Gong, Z., 2017. The p53-binding protein 1-Tudor-interacting repair regulator complex participates in the DNA damage response. J Biol Chem 292, 6461–6467. https://doi.org/10.1074/jbc.M117.777474

Zhang, Y., Rowley, J.D., 2006. Chromatin structural elements and chromosomal translocations in leukemia. DNA Repair, Mechanisms of chromosomal translocation 5, 1282–1297. https://doi.org/10.1016/j.dnarep.2006.05.020

Zhao, X., Wei, C., Li, Jingjing, Xing, P., Li, Jingyao, Zheng, S., Chen, X., 2017. Cell cycle-dependent control of homologous recombination. Acta Biochimica et Biophysica Sinica 49, 655–668. https://doi.org/10.1093/abbs/gmx055

License CC BY-NC-ND 4.0

Abstract

In normal B cells, Activation Induced-cytidine deaminase (AID) is the key enzyme for class switch recombination (CSR) and somatic hypermutation of (SHM) on the heavy chain (H) and the light chain (for SHM) of Immunoglobulin (Ig). AID is also implicated in another *IgH* rearrangement, the locus suicide recombination (LSR). LSR occurs in activated B cells and recombines the *IgH* locus between the switch µ (Sµ) region and the 3'regulatory region (3'RR) of *IgH* locus. LSR results in the complete deletion of the cluster of *IgH* constant genes. When LSR hits the active *IgH* locus, it induces the loss of BCR expression and the death of the concerned B cells. CSR and d LSR proceed by introduction of double strand breaks (DSB) followed by DNA repair and junction production. Chronic lymphocytic leukemia (CLL) is an indolent non-Hodgkin B cell lymphoma. CLL is characterized by the clonal expansion of tumor cells (CD5+, CD23+ CD19+). Tumor cells weakly express a B cell receptor (BCR) on the surface, it is composed in the vast majority of cases of Immunoglobulins (Ig) IgM and IgD. CLL tumor cells are rarely switched, raising the question of abnormalities in the Ig gene recombination machinery in this B cell lymphoma. In our study, and based on the count of LSR junction we identified two groups of CLL patients. A group with High LSR junction count (LSR^{High}) and a group with low LSR junction count (LSR^{Low}) based on the mean count of LSR junctions obtained in healthy peripheral mononuclear blood cells (PBMC). Deep analysis of these groups of CLL patients showed that in LSR^{High} CLLs cells, the accessibility of *IgH* locus could be increased in a MYC dependent manner resulting in shorter survival and implying an additional MYC driven AID independent mechanism of *IgH* recombination. Also, LSR^{High} and ^{Low} CLLs appear to be characterized by different features certainly due to different CLL tumoral transformation mechanisms. We showed also similarity of LSR junctions between CLL LSR^{Low} samples and healthy tonsils. We propose tumoral cells, in LSR^{Low} CLL, emerge from B cell population which is normally restricted to the compartment of B cell activation achievement.

Key words High LSR count, low LSR count, CSR, MYC, CLL, prognosis, cell of origin.

Résumé

Dans les lymphocytes B (LB) normaux, l'Activation Induced-cytidine Deaminase (AID) est l'enzyme clé des mécanismes de commutation de classe (CSR) et l'hyper-mutation somatique (SHM) des chaînes lourde (H) et légère (L) d'immunoglobuline (Ig). AID est impliquée dans un autre mécanisme de réarrangement du locus *IgH*, la recombinaison suicide du locus *IgH* (LSR). La LSR se produit dans les cellules B activées et recombine le locus *IgH* entre la région de commutation µ (Sµ pour switch µ) et la région régulatrice (3'RR) en 3' du locus *IgH*. La LSR entraîne la suppression des gènes constants du locus *IgH*. Quand la LSR touche le locus *IgH* sur l'allèle productif, elle induit la perte d'expression du BCR et la mort des LB concernés. Les mécanismes de CSR et LSR nécessitent des cassures doubles brin (CDB) de l'ADN qui vont être réparées et générer la production de jonctions de recombinaison. La leucémie lymphoïde chronique (LLC) est un lymphome indolent non hodgkinien affectant les cellules B. la LLC est caractérisée par une prolifération clonale de cellules tumorales (CD5+, CD23+, CD19+). Les cellules tumorales expriment faiblement le BCR et l'Ig est majoritairement une IgM coexprimée avec l'IgD. Les cellules tumorales expriment rarement une Ig de classe commutée, ce qui pose la question sur une altération du processus permettant le réarrangement du locus *IgH* dans ces cellules cancéreuses. En utilisant le nombre de jonctions LSR détectées dans des prélèvements sanguins de patients atteints de LLC, nous avons identifié deux groupes distincts. Le premier groupe se présente avec un nombre augmenté de jonctions de LSR ($LSR^{augmentée}$), le second groupe, avec un nombre diminué de jonctions LSR, ($LSR^{diminuée}$) par rapport à la moyenne du compte de jonctions LSR d'échantillons de cellules mononuclées du sang périphérique (PBMC) de volontaires sains. L'analyse en détails de ces deux groupes a permis de montrer que dans les cellules du groupe $LSR^{augmentée}$ l'accessibilité du locus *IgH* est augmentée, une prolifération accrue, la surexpression de *MYC* et des indicateurs de mauvais pronostic. Ces cellules apparaissent subies un mécanisme de recombinaison du locus *IgH* aboutissant à la LSR indépendant de l'AID mais dépendant de MYC. Par ailleurs, nos résultats montrent que les LLC $LSR^{augmentée}$ et $LSR^{diminuée}$ présentent des caractéristiques différentes et suggèrent des mécanismes de transformation tumorale distincts. Nous avons également montré la similitude des jonctions LSR des cellules de LLC $LSR^{diminuée}$ et de cellules issues des amygdales de volontaires sains. Nous proposons que les cellules tumorales, dans la LLC $LSR^{diminuée}$, émergent de la population de cellules B qui est normalement limitée aux compartiments impliqués dans l'activation des cellules B.

Mots clés LSR augmentée, LSR diminuée, CSR, MYC, LLC, pronostic, Cellule d'origine.

License CC BY-NC-ND 4.0

License CC BY-NC-ND 4.0